
Electronic Thesis and Dissertation Repository

4-18-2022 2:30 PM

Application Of A Polynomial Affine Method In Dynamic Portfolio Choice

Yichen Zhu, *The University of Western Ontario*

Supervisor: Marcos, Escobar-Anel, *The University of Western Ontario*

Joint Supervisor: Matt, Davison, *The University of Western Ontario*

A thesis submitted in partial fulfillment of the requirements for the Doctor of Philosophy degree in Statistics and Actuarial Sciences

© Yichen Zhu 2022

Follow this and additional works at: <https://ir.lib.uwo.ca/etd>



Part of the [Finance Commons](#), [Management Sciences and Quantitative Methods Commons](#), and the [Operational Research Commons](#)

Recommended Citation

Zhu, Yichen, "Application Of A Polynomial Affine Method In Dynamic Portfolio Choice" (2022). *Electronic Thesis and Dissertation Repository*. 8467.

<https://ir.lib.uwo.ca/etd/8467>

This Dissertation/Thesis is brought to you for free and open access by Scholarship@Western. It has been accepted for inclusion in Electronic Thesis and Dissertation Repository by an authorized administrator of Scholarship@Western. For more information, please contact wlsadmin@uwo.ca.

Abstract

This thesis develops numerical approaches to attain optimal multi-period portfolio strategies in the context of advanced stochastic models within expected utility and mean-variance theories. Unlike common buy-and-hold portfolio strategies, dynamic asset allocation reflects the investment philosophy of a portfolio manager that benefits from the most recent market conditions to rebalance the portfolio accordingly. This enables managers to capture fleeting opportunities in the markets thereby enhancing the portfolio performance. However, the solvability of the dynamic asset allocation problem is often non-analytical, especially when considering a high-dimensional portfolio with advanced models mimicking practical asset's return. To overcome this issue, this thesis presents a competitive methodology to approximate optimal dynamic portfolio strategies.

The thesis can be categorized into two large sections. The development, algorithmic description, testing and extension of the methodology are presented in detail in the first section. Specifically, the main method, named PAMC, is originally developed for constant relative risk aversion investors. In a comparison with two existing well-known benchmark methods, our approach demonstrates superior efficiency and accuracy, this is not only for cases with no known solution but also for models where the analytical solution is available. We consequently extend the method into the wider hyperbolic absolute risk aversion utility family which is more flexible in capturing the risk aversion of investors. This extension permits the applicability of our method to both expected utility theory and mean-variance theory. Furthermore, the quality of portfolio allocation is directly linked to the quality of the portfolio value function approximation. This generates another important extension: the replacement of the polynomial regression in the original method by neural networks. Besides, we successfully implement the method on two important but models that have not been solved in closed-form: the Ornstein-Uhlenbeck 4/2 model and the Heston model with a stochastic interest rate, which further confirms the practicality and effectiveness of our novel methodology.

The second part of the thesis addresses the application of our numerical method to investments involving financial derivatives. In addition to portfolio performance maximization, we propose another criterion, namely, risk exposure minimization, to help investors meet regulatory constraints and protect their capital in the case of a market crash. The complexity of derivatives' price dynamics leads to new challenges on the solvability of the optimal allocation for a derivative-based portfolio. With proper modifications, our method is applicable to this type of problem. We then consider a portfolio construction with equity options and volatility index (VIX) options in the presence of volatility risk, providing insight into best investment practices with derivatives.

Keywords: Dynamic programming, Quadratic-Affine processes, Expected Utility, Portfolio optimization, derivatives market, Volatility risk

Summary for lay audience

Financial markets, i.e. markets for financial securities, are important mediums for economic development. There are two typical players in financial markets. The demand side refers to participants who seek funds for daily operational cash flows, bridge financing or long-term special projects. In contrast, the supply side refers to those who have excess money that can be used in favor of demand side thereby earning appreciation of their capital. This “dedication” of assets is often called investment, which is investigated in a scientific way in this thesis.

In practice, investment is a systematic process for large institutional investors including defining objectives, security selection, ongoing monitoring, etc. In this thesis, we focus on one of the most important steps, i.e. portfolio construction. A portfolio is a collection of financial investments like stocks, bonds, commodities, that take advantage of the wisdom of diversification—which simply means never put all your eggs in one basket. Moreover, we consider the portfolio in a continuous-time framework which allows investors to adjust their portfolio allocation in real time in response to new information that can appear at any time. Thus, Chapters 2, 3 and 4 are mainly concerned on the methodologies for approximating the optimal portfolio strategy.

Financial derivatives, defined as contracts that derive value from the performance of underlying assets, are widely used for hedging, speculation and taking arbitrage opportunities. There are numerous studies showing that derivatives may effectively enhance portfolio performance. This generates interest in the theme of the last two chapters: investments across traditional financial markets and derivatives markets. Specifically, Chapter 5 develops a new framework for derivatives-based portfolios. Chapter 6 illustrates an application of derivatives-based portfolios in presence of volatility risk.

Co-authorship statement

This thesis consists of materials based on five jointly authored research papers. All of these papers were co-authored with my supervisors: Dr. Marcos Escobar-Anel and Dr. Matt Davison. All co-authors contributed equally to co-authored papers. The detailed information on co-authorship is as follows,

1. The first paper titled “A polynomial-Affine approximation for dynamic portfolio choice” was co-authored with Dr. Marcos Escobar-Anel and Dr. Matt Davison. The paper is in the first round of revision and was in the second round of revision to *Computational Economics* in Apr 2022.
2. The second paper titled “Polynomial affine approach to the HARA utility with application to OU 4/2 model” (see [91]) was co-authored with Dr. Marcos Escobar-Anel. It has been published in *Applied Mathematics and Computation*.
3. The third paper titled “A Neural Network Monte Carlo Approximation for Expected Utility Theory” (see [90]) published in the *Journal of Risk and Financial Management* was co-authored with Dr. Marcos Escobar-Anel.
4. The fourth paper “Derivatives-based portfolio decisions. An expected utility insight” (see [36]) was co-authored with Dr. Marcos Escobar-Anel and Dr. Matt Davison. The paper was accepted by *Annals of Finance* in Apr 2021.
5. The fifth paper “Optimal market completion through financial derivatives with applications to volatility risk” (see [28]) was co-authored with Dr. Matt Davison and Dr. Marcos Escobar-Anel. This paper was submitted to *Quantitative Finance* in Feb 2022;

I certify that this thesis and its preliminary results incorporate materials that are direct results of my efforts. Dr. Marcos Escobar-Anel and Dr. Matt Davison supervised the research direction, provided critical feedback, and helped shape the research, analysis and manuscript. I would like to sincerely thank Dr. Marcos Escobar-Anel and Dr. Matt Davison for their guidance, support and supervision on all of my research.

Acknowledgements

I have received a lot of support and assistance throughout the writing of this thesis.

I would like to thank my supervisor, Dr. Marcos Escobar-Anel for his precious advice and continuous support. It was a privilege to work with him. His immense knowledge and patient guidance had encouraged me in all the time of my academic research and daily life and pushed me to sharpen my thinking and brought my work to a higher level. It is his kind help that has made my study and life at Western University a wonderful time.

I would also like to thank my supervisor, Dr. Matt Davison, whose expertise was invaluable in formulating the research questions and methodology. His insightful feedback often enlightened me during my research. He is also a life mentor for me who always encourages me to challenge difficulties and to stick to the career path that I desire.

In addition, I would like to thank all my colleagues and friends at Western University. Finally, I would like to express my gratitude to my parents for their encouragement and support throughout my studies.

Contents

Abstract	ii
Summary for lay audience	iii
Co-authorship statement	iv
Acknowledgements	v
List of Figures	x
List of Tables	xii
Preface	xiv
1 Introduction	1
1.1 Motivation and background	1
1.1.1 Contributions	4
1.1.2 Connection among chapters	7
1.2 Stochastic optimal control for dynamic asset allocation	8
1.2.1 Martingale method	9
1.2.2 Dynamic programming approach	11
1.2.3 Pre-commitment strategy within MVT	13
1.3 Numerical methods for dynamic portfolio choice	13
1.3.1 BGSS method	15
1.3.2 SVD approach	17
1.3.3 SGBM	18
1.3.4 Denault’s method	19
1.3.5 Cvitanic’s method	20
1.4 An overview of neural network	22
1.4.1 Artificial neural network	22
1.4.2 Backpropagation	23
1.5 A LSMC approach for the American option Valuation	24
2 A polynomial-Affine approximation for dynamic portfolio choice	27
2.1 Introduction	27
2.2 A methodology based on a polynomial-affine approximation	30
2.2.1 PAMC-VFI	32

2.2.2	PAMC-PWI	34
2.3	Examples of problems and solutions	34
2.3.1	Geometric Brownian motion	34
2.3.2	Stochastic volatility (SV) model	35
2.3.3	Mean-reverting log stock price process	35
2.4	Assessing accuracy and efficiency of the PAMC	36
2.4.1	Geometric Brownian motion	37
2.4.2	VAR model	37
2.4.3	Stochastic volatility (SV) model.	38
2.4.4	Exponential Ornstein–Uhlenbeck (OU) model	40
2.5	The Heston model with stochastic interest rate.	41
2.6	Conclusion	42
2.7	Proof of Theorem 2.2.1.	43
2.8	Relation to the BGSS	45
2.9	Tables and Figures.	47
3	Polyomial affine approach to the HARA utility with application to OU 4/2 model	60
3.1	Introduction	60
3.2	Polynomial-affine method for HARA utilities	64
3.3	Accuracy of the approximation for GBM 1/2 model	67
3.3.1	Closed-form solution of GBM 1/2 model	67
3.3.2	Accuracy for DRRA investors	68
3.3.3	Accuracy for IRRA investors	70
3.3.4	Application to a n-dim Heston model	71
3.4	Applications to the OU 4/2 family of models	72
3.4.1	Analysis of a DRRA investor	73
3.4.2	Analysis of IRRA investors—the mean-variance case	75
3.4.3	Suboptimality analysis for CRRA investors – the OU 1/2 model	78
3.5	Conclusions	80
3.6	Notation and algorithm for our methodology	81
3.6.1	Algorithm	81
3.7	Proof of Theorem 3.2.1	83
4	A neural network Monte Carlo approximation for expected utility theory	86
4.1	Introduction	86
4.2	Problem Setting and Architectures of the Deep Learning Model	88
4.2.1	Architectures of the deep learning model	89
4.2.1.1	Sum of exponential network	89
4.2.1.2	Improving Exponential Network	91
4.2.2	Initialization, Stopping Criterion and Activation Function	92
4.3	Notation and Algorithm of the Methodology	93
4.3.1	Algorithm	94
4.4	Application to 4/2 model	94
4.4.1	A solvable case	94
4.4.2	An unsolvable case, 4/2 Model with jumps	96

4.4.3	An unsolvable case, market price of risk proportional to volatility	98
4.5	Application to the OU 4/2 model	98
4.6	Conclusions	99
5	Derivatives-based portfolio decisions. An expected utility insight	108
5.1	Introduction	108
5.2	Mathematical setting and results	110
5.2.1	Derivative selection criterion: minimizing ℓ_1 risk exposure	112
5.3	Applications to one-asset derivatives	113
5.3.1	Put and call options	115
5.3.2	Straddles	118
5.4	Multi-asset option selection	121
5.5	Conclusions	123
5.6	Proofs	125
5.6.1	Proof of Proposition 5.2.1	125
5.6.2	Proof of Proposition 5.2.2	125
5.6.3	Proof of Proposition 5.3.1	127
5.6.4	Proof of Proposition 5.3.2	127
5.6.5	Proof of Corollary 5.3.3	128
5.6.6	Proof of Proposition 5.3.4	130
5.6.7	Proof of Proposition 5.4.1	131
5.6.8	Proof of Proposition 5.4.2	131
5.6.9	Comparison between the one-asset option and multi-asset option subsets	132
6	Optimal market completion through financial derivatives with applications to volatility risk	133
6.1	Introduction	133
6.2	Investor's problem	136
6.3	Polynomial affine method for CRRA utilities in financial derivatives market . .	138
6.3.1	The PAMC-indirect	139
6.4	Derivatives selection	141
6.4.1	Derivatives selection within options on stock	142
6.4.2	Derivatives selection within VIX products	144
6.5	Conclusion	146
6.6	Proofs	147
6.6.1	Proof of Proposition 6.2.1	147
6.6.2	Proof of Proposition 6.3.1	148
6.7	Alternative approximation method and comparison	150
6.7.1	Direct method	150
6.7.2	Comparison between the PAMC-direct method and the PAMC-indirect method	152
7	Summary and Future Research	154
	Bibliography	156

List of Figures

1.1	Classification of the numerical methods	14
1.2	Structure of the neural network	22
2.1	Different periods (Heston), (a) shows computational time versus number of period. (b) shows annualized certainty equivalent rate (CER) versus number of period. (c) shows mean L2 distance of optimal allocations at mid point versus number of period. We set $\gamma = 4$ and use other parameters in table 2.5 to produce above plots.	47
2.2	CER versus time to maturity T , $\gamma = 10$	48
2.3	Different periods (Mean-reverting Model), (a) shows computational time versus number of period. (b) shows annualized certainty equivalent rate (CER) versus number of period. (c) shows mean L2 distance of optimal allocations at mid point versus number of period. We set $\gamma = 4$ and use other parameters in table 2.5 to produce above plots.	48
2.4	The optimal strategy and CER across different value of ρ_{Sr} and ρ_{Xr} (Heston model with stochastic interest rate), $\gamma = 4$. Results from PAMC-VFI and PAMC-PWI are visually overlapped.	52
2.5	Comparison in Heston model with stochastic interest rate given $\rho_{Xr} = 0$: (a) optimal strategy, (b) CER and (c) computational time from PAMC, BGSS and SGBM across different value of ρ_{Sr}	59
3.1	Expected utility and certainty equivalent rate (CER) versus F (geometric Brownian motion [GBM] 1/2 model).	69
3.2	Expected utility and certainty equivalent rate (CER) versus λ_S with non-well-defined parametrization (geometric Brownian motion [GBM] 1/2 model).	70
3.3	Expected utility, certainty equivalent rate (CER), mean of relative strategy error, and computational time versus dimension n (multi-factor stochastic volatility model).	72
3.4	Expected utility and CER versus F (OU 4/2 model).	75
3.5	Optimal allocation for decreasing relative risk aversion (DRRA) investor versus a_S and b_S (OU 4/2 model).	75
3.6	Efficient frontier (OU 4/2 model).	77
3.7	Optimal allocation for IRRA investor versus a_S and b_S (OU 4/2 model).	78
3.8	Expected utility and CER versus γ (OU 1/2 model).	80
3.9	Optimal allocation versus θ_X and σ_X (OU 1/2 model).	80
4.1	Sum of exponential network (SEN).	90

4.2	Improving exponential polynomial.	91
4.3	S_t follows the 4/2 model with market price of risk $\lambda_S \sqrt{X_t}$, (a) shows the Expected utilities obtained with theoretical results and approximation methods versus investment horizon T , (b) shows the CERs versus investment horizon T given $\gamma = 2$	97
4.4	S_t follows a 4/2 model with stochastic jump, (a) shows the Expected utilities obtained with the approximation methods versus investment horizon T , (b) shows CERs versus investment horizon T given $\gamma = 2$	97
4.5	S_t follows the 4/2 model with market price of risk $\lambda_S(a\sqrt{X_t} + \frac{b}{\sqrt{X_t}})$, (a) shows the Expected utilities obtained with theoretical results and approximation methods versus investment horizon T , (b) shows the CERs versus investment horizon T given $\gamma = 2$	98
4.6	S_t follows the OU 4/2 model, (a) shows the Expected utilities obtained via approximation methods versus investment horizon T , (b) shows the CERs versus investment horizon T given $\gamma = 2$	99
5.1	Allocation on options versus strike price	117
5.2	Certainty equivalent rate (CER) versus strike price with different rebalancing frequencies	118
5.3	Allocation on straddle versus $\frac{K^{(i,j)}}{S_0^{(i,j)}}$	120
5.4	Straddle analysis	121
5.5	$\ \pi_t\ _1$ versus strike price (Basket option)	123
5.6	Derivatives selection $O_t^{(2,j_2)}$	124
5.7	Derivatives selection $O_t^{(2,j_2)}$ ($\rho = -0.4$)	132
5.8	Derivatives selection $O_t^{(2,j_2)}$ (exchange assets' parameter)	132
6.1	The $\ \pi_t\ _1$ versus moneyness: The Y-axis is the risk exposure of a portfolio containing different derivatives. The X-axis indicates the moneyness K/S_0 of calls, puts and straddles. The strangle is synthesized with an OTM put and an OTM call. Given moneyness of the OTM put indicated by the X-axis, the strike price of the OTM call is the one achieving minimum $\ \pi_t\ _1$ within the range $[S_0, 110\%S_0]$	143
6.2	Impact of the OTM put's moneyness on the strangle. Left vertical axis indicates the optimal moneyness of the OTM call within $[100\%S_0, 110\%S_0]$. Right vertical axis indicates the allocation on the stock and the strangle.	143
6.3	Sensitivity of strangle option price $O_t^{(C)}$ to instantaneous variance X_t versus time to maturity T_{op} . The legend indicates the moneyness of component put, and the call option is the one achieving minimum risk exposure. Note that there is no boundary for the strike price of the component call.	144
6.4	The $\ \pi_t\ _1$ for VIX products	146
6.5	Allocation on straddle versus γ	152

List of Tables

1.1	Notation (BGSS)	16
1.2	Notation (LSMC-S&D)	19
1.3	Notation (LSMC)	24
2.1	Notation	33
2.2	Parameter value for Merton's problem	51
2.3	Parameter value for VAR model	51
2.4	Parameter value for the SV case, after [34]	51
2.5	Parameter value for mean-reverting model, after [19]	51
2.6	Parameter value for the Heston model with stochastic interest rate, after [35]	52
2.7	Results for GBM	53
2.8	Results for VAR model	54
2.9	Results for stochastic volatility	55
2.10	Results for Heston model with different degree of polynomial	56
2.11	Error between numerical and theoretical allocation at mid point Heston Model	56
2.12	Results for mean-reverting case	57
2.13	Results for mean-reverting case with different degree of polynomial	58
2.14	Error between numerical and theoretical allocation at mid point Mean-reverting Model	58
3.1	Special cases of the hyperbolic absolute risk aversion (HARA) utility	65
3.2	Parameter value for geometric Brownian motion (GBM) 1/2 model.	68
3.3	Results for GBM 1/2 model with decreasing relative risk aversion (DRRA) investor.	69
3.4	Results for GBM 1/2 model with increasing relative risk aversion (IRRA) investor.	70
3.5	Parameter value for OU 4/2 model.	73
3.6	Results for OU 4/2 model with DRRA investor.	74
3.7	Results for OU 4/2 model with IRRA investor.	77
3.8	Parameter values for OU 1/2 model.	79
3.9	Notation and definitions	81
4.1	Notations for NNMC for NNMC is listed here.	93
4.2	Parameter values for 4/2 model.	102

4.3	Results for the 4/2 model with market price of risk $\lambda_S \sqrt{X_t}$. We report the optimal weights, expected utility, and CER obtained with theoretical result and with the approximation method for different levels of risk aversion γ . The standard deviation of estimated expected utility and CER from 100 runs is displayed in parentheses.	103
4.4	Results for the 4/2 model with stochastic jumps. We report the optimal weights, expected utility and CER obtained via the approximation methods for different levels of risk aversion γ . The standard deviation of estimated expected utility and CER from 100 runs is displayed in parentheses.	104
4.5	Results for the 4/2 model with market price of risk $\lambda_S(a_S \sqrt{X_t} + \frac{b_S}{\sqrt{X_t}})$. We report the estimation of optimal weights, expected utility and CER obtained via approximations given different levels of risk aversion γ . The standard deviation of estimated expected utility and CER from 100 runs is displayed in parentheses.	105
4.6	Parameter value for the OU 4/2 model.	106
4.7	Results for the OU 4/2 model. We report the estimation of optimal weights, expected utility and CER obtained via approximations for different levels of risk aversion γ . The standard deviation of estimated expected utility and CER from 100 runs is provided in parentheses.	107
5.1	Parameter Value	114
6.1	Notation and definitions	140
6.2	Parameter value for the Heston model.	142

Preface

In this thesis new, fast, and accurate numerical methods are developed to solve for asset allocation (and the associated value function) in dynamic portfolio problems. These methods are validated and widely tested for accuracy and speed on various models. The newly developed tools are used to extract insights about portfolio allocation in previously unsolvable cases. Five related but distinct projects are completed. These projects, each of which is its own stand alone paper are presented as chapters 2 through 6 in the thesis. The introductory chapter 1 provides the necessary preliminaries.

The first project, presented in chapter 2, proposes a new polynomial affine methodology to study portfolio allocation to various stocks (or indexes) and one money market fund where the investor maximizes its expected constant relative risk aversion (CRRA) utility. This method is termed PAMC, which stands for polynomial affine method for CRRA. The methodology is applied on four different widely used models: a geometric Brownian motion (GBM), a Heston $1/2$ stochastic volatility (SV), an exponential Ornstein Uhlenbeck (OU) model (the first three models allow comparison with the appropriate closed form solution), and a vector autoregressive (VAR) model. The optimal allocation vector and the value function obtained with PAMC are compared to closed form solutions and/or the solutions arising from other existing numerical methods. These results demonstrate the superior accuracy and efficiency of the PAMC. Furthermore, we exemplify the application of PAMC on an unsolvable model, i.e. the Heston model with stochastic interest rate. In particular, we learn about the impact of the various correlation on optimal portfolio decisions.

The second project, presented in chapter 3, extends the work of chapter 2 to the wider Hyperbolic Absolute Risk Aversion (HARA) utility class for a somehow narrower family of multidimensional models. As such this method is denoted by PAMH. Given the flexibility of the HARA structure, the methodology is applicable not only to expected utility theory (EUT) but also to mean variance theory (MVT). The accuracy and efficiency of the approximation is examined in a comparison to known closed-form solutions for the one dimensional Heston model, and a high dimensional stochastic covariance model. Moreover, the PAMH is applied to a setting in which the risky asset is a commodity modelled by the OU $4/2$ model which captures two stylized facts of financial data: mean reverting drift and SV. This is the first analysis of such a new model leading to interesting conclusions summarized next.

In this chapter, the optimal strategies for both a decreasing relative risk aversion (EUT) investor and an increasing relative risk aversion (MVT) investor are presented. The former incorporates a minimum capital guaranteed, while the latter delivers what is known as a pre-commitment solution due to the time-inconsistent nature of the problem. Sensitivity analysis of the optimal strategies with respect to key parameters of the commodity model and risk aversion are conducted. We also studied the certainty equivalent return (CER) loss in case of the OU $1/2$ model given two sub-optimal strategies: a myopic strategy (Merton's solution) ignoring future movements of state variables; and a strategy adopted by investors who ignores the SV feature of asset dynamics. We conclude that, for a particular market-calibrated set of parameters, a myopic strategy is preferable to a strategy ignoring SV.

The third project, described in chapter 4, combines neural network and PAMC, namely NNMC. Two customized architectures of the neural network are introduced, both nesting the polynomial choice of chapter 2. The methodologies are applied on four settings: a $4/2$ SV

model with two types of market price of risk, a 4/2 model with jumps, and an OU 4/2 model. The results of these, both in computing the value surface and in computing the asset allocations, are demonstrated in a one money market, one risky asset CRRA setting. Even through the NNMC fails to outperform and is not as efficient as PAMC, it demonstrates a way to tackle more advanced models along the lines of Markov switching, Lévy processes, and fractional Brownian processes.

The previous chapters work with incomplete market solutions, e.g. no additional asset hedging the SV risk. Projects four and five address the complete market problem, first from a theoretical perspective (chapter 5), and then mostly numerically in chapter 6. The portfolios here can use derivatives on the underlying to ensure completion, therefore infinitely many choices of portfolio assets become available. In particular, an additional optimization criterion (i.e. risk exposure minimization) inspired by regulatory constraints is proposed in chapter 5. In this chapter, for simplicity and to gain a better understanding of the problematic, we work in the context of the Black-Scholes-Merton setting. Here, we prove the minimum number of derivatives needed to simultaneously maximize expected utility and minimize risk exposure for investors. To help investors make a practical derivatives selection, a comparison is conducted within one-asset options (e.g. American, European and Asian puts and calls), synthetic straddle options are studied as well. In addition, the superiority of multi-asset options (i.e. basket options) over one-asset options in many realistic situations is confirmed.

Finally, the last project of the thesis extends the work of chapter 5 to a generalized diffusion model family. Chapter 6 focuses on two issues in derivatives-based portfolio choice problem: the computation of the optimal allocation on derivatives, and the selection of derivatives for risk exposure minimization purpose. Advanced models with various stylized facts often endanger the mathematical tractability of optimal allocation of common assets, let alone derivatives with complex structures. To overcome this problem, we propose two variants of PAMC, namely PAMC-direct and PAMC-indirect. The PAMC-direct is a straightforward application of PAMC, where derivatives are taken as assets whose dynamics is explicitly known. In contrast, the PAMC-indirect first computes the optimal strategy for a pure factor portfolio; and the optimal derivatives strategy is obtained with financial replication techniques. The accuracy and efficiency of the PAMC-direct and the PAMC-indirect are compared. The selection of derivatives is explored within the Heston SV model, where we consider 4 popular products on stocks: call/put options, synthetic straddle and strangle options. Straddle and strangle options are preferable for their intrinsic exposure to the volatility risk. Furthermore, we studied VIX products, such as VIX options, thereby describing interesting conclusions in the chapter.

Chapter 1

Introduction

1.1 Motivation and background

Portfolio construction is one of the most important segments in the business of asset management and investment companies. Tracing back to Markowitz 1952, [73] was the first to analyze a portfolio in a quantitative way, where the author minimized the variance of terminal wealth given a specific expected return. His work laid the foundations for the development of portfolio analysis in both academia and industry. However, the result was based on the assumption of single period investment, hence a major criticism of Markowitz's work is that it only allows investors to allocate their wealth myopically and fails to account for the opportunity of rebalancing when the market state fluctuates.

Seventeen years later, Samuelson, in [83] first formulated and solved a multi-period portfolio selection problem corresponding to lifetime planning of consumption and investment decisions. His work provided instructions for an investor who has constant relative risk aversion through his whole life. [46] presented a discrete-time model for an investor's economic decision under risks and obtained closed-form optimal strategies with constant relative risk aversion (CRRA) and constant absolute risk aversion (CARA) utilities. Dynamic multi-period portfolio analysis is certainly an important extension of Markowitz's work, it allows investors to rebalance their portfolio at pre-determined dates. However, scholars soon shifted their attention to the continuous-time portfolio analysis because of its more flexible and practical setting that allows investors to react to new information immediately while producing closed-form solutions.

The seminal work of Merton [76] initiated research on continuous-time portfolio optimization. The author obtained optimal allocation and consumption policy with a dynamic programming technique and the use of Hamilton-Jacobi-Bellman equations (HJB), assuming the stock price follows a geometric Brownian motion (GBM). Compared to Markowitz's work and those in multi-period analysis, his portfolio construction process assumed a more realistic rebalancing policy, which has now become an indispensable component in investment management. In the late 80s, [54] and [25] pioneered the martingale method to solve portfolio optimization problems via a combination of static optimization and financial replication. Both, dynamic programming, and martingale methods are mainly applied when the investor's preference is represented by a utility function (i.e. expected utility theory [EUT]), although it can also be

used, with some limitations, in the context of mean-variance theory (MVT) considered in [73]. EUT and MVT reflect different investment objectives from a financial viewpoint. While both approaches reward return and penalize volatility, EUT does this through utility function which provides convex “enjoyment” of wealth, while MVT just takes return good and volatility bad as axiomatic. Following [43], it can be shown that the EUT problem can approximately be described as a maximization problem with respect to a mean-variance criterion on the portfolio return. This shows a strong mathematical relation between the theories. Debate continues about the better framework, EUT or MVT. The reality is that EUT and MVT have become the two major branches of portfolio optimization analysis.

Financial markets are constantly evolving dynamical systems, a variety of financial assets and indices appear which display distinct intrinsic characteristic in their time series data. Consequently, detecting and modeling stylized facts of financial time series is an active area of research. For example, the Vasicek model (see [86]) and the Hull–White model (see [51]) were proposed, as improvements over the GBM, to describe the evolution of interest rates, which play an essential role in bond and interest rate derivatives valuation. In equity markets, the Heston’s $1/2$ model was introduced in [48] to fit popular market indexes like S&P500 incorporating stochastic volatility, now fully accepted as confirmed by the existence of volatility indexes like VIX. The OU $4/2$ model (see [37]), developed in 2020 is, at the time of writing, the latest substantial achievement in commodity price modelling, this incorporates both mean-reverting price patterns and an advanced stochastic volatility structured on a single model. Many portfolio researchers, inspired by the rise of advanced financial model, seek the optimal investment policy for investor focusing on these specific asset classes.

Within EUT, dynamic portfolio choice for CRRA type investors has been widely studied with several closed-form results in the literature, which we list next for models with only one extra state variable. [59] solved the associated HJB equation and obtained the optimal strategy when the stock price follows the Heston’s $1/2$ stochastic volatility (SV) model. [19] considered the optimal investment problem for an insurer, who invests in assets modelled by an exponential Ornstein–Uhlenbeck (OU) process, subject to random payments of insurance claims. [38] constructed a portfolio across the equity and fixed-income markets, their optimal allocation provides intuition about how to hedge against interest rate risk. [13] hedged against both stochastic volatilities and correlations risk solving the optimal allocation problem for incomplete markets. [34] derived optimal portfolio decision in complete and incomplete markets for a multivariate setting where the principal components have stochastic eigenvalues, generalizing the multi-factor model of [22]. The optimal portfolio problem given the GBM $4/2$ model with certain types of market price of risk (MPR) was studied in [18]. The results have been extended to Hyperbolic absolute risk aversion (HARA) class of utility functions that are popular due to its flexibility to capture risk aversion preferences. For a risk-averse investor with a HARA utility, the explicit solution of optimal strategy with stochastic market price of risk or SV is presented in [61]. [33] considered a regime switching bond-stock market, obtaining the optimal strategy even with multi stochastic factors.

There has been also plenty of progress in the study of dynamic portfolio choice within the framework of MVT. This is in spite of the difficulty of applying classical dynamic programming techniques coming from the presence of a variance term in the objective function with time-inconsistency implications. A pre-commitment strategy, proposed in [89], was obtained by solving a class of auxiliary stochastic linear-quadratic (LQ) problems. [21] followed

the method suggested in [5], and derived a time-consistent strategy when the stock price is modelled by a exponential OU process. All these results confirm the interest and promote the application of portfolio theory in real-world investment settings. But obtaining analytical portfolio solutions is getting harder by the decade.

Financial markets are growing in terms of volume and complexity at a rapid speed, hence any adequate strategy for investors must rely on emerging models reflecting new stylized facts of these evolving markets. However, the complexity of advanced models jeopardizes the solvability of optimal portfolio problems. This generates more interest on approximation methods for dynamic portfolio analysis. Most numerical methods for dynamic portfolio focus on EUT, incorporating ideas from the martingale method or dynamic programming technique in the construction of the methodology. The explicit representation of the optimal terminal wealth obtained via the martingale method was utilized in [26] to estimate the optimal allocation through Monte Carlo simulation. [30] achieved better accuracy with the application of Malliavin derivatives. In addition, avoiding the limitations of a complete market setting, the seminal paper [10] extended the least-squares Monte Carlo (LSMC) method (see [72]) to the context of dynamic portfolio optimization. Their method, namely BGSS, recursively estimates the value function, which follows the dynamic programming principle. [39] and [41] targeted the optimal allocation approximation and proposed to expand the value function based on a nonlinear decomposition. [24], enlightened by the stochastic grid bundling method (SGBM) for conditional expectation estimation introduced in [53], further enhanced the accuracy of the BGSS.

This thesis studies five topics related to dynamic portfolio choice. We first introduce related background information for this thesis in chapter 1. We provide a brief overview on the two fundamental methodologies: the dynamic programming approach and the martingale method, and demonstrate the pre-commitment strategy for dynamic mean-variance portfolio. Next, several representative numerical methods for dynamic portfolio are presented with the intention of providing a wide overview of relevant, existing numerical approaches. We also concisely mention the architecture of artificial neural network and a learning algorithm: backpropagation. A LSMC method for American option valuation is also described in details.

In chapter 2, we introduce the polynomial affine method for CRRA utilities (PAMC), which offers a new competitive numerical methodology to approximate the optimal strategy and the value function. The PAMC, inspired by the quadratic-affine family of portfolio solutions described in the celebrated paper [70], estimates the value function via an exponential polynomial function. The PAMC is divided into two branches: the value function iteration (VFI) method and the portfolio weight iteration (PWI) method, distinguished by the approach to obtain the value function. The implementation of PAMC-VFI, PAMC-PWI, SGBM and BGSS on each of Merton's model, Heston's model, the exponential OU model, and the (discrete-time) vector autoregressive (VAR) model are conducted for comparison purposes. The efficiency and accuracy of PAMC are demonstrated by considering the several metrics: computational time, relative error of the optimal allocation and of the expected utility at initial time, and mean L_2 error of the optimal allocation at the mid point of the investment horizon.

Chapter 3 constructs optimal portfolios in a commodity market, where the asset's price follows the OU 4/2 model. We first extend the PAMC to the wider HARA utility family and propose the so-called polynomial affine method for HARA (PAMH). The accuracy of the PAMH is examined on a variety of models for which closed-form solutions are known, some of which are highly multivariate. The PAMH produces optimal strategies in the contexts of EUT, this is

for decreasing relative risk aversion (DRRA), as well as in the framework of MVT, which can be interpreted as an increasing relative risk aversion (IRRA). We conduct the sensitivity analysis of optimal strategies for both DRRA and IRRA with respect to volatility group parameters. The efficient frontier of dynamic mean-variance portfolio is also reported. Moreover, certainty equivalent return (CER) losses from sub-optimal strategies mostly based on ignoring key parameters, are studied.

Most numerical methods for portfolio optimization, including PAMC and PAMH, approximate the value function with a classical regression model. An alternative way is using a neural network, such functions have recently displayed their superiority in many real world applications. In chapter 4, we replace the regression model with a deep learning model within the PAMC methodology seeking better portfolio performance. Two network architectures aimed at fitting the value function are presented in details. Comparisons between portfolio allocations obtained with the original PAMC and the new PAMC incorporating the neural networks, are conducted for various advanced stochastic models.

In chapter 5, we reveal the optimal derivatives-based portfolio strategy for maximizing expected utility investors. Given a set of derivatives, there are infinitely many strategies available, all producing the same maximum of the value function in a frictionless market. We take advantage of this to further propose an additional criterion (i.e. risk exposure minimization) for a practical derivative selection. The new criterion help investors meet potential regulatory constraints in terms of portfolio total exposure to risky assets, hence protecting the investor's capital from risks. We determine the minimum number of derivatives needed to achieve both of investors' objectives, these are expected utility maximization and risk exposure minimization. We also investigate the selection of derivatives among three specific option classes: (i) American, European and Asian calls and puts; (ii) American, European and Asian synthetic straddles; and (iii) basket options. Furthermore, one-asset options and multi-asset options are compared in several realistic situations.

Chapter 6 extends the work in chapter 5 to a generalized diffusion model. The lack of analytical solutions for the optimal strategy lays obstacles for the implementation of derivatives-based portfolio, this generates the interest on two variants of the PAMC: the PAMC-direct which is a straightforward application of PAMC; and the PAMC-indirect which bridges derivatives-based portfolio strategies and pure factor strategies. A numerical study demonstrates the superiority of the PAMC-indirect in terms of accuracy and computational efficiency. In addition, we explore derivatives selection in the context of the Heston SV model. We study two major derivatives classes for hedging the volatility risk: (i) options on the stock (e.g. call, put, straddle and strangle options) and (ii) VIX products, e.g. options on the VIX. Advantages and disadvantages of each derivative class are illustrated.

1.1.1 Contributions

In this section, we summarize the innovations and contributions in each chapters.

Chapter 2

- We introduce two methodologies (PAMC-VFI and PAMC-PWI) based on polynomial-Affine structures to approximate the optimal solution of a portfolio investment problem.

- We demonstrate, with the help of three popular continuous-time and one discrete-time model, the accuracy and computational efficiency of PAMC in capturing both value functions and optimal strategies. For this we rely on the annualized certainty equivalent rate, the relative errors at the initial time for value function and optimal strategies, and the mean $L2$ error for optimal strategies at mid point of investment horizon.
- We demonstrate that PAMC-VFI could be three times faster, while producing 90% more accurate results than other approaches, in capturing optimal strategies. The efficiency could be even more significant for higher levels of precision.
- The PAMC is applied to an important unsolvable case, i.e. the Heston model with a stochastic interest rate. We show that PAMC delivers the highest CER, while the optimal strategy and portfolio performance are affected more by the correlation between stock price and interest rate than by the correlation between SV and interest rate.

Chapter 3

- A numerical method (PAMH) is presented to approximate optimal allocation and value function for a risk-averse investor in a general HARA setting, hence embedding both EUT (i.e. decreasing relative risk aversion [DRRA]) and MVT (i.e. increasing relative risk aversion [IRRA]) cases. The method relies on the wealth and state variables separability of the value function to fit the value function via an exponential polynomial. With this we generalize the family of exponential quadratic solutions (see [70]).
- A high level of accuracy of the methodology and low computational time on a standard PC of the PAMH are examined in a comparison to known closed-form solutions for a one dimensional ($n = 1$) geometric Brownian motion with a CIR stochastic volatility model (i.e. GBM 1/2 or Heston model), and a high dimensional (up to $n = 35$) stochastic covariance model.
- The optimal strategy, optimal wealth and value function are numerically studied for an OU 4/2 model in the context of EUT (decreasing RRA). Sensitivities to risk aversion level, minimum capital guarantee and 4/2 parameters are presented. The analysis confirms substantial changes in allocations due to relatively small changes in these parameters.
- An efficient frontier of pre-commitment strategies for dynamic MVT (increasing RRA investor) is obtained. A sensitivity to 4/2 parameters and multipliers is presented, confirming the findings of the DRRA case.
- The suboptimality of myopic strategies in terms of the certainty equivalent rate (CER), for OU 4/2 models, is corroborated. A similar analysis of CER performance in the popular OU 1/2 model confirms low CERs for investors ignoring SV, to the point that a myopic strategy may be preferable to a strategy that neglects SV.

Chapter 4

- An approximation method, namely NNMC, for optimal continuous-time portfolio strategies based on a combination of neural networks and Monte Carlo is proposed.
- We design two architectures enriching an embedded quadratic-affine structure to fit the portfolio value function, i.e. sum of exponential network (NNMC-SEN) and improving exponential network (NNMC-IEN), and we explore three types of activation functions.
- The NNMC is applied on four settings: a 4/2 SV model with two types of market price of risk, a 4/2 model with jumps, and an Ornstein–Uhlenbeck 4/2 model. We report the accuracy of the various settings in terms of optimal strategy, portfolio performance and computational efficiency, highlighting the potential of NNMC to tackle complex dynamic models.

Chapter 5

- We study a derivatives-based portfolio choice problem. In addition to the expected utility maximization, we explore an additional optimization criterion, namely risk exposure minimization, which is motivated by investor needs for practical derivatives selection.
- Given two one-factor (e.g. GBM) assets, we illustrate that investors need only two derivatives for the expected utility to be maximized and risk exposure to be minimized simultaneously.
- Comparison among simple one-asset options (e.g. American, European and Asian calls and puts) reveal that a deep out-of-the-money Asian option is the preferable derivative choice. Furthermore, we illustrate that a synthetic straddle is practically useful because its optimal strategies refrain from boundary optimality, which leads to a product with acceptable liquidity for investor.
- We investigate the benefit of multi-asset derivatives, it's shown that a basket option could be a better choice than one-asset option in many realistic situations.

Chapter 6

- The multitude of financial derivatives available in the market offers investors non-unique optimal choice in terms of EUT maximization. Hence, we extend the additional optimization criterion propose [36], namely risk exposure minimization, from the family of GBM to SV models. This aids investors with practical derivative selection in a popular modelling setting of stock markets.
- A numerical method (i.e. PAMC-indirect) is proposed to approximate the optimal allocation for a CRRA investor investing in the derivatives market. The superior accuracy and efficiency of the methodology are verified on the Heston model.
- Targeting equity and volatility risk, we first consider the optimal choice among equity options (e.g. calls, puts, straddles and strangles). We demonstrate that strangles are the best options for minimizing risk exposure in many practical situations.

- We also investigate the usage of financial derivatives on the VIX as a means of completing the market, and we conclude that investors would prefer VIX options to equity strangle when only long-term maturity options are available.

In summary, the thesis presents a competitive methodology for dynamic portfolio choice. The method can be applied to various types of investors (e.g. HARA, CRRA and constant absolute risk aversion [CARA]). The analysis presented here allows the investor to freely alter the dynamic model for asset prices according to the asset's features and market condition. The thesis applies this methodology to answer many practical questions. The methodology is developed and expounded in Chapter 2 for CRRA investors. Chapter 3, targeting commodity market investment, constructs the optimal portfolio for risky assets which follow the OU 4/2 model in a context of HARA utilities. Chapter 4 describes an attempt to enhance the methodology with a deep learning model; two architectures estimating the portfolio value function are proposed. Chapter 5 builds a new criterion for derivatives-based portfolio selection aiming at market completion. Finally, two variants of the methodology for derivatives-based portfolio are proposed in chapter 6, the optimal derivative choice for hedging volatility risk is studied.

1.1.2 Connection among chapters

The thesis will focus on approximation methods for dynamic portfolio choice, as well as the applications of these methods. The connection among the core chapters (i.e. chapter 2-6) and the internal logic of this thesis are provided in this section.

Chapter 2 is the foundation of the whole thesis; subsequent chapters are constructed on its foundation. The main objective of this chapter is the introduction of the new PAMC approximation method, which targets a high-frequency re-balancing/continuous-time dynamic portfolio. The algorithm is described in detail to help readers better understand the PAMC. Furthermore, we validate the robustness of the PAMC by the implementation of several popular models. PAMC exhibits superior accuracy and efficiency in comparison with other existing methods. However, there are two potential limitations in the PAMC. First, the PAMC is only applicable to EUT when the investor's risk preference is modelled by a CRRA utility. The PAMC also requires the dynamics of assets' prices to follow explicit structures within Ito's processes as explained in the chapter.

Chapter 3 illustrates both an extension and an application of chapter 2. We first extend the PAMC to a wider HARA utility family, proposing the PAMH. This extension addresses the first limitation of the PAMC, the PAMH is not only applied to EUT with common utilities (e.g. HARA, CRRA and CARA), but it can also be used to find the pre-commitment strategy for a dynamic mean-variance portfolio. Note that, even though PAMH and PAMC have similar algorithms, PAMH adopts a new structure of the value function to adapt the flexibility of HARA utility in capturing the risk preference. Moreover, the PAMH is applied to an important and unsolvable model (i.e. OU 4/2 model). Optimal dynamic portfolios within both EUT and MVT are studied, and we conduct a sensitivity analysis to investigate the impact of key parameters on portfolio allocation and a sub-optimal analysis to quantify the loss from sub-optimal strategies that might be used by investors.

Chapter 4 enhances the accuracy of the PAMC. Both PAMC and PAMH approximate the portfolio value function with a polynomial regression model. Even though the Stone–Weierstrass

theorem guarantees that any continuous function in a compact support can be approximated arbitrarily well in a polynomial class, estimating a non-polynomial function with a polynomial regression may still lead to significant errors. We, therefore, investigate if the neural network is a better choice in value function approximation, and we propose two architectures for this problem.

The last two chapters consider investment in derivatives markets. The dynamics of derivatives price can be written explicitly only on a few occasions, therefore this problem emphasizes the second limitation of the PAMC. The framework for the derivatives-based portfolio is first constructed in chapter 5. We introduce an additional portfolio criterion that helps investors select the best financial derivatives to be included in the portfolio. The derivatives-based portfolio framework minimizes the unexpected loss for investors while keeping the best portfolio performance. Furthermore, in the context of GBM, the derivative selection within the subset of one-asset options (e.g. American, European and Asian calls, puts and straddles) and within the subset of multi-asset options (e.g. basket options) are studied.

Chapter 6 integrates the achievements in chapter 2 and chapter 5 by extending the derivatives-based portfolio to a generalized diffusion model family. Inspired by the PAMC, a new approximation method, termed PAMC-indirect, is proposed to obtain the optimal strategy for derivatives-based portfolio. We specifically considered a market characterized by volatility risk and investigate derivatives selection among four popular equity options. Finally, the comparison between equity options and VIX options is also illustrated.

1.2 Stochastic optimal control for dynamic asset allocation

The application of dynamic portfolio choice was pioneered by [76], which extended the dynamic programming technique to the context of continuous-time portfolio optimization within EUT. [54] and [25] considered the same problem, while they focused on the replication of the static optimum, and proposed the so-called martingale method. In the following years, these two methods inspired many papers and books in the field of analytical and numerical portfolio optimization. In this section, we first convey the ideas of these two methods, and summarize their basic procedures. Furthermore, as optimal strategy for MVT is ingeniously related to the optimal strategy within EUT (see [89]), we illustrate the connection between these two optimal strategies in Section 1.2.3. This lays the foundation for solving dynamic portfolio problems within the MVT in later Chapters. The investor's problem used to implement the dynamic programming technique and the martingale method is described as follows:

We assume the stochastic processes describing the financial market is defined on a complete probability space $(\Omega, \mathcal{F}, \mathbb{P})$ with a right-continuous filtration $\{\mathcal{F}_t\}_{t \in [0, T]}$. A frictionless market consists of a money account (S_t^0) and N risky assets $S_t = [S_t^1, S_t^2, \dots, S_t^N]^T$, where investors can freely trade assets at prices without market impact and transaction costs. Moreover, the dynamics of assets' price are also determined by a M dimensional state variable

$$H_t = [H_t^1, H_t^2, \dots, H_t^M]^T:$$

$$\begin{cases} \frac{dS_t^0}{S_t^0} = r(H_t)dt \\ dS_t = \text{diag}(S_t)(\mu(t, H_t)dt + \Sigma(t, H_t)dB_t) \\ \quad = \text{diag}(S_t)(r(X_t) + \Sigma(t, H_t)\lambda(t, H_t)dt + \Sigma(t, H_t)dB_t) \\ dH_t = \mu^H(H_t)dt + \Sigma^H(H_t)dB_t^H \\ \langle dB_t, dB_t^H \rangle = \rho dt, \end{cases} \quad (1.1)$$

where $B_t = [B_t^1, B_t^2, \dots, B_t^N]^T$ and $B_t^H = [B_t^{H,1}, B_t^{H,2}, \dots, B_t^{H,M}]^T$ are N and M dimensional Brownian motions with independent components, $r(H_t)$ is the risk-free rate, $\mu(t, H_t)$ and $\Sigma(t, H_t)$ are the drift and volatility matrix of the price process, $\lambda(t, H_t)$ is the market price of risk. We denote the drift and volatility of the state variable H_t by $\mu^H(H_t)$ and $\Sigma^H(H_t)$. Elements in the correlation matrix ρ are between $[-1, 1]$ (i.e. $|\rho^{i,j}| \leq 1$) and ρ is positive definite. With a specific trading strategy π_t , the corresponding wealth process W_t is given by

$$\frac{dW_t}{W_t} = (r(X_t) + \pi_t^T(\Sigma(t, H_t))\lambda(t, H_t))dt + \pi_t^T \Sigma(t, H_t)dB_t, \quad (1.2)$$

We define a utility function U to represent the investor's degree of satisfaction associated with the terminal wealth W_T .

Definition 1.2.1 (Utility function) *A continuously differentiable and strictly concave function $U : (0, \infty) \rightarrow \mathbb{R}$, which satisfies the conditions*

$$U'(0) = \lim_{w \downarrow 0} U'(w) = \infty \quad U'(\infty) = \lim_{w \uparrow \infty} U'(w) = 0 \quad (1.3)$$

is called a utility function.

An investor is assumed to be able to freely trade at any time and wants to derive an investment strategy π_t that will maximize the expected utility from terminal wealth W_T . The investor's problem at time $t \in [0, T]$ can be written as,

$$V(t, W, H) = \max_{\pi_{\{s \geq t\}}} \mathbb{E}^{\mathbb{P}}(U(W_T) | \mathcal{F}_t), \quad (1.4)$$

where $V(t, W, H)$ is the value function at time t . Both the martingale method and the dynamic programming technique provide methodologies for obtaining the optimal investment strategy π_t^* and the value function $V(t, W, H)$ for the investor.

1.2.1 Martingale method

The martingale method was introduced in [54] and [25] in the late 80's. The method obtains the optimal terminal wealth through a static optimization. If markets are complete (i.e. ρ is the identity matrix), there is a replicating strategy for the optimal terminal wealth.

The risk-neutral probability measure \mathbb{Q} is defined by the Radon-Nikodym derivative

$$\frac{d\mathbb{Q}}{d\mathbb{P}} = \exp\left(-0.5 \int_0^t \|\lambda(s, H_s)\|^2 ds - \int_0^t \lambda(s, H_s)^T dB_s\right) = \xi_t. \quad (1.5)$$

The expectation of any stochastic payoff X_T under measure \mathbb{Q} and \mathbb{P} at time t is connected by

$$\mathbb{E}_t^{\mathbb{Q}}(X_T) = \mathbb{E}_t^{\mathbb{P}}\left(\frac{\xi_T}{\xi_t} X_T\right). \quad (1.6)$$

The martingale method is based on two important theorems. The first theorem states a constraint on the portfolio terminal wealth.

Theorem 1.2.1 *If π_t is a feasible strategy, then*

$$\mathbb{E}_0^{\mathbb{Q}}\left(\exp\left(\int_0^T -r(H_s)ds\right) W_T\right) = \mathbb{E}_0^{\mathbb{P}}\left(\exp\left(\int_0^T -r(H_s)ds\right) \xi_T W_T\right) \leq W_0, \quad (1.7)$$

where W_T is the terminal wealth induced by the strategy π_t .

Proof [55] Theorem 1.5.6.

Theorem 1.2.1 indicates that the investor's problem is to maximize the expected utility of terminal wealth, whose expectation is less than W_0 under the risk-neutral measure.

$$\begin{aligned} & \max_{\pi_{\{s \geq 0\}}} \mathbb{E}_0^{\mathbb{P}}(U(W_T)) \\ \text{s.t. } & \mathbb{E}_0^{\mathbb{P}}\left(\exp\left(\int_0^T -r(H_s)ds\right) \xi_T W_T\right) = W_0. \end{aligned} \quad (1.8)$$

The Lagrangian for constrained optimization problem (1.8) is given by

$$\mathcal{L} = \mathbb{E}_0^{\mathbb{P}}(U(W_T)) - y \left(\mathbb{E}_0^{\mathbb{P}}\left(\exp\left(\int_0^T -r(H_s)ds\right) \xi_T W_T\right) - W_0 \right), \quad (1.9)$$

where y is a Lagrange multiplier. Let I denote the inverse of the utility's first derivative $(U')^{-1}$. Then, the candidate optimal terminal wealth has the representation

$$W_T^* = I\left(y \exp\left(\int_0^T -r(H_s)ds\right) \xi_T\right), \quad (1.10)$$

where y is chosen such that Equation (1.7) holds for W_T^* . The next theorem illustrates that the optimal terminal wealth in the static problem is feasible and optimal in the dynamic problem.

Theorem 1.2.2 *Under the optimal strategy, the optimal terminal wealth is given in (1.10). And the wealth process is given by*

$$W_t^* = \mathbb{E}_t^{\mathbb{Q}}\left(\exp\left(\int_t^T -r(H_s)ds\right) W_T^*\right). \quad (1.11)$$

Proof [55] Theorem 3.7.6.

Hence, if the strategy π_t^* is feasible and generates a terminal wealth of W_T^* , then it must be the optimal strategy. Next, we define the optimal wealth process W_t^* such that $\exp\left(\int_0^t -r(H_s)ds\right)\xi_t W_t^* = \mathbb{E}^{\mathbb{P}}\left(\exp\left(\int_0^T -r(H_s)ds\right)\xi_T W_T^*\right)$. Due to the martingale representation theorem, there is a process ϕ_t such that

$$d \exp\left(\int_0^t -r(H_s)ds\right)\xi_t W_t^* = \phi_t dB_t. \quad (1.12)$$

Consider a portfolio wealth process W_t generated by a strategy π_t ,

$$\frac{d \exp\left(\int_0^t -r(H_s)ds\right)\xi_t W_t}{\exp\left(\int_0^t -r(H_s)ds\right)\xi_t W_t} = (\pi_t^T \Sigma_t(t, H_t) - \lambda^T(t, H_t))dB_t. \quad (1.13)$$

Apparently, when π_t satisfies

$$\pi_t = (\Sigma_t(t, H_t)^T)^{-1} \left(\frac{\phi_t^T}{\exp\left(\int_t^T -r(H_s)ds\right)\xi_t W_t} + \lambda(t, H_t) \right), \quad (1.14)$$

W_t has the same dynamic as W_t^* , which results in $W_T = W_T^*$.

Furthermore, the value function is rewritten by

$$V(t, W, H) = \mathbb{E}^{\mathbb{P}}(U(W_T^*)|\mathcal{F}_t). \quad (1.15)$$

Finally, we summarize the procedure for finding optimal strategies and value function via the martingale method as follows:

1. Compute the representation of the optimal terminal wealth $W_T^* = I(y \exp(\int_t^T -r(H_s)ds) \frac{\xi_T}{\xi_t})$.
2. Obtain the Lagrange multiplier y such that $\mathbb{E}_0^{\mathbb{Q}}(W_T^*) = W_0$.
3. Solve the $\exp\left(\int_0^t -r(H_s)ds\right)\xi_t W_t^*$ in closed form and find the process ϕ_t with Ito's lemma.
4. Calculate the optimal strategy with Equation (1.14) and the value function with (1.15).

1.2.2 Dynamic programming approach

The dynamic programming technique was first applied to a continuous-time optimal consumption/investment problem in [76] and [78]. It relies on the Bellman principle and the explicit solution for the optimal strategy and value function are found by solving an associated Hamilton-Jacobi-Bellman (HJB) equation. Unlike the martingale method, the dynamic programming technique is applicable even if the financial market is incomplete. However, the HJB equation is a non-linear, high-order partial differential equation, which is not usually solvable.

We first consider a discrete-time multi-period portfolio problem. According to the Bellman principle, the value function at time t can be expressed as:

$$V(t, W_t, H_t) = \sup_{\pi_t} \mathbb{E}(V(t + \Delta t, W_t + \Delta t, H_t + \Delta t)). \quad (1.16)$$

We move the $V(t, W_t, H_t)$ to the right hand side, and divide both sides by Δt . Then,

$$0 = \sup_{\pi_t} \frac{V(t + \Delta t, W_t + \Delta t, H_t + \Delta t) - V(t, W_t, H_t)}{\Delta t}. \quad (1.17)$$

As $\Delta t \rightarrow 0$, investors rebalance their allocation continuously. Moreover,

$$\lim_{\Delta t \rightarrow 0} \frac{V(t + \Delta t, W_t + \Delta t, H_t + \Delta t) - V(t, W_t, H_t)}{\Delta t} = \frac{dV(t, W_t, H_t)}{dt}. \quad (1.18)$$

The numerator $dV(t, W_t, H_t)$ is obtained by Ito's lemma. Therefore, Equation (1.16) in the continuous-time setting converges to the HJB equation, i.e.

$$\begin{aligned} 0 = \sup_{\pi_t} & \left\{ V_t(t, W_t, H_t) + V_{W_t}(t, W_t, H_t)W_t(r_t(H_t) + \pi_t^T \Sigma \lambda) \right. \\ & + (\mu^H)^T V_{H_t}(t, W_t, H_t) + \frac{1}{2} V_{W_t W_t}(t, W_t, H_t) W_t^2 \pi_t^T \Sigma \Sigma^T \pi_t \\ & \left. + W_t \pi_t^T \Sigma \rho(\Sigma^H)^T V_{H_t W_t}(t, W_t, H_t) + \frac{1}{2} Tr((\Sigma^H)^T \Sigma^H V_{H_t H_t}(t, W_t, H_t)) \right\}, \end{aligned} \quad (1.19)$$

where r_t , Σ , λ , μ^H , Σ^H are the abbreviations of $r_t(H_t)$, $\Sigma(t, H_t)$, $\lambda(t, H_t)$, $\mu^H(H_t)$ and $\Sigma^H(H_t)$ respectively. Note that Equation (1.19) is a quadratic function of the allocation π_t . Assuming $V(t, W, H)$ is concave with respect to W , the optimal allocation is given by

$$\pi_t^* = -(\Sigma \Sigma^T)^{-1} \frac{V_{W_t}(t, W_t, H_t) \Sigma \lambda + \Sigma \rho(\Sigma^H)^T V_{H_t W_t}(t, W_t, H_t)}{V_{W_t W_t}(t + dt, W_t, H_t) W_t}. \quad (1.20)$$

We substitute (1.20) into (1.19), the value function therefore satisfies the partial differential equation (PDE)

$$\begin{aligned} 0 = & V_t + V_W(rW - ((\Sigma \Sigma^T)^{-1} \frac{V_W \Sigma \lambda + \Sigma \rho(\Sigma^H)^T V_{HW}}{V_{WW}})^T \Sigma \lambda) + (\mu^H)^T V_H \\ & + \frac{1}{2} V_{WW} ((\Sigma \Sigma^T)^{-1} \frac{V_W \Sigma \lambda + \Sigma \rho(\Sigma^H)^T V_{HW}}{V_{WW}})^T (V_W \Sigma \lambda + \Sigma \rho(\Sigma^H)^T V_{HW}) \\ & - ((\Sigma \Sigma^T)^{-1} \frac{V_W \Sigma \lambda + \Sigma \rho(\Sigma^H)^T V_{HW}}{V_{WW}})^T \Sigma \rho(\Sigma^H)^T V_{HW} + \frac{1}{2} Tr((\Sigma^H)^T \Sigma^H V_{HH}). \end{aligned} \quad (1.21)$$

With the terminal condition: $V(T, W, H) = U(W)$. Finally, we summarize the steps for finding optimal strategies and value function via the dynamic programming technique as follows:

1. Write the HJB equation.
2. Assume the value function V is concave w.r.t the wealth, and obtain the optimal strategy π_t^* (i.e. a the function of the value function's derivatives).
3. Substitute π_t^* back into the HJB equation, and derive the PDE for the value function V .
4. Find the explicit solution for the value function V as well as the optimal strategy π_t^* .
5. Check all necessary conditions.

1.2.3 Pre-commitment strategy within MVT

Both the martingale method and the dynamic programming technique are applicable within EUT (i.e. the investor's preference is represented by a utility function), which is widely used in economic studies. In contrast, the framework proposed in [73] (i.e. MVT) measures the investment risk with the variance of the portfolio terminal wealth, and investors aim at maximizing the expected portfolio terminal wealth given a specific upper bound B for the variance

$$\begin{aligned} & \max_{\pi_{(s \geq t)}} \mathbb{E}(W_T | \mathcal{F}_t) \\ & s.t. \quad \text{Var}(W_T | \mathcal{F}_t) \leq B. \end{aligned} \quad (1.22)$$

Equivalently,

$$V(t, W_t, H_t) = \max_{\pi_{(s \geq t)}} \mathbb{E}(W_T | \mathcal{F}_t) - y(\text{Var}(W_T | \mathcal{F}_t) - B), \quad (1.23)$$

where $y > 0$ is a Lagrange multiplier. [89] demonstrated that problem (1.23) can be embedded into a class of auxiliary stochastic linear-quadratic (LQ) problems that can be solved analytically.

Theorem 1.2.3 *If $\pi_{s \geq t}^*$ is the optimal strategy for problem (1.23), $\pi_{s \geq t}^*$ is the optimal strategy for*

$$\max_{\pi_{(s \geq t)}} -\mathbb{E}((W_T - \mu)^2 | \mathcal{F}_t), \quad (1.24)$$

where $\mu = \frac{1}{2y} + \mathbb{E}(W_T^* | \mathcal{F}_t)$ and W_T^* is the terminal wealth induced by $\pi_{s \geq t}^*$.

Proof See [89], Theorem 3.1.

Theorem 1.2.3 illustrates that, if the following two conditions are satisfied—① optimal strategy for (1.23) exists, and ② optimal strategy for (1.24) is unique—the optimal strategy for (1.23) can be found by solving (1.24). Then, the dynamic portfolio choice problem within MVT is converted to a dynamic portfolio choice problem for an investor with risk preference as per a quadratic utility.

1.3 Numerical methods for dynamic portfolio choice

As shown in Figure 1.1, we can divide the existing popular numerical methods for dynamic portfolio choice into two categories. One uses the representation of the optimal terminal wealth in the martingale method and attempt to find the replicating strategy for it. The other follows the principle of dynamic programming and approximates the value function and optimal allocation recursively. Moreover, the later category can be further classified by the approaches to obtain the optimal strategy. Some explanations and clarifications of Figure 1.1 are provided next.

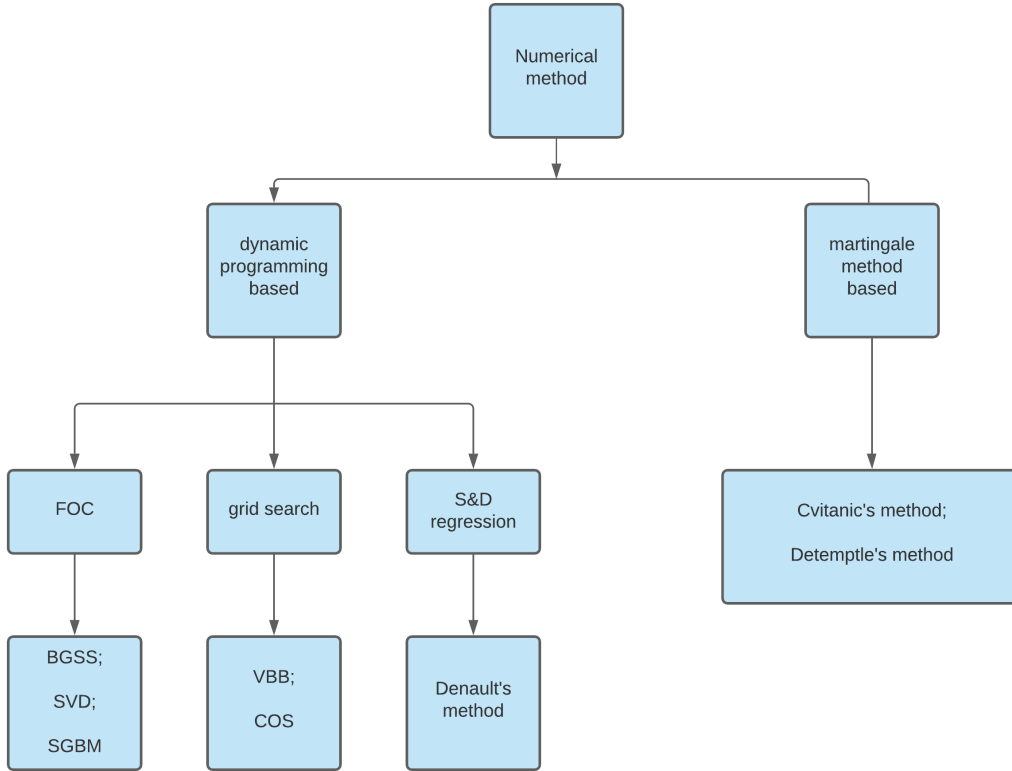


Figure 1.1: Classification of the numerical methods

In this section, we first present three methods that approximate value function recursively and compute the optimal allocation with the first order condition (FOC). These three methods, namely the BGSS (see [10]), the State Variable Decomposition (SVD) (see [39]) and the Stochastic Grid Bundling Method (SGBM, see [24]); target a CRRA-type investor whose preference on terminal wealth W is given by

$$U(W) = \frac{W^{1-\gamma}}{1-\gamma}, \quad (1.25)$$

where γ ($\gamma > 0, \neq 1$) shows the level of risk aversion. Given wealth level W_t and set of state variables H_t , the value function is assumed to follow a separable representation:

$$V(t, W_t, H_t) = \mathbb{E}_t(U(W_T) | W_t, H_t) = W_t^{1-\gamma} f(t, H_t). \quad (1.26)$$

This is, the value function is separable into wealth $W_t^{1-\gamma}$ and a state variable function $f(t, H_t)$. The methods, BGSS, SVD and SGBM, benefit from the separable property, and hence only estimate the state variable function. In the next step, the value function is expanded so that the optimal strategy can be calculated by the FOC.

In contrast, the VBB (see [85]) and the Fourier cosine series (COS) technique (see [24]) rely on grid-searching to tackle the optimization problem. However, grid-searching methods suffer from the curse of dimensionality, which makes those methods unsuitable for the targeting problem in this thesis. In section 1.3.4, we present a method based on regressing the value

function over both state variables and decision variables (S&D regression method). The method is quite general and applicable to both differentiable and non-differentiable utility functions. Unlike the other methods mentioned above, Cvitanic's method (see [26]) does not involve any estimation of value function. The method aims at a complete market portfolio and seeks the financial replication for the optimal terminal wealth. [30] developed a comprehensive approach for the calculation of optimal portfolios in asset allocation problems within complete markets, and the application of Malliavin calculus enhances its accuracy. Both above two methods are based on the martingale approach, we introduce Cvitanic's method in detail at end of this section for its operational simplicity.

1.3.1 BGSS method

BGSS was introduced in [10], it first applies the LSMC method (see [72]) in the context of dynamic portfolio problem as a way to develop the BGSS methodology. One of the innovation of BGSS is that it approximates the optimal allocation by expanding the value function with respect to wealth. For simplicity, we illustrate with the case of a second-order expansion. Note that the extension to higher order expansion is feasible, which further enhances the accuracy of the method. We denote the excess return of the stock by R_t^e and the risk-free return by R^f . Given portfolio allocation π_t , the wealth process is

$$W_{t+\Delta t} = W_t(\pi_t^T R_{t+\Delta t}^e + R^f), \quad (1.27)$$

and the value function is expanded at $W_t R^f$

$$\begin{aligned} V(t, W_t, H_t) &= \max_{\pi_t} \mathbb{E}_t(V(t + \Delta t, W_{t+\Delta t}, H_{t+\Delta t})) \\ &\approx \max_{\pi_t} \mathbb{E}_t \left(V(t + \Delta t, W_t R^f, H_{t+\Delta t}) + \frac{\partial V(t + \Delta t, W_t R^f, H_{t+\Delta t})}{\partial W_t R^f} (W_t \pi_t^T R_{t+\Delta t}^e) \right. \\ &\quad \left. + \frac{1}{2} \frac{\partial^2 V(t + \Delta t, W_t R^f, H_{t+\Delta t})}{\partial (W_t R^f)^2} (W_t \pi_t^T R_{t+\Delta t}^e)^2 \right). \end{aligned} \quad (1.28)$$

Therefore, the value function is realized when a quadratic function of allocation π_t reaches the optimum. In order to compute the partial derivatives of the value function, a terminal wealth \hat{W}_T is generated

$$\hat{W}_T = W_t R^f \prod_{s=t+\Delta t}^{T-\Delta t} (\pi_s^T R_{s+\Delta t}^e + R^f), \quad (1.29)$$

and the partial derivatives are conditional expectations as follows:

$$\begin{aligned} \frac{\partial V(t + \Delta t, W_t R^f, H_{t+\Delta t})}{\partial W_t R^f} &= \mathbb{E}_{t+\Delta t} \left(\frac{dU(\hat{W}_T)}{d\hat{W}_T} \prod_{s=t+\Delta t}^{T-\Delta t} (\pi_s^T R_{s+\Delta t}^e + R^f) \right) \\ \frac{\partial^2 V(t + \Delta t, W_t R^f, H_{t+\Delta t})}{\partial (W_t R^f)^2} &= \mathbb{E}_{t+\Delta t} \left(\frac{d^2 U(\hat{W}_T)}{d\hat{W}_T^2} \prod_{s=t+\Delta t}^{T-\Delta t} (\pi_s^T R_{s+\Delta t}^e + R^f)^2 \right). \end{aligned} \quad (1.30)$$

Substituting (1.30) into (1.28), then the optimal allocation π_t^* can be approximated by,

$$\pi_t^* = - \left\{ \mathbb{E}_t \left(\frac{d^2 U(\hat{W}_T)}{d\hat{W}_T^2} \prod_{s=t+\Delta t}^{T-\Delta t} (\pi_s^T R_{s+\Delta t}^e + R^f)^2 R_{t+\Delta t}^e (R_{t+\Delta t}^e)^T \right) W_t \right\}^{-1} \mathbb{E}_t \left(\frac{dU(\hat{W}_T)}{d\hat{W}_T} \prod_{s=t+\Delta t}^{T-\Delta t} (\pi_s^T R_{s+\Delta t}^e + R^f) R_{t+\Delta t}^e \right). \quad (1.31)$$

The BGSS applies a back-to-front estimation. At each rebalancing time t , subsequent optimal allocations has already been obtained which provide sufficient information to compute the current optimal strategy. In this way, the BGSS recursively approximates the optimal strategies covering the whole investment horizon. The notation for the BGSS method is summarized in the Table 1.1.

Notation	Meaning
B_t^m	Brownian motion at time t in m_{th} simulated path
S_t^m	Stock price at time t in m_{th} simulated path
$R_t^{e,m}$	Excess return of stock during $[t - \Delta t, t]$ in m_{th} simulated path
R^f	Risk-free return
H_t^m	state variable at time t in m_{th} simulated path
n_r	Number of simulated path
\hat{W}_T^m	Simulated terminal wealth for computing the realized value of value function's partial derivatives
$\pi_t^{*,m}$	The optimal allocation at time t in m_{th} simulated path
$L^1(t, H)$	Regression function approximating the numerator in (1.31)
$L^2(t, H)$	Regression function approximating the denominator in (1.31)

Table 1.1: Notation (BGSS)

Next, we present the step by step BGSS algorithm.

Algorithm 1: BGSS

Input: S_0, W_0, H_0 , dynamics of all processes involved

Output: Optimal current trading strategy π_0^* , expected utility $V(0, W_0, H_0)$

1 initialization;

2 Generating n_r paths of S_t^m, H_t^m and compute corresponding $R_t^{e,m}$ for $m = 1 \dots n_r$;

3 **while** $t = T - \Delta t$ **do**

4 Let $W_{T-\Delta t}^m = 1$ and $\hat{W}_T^m = R_f$, compute $A_{T-\Delta t}^m = \frac{dU(\hat{W}_T^m)}{d\hat{W}_T^m} R_T^{e,m}$ and

$$B_{T-\Delta t}^m = \frac{d^2 U(\hat{W}_T^m)}{d\hat{W}_T^{m2}} R_{t+\Delta t}^{e,m} (R_{t+1}^{e,m})^T;$$

5 Regress $A_{T-\Delta t}^m$ and $B_{T-\Delta t}^m$ over the polynomial base of state variable $H_{T-\Delta t}^m$ and obtain $L^1(T - \Delta t, H)$ and $L^2(T - \Delta t, H)$;

6 The optimal allocation is $\pi_{T-\Delta t}^{*,m} = -\frac{L^1(T-\Delta t, H_{T-\Delta t}^m)}{L^2(T-\Delta t, H_{T-\Delta t}^m)}$;

7 **for** $t = T - \Delta t$ **to** Δt **do**

8 Let $W_t^m = 1$ and $\hat{W}_T^m = R_f \prod_{s=t+\Delta t}^{T-\Delta t} ((\pi_s^m)^T R_{s+\Delta t}^{e,m} + R^f)$, compute

$$A_t^m = \frac{dU(\hat{W}_T^m)}{d\hat{W}_T^m} \prod_{s=t+\Delta t}^{T-\Delta t} ((\pi_s^m)^T R_{s+\Delta t}^{e,m} + R^f) R_T^{e,m} \text{ and}$$

$$B_t^m = \frac{d^2 U(\hat{W}_T^m)}{d\hat{W}_T^{m2}} \prod_{s=t+\Delta t}^{T-\Delta t} ((\pi_s^m)^T R_{s+\Delta t}^{e,m} + R^f)^2 R_{t+1}^{e,m} (R_{t+\Delta t}^{e,m})^T;$$

9 Regress A_t^m and B_t^m over the polynomial base of state variable H_t^m and obtain $L^1(t, H)$ and $L^2(t, H)$;

10 The optimal allocation is $\pi_t^{*,m} = -\frac{L^1(t, H_t^m)}{L^2(t, H_t^m)}$;

11 **while** $t = 0$ **do**

12 Let $W_0^m = 1$ and $\hat{W}_T^m = R_f \prod_{s=\Delta t}^{T-\Delta t} ((\pi_s^m)^T R_{s+\Delta t}^{e,m} + R^f)$, compute

$$A_0 = \frac{1}{n_r} \sum_{m=1}^{n_r} \frac{dU(\hat{W}_T^m)}{d\hat{W}_T^m} \prod_{s=\Delta t}^{T-\Delta t} ((\pi_s^m)^T R_{s+\Delta t}^{e,m} + R^f) R_T^{e,m} \text{ and}$$

$$B_0 = \frac{1}{n_r} \sum_{m=1}^{n_r} \frac{d^2 U(\hat{W}_T^m)}{d\hat{W}_T^{m2}} \prod_{s=\Delta t}^{T-\Delta t} ((\pi_s^m)^T R_{s+\Delta t}^{e,m} + R^f)^2 R_{t+\Delta t}^{e,m} (R_{t+1}^{e,m})^T;$$

13 The optimal allocation at initial time is $\pi_0^* = -\frac{A_0}{B_0}$;

14 Compute $W_T^m = W_0 ((\pi_0^*)^T R_{\Delta t}^{e,m} + R^f) \prod_{s=\Delta t}^{T-\Delta t} ((\pi_s^*)^T R_{s+\Delta t}^{e,m} + R^f)$.

15 The expected utility is, $\hat{V}(0, W_0, H_0) = \frac{1}{n_r} \sum_{m=1}^{n_r} U(W_T^m)$

16 **Return** π_0^* and $\hat{V}(0, W_0, H_0)$.

1.3.2 SVD approach

[39] introduced the SVD approach, which improves the recursive approximation method exhibited in BGSS. There are two innovations in the SVD approach: ① The value function is expanded based on a Nonlinear Decomposition. ② It applies the inverse utility transformation

on the value function. The SVD approach still targets a CRRA investor, whose value function is separable into wealth and a state variable function. With the Bellman principle, the value function is given by

$$\begin{aligned} V(t, W_t, H_t) &= W^{1-\gamma} f(t, H_t) = W^{1-\gamma} V(t, 1, H_t) = W^{1-\gamma} U(J(t, 1, H_t)) \\ &= W^{1-\gamma} \max_{\pi_t} \mathbb{E}_t(U(\pi_t^T R_{t+\Delta t}^e + R^f) J(t + \Delta t, H_{t+\Delta t})^{1-\gamma}), \end{aligned} \quad (1.32)$$

where $J = U^{-1}(V)$. Substituting the log excess return r_t^e (i.e. $R_t^e = R^f(\exp(r_t^e) - 1)$) into (1.32), the expansion of the value function has the representation

$$V(t, W_t, H_t) = W^{1-\gamma} \max_{\pi_t} \mathbb{E}_t(U(\pi_t^T R^f(\exp(r_{t+\Delta t}^e) - 1) + R^f) J(t + \Delta t, H_{t+\Delta t})^{1-\gamma}). \quad (1.33)$$

The log excess return and state variables are decomposed into the conditional mean and the random source i.e. $r_{t+\Delta t}^e = \mu_{t+\Delta t}^r + \epsilon_{t+\Delta t}^r$, $H_{t+\Delta t} = \mu_{t+\Delta t}^H + \epsilon_{t+\Delta t}^H$ where $\mathbb{E}_t(\epsilon_{t+\Delta t}^r) = \mathbb{E}_t(\epsilon_{t+\Delta t}^H) = 0$. [39] proposed two versions of SVD approach. The partial SVD (PSVD) expands the value function only with respect to the $\epsilon_{t+\Delta t}^r$

$$V(t, W_t, H_t) = W^{1-\gamma} \max_{\pi_t} \sum_{m=0}^M \frac{1}{m!} \frac{d^m G_{t+\Delta t}(0)}{d\epsilon_{t+\Delta t}^r{}^m} \mathbb{E}_t((\epsilon_{t+\Delta t}^r)^m J(t + \Delta t, H_{t+\Delta t})^{1-\gamma}), \quad (1.34)$$

where $G_{t+\Delta t}(\epsilon_{t+\Delta t}^r) = U(\pi_t^T R^f(\exp(\mu_{t+\Delta t}^r + \epsilon_{t+\Delta t}^r) - 1) + R^f)$. The full SVD (FSVD) expands the value function with respect to both, $\epsilon_{t+\Delta t}^r$ and $\epsilon_{t+\Delta t}^H$

$$V(t, W_t, H_t) = W^{1-\gamma} \max_{\pi_t} \sum_{0 \leq m_1 + m_2 \leq M} \frac{1}{m_1! m_2!} \frac{d^{m_1 + m_2} K_{t+\Delta t}(0, 0)}{d\epsilon_{t+\Delta t}^r{}^{m_1} d\epsilon_{t+\Delta t}^H{}^{m_2}} \mathbb{E}_t((\epsilon_{t+\Delta t}^r)^{m_1} (\epsilon_{t+\Delta t}^H)^{m_2}), \quad (1.35)$$

where $K_{t+\Delta t}(\epsilon_{t+\Delta t}^r, \epsilon_{t+\Delta t}^H) = U(\pi_t^T R^f(\exp(\mu_{t+\Delta t}^r + \epsilon_{t+\Delta t}^r) - 1) + R^f) J(t + \Delta t, \mu_{t+\Delta t}^H + \epsilon_{t+\Delta t}^H)^{1-\gamma}$. The allocation π_t is embedded in the partial derivatives of $G_{t+\Delta t}$ or $K_{t+\Delta t}$.

At each rebalancing point t , an approximation of $J(t + \Delta t, H_{t+\Delta t})$ has already been obtained. The SVD approach computes the conditional expectations with the cross-path regression method used in BGSS. Then, the optimal allocation π_t^* is immediately known by the optimization search. Using these values, the function $J(t, H_t)$ is fitted by a polynomial regression. The SVD approach moves backwards and repeat these procedures until reaching the initial time.

1.3.3 SGBM

[24] equipped the BGSS with a recently developed method (i.e. Stochastic Grid Bundling Method [SGBM]) for calculating the conditional expectation, which results in a lower biased approximation of the optimal allocation. Compared with Algorithm 1, at each rebalancing time t , the SGBM sorts the simulated paths by the size of state variable H_t^m and bundles those paths into B non-overlapping partitions denoted by $\mathcal{B}_t(1), \mathcal{B}_t(2), \dots, \mathcal{B}_t(B)$. The realized value of numerator A_t^m and denominator B_t^m of the optimal allocation are regressed over the polynomial basis of H_t^m within the bundle $\mathcal{B}_t(b)$, so the regression function $L^{1,b}(t, H)$ and $L^{2,b}(t, H)$

are obtained. The optimal allocation is computed by $\pi_t^{*,m} = -\frac{L^{1,b}(t,H_t^m)}{L^{2,b}(t,H_t^m)}$. Repeating the same procedures for all bundles, the optimal allocation for each path is found.

[24] further extended the SGBM method by applying the Taylor expansion based on a non-linear decomposition of the value function which is introduced in the SVD approach, while it chooses a different expansion center $r_{t+\Delta t}^e = 0$. The author claimed that the new expansion center is superior according to the numerical test result. In the SGBM with log Taylor expansion (SGBM-LT), the value function is expanded as follows:

$$V(t, W_t, H_t) = W^{1-\gamma} \max_{\pi_t} \sum_{m=0}^M \frac{1}{m!} \frac{d^m G_{t+\Delta t}(0)}{dr_{t+\Delta t}^{em}} \mathbb{E}_t((r_{t+\Delta t}^e)^m f(t + \Delta t, H_{t+\Delta t})), \quad (1.36)$$

where $G_{t+\Delta t}(r_{t+\Delta t}^e) = (\pi_t^T R^f (\exp(r_{t+\Delta t}^e) - 1) + R^f)^{1-\gamma}$. The allocation π_t is embedded in the partial derivatives of $G_{t+\Delta t}$ and is obtained by searching the optimum point of a polynomial.

1.3.4 Denault's method

All the methods above solve the dynamic portfolio choice problem for CRRA-type investor, where the value function is expanded to obtain the optimal strategy. [29] presented a Least-Squares Monte Carlo method that regresses the post decision value function with respect to both state variables and decision variable (LSMC-S&D). The method do not rely on a Taylor expansion nor the derivatives of the utility function, which makes it suitable for both differentiable and non-differentiable utilities. The notations for LSMC-S&D is listed in table 1.2.

Notation	Meaning
S_t^m	Stock price at time t in m_{th} simulation path
$R_t^{e,m}$	Excess return at time t in m_{th} simulation path
R_f	Risk-free return
H_t^m	State variable at time t in m_{th} simulation path
n_r	Size of simulated path
$n_w(t)$	Size of wealth grid at time t
n_x	Size of trading allocation grid
$W_{k,t}$	k_{th} value on the representative future wealth grid at time t
$\left\{ v_{k,t+\Delta t}^m, W_{k,t+\Delta t} \right\}_{k=1}^{n_w(t+\Delta t)}$	Surface of value function and wealth at time t in m_{th} simulation path
$L_{k,t}(\pi, H)$	Regression function estimating the value function at time t given wealth $W_{k,t}$

Table 1.2: Notation (LSMC-S&D)

The method is divided into two stages. In the stage of forward simulation, the paths of stock prices and state variables are generated, then the LSMC-S&D computes a grid of representative future wealths. In the stage of backward recursion, LSMC S&D considers the post-decision value function $V(t, W_t, H_t, \pi_t)$ defined by

$$V(t, W_t, H_t, \pi_t) = \max_{\pi_s \geq t + \Delta t} \mathbb{E}_t(V(t + \Delta t, W_{t+\Delta t}, H_{t+\Delta t})). \quad (1.37)$$

At each rebalancing time t , a wealth at $t + \Delta t$ is generated given wealths at t , i.e. W_t^k , state variable H_t and allocation π_t . The realized value of the post decision value function at $t + \Delta t$

is found by interpolation on the surface of the value function with representative wealths. An approximation function $L_{k,t}(\pi, H)$ to $V(t, W_t^k, H, \pi)$ is then obtained by regressing the value of post decision value functions over the polynomial basis of state variables H_t and decision variable π_t . Lastly, the optimal strategy is found by searching the optimum of the $L_{k,t}(\pi, H)$. Next, the LSMC-S&D is presented step by step in Algorithm 2 and 3 .

Algorithm 2: LSMC–S&D-Forward Simulation

Input: S_0, H_0, W_0

Output: $S_t^m, H_t^m, R_t^{e,m}$, portfolio allocation grid π_i , representative future wealth grid $W_{k,t}$

- 1 initialization;
- 2 Generate n_r paths of S_t^m, H_t^m and compute corresponding $R_t^{e,m}$ for $m = 1 \dots n_r$;
- 3 Compute a grid of portfolio allocation π_i , for $i = 1 \dots n_x$;
- 4 Calculate the future wealth level $\widetilde{W}_{j,t}$ by keeping a large allocation on risky assets. The wealth level percentile grid is given by

$$W_{k,t} = \text{percentile}(\{\widetilde{W}_{m,t}\}_{j=1}^{n_r}, P_k) \quad \text{for } k = 1 \dots n_w(t) \quad (1.38)$$

In step 4 of the Algorithm 2, simulated wealth $\widetilde{W}_{j,t}$ is generated by a relatively risky strategy (i.e. keeping a large proportion of wealth on the risky assets). Then, the range of $\widetilde{W}_{j,t}$ is wide enough to cover most feasible outcomes given a substantial simulation size adapted to the problem, which makes the percentile grid of $\widetilde{W}_{j,t}$, i.e. $W_{k,t}$, an ideal grid for the representative future wealth.

1.3.5 Cvitanic's method

All the methods above rely on the Bellman principle and dynamic programming techniques, which approximate the value function and the optimal allocation recursively. Targeting dynamic portfolio in complete market, [26] proposed a pure Monte Carlo simulation method based on the Martingale approach. The method is quite general and can be applied to any type of time additive utility function as long as: ① Markets are complete, ② The dynamics of all the processes involved are known. To simplify the presentation, we illustrate Cvitanic's method in one dimension with the investor's preference as per power utility (see (1.25)). The key of the method is to find the replication strategy of the optimal wealth process. Under the risk-neutral measure Q , the optimal wealth process satisfies

$$\frac{dW_t^*}{W_t^*} = rdt + \sigma_t^W dB_t^Q. \quad (1.39)$$

The investor's wealth process given the strategy π_t can be written as

$$\frac{dW_t}{W_t} = rdt + \pi_t \sigma_t^S dB_t^Q, \quad (1.40)$$

where σ_t^S is the instantaneous volatility of the stock price. The investor's wealth process is identical to the optimal wealth process when the optimal strategy π_t^* is adopted. Comparing

Equation (1.40) with (1.39), the optimal allocation π_t^* is immediately known if the σ_t^W is computed.

According to the Martingale method, the optimal terminal wealth is given by,

$$W_T^* = \left(y \exp \left(- \int_0^T r_s ds \right) \xi_T \right)^{-\frac{1}{\gamma}}, \quad (1.41)$$

where y is the Lagrange multiplier, $\xi_T = \exp(-0.5 \int_0^T \lambda_s^2 ds - \int_0^T \lambda_s dB_s)$ denotes the Radon-Nikodym derivative and the market price of risk is denoted by λ_t . Furthermore, the optimal wealth process is equivalent to a conditional expectation of the optimal terminal wealth under the measure Q .

$$W_{t+\Delta t}^* = \mathbb{E}_{t+\Delta t}^Q \left(\exp \left(- \int_{t+\Delta t}^T r_s ds \right) W_T^* \right). \quad (1.42)$$

Therefore, $W_{t+\Delta t}^*$ can be approximated by a Monte Carlo simulation. In addition, the instantaneous volatility of optimal wealth process satisfies

$$\sigma_t^W = \lim_{\Delta t \rightarrow 0} \mathbb{E}_t \left(\frac{(W_{t+\Delta t}^* - W_t^*)(B_{t+\Delta t} - B_t)}{\Delta t} \right), \quad (1.43)$$

which is also obtained with a Monte Carlo simulation. Finally, the optimal strategy is computed by $\pi_t^* = \frac{\sigma_t^W}{\sigma_t^S}$. Next, we present the step by step algorithm,

Algorithm 4: Cvitanic's method

Input: S_0, H_0, W_0

Output: Optimal allocation π_0^*

- 1 initialization;
 - 2 Generate N paths of S_t^m, H_t^m and compute corresponding pricing kernel ξ_t^m
 $m = 1 \dots N$;
 - 3 Find the y Lagrange multiplier that makes $W_0 = \frac{1}{N} \sum_{m=1}^N \left(y \exp \left(- \int_0^T r_s ds \right) \xi_T^m \right)^{-\frac{1}{\gamma}}$;
 - 4 Generate the value at $t = \Delta t, S_{\Delta t}^i, H_{\Delta t}^i, B_{\Delta t}^i$ and compute pricing kernel $\xi_{\Delta t}^i \quad i = 1 \dots K$;
 - 5 **for** $i = 1$ **to** K **do**
 - 6 Generate M paths of $S_t^{i,j}, H_t^{i,j}$ and compute corresponding pricing kernel $\xi_t^{i,j}$
 starting from $S_{\Delta t}^i, H_{\Delta t}^i$ and $\xi_{\Delta t}^i \quad j = 1 \dots M$;
 - 7 Compute optimal terminal wealth $W_T^{i,j} = \left(y \exp \left(- \int_0^T r_s ds \right) \xi_T^{i,j} \right)^{-\frac{1}{\gamma}} \quad j = 1 \dots M$;
 - 8 Calculate the optimal wealth at $t = \Delta t, W_{\Delta t}^i = \frac{1}{M} \sum_{j=1}^M \exp \left(- \int_{\Delta t}^T r_s ds \right) \frac{\xi_T^{i,j}}{\xi_{\Delta t}^i} W_T^{i,j}$;
 - 9 Obtain instantaneous volatility of optimal wealth process $\sigma_0^W = \frac{1}{M} \sum_{i=1}^K \frac{(W_{\Delta t}^i - W_0) B_{\Delta t}^i}{W_0 \Delta t}$;
 - 10 Finally compute optimal allocation $\pi_0^* = \frac{\sigma_0^W}{\sigma_0^S}$;
-

1.4 An overview of neural network

In this section, we briefly introduce the architecture of artificial neural networks (ANN) and the backpropagation i.e. a widely used algorithm for training neural networks.

1.4.1 Artificial neural network

Artificial neural networks is a general method for learning real value functions with unknown form. It is inspired by the biological neural networks and try to mimic the way the human brain analyzes and processes information. For simplicity, we illustrate with the two hidden layers network depicted in the Figure 1.2.

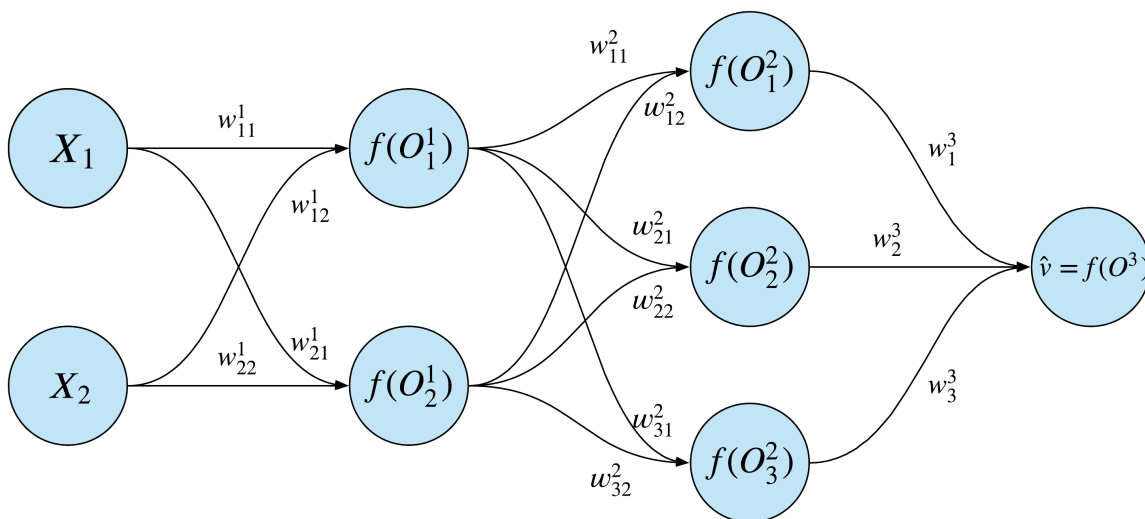


Figure 1.2: Structure of the neural network

We denote the vector of input by $X = [X_1, X_2]^T$ and output by \hat{v} . Then, the ANN is equivalent to the function:

$$\hat{v} = f(\underbrace{W^3 f(\underbrace{W^2 f(\underbrace{W^1 X + B^1}_{O^1}) + B^2}_{O^2}) + B^3}_{O^3}), \quad (1.44)$$

where $O_1 = [O_1^1, O_1^2]$, $O_2 = [O_2^1, O_2^2, O_2^3]$ are the hidden neurons and

$$\begin{aligned} W^1 &= \begin{bmatrix} w_{11}^1 & w_{12}^1 \\ w_{21}^1 & w_{22}^1 \end{bmatrix} & W^2 &= \begin{bmatrix} w_{11}^2 & w_{12}^2 \\ w_{21}^2 & w_{22}^2 \\ w_{31}^2 & w_{32}^2 \end{bmatrix} & W^3 &= \begin{bmatrix} w_1^3 & w_2^3 & w_3^3 \end{bmatrix} \\ B^1 &= \begin{bmatrix} b_1^1 & b_2^1 \end{bmatrix}^T & B^2 &= \begin{bmatrix} b_1^2 & b_2^2 & b_3^2 \end{bmatrix}^T & B^3 &= \begin{bmatrix} b^3 \end{bmatrix} \end{aligned} \quad (1.45)$$

are the weights of ANN to be fitted with the sample data. f represents the activation function that connects the neurons and provides the nonlinearity for the ANN. The architecture of ANN is determined by the number of hidden layers, the number of hidden neurons and the activation function, which are selected according to the target function to be fitted. We summarize some representative activation functions as follows:

1. Rectified linear unit (ReLU)

$$f(x) = \begin{cases} x & x \geq 0 \\ 0 & x < 0. \end{cases} \quad (1.46)$$

ReLU neural network will provide a piece-wise function.

2. Exponential linear unit (ELU)

$$f(x) = \begin{cases} x & x \geq 0 \\ \alpha(e^x - 1) & x < 0. \end{cases} \quad (1.47)$$

3. Scaled Exponential linear unit (SELU)

$$f(x) = \begin{cases} \lambda x & x \geq 0 \\ \lambda \alpha(e^x - 1) & x < 0. \end{cases} \quad (1.48)$$

SELU function is a general case of ELU.

4. SoftPlus

$$f(x) = \ln(1 + e^x). \quad (1.49)$$

5. Sigmoid

$$f(x) = \frac{1}{1 + e^{-x}}. \quad (1.50)$$

1.4.2 Backpropagation

The algorithm of backpropagation was originally invented in [69]. However, the importance of backpropagation wasn't fully appreciated until [82] demonstrated that it could provide interesting distribution representations. The backpropagation is used to approximate the value of weights in the ANN, i.e. W^1 , W^2 , W^3 , B^1 , B^2 and B^3 in the above example. It employs the gradient descent method to minimize the error between the output of ANN and target value from the sample data.

Given the input variables (X_1, X_2, \dots, X_N) in the sample data, ANN generates a set of predict value for the output variables $(\hat{v}_1, \hat{v}_2, \dots, \hat{v}_N)$. The sum of error is hence calculated with the predict values and target values (Y_1, Y_2, \dots, Y_N) .

$$Er = \sum_{i=1}^N L(\hat{v}_i, Y_i), \quad (1.51)$$

where L is a loss function. The derivative of error Er with respect to the each weight (i.e. $\frac{dEr}{dW^i}$ and $\frac{dEr}{dB^i}$) can be computed with the chain rule. Next, the backpropagation algorithm update the weights with

$$\begin{aligned} W^i(\text{updated}) &= W^i(\text{old}) - l \frac{dEr}{dW^i} \\ B^i(\text{updated}) &= B^i(\text{old}) - l \frac{dEr}{dB^i}, \end{aligned} \quad (1.52)$$

where l is the learning rate. The predicted value for the output variables ($\hat{v}_1, \hat{v}_2, \dots, \hat{v}_N$) are regenerated with the updated weights. In this way, the error between ANN's predict values and target values diminishes, and weights in ANN iteratively converge to the optimal value to fit the target function. The backpropagation algorithm stop when the error Er is smaller than a pre-determined threshold.

1.5 A LSMC approach for the American option Valuation

There are plenty of analytical results in the valuation of European options, where the price function is rewritten as the conditional expectation of terminal payoff under the risk neutral measure and options' price are the solutions of Feynman–Kac PDEs. For example, the seminal paper [8] obtained the closed form call and put price given a single factor model (GBM); another substantial achievement (see [48]) incorporated the volatility risk into option valuation, which better captures the implied volatility surface. In contrast, analytical results for path-dependent options (e.g. the American option) are more rare. The involvement of optimal stopping time jeopardizes the solvability, even in the context of Black–Scholes–Merton setting, closed form solution for American option price has not been found yet. Some researchers explore the application of numerical PDEs, like for example finite-difference method (FDM), which is effective for a limited amount of underlying assets and state variables. This method suffers from the curse of dimensionality, so it is inefficient for high-dimensional problem. Alternatively, [72] proposed a powerful simulation based method, namely LSMC. The LSMC is accurate, easy to apply and computational efficient, which has led to its extensive use in both industry and academia. We first summarize the notation for LSMC in Table 1.3.

Notation	Meaning
S_t^m	Stock price at time t in m_{th} simulated path
r^f	Risk-free return
H_t^m	state variable at time t in m_{th} simulated path
n_r	Number of simulated path
n_t^I	Number of in the money simulated path at time t
τ^m	The optimal stopping time in m_{th} simulated path
$L(t, S, H)$	Regression function approximating the option price
$U(t, \tau, S)$	Discounted option payoff $U(t, \tau, S) = \exp(-(\tau - t)r^f)U(\tau, \tau, S)$
P_0	Price of the option at $t = 0$

Table 1.3: Notation (LSMC)

Next, we present the step by step algorithm for LSMC.

Algorithm 5: LSMC

Input: S_0, H_0 , dynamics of all processes involved

Output: Price of the option at $t = 0$

1 initialization;

2 Generating n_r paths of S_t^m, H_t^m under the risk neutral measure, and let $\tau^m = T$
 for $m = 1 \dots n_r$;

3 **for** $t = T - \Delta t$ to Δt **do**

4 Find the in-the-money simulated path subset (i.e. $U(t, t, S_t^m) > 0$);

5 Within the subset, compute the discounted option payoff $U(t, \tau^m, S_{\tau^m}^m)$
 for $m = 1 \dots n_t^I$;

6 Regress $U(t, \tau^m, S_{\tau^m}^m)$ over S_t^m and H_t^m and obtain $L(t, S, H)$;

7 **if** $L(t, S_t^m, H_t^m) < U(t, t, S_t^m)$ **then**

8 | let $\tau^m = t$;

9 **while** $t = 0$ **do**

10 Compute the average of discounted option payoff: $\bar{U} = \frac{1}{n_r} \sum_{i=1}^{n_r} U(0, \tau^m, S_{\tau^m}^m)$;

11 $P_0 = \max \{ \bar{U}, U(0, 0, S_0) \}$;

12 Return P_0 .

Algorithm 3: LSMC-S&D–Backward recursion**Input:** representative future wealth grid $W_{k,t}$,simulated paths $S_t^m, H_t^m, R_t^{e,m} \quad m = 1 \dots n_r$ portfolio allocation grid $\pi_i \quad i = 1, 2, \dots, n_x$ **Output:** Optimal strategy π_0^*

```

1 while  $t = T - \Delta t$  do
2   for  $k = 1$  to  $n_w(T - \Delta t)$  do
3     Generate  $n_x \times n_r$  wealth at time  $T$ :
4        $W_{k,T}^m(\pi_i, R_T^{e,m}) = W_{k,T-\Delta t}(R^f + \pi_i^T R_T^{e,m}), \quad m = 1 \dots n_r$  and  $i = 1, 2, \dots, n_x$ ;
5     Compute realized value  $v_{k,T}^{i,m} = U(W_{k,T}^m(\pi_i, R_T^{e,m}))$ ;
6     Regress  $v_{k,T}^{i,m}$  over the polynomial basis of  $(\pi_i, H_{T-\Delta t}^m)$  and obtain  $L_{k,T-\Delta t}(\pi, H)$ ;
7     Calculate the optimal strategy  $\pi_{k,T-\Delta t}^m = \arg \max_{\pi} L_{k,T-\Delta t}(\pi, H_{k,T-\Delta t}^m) \quad m = 1 \dots n_r$ ;
8   Compute  $W_{k,T}^m(\pi_{k,T-\Delta t}^m, R_T^{e,m}) = W_{k,T-\Delta t}(R^f + (\pi_{k,T-\Delta t}^m)^T R_T^{e,m})$ ,
9      $v_{k,T-\Delta t}^m = U(W_{k,T}^m(\pi_{k,T-\Delta t}^m, R_T^{e,m})) \quad m = 1 \dots n_r$  and  $k = 1, 2, \dots, n_w(T - \Delta t)$ ;
10  Construct surface  $\{v_{k,T-\Delta t}^m, W_{k,T-\Delta t}\}_{k=1}^{n_w(T-\Delta t)} \quad m = 1 \dots n_r$ ;
11 for  $t = T - 1\Delta t$  to  $\Delta t$  do
12   for  $k = 1$  to  $n_w(t)$  do
13     Generate  $n_x \times n_r$  wealth at time  $t + \Delta t$ :
14        $W_{k,t+\Delta t}^m(\pi_i, R_{t+\Delta t}^{e,m}) = W_{k,t}(R^f + \pi_i^T R_{t+\Delta t}^{e,m}), \quad m = 1 \dots n_r$  and  $i = 1, 2, \dots, n_x$ ;
15     Compute realized value  $v_{k,t+\Delta t}^{i,m}$  by interpolating  $W_{k,t+\Delta t}^m(\pi_i, R_{t+\Delta t}^{e,m})$  through
16        $\{v_{k,t+\Delta t}^m, W_{k,t+\Delta t}\}_{k=1}^{n_w(t+\Delta t)}$ ;
17     Regress  $v_{k,t+\Delta t}^{i,m}$  over the polynomial basis of  $(\pi_i, H_t^m)$  and obtain  $L_{k,t}(\pi, H)$ ;
18     Calculate the optimal strategy  $\pi_{k,t}^m = \arg \max_{\pi} L_{k,t}(\pi, H_{k,t}^m) \quad m = 1 \dots n_r$ ;
19   Compute  $W_{k,t+\Delta t}^m(\pi_{k,t}^m, R_{t+\Delta t}^{e,m}) = W_{k,t}(R^f + (\pi_{k,t}^m)^T R_{t+\Delta t}^{e,m})$ ,  $v_{k,t}^m$  is calculated by
20     interpolating  $W_{k,t+\Delta t}^m(\pi_{k,t}^m, R_{t+\Delta t}^{e,m})$  through  $\{v_{k,t+\Delta t}^m, W_{k,t+\Delta t}\}_{k=1}^{n_w(t+\Delta t)} \quad m = 1 \dots n_r$  and
21      $k = 1, 2, \dots, n_w(t)$ ;
22   Construct surface  $\{v_{k,t}^m, W_{k,t}\}_{k=1}^{n_w(t)} \quad m = 1 \dots n_r$ ;
23 while  $t = 0$  do
24   Generate  $n_x \times n_r$  wealth at time  $\Delta t$ :  $W_{\Delta t}^m(\pi_i, R_{\Delta t}^{e,m}) = W_0(R^f + \pi_i^T R_{\Delta t}^{e,m}), \quad m = 1 \dots n_r$ 
25     and  $i = 1, 2, \dots, n_x$ ;
26   Compute realized value  $v_{k,\Delta t}^{i,m}$  by interpolating  $W_{\Delta t}^m(\pi_i, R_{\Delta t}^{e,m})$  through
27      $\{v_{k,t+\Delta t}^m, W_{k,t+\Delta t}\}_{k=1}^{n_w(t+\Delta t)}$ ;
28   Regress  $v_{k,\Delta t}^{i,m}$  over the polynomial basis of  $(\pi_i, H_t^m)$  and obtain  $L_0(\pi)$ ;
29   Calculate the optimal strategy  $\pi_0^* = \arg \max_{\pi} L_0(\pi) \quad m = 1 \dots n_r$ ;
30 Return  $\hat{\pi}_0$ 

```

Chapter 2

A polynomial-Affine approximation for dynamic portfolio choice

Chapter summary:

This chapter proposes an efficient and accurate simulation-based method to approximate the solution of a continuous-time dynamic portfolio optimization problem for multi-asset and multi-state variables within expected utility theory (EUT). The performance of this methodology is demonstrated in five settings of a risky asset. Closed-form solutions are available for three of these settings—a geometric Brownian motion, a stochastic volatility (SV) model, and an exponential Ornstein-Uhlenbeck process—which help assess performance. The fourth setting is a discrete-time vector autoregressive (VAR) parametrization, which is popular in this area of research. In these cases, we compare our method to at least two relevant benchmarks in the literature: the BGSS methodology of [10] and the SGBM approach of [24]. Our method delivers accurate and fast results for the optimal investment and value function, comparable to analytical solutions. Moreover, it is also significantly faster for a given precision level than the aforementioned competing simulation-based methodologies. Lastly, we explore the solution to a model with mean-reverting SV and interest rate, under full correlation; this last assumption makes it unsolvable in closed-form. Our analysis shows a significant impact of correlation between stock and interest rate on allocation and Annualized certainty equivalent rate (CER).

Status: Second round at *Computational Economics*.

2.1 Introduction

Since the late 20th century, financial markets have become increasingly complex. The list of stylized facts required to characterize even simple equity time series gets longer every decade. For instance, the modeling of a popular market index like the S&P 500 must include stochastic volatility (SV) and stochastic volatility of volatility (SVV), both of which are indisputable with the appearance of volatility indexes quoted by Chicago Board Options Exchange (CBOE): volatility index (VIX) as a proxy for SV and VIX volatility index (VVIX) to track SVV. Non-constant leverage effects, stochastic market prices of risk and periods of mean-reverting patterns are simply additional complexities reported in real data. Such stylized facts concern a one-dimensional series (S&P 500), but the reality is that the surface has barely been scratched

in terms of joint assets behaviour; one popular stylized fact in multidimensions is stochastic correlation, which is partially targeted with the introduction of the CIX index (CBOE). Making decisions that adequately mirror this complexity requires the introduction of more complicated stochastic models. Unfortunately, these challenging models and the additional sources of randomness they entail jeopardise the analytic solvability of important financial problems like, for instance, optimal investment allocation. This highlights the need for an accurate and fast numerical method that can keep up with the ever increasing challenges.

Portfolio optimization for continuous-time processes within the framework of expected utility theory (EUT) began in the 1960s with the seminal papers [76] and [78], in which the associated Hamilton-Jacobi-Bellman (HJB) problem was solved in closed-form, hence producing the optimal trading strategy, value functions, and wealth for stock prices modelled with a geometric Brownian motion (GBM). In the 1980s, [54] and [25] pioneered the martingale method to solve the portfolio optimization problem via a combination of static optimization and financial replication. These approaches have generated a large amount literature on analytical solutions for a variety of models. For example, [59] obtained closed-form solution of optimal strategies with Heston's SV model. [19] considered the portfolio problem for stocks with prices that follow mean-reverting processes, obtaining analytic solutions up to a system of ordinary differential equations (ODEs). More recently, [38] solved the optimal portfolio for investors allocating their wealth to stocks and bonds (stochastic interest rates). [13] considered a model with stochastic volatilities and correlations solving the optimal allocation for incomplete markets. Similarly, [34] assumed a multivariate setting where the principal components have stochastic eigenvalues, generalizing the multi-factor model of [22].

All the cases described above belong to the family of linear-affine models,¹ which explains their solvability. This family of solvable models was extended to include quadratic-affine models in the celebrated paper of [70]. This latest family is, to the best of our knowledge, one of the broadest families solvable in closed form. It accommodates stochastic processes for the underlying with drifts and quadratic variations (coefficients of the infinitesimal generator, [IG]), which can be represented as quadratic polynomials in the variables. In such cases, the optimal value function is separable into a function of wealth and an exponential quadratic function on state-variables; such a setting also permits analytical optimal strategies. On the other hand, there are many reasonable and interesting models for which analytical solutions are not available. In particular, IG coefficients with either non-polynomial structures, displaying a polynomial of an order higher than 2, or non-integer exponents are rarely solvable in the context of portfolio optimization.

These limitations have generated a literature on approximations to the underlying optimal control problem, with a minority of papers focusing on the financial applications and implications. One of the key breakthroughs in terms of methodology and financial applications is the seminal work of [10]. Their method (BGSS) applies least-square Monte Carlo (LSMC, [72]) to the context of portfolio optimization with excellent results in terms of accuracy and time efficiency. Subsequently, [85] compared the numerical performance of two sub-methodologies—the value function iteration (VFI) and the portfolio weight iteration (PWI)—and concluded that VFI shows a higher bias in the solution. [39] argue that VFI can also produce accurate results if a proper transformation on value function is applied. [40] improve [10] by applying an inverse

¹Portfolio value function is an exponential linear function when asset prices follow a linear-affine model.

utility transformation to the value function and choosing a different expansion center. [57] combine an endogenous grid method and a simulation-based technique to accommodate life cycles that are characterized by endogenous variables. More recently, [29] proposed a new algorithm using both regression and interpolation estimation methods for non-differentiable utility functions. In the same spirit, [24] enhance [10] by replacing the standard regression method by a technique called the Stochastic Grid Bundling Method (SGBM), which was introduced in [53]. A VFI method is introduced in [12] that takes certainty equivalent transformation on value functions and exhibits better accuracy than some Taylor series expansion based methods.

All approximation methods mentioned above focus on multi-period portfolio construction with a relatively low re-balancing frequency, which reflects the investment philosophy that portfolio managers acquire new information from traditional sources, such as quarterly and annual financial reports, and adjust their allocation at a slow pace. This is perfectly suitable for large-scale funds, which are under the constraints of portfolio turnover due to non-negligible transaction costs and market impact. More recently, small-scale investors have benefited from the availability of data, which enables them to make extra profits by capturing fleeting opportunities in the markets. In this case, the investors move their attention to continuous-time assets' price models, which are not subject to a specific time interval. However, approximation methods targeting unsolvable continuous-time models are rarely studied. To fill this research gap, a new method, namely the polynomial affine method for constant relative risk aversion utility (PAMC), is proposed in this chapter. Our focus is on investors who may want to make transactions in near continuous time (rebalancing at will) and prefer to use advanced stochastic models with common factors (e.g., SV and interest rate) or unconventional factors (e.g., natural language processing indicator) to detect any profitable chance.

Inspired by the applicability of the quadratic-affine family of models in [70], we approximate the optimal investment strategy for any given stochastic process model using an order k polynomial affine structure on the value function. This approach automatically detects if the given problem has a low-order polynomial affine structure, therefore delivering a highly precise solution to the embedded quadratic-affine family of models. We demonstrate the accuracy and efficiency of our approximation on three well-known cases for practitioners in finance and economics: a GBM (Merton's solution, [78]), Heston's SV model for an incomplete market (see [59]), and an exponential Ornstein-Uhlenbeck (OU) process (see [19]) targeting commodities. We compare our approach to what can be considered two leading, gold-standard methodologies: the BGSS (see [10]) and the SGBM (see [24]). To ensure the fairness of the comparison and also to demonstrate the applicability of the PAMC in discrete-time cases, we implement all the methods on the vector autoregression (VAR) setting reported in both [10] and [24]. Finally, we exemplify the application of PAMC on an unsolvable model of significance in the financial industry with a full correlation between SV, stochastic interest rate, and stock prices.

The contributions of the chapter can be summarized as follows:

- We introduce two methodologies (PAMC-VFI and PAMC-PWI) based on polynomial-affine structures to approximate the optimal solution of a portfolio investment problem.
- We demonstrate, via three popular continuous-time models and one discrete-time model, the accuracy and computational efficiency of our methods capturing value function (V) and optimal strategies (π). For this, we use the annualized certainty equivalent rate

(CER), the relative errors at the initial time for V and π_0 , and the mean $L2$ error for $\pi_{T/2}$.

- In particular, VFI could be three times faster, while producing 90% more accurate results than other approaches (e.g. BGSS and SGBM), in capturing optimal strategies. The efficiency could be even more significant for higher levels of precision.
- We implement the PAMC on the Heston model with a stochastic interest rate, which is not solvable in closed form. We show that PAMC delivers the highest CER, while the optimal strategy and portfolio performance are affected more by the correlation between stock price and interest rate than by the correlation between SV and interest rate.

The chapter is organized as follows: Section 2.2 introduces the problem and approximation solution methodology. Section 2.3 provides examples of models with closed-form solutions to be used for comparison purposes. The assessment of the accuracy and efficiency of our proposal is conducted in Section 2.4, where all models are studied separately. Section 2.5 provides an example of solving the optimal portfolio strategy given an unsolvable model with our methods. Lastly, Section 2.6 concludes. Section 2.7 and 2.8 provide mathematical proofs and a gold-standard method for comparison, respectively, while Section 2.9 reports all long tables and figures.

2.2 A methodology based on a polynomial-affine approximation

Let $(\Omega, \mathcal{F}, \mathbb{P})$ be a complete probability space with a right-continuous filtration $\{\mathcal{F}_t\}_{t \in [0, T]}$. The stochastic processes introduced later in the chapter are defined on this probability space. We consider an economy with a money market account (cash, M), n stocks $S = (S^{(1)}, \dots, S^{(n)})$ and an agent with constant relative risk aversion (CRRA) utility $U(W) = \frac{W^{1-\gamma}}{1-\gamma}$, $\gamma \geq 0$, $\gamma \neq 1$. The investor wants to derive an investment strategy π (percentage of wealth allocated to the stock) for the time interval $[0, T]$ that will maximize the expected utility from the terminal wealth W_T .

Assume investors can trade their desired quantity without transaction costs at the pre-determined set of re-balance $(0, \Delta t, 2\Delta t, \dots, T - \Delta t)$. We suppose the log stock price follows a generalized process with a d dimensional state variable H :

$$\begin{cases} \frac{dM_t}{M_t} = r(H_t)dt \\ d \ln S_t^{(i)} = \theta_i(H_t, \ln S_t)dt + \sum_{j=1}^n \sigma_{i,j}(H_t, \ln S_t)dB_t^{(j)}, \quad i = 1, \dots, n \\ dH_t^{(j)} = a_j(H_t^{(j)})dt + b_j(H_t^{(j)})dB_t^{(H,j)}, \quad j = 1, \dots, d \\ \langle dB_t^{(i)}, dB_t^{(H,j)} \rangle = \rho_{i,j}dt, \quad i = 1, \dots, n, \quad j = 1, \dots, d \\ \langle dB_t^{(H,i)}, dB_t^{(H,j)} \rangle = \rho_{H,i,j}dt, \quad i, j = 1, \dots, d, \end{cases} \quad (2.1)$$

where $B_t^{(i)}$, $B_t^{(H,j)}$ for $i = 1, \dots, n$, $j = 1, \dots, d$ are Brownian motions; $r(H_t)$ is the risk-free rate; and $\theta_i(H_t, \ln S_t)$, $\sigma_i(H_t, \ln S_t)$, $a_j(H_t)$, and $b_j(H_t)$ are measurable functions satisfying standard growth and Lipschitz conditions. We also assume that the covariance matrix $\Sigma = \sigma(H_t, \ln S_t)\sigma(H_t, \ln S_t)^T$ is definite positive.

The corresponding wealth process is

$$\begin{aligned} \frac{dW_t}{W_t} &= \left(r(H_t) + \sum_{i=1}^n \pi_t^{(i)} \left(\theta_i(H_t, \ln S_t) + \sum_{j=1}^n \frac{1}{2} \sigma_{i,j}^2(H_t, \ln S_t) - r(H_t) \right) \right) dt \\ &+ \sum_{i=1}^n \pi_t^{(i)} \left(\sum_{j=1}^n \sigma_{i,j}(H_t, \ln S_t) dB_t^{(j)} \right). \end{aligned} \quad (2.2)$$

The investor's problem at any time $t \in [0, T]$ can be written as

$$V(t, W, \ln S, H) = \max_{\pi_{\{s \geq t\}}} \mathbb{E}(U(W_T) | \mathcal{F}_t). \quad (2.3)$$

$V(t, W, \ln S, H)$ is the value function at time t .

Here is where the main novelty in our approach is realized. Inspired by the structure of the value function within the quadratic-affine model class,² we propose the following representation for V :

$$V(t, W, \ln S, H) = \frac{W^{1-\gamma}}{1-\gamma} [f(t, \ln S, H)]^\gamma, \quad (2.4)$$

where $f = \exp\{P_k\}$, and P_k is a polynomial of order k with time-dependent coefficients. This is equivalent to the following representation:

$$\ln(-V(t, W, \ln S, H)) = (1-\gamma) \ln W + P_k(t, \ln S, H). \quad (2.5)$$

We name our method the PAMC because of the exponential polynomial representation of the value function (2.5). This is a natural way to generalize the quadratic-affine subclass that contains the vast majority of solvable models in the literature. The Stone-Weierstrass theorem guarantees that any continuous function on a compact support can be approximated arbitrarily well in the polynomial class. Although this conflicts with the existence of unbounded paths for the processes H and $\ln S$, the small probability of such paths for finite horizons and the choice of high-order polynomials grant soundness to the methodology, as endorsed by the numerical sections. The only hard assumption is the separability of wealth W and state variables $H, \ln S$, which is compatible with all known solvable cases in the literature.³ The assumption of an exponential polynomial with separable wealth value function (2.4) still holds with intermediate consumption.

PAMC is a backward approximation method. At arbitrary re-balancing time t , PAMC uses the approximation of value function at $t + \Delta t$ to compute the optimal strategies. Based on these strategies, the value function at t can be approximated. Structure shown in Equation (2.5) allows us to estimate the value function $V(t, W, \ln S, H)$ by a polynomial regression over the time $t + \Delta t$ vector $(H, \ln S)$. Once we estimate the coefficient of the regression function, we completely specify the value function at time t . Next theorem states the representation for the optimal strategy.

²Portfolio value function is an exponential quadratic function when asset prices follow a quadratic-affine model.

³The separability of wealth and existence of intermediate consumption (i.e. money withdrawn from the portfolio) will be incorporated in future research.

Theorem 2.2.1 *The optimal allocation $\pi_t^* = (\pi_t^{(*,1)}, \dots, \pi_t^{(*,n)})$ for investors with market dynamics shown in Equation (2.1) can be approximated by the unique solution to the following system of equations:*

$$\sum_{j=1}^n g_{i,j}(t, W_t, \ln S_t, H_t) \pi_t^{(*,j)} = g_i(t, W_t, \ln S_t, H_t), \quad i = 1, \dots, n \quad (2.6)$$

where

$$\begin{aligned} g_{i,j}(t, W_t, \ln S_t, H_t) &= \gamma \left(\sum_{m=1}^n \sigma_{i,m}(H_t, \ln S_t) \sigma_{j,m}(H_t, \ln S_t) \right) \\ g_i(t, W_t, \ln S_t, H_t) &= \left(\theta_i(H_t, \ln S_t) + \frac{1}{2} \sum_{j=1}^n \sigma_{i,j}^2(H_t, \ln S_t) - r(H_t) \right) \\ &+ \sum_{j=1}^n \frac{\partial P_k(t+dt, \ln S_t, H_t)}{\partial \ln S_t^{(j)}} \left(\sum_{m=1}^n \sigma_{i,m}(H_t, \ln S_t) \sigma_{j,m}(H_t, \ln S_t) \right) \\ &+ \sum_{j=1}^d \frac{\partial P_k(t+dt, \ln S_t, H_t)}{\partial H_t^{(j)}} \left(\sum_{m=1}^n \sigma_{i,m}(H_t, \ln S_t) b_j(H_t^{(j)}) \rho_{m,j} \right). \end{aligned} \quad (2.7)$$

Under this strategy, the wealth process $W_t \geq 0$ with a unique path-wise solution.

Proof See Section 2.7.

Note that the functions $g_{i,j}$ and g_i in Equation (2.6) can then be directly and harmoniously⁴ computed by taking the derivative of the regression function obtained. Therefore, the optimal allocation at time t is a function of the current state variable and coefficients in the regression function, which can be directly computed.

At this point, the PAMC separates into two branches: the VFI and the PWI, which are described in detail in Section 2.2.1 and 2.2.2, respectively.

2.2.1 PAMC-VFI

We first introduce PAMC-VFI. Given the initial value of stock prices and state variables, the first step of the PAMC-VFI is the (forward) simulation via Euler on the dynamics in Equation (2.1). This leads to path-wise stock prices and state variables. Next, a backward approximation is conducted. Starting at the last re-balancing time $T - \Delta t$, we compute the optimal strategy via Theorem 2.2.1 for each path generated in the forward simulation. This is feasible because the value function at terminal is the utility function. Note that the investor wealth level is independent of the optimal strategy and of the value function because of its separability (2.4). Hence, we simply let the wealth level at each re-balancing time be $W_t = W_0$. With the optimal strategies, it is easy to simulate the optimal terminal wealth W_T^* and estimate the path-wise expected utilities.

⁴Other approaches separate the calibration of $g_{i,j}$ from that of g_i , hence creating an inconsistency with the primal representation of V . See Section 2.7.

We then regress the modified log expected utility $(\ln(-V(T - \Delta t, W, \ln S, H)) - (1 - \gamma) \ln W_0)$ over stock prices and state variables via a polynomial regression, creating $P_k(T - \Delta t, \ln S, H)$ in Equation (2.5). Lastly, we move backward to time $T - 2\Delta t$. The optimal strategy is found using $P_k(T - \Delta t, \ln S, H)$. The VFI method uses the Bellman equation

$$V(T - 2\Delta t, W_t, \ln S_t, H_t) = \max_{\pi_{T-\Delta t}} \mathbb{E}_t(V(T - \Delta t, W_{T-\Delta t}, \ln S_{T-\Delta t}, H_{T-\Delta t}))$$

to compute the expected utility. At each path, the wealth, stock prices, and state variables at $T - \Delta t$ are generated and substituted into the approximated value function

$$V(T - \Delta t, W, \ln S, H) \approx \frac{W^{1-\gamma}}{1-\gamma} P_k(T - \Delta t, \ln S, H).$$

The average of these simulated value functions approximates the expected utility. We follow a similar procedure at each re-balancing time until the optimal initial strategy π_0^* is obtained. Finally, we re-generate the path of stock prices and states variables. The optimal strategies at each path are obtained via Theorem 2.2.1. We simulate the portfolio wealth and evaluate the portfolio performance.⁵ We clarify the notation in Table 2.1 and illustrate the PAMC-VFI method in Algorithm 6 in detail.

Notation	Meaning
$B_t^{(j,m)}, B_t^{(j,m)}$	Brownian motion at time t in m_{th} simulated path
S_t^m	Stock price at time t in m_{th} simulated path
H_t^m	State variable, such as interest rate or volatility
n_r	Number of simulated paths
N	Number of simulations to compute expected utility for a given set (W_0, S_t^m, H_t^m)
$\hat{W}_s^{m,n}(\pi^m)$	A simulated wealth level at $s > t$, given that wealth, stock price and other, state variables at t are $W_t = W_0, S_t^m$ and H_t^m
$\hat{S}_s^{m,n}$	Simulated stock price at $s > t$
$\hat{H}_s^{m,n}$	Simulated state variable at $s > t$
$V(t, W, \ln S, H)$	Value function at time t given wealth W , stock price S , and state variable H
\hat{V}^m	Estimation of $\log(-V(t, W_t^m, H_t^m)) - (1 - \gamma) \log(W_t^m)$. Regressand in regression, superscript m, i indicate the corresponding regressor (W_t^m, H_t^m)
$L_t(H, \ln S)$	The regression function to be used to approximate $\log(-V(t, W, \ln S, H)) - (1 - \gamma) \log(W)$
π_t^m	Optimal strategy at time t given stock price and other state variables: S_t^m and H_t^m
$\pi_s^{m,n}$	Optimal strategy at time $s > t$ given stock price and other state variables $\hat{S}_s^{m,n}$ and $\hat{H}_s^{m,n}$
$\hat{V}(0, W_0, \ln S_0, H_0)$	Estimation of expected utility at time 0

Table 2.1: Notation

⁵PAMC computes expected utilities and CERs with an independent set of simulations, while BGSS and SGBM use the same set of simulations in building the optimal strategies.

2.2.2 PAMC-PWI

Next, we describe the PWI method. PAMC-PWI follows the same procedures as PAMC-VFI in the forward simulation and backward approximation at $T - \Delta t$. For an earlier re-balancing time, the approximation of the expected utility of the PWI method relies directly on (Equation (2.3))

$$V(t, W_t, \ln S_t, H_t) = \mathbb{E}_t(U(W_T)).$$

This means that, at re-balancing time t , we simulate the path of stock price $S_{s>t}$ and state variable $H_{s>t}$, and we calculate the optimal allocation $\pi_{s>t}$ via Theorem 2.2.1 and $P_k(s, \ln S, H)$, by which the optimal terminal wealth W_T is computed. The mean of simulated utilities approximates expected utility, and we regress the modified log expected utilities $\ln(-V(t, W, \ln S, H)) - (1 - \gamma) \ln W_0$ over stock prices and state variables to produce $P_k(t, \ln S, H)$. We repeat the procedure at each re-balancing time until the π_0^* is obtained. The pseudo code for the PWI method is rendered in Algorithm 7.

Differences between our methodology and BGSS from [10], which we selected for comparison, are explained in detail in Section 2.7.

2.3 Examples of problems and solutions

In this section, we provide a concise review of popular models and their implied closed-form solutions, which will be used for comparison purposes in the rest of the chapter. All of the problems maximize the expected discounted future utility of a portfolio containing one risky and one risk-free asset, where the uncertainty is driven only by the single risky asset.

We start with a reminder of the closed-form solution for Merton's model, in which the stock price process follows a GBM, which is driven by a single Wiener process with a constant return rate and volatility. We then report the solution for the Heston stock price model. The Heston stock model is like GBM, except the instantaneous variance follows a Cox-Ingersoll-Ross (CIR) process, which is itself driven by a second Wiener process correlated to the stock process. Finally, we provide the existing solution for the portfolio problem in which the log of the risky asset price follows a mean-reverting OU process. This model is commonly used to describe the evolution of commodity prices and volatility indexes. A fully closed-form solution has not yet been discovered in this case, and the portfolio problem's solution can be represented in terms of the solution of ordinary differential equations, whose numerical solution is straightforward.

2.3.1 Geometric Brownian motion

We start with Merton's case where all coefficients involved are constant. Here the dynamics are given by the following:

$$\begin{cases} \frac{dM_t}{M_t} = r dt \\ \frac{dS_t}{S_t} = (r + \lambda_S \sigma) dt + \sigma dB_t, \end{cases} \quad (2.8)$$

where λ_S captures the market price of equity risk. This is the one-dimensional case of Equation (2.1), when state variable H_t , drift $\theta(H_t, \ln S_t)$, and volatility $\sigma(H_t, \ln S_t)$ of stock are constants. The optimization problem, with power utility function, was solved by [78], and the optimal trading strategy π_t^* and the corresponding value function are given by

$$\begin{aligned}\pi_t^* &= \frac{1}{\gamma\sigma}\lambda_S \\ V(t, W) &= \frac{W^{1-\gamma}}{1-\gamma} (e^{(r+\frac{1}{2\gamma}\lambda_S^2)(T-t)})^{1-\gamma}.\end{aligned}\quad (2.9)$$

2.3.2 Stochastic volatility (SV) model

[59] provides a closed-form solution for Heston's SV model ([48]). The dynamics can be summarized by the following:

$$\begin{cases} \frac{dM_t}{M_t} = rdt \\ \frac{dS_t}{S_t} = (r + \lambda_S X_t)dt + \sqrt{X_t}dB_t^S \\ dX_t = \kappa_X(\theta_X - X_t)dt + \sigma_X \sqrt{X_t}dB_t^X \end{cases} \quad \langle B^S, B^X \rangle_t = \rho_{SX}.\quad (2.10)$$

The Heston model is a special case of Equation (2.1), with state variable H_t be the SV X_t , $\sigma(H_t, \ln S_t) = \sqrt{X_t}$ and $\theta(H_t, \ln S_t) = r + (\lambda_S - 0.5)X_t$. The optimal trading strategy and value function for a CRRA investor are given by the following:

$$\begin{aligned}V(t, W, X) &= \frac{W^{1-\gamma}}{1-\gamma} e^{\gamma a(T-t) + \gamma b(T-t)X} \\ \pi_t^* &= \frac{1}{\gamma} + \lambda_S + \rho_{SX}\sigma_X b(T-t),\end{aligned}\quad (2.11)$$

where the functions $a(\tau)$ and $b(\tau)$ are

$$\begin{aligned}a(\tau) &= \frac{2\kappa_X\theta_X}{k_4} \ln \frac{2k_2 e^{0.5(k_1+k_2)\tau}}{2k_2 + (k_1 + k_2)(e^{k_2\tau} - 1)} \\ b(\tau) &= \frac{k_3(e^{k_2\tau} - 1)}{2k_2 + (k_1 + k_2)(e^{k_2\tau} - 1)}\end{aligned}\quad (2.12)$$

with auxiliary parameters

$$\begin{aligned}k_1 &= \kappa_X + \frac{\gamma-1}{\gamma}\rho_{SX}\sigma_X\lambda_S, k_2 = \sqrt{k_1^2 - k_3k_4} \\ k_3 &= \frac{1-\gamma}{\gamma^2}\lambda_S^2, k_4 = \sigma_X^2((1-\gamma)(\rho_{SX}^2 - 1) + 1).\end{aligned}\quad (2.13)$$

2.3.3 Mean-reverting log stock price process

The last case is the exponential OU model, where the log of the stock price follows an OU process:

$$\begin{cases} \frac{dM_t}{M_t} = r_t dt \\ d \ln S_t = (\theta - A \ln S_t)dt + \sigma dB_t.\end{cases}\quad (2.14)$$

If we let $\sigma(H_t, \ln S_t) = \sigma$ and $\theta(H_t, \ln S_t) = \theta - A \ln S_t$, the generalized model (2.1) is exactly the exponential OU model. The corresponding wealth process is given by

$$\frac{dW_t}{W_t} = (r + \pi_t \beta_t) dt + \pi_t \sigma dB_t, \quad (2.15)$$

where $\beta_t = \theta - A \ln S_t + \frac{1}{2} \Sigma - r$, $\Sigma = \sigma^2$. [19] solved the optimal strategy and value function for a CRRA investor in closed form:

$$\begin{aligned} \pi_t^* &= \frac{1}{\gamma} \left(\left(\frac{1}{\Sigma} - AK(t) \right) \beta_t - AN(0, t) \right) \\ V(0, W, \ln S_0) &= \frac{W^{1-\gamma}}{1-\gamma} e^{\frac{1}{2} \beta_0^2 K(T) + N(0, T) \beta_0 + M(0, T)} \end{aligned} \quad (2.16)$$

where $K(t)$, $N(t, T)$, and $M(t, T)$ can be obtained by solving ODEs, leading to $K(t) = R_2(t)R_1^{-1}(t)$, $R = (R_1(t), R_2(t))$, and

$$\begin{aligned} R(t) &= \exp \left(\begin{pmatrix} \frac{1}{\gamma} A & -\frac{1}{\gamma} A^2 \Sigma \\ \frac{1-\gamma}{\gamma \Sigma} & -\frac{1}{\gamma} A \end{pmatrix} t \right) \begin{pmatrix} 1 \\ 0 \end{pmatrix} \\ N(T-t) &= N(t, T) = \frac{\int_0^{T-t} \theta K(s) \Phi_H(s, 0) ds}{\Phi_H(T-t, 0)} \end{aligned} \quad (2.17)$$

where

$$\frac{d\Phi_H(t, s)}{dt} = H(t) \Phi_H(t, s), \quad H(t) = \frac{1}{\gamma} (A - A^2 \Sigma K(t)) \quad \Phi_H(s, s) = 1 \quad (2.18)$$

$$M(T-t) = M(t, T) = \int_0^{T-t} \left\{ N(s) \theta_s + \frac{1}{2} K(s) A^2 \Sigma + \frac{1}{2\gamma} N(s) A^2 \Sigma N(s) + (1-\gamma)r \right\} ds. \quad (2.19)$$

2.4 Assessing accuracy and efficiency of the PAMC

In this section, we examine the accuracy and efficiency of the PAMC (VFI and PWI) by implementing GBM (Section 2.4.1), the Heston model (Section 2.4.3), exponential OU model (Section 2.4.4), and the VAR model (Section 2.4.2). We compare optimal allocation at time 0 and time $T/2$ as well as expected utility at time 0 for seven methodologies. These are as follows: PAMC-VFI and PAMC-PWI; BGSS with 2nd order and with fourth-order Taylor expansions of the utility function;⁶ the SGBM and the SGBM with log, both with 4th order Taylor expansion (SGBM-LT);⁷ and, lastly, the true theoretical results. We always generate 2×10^6 paths to evaluate the performance and employ 20 bundles in SGBM and SGBM-LT. We also report the annualized CER from all methodologies, where the CER is defined as follows:

$$U(W_0(1 + CER)^T) = V(0, W_0, \ln S_0, H_0), \quad (2.20)$$

⁶More details about the difference between BGSS 2nd and BGSS 4th can be found in [10].

⁷More details about the difference between SGBM and SGBM-LT can be found in [24].

hence describing the annualized rate of return of a risk-free asset that yields the same utility of wealth obtained from the dynamic portfolio strategy. The initial optimal allocation and expected utility is computed for all approaches (PAMC-VFI, PAMC-PWI, BGSS 2nd, BGSS 4th, SGBM, SGBM-LT, and theoretical) using their corresponding optimal allocation along paths.

To study the impact from discretization error, we implement all seven methods for different number of periods and provide the numerical weights at time 0. We show that the numerical approximation converges to the theoretical result (re-balance continuously), as the number of periods is large.

To assess the accuracy of optimal allocations at mid point, we compute the mean of the L_2 distance, which is defined as follows:

$$\text{mean of } L_2 \text{ error} = \frac{1}{N} \sqrt{\sum_{i=1}^N (\pi_{\frac{T}{2}}^{appro,i} - \pi_{\frac{T}{2}}^{*,i})^2} \quad (2.21)$$

where $\pi_{\frac{T}{2}}^{*,i}$ and $\pi_{\frac{T}{2}}^{appro,i}$ are the theoretical optimal allocation and numerical allocation at mid point respectively. Note that the error is roughly symmetric about 0, which indicates the low bias of the PAMC.

We also investigate the impact of the number of periods on the computational time for both the Heston and the exponential OU model.

Finally, we investigate the impact of the choice of polynomial degree k on the approximation quality. For the (Section 2.4.3) and exponential OU model (Section 2.4.4), we allow this degree to be unknown and let the methodology select the proper order by studying the improvement in accuracy. We do not report the results of this analysis in the case of Merton (Section 2.4.1) due to its simplicity.

2.4.1 Geometric Brownian motion

We start with the simplest model, where the stock follows a geometric Brownian motion, Equation (2.8). In this case, the value function is only dependent on time t and wealth W ; hence, the function f is in theory a constant. The chosen parameters for the GBM case are shown in Table 2.2.

Table 2.7 compares theoretical and all three numerical optimal strategies at time 0, π^* , the expected utility $V^*(0, W_0)$, the CER, and the computational time needed for all numerical methods. Table 2.7 demonstrates that all methods—PAMC (VFI and PWI), BGSS methods, SGBM, and SGBM-LT—can produce accurate results. Our methods are much faster with VFI, boasting a slight computational edge over PWI. PAMC produces similar CER values, which are slightly smaller than the CER of the theoretical result.

[Table 2.7 about here.]

2.4.2 VAR model

In this section, we consider a VAR model to describe the dynamics of the log excess return r_t^e of the risky asset and its log dividend yield d_t , which is the state variable. The dynamics

involved are given by

$$\begin{aligned} r_{t+1}^e &= a^r + b^r d_t + \epsilon_{t+1}^r \\ d_{t+1} &= a^d + b^d d_t + \epsilon_{t+1}^d, \end{aligned} \tag{2.22}$$

where $\begin{bmatrix} \epsilon_{t+1}^r \\ \epsilon_{t+1}^d \end{bmatrix} \sim N(\mu, \Sigma)$, $\mu = \begin{bmatrix} \mu^r \\ \mu^d \end{bmatrix}$ and $\Sigma = \begin{bmatrix} \sigma_r^2 & \rho\sigma_r\sigma_d \\ \rho\sigma_r\sigma_d & \sigma_d^2 \end{bmatrix}$.

R^f is the gross return of the risk-free asset, while the stock price can be written as $S_{t+1} = S_t(R^f + R_{t+1}^e)$ with $R_{t+1}^e = R^f(\exp(r_{t+1}^e) - 1)$ as the excess return. The VAR model is actually a discretized constant volatility model with an excess return following an OU process, so the PAMC is applicable. We impose borrowing and short-selling constraints on allocation: in other words, $\pi \in [0, 1]$. The model and this particular parametric setting have been widely used by other authors, including [10], [85], [39], and [24]. The parameters involved are estimated from quarterly data and shown in Table 2.3.

In the VAR model, results from a Fourier cosine series expansion (COS) (see [24])⁸ are also reported as a benchmark. The COS is a quadrature method instead of a simulation-based method, where the conditional expectation is computed with numerical integration, and the optimal strategy is obtained with the grid-searching technique. Table 2.8 shows that both PAMC methods and the COS method achieve similar expected utility and CER, which are higher than the results from BGSS and SGBM. Furthermore, the PAMC-VFI method is as fast as BGSS 2nd, both of which are the most computationally efficient and take less than a quarter of the computational time needed by other methods.

[Table 2.8 about here.]

2.4.3 Stochastic volatility (SV) model.

We implement methodologies from Heston's SV model (Section 2.3.2), and the dynamics involved are given in Equation (2.10), where the squared volatility follows a CIR process. The parameters used in the numerical example come from the source paper and are shown in Table 2.4. In the simulations, regardless of the re-balancing time interval, we simulate the path of the stock's price and volatility by the Euler scheme, with $dt = \frac{1}{60}$ to decrease the discretization error and make the result comparable to the theoretical solution of the continuous model.

Table 2.9 reports several results at time 0. Note that Equation (2.11) shows that the correct degree of P_k for this model is $k = 1$. First, we can see that the smaller the investor's risk aversion level, γ , the more precise the optimal allocation and value functions are. We can also observe that most methods—VFI, PWI, SGBM, SGBM-LT, and BGSS 4th—achieve similar accuracy, outperforming BGSS 2nd, while VFI is the most computationally efficient. Lastly, the expected utility and CER, with 10 re-balancing times, is close to the true maximum expected utility (resulting from continuous re-balancing), which means that a portfolio optimization with the Heston model does not require frequent re-balancing.

⁸Grids for numerical integration and optimal strategy searching in the COS method are identical to the set given in [24].

[Table 2.9 about here.]

Tables 2.10 compares the allocation and the CER when choosing different degrees of the P_k . Increasing the degree above 1 has a small impact on the accuracy of allocation and the CER, but it increases computational time; hence, $k = 1$ is the optimal degree, as expected.

[Table 2.10 about here.]

Table 2.11 presents the mean of the L_2 distance of optimal allocation at mid point for all methods including various degrees of P_k . The L_2 distance shows little difference for different degrees. It also demonstrates that PAMC-PWI delivers a more precise allocation at mid point compared to PAMC-VFI, both BGSSs, SGBM, and SGBM-LT.

[Table 2.11 about here.]

Next, we investigate the impact of the number of periods for a fixed time to maturity T in Figure 2.1. The number of simulations used to compute expected utility in our methods for a given set (W_t^m, S_t^m, X_t^m) was $N = 2000$.⁹ (a) shows the computational time varying with respect to the number of periods. The computational time required by PWI increases much faster than VFI, which is linear with the number of periods. This is because PWI always needs to compute the value at terminal at each period which significantly increases the computational complexity when the number of periods increases. BGSS 2nd is the most efficient, which is followed by our VFI method. BGSS 4th is slower than our VFI when the number of periods is greater than 12. (b) shows the CER obtained using all methods. Both of the PAMCs and BGSS 4th outperform BGSS 2nd in terms of CER regardless of the number of periods. SGBM and SGBM-LT obtain similar CERs as our methods when the number of periods is large.¹⁰

[Figure 2.1 about here.]

The mean L2 error of optimal allocation at mid point is shown in (c). PAMC-VFI and PAMC-PWI produce significantly more accurate allocations at mid point than BGSS, SGBM, and SGBM-LT. As the number of periods increases, the bias from discretization diminishes while the number of coefficients increases; this leads to a greater estimation error. In PAMC and SGBM, the discretization bias dominates the mean L2 error of optimal allocation at mid point, which thus decreases with the number of periods. In BGSS, the estimation error is important, and the mean L2 error of optimal allocation at mid point increases with the number of periods. Finally, we take account of these three criteria, and only PAMC-VFI achieves superior CERs and accuracy of optimal strategy while maintaining excellent efficiency given a high re-balancing frequency.

In Figure 2.2 (a), we increase the number of periods proportionally to the time to maturity T and plot the CER versus T . One can observe a decreasing CER for all methods, and the BGSS 2nd always achieves slightly smaller CER than other methods.

[Figure 2.2 about here.]

⁹We noticed little improvements in accuracy when taking $N = 200000$ at the expense of more computational time

¹⁰In all cases, CER increases with the number of periods, converging slowly to the true optimal (e.g., number of periods greater than 100).

2.4.4 Exponential Ornstein–Uhlenbeck (OU) model

The last model considered is the exponential OU model, where log prices follow a mean-reverting process. The dynamics involved are shown in Equation (2.14), and the parameters used in the numerical example are shown in Table 2.5.

Table 2.12 reports initial optimal allocations and value functions for $k = 2$. PAMC-VFI and PAMC-PWI achieve similar accuracy, with the former being more efficient and outperforming all other methods. SGBM, SGBM-LT, and BGSS 4th obtain CERs slightly higher than BGSS 2nd. Compared to the Heston model, the expected utility and CER with 10 re-balancing times is farther away from the continuous-time optimal values, which highlights the need for even more frequent re-balancing in an exponential OU model.

[Table 2.12 about here.]

Equation (2.16) illustrates that the correct degree of P_k for this model is $k = 2$. Table 2.13 confirms that both $k = 2$ and $k = 3$ give substantially better results than $k = 1$ in terms of allocation and CER. The results of Tables 2.13 are less conclusive when comparing $k = 2$ and $k = 3$. Here, one may argue that on accuracy, there is not much difference, but on speed, $k = 2$ is best.

[Table 2.13 about here.]

Table 2.14 shows the mean of L_2 distance of optimal allocation at mid point. Here, we display results from the BGSS, the SGBM, and the PAMC with different degrees of P_k . L_2 distance is much smaller when we choose the degree 2 or 3. For both VFI and PWI, choosing a smaller degree will result in a larger bias than choosing a large degree. It also shows that VFI produces more precise allocation at mid point compared to PWI. Compared with SGBM and SGBM-LT, PAMC-VFI and PAMC-PWI have a smaller mean of L_2 distance, which demonstrates the superior accuracy of the PAMC.

[Table 2.14 about here.]

As with the Heston case, we investigate the impact of the number of periods with a fixed number of simulation $N = 2000$ and time to maturity T , as shown in Figure 2.3. Figure 2.3 (a) shows how the computational time varies with the number of periods. BGSS 2nd and VFI are the most computationally efficient. PWI is faster than BGSS 4th, SGBM, and SGBM-LT when the number of periods is small but slower when the number of periods is large.

Figure 2.3 (b) displays the CER for all methods. The two PAMCs achieve similar CERs with different numbers of periods, and both are higher than the CER from BGSS, while SGBM and SGBM-LT are close to the PAMC when the number of periods is large. We also noticed that BGSS 4th performs better than BGSS 2nd when the number of periods is small, but it is surpassed as the number of periods increases. A possible explanation is that increasing the order of expansion on utility function improves accuracy when Δt is large but has more coefficients to estimate, which increases the estimation error simultaneously. Furthermore, the CER grows faster when the number of periods is small, which comes from the mean-reverting nature of prices and investors enhancing profit by reacting swiftly to the under/overpricing

opportunity. The mean of L2 distance of the optimal allocation at mid point is shown in Figure 2.3 (c). Both VFI and PWI lead to more accurate allocations at mid point. It is concluded that PAMC-VFI exhibits excellent portfolio performance, accurate optimal strategies, and a modest growth rate of computational time to the number of periods, which makes it best suited for high-frequency investors in this case.

We study the impact of time to maturity on CERs in Figure 2.2 (b). The optimal CER increases with the time to maturity T , and all numerical methods increase as well. On the other hand, the difference between PAMC and BGSS 2^{nd} increases with T . BGSS 4^{th} , SGBM, and SGBM-LT produce CER values between our methods and BGSS 2^{nd} for $T \leq 2$, but they fail to avoid negative terminal wealth when $T > 2$.

[Figure 2.3 about here.]

2.5 The Heston model with stochastic interest rate.

The superiority of PAMC in terms of accuracy and efficiency has been verified for the solvable cases: GBM, the Heston model, and the exponential OU model. In this section, we apply PAMC to an important unsolvable problem, which is a situation with fully correlated stochastic asset price, volatility, and interest rate:

$$\begin{cases} \frac{dM_t}{M_t} = r_t dt \\ \frac{dS_t}{S_t} = (r_t + \lambda_S X_t) dt + \sqrt{X_t} dB_t^S \\ dX_t = \kappa_X (\theta_X - X_t) dt + \sigma_X \sqrt{X_t} dB_t^X \\ dr_t = \kappa_r (\theta_r - r_t) dt + \sigma_r \sqrt{r_t} dB_t^r \\ \langle B^S, B^X \rangle_t = \rho_{SX} \\ \langle B^S, B^r \rangle_t = \rho_{Sr} \\ \langle B^X, B^r \rangle_t = \rho_{Xr}. \end{cases} \quad (2.23)$$

This is a specific case of the generalized model (2.1), where $n = 1$, $d = 2$, $r_t = H_t^{(1)}$, $X_t = H_t^{(2)}$, $\sigma_1(H_t, \ln S_t) = \sqrt{X_t}$, and $\theta(H_t, \ln S_t) = r_t + \lambda_S X_t$, $\lambda_S \theta_X = \lambda_X \rho_{SX} \theta_X + \lambda_r \nu \theta_r \rho_{Sr} + \lambda_S^{old} (\theta_X \sqrt{1 - \rho_{SX}^2} + \theta_r \sqrt{1 - \rho_{Sr}^2})$. The set of parameters for this model, calibrated with the daily time series of the S&P500 and 10 years to maturity bond prices (see [35]), are shown in Table 2.6.

Correlations ρ_{Sr} and ρ_{Xr} are the key parameters stopping the expected utility problem from having a closed-form solution, which is why we focus on studying their impact on the solution. Figure 2.4 (a) illustrates how the optimal strategy varies with the correlation ρ_{Sr} and ρ_{Xr} . There is little improvement when the degree of polynomial goes beyond 1, so we let $k = 1$. The optimal strategies from the PAMC-VFI and the PAMC-PWI are visually overlapped. The correlation between the interest rate and variance ρ_{Xr} has little impact on the optimal portfolio allocation. Furthermore, it is shown that the investor should allocate more wealth on the stock as the stock and interest rate become less correlated: in other word, when $|\rho_{Sr}| \approx 0$. The CER as a function of the correlation ρ_{Sr} and ρ_{Xr} is also reported: see Figure 2.4 (b). Here we continue to witness a parabolic cylindrical surface. A small correlation $|\rho_{Sr}|$ leads to a better portfolio performance.

[Figure 2.4 about here.]

Given the little impact of ρ_{Xr} , we specify $\rho_{Xr} = 0$ and compare PAMC, BGSS, and SGBM in terms of optimal strategy as well as CER and the computational time in Figure 2.5. Part (a) shows the optimal strategy across different values of ρ_{Sr} : PAMC-PWI and VFI yield the most aggressive position, followed by SGBM-LT. Note that the optimal initial strategy from SGBM and BGSS 4th are close. We plot the CER versus ρ_{Sr} in (b), and PAMC-VFI and PWI achieve the best portfolio performance. All the methods confirm that stronger portfolio performance is attainable when correlation $|\rho_{Sr}|$ is small. Furthermore, BGSS 2nd leads to a much lower CER than other methods. Part (c) in the figure shows the computational time for each method: BGSS 2nd is the most efficient, as it is slightly faster than PAMC-VFI. Thus, BGSS 2nd and PAMC-VFI have obvious advantages over other methods in terms of computational efficiency.

[Figure 2.5 about here.]

2.6 Conclusion

This chapter introduces a new numerical method for portfolio dynamic optimization in the context of EUT. Our method is based on an approximation of the value function via a polynomial-affine structure inspired by the popular family of quadratic-affine models. This allows us to estimate the value function with a polynomial fitting, which also produces closed-form optimal strategies. We divided our method into two branches: the PAMC-VFI method and the PAMC-PWI method. We implemented both methods, as well as SGBM and SGBM-LT ([24]) and the BGSS method from [10], on four models: three continuous-time models with analytical solutions (Merton's model, Heston's model, and a mean-reverting model) and a discrete-time model (VAR) popular for comparison purposes. These analyses helped us study the accuracy and efficiency of our methodologies. The four models were chosen for their popularity.

In comparison to BGSS, SGBM, and SGBM-LT, our methods are, in most cases, significantly more accurate in terms of value function and optimal allocation at initial time and at mid point. They are also better in terms of CER performance. The largest differences are found in optimal allocation at mid point. Furthermore, the PAMC-VFI maintains efficiency and accuracy as the re-balancing frequency increases, which makes it an ideal methodology for high turnover funds capturing fleeting market opportunities. We compared the result from the PAMC by selecting different degrees of the fitting polynomial; in all cases, the method finds the right degree with minimum impact from choosing higher degrees. We investigated the impact of the number of periods on the accuracy of the PAMC, confirming, as expected, more precise results as the number of periods increases.

As the PAMC is proposed to approximate the optimal strategy when closed-form solutions are not available, we also applied our methodology to an important unsolvable case. This was a fully correlated model with stochastic assets, volatility, and interest rate. In this model, the instantaneous variance and short rate followed CIR processes. We demonstrated how the correlations between stock price and interest rate and between instantaneous variance and interest rate impact the optimal strategies and portfolio performance. Moreover, the PAMC achieves

superior portfolio performance to other approximation methods while keeping the best computational efficiency.

The approximation method proposed in this chapter, PAMC, can work with an unsolvable multi-factor continuous-time model; hence, it is flexible enough in terms of rebalancing frequency and stochastic complexity to accommodate institutional and individual investors. Especially with the evolution of financial markets, many asset prices exhibit complex structures in their dynamics, while the availability of data permits a higher frequency of trading. Like most approximation methods for the dynamic portfolio choice problem, the PAMC relies on the assumption of a frictionless market, where no transaction cost and no market impact exist. Furthermore, the method can be extended to more general utility families (e.g., hyperbolic absolute risk aversion) and can entertain derivatives-based portfolios needed for market completion. These are topics for future research.

2.7 Proof of Theorem 2.2.1.

According to the Bellman equation, the value function can be rewritten as,

$$\begin{aligned} V(t, W, \ln S, H) &= \mathbb{E}_t(V(t + dt, W_{t+dt}, \ln S_{t+dt}, H_{t+dt}) \mid W, \ln S, H) \\ &= \max_{\pi_t} \mathbb{E}_t(V(t + dt, W_{t+dt}, \ln S_{t+dt}, H_{t+dt}) \mid W, \pi, \ln S, H). \end{aligned} \quad (2.24)$$

We expand $V(t + dt, W_{t+dt}, \ln S_{t+dt}, H_{t+dt})$ at $t + dt$ in terms of all the variables.

$$\begin{aligned} V(t + dt, W_{t+dt}, \ln S_{t+dt}, H_{t+dt}) &= V(t + dt, W_t, \ln S_t, H_t) + V_{W_t}(t + dt, W_t, \ln S_t, H_t)dW_t \\ &+ \frac{1}{2} V_{W_t W_t}(t + dt, W_t, \ln S_t, H_t)(dW_t)^2 \\ &+ \sum_{i=1}^n (V_{\ln S_t^{(i)}}(t + dt, W_t, \ln S_t, H_t)d \ln S_t^{(i)}) + \sum_{i=1}^n (V_{H_t^{(i)}}(t + dt, W_t, \ln S_t, H_t)dH_t^{(i)}) \\ &+ \frac{1}{2} \sum_{i,j=1}^n (V_{\ln S_t^{(i)} \ln S_t^{(j)}}(t + dt, W_t, \ln S_t, H_t)d \ln S_t^{(i)} d \ln S_t^{(j)}) \\ &+ \frac{1}{2} \sum_{i,j=1}^d (V_{H_t^{(i)} H_t^{(j)}}(t + dt, W_t, \ln S_t, H_t)dH_t^{(i)} dH_t^{(j)}) + \sum_{i=1}^n (V_{W_t \ln S_t^{(i)}}(t + dt, W_t, \ln S_t, H_t)dW_t d \ln S_t^{(i)}) \\ &+ \sum_{i=1}^d (V_{W_t H_t^{(i)}}(t + dt, W_t, \ln S_t, H_t)dW_t dH_t^{(i)}) \\ &+ \sum_{i=1}^n \sum_{j=1}^d (V_{\ln S_t^{(i)} H_t^{(j)}}(t + dt, W_t, \ln S_t, H_t)d \ln S_t^{(i)} dH_t^{(j)}) + o(dt). \end{aligned} \quad (2.25)$$

Substituting dW_t , $d \ln S_t$, dH_t which can be found in Equation (2.1), taking conditional expectation on both sides, and rewriting $V(t, W_t, \ln S_t, H_t)$ in a quadratic form with respect to π leads to

$$\begin{aligned}
V(t, W_t, \ln S_t, H_t) &= \max_{\pi_t} \left(\sum_{i,j=1}^n f_{i,j}(t, W_t, \ln S_t, H_t) \pi_t^{(i)} \pi_t^{(j)} + \sum_{i=1}^n f_i(t, W_t, \ln S_t, H_t) \pi_t^{(i)} + f_0(t, W_t, \ln S_t, H_t) \right) \\
f_{i,j}(t, W_t, \ln S_t, H_t) &= \frac{1}{2} V_{W_t W_t}(t + dt, W_t, \ln S_t, H_t) W_t^2 \left(\sum_{m=1}^n \sigma_{i,m}(H_t, \ln S_t) \sigma_{j,m}(H_t, \ln S_t) \right) dt \\
f_i(t, W_t, \ln S_t, H_t) &= V_{W_t}(t + dt, W_t, \ln S_t, H_t) W_t \left(\theta_i(H_t, \ln S_t) + \frac{1}{2} \sum_{j=1}^n \sigma_{i,j}^2(H_t, \ln S_t) - r(H_t) \right) dt \\
&\quad + \sum_{j=1}^n V_{W_t \ln S_t^{(j)}}(t + dt, W_t, \ln S_t, H_t) W_t \left(\sum_{m=1}^n \sigma_{i,m}(H_t, \ln S_t) \sigma_{j,m}(H_t, \ln S_t) \right) dt \\
&\quad + \sum_{j=1}^d V_{W_t H_t^{(j)}}(t + dt, W_t, \ln S_t, H_t) W_t b_j(H_t^{(j)}) \sum_{m=1}^n \sigma_{i,m}(H_t, \ln S_t) \rho_{m,j} dt \\
f_0(t, W_t, \ln S_t, H_t) &= V(t + dt, W_t, \ln S_t, H_t) + V_{W_t}(t + dt, W_t, \ln S_t, H_t) W_t r dt \\
&\quad + \sum_{i=1}^n V_{\ln S_t^{(i)}}(t + dt, W_t, \ln S_t, H_t) \theta_i(H_t, \ln S_t) dt \\
&\quad + \sum_{i=1}^d \left(V_{H_t^{(i)}}(t + dt, W_t, \ln S_t, H_t) a_i(H_t^{(i)}) \right) dt \\
&\quad + \sum_{i,j=1}^d \left(\frac{1}{2} V_{H_t^{(i)} H_t^{(j)}}(t + dt, W_t, \ln S_t, H_t) b_i(H_t^{(i)}) b_j(H_t^{(j)}) \rho_{H,i,j} \right) dt \\
&\quad + \frac{1}{2} \sum_{i,j=1}^n V_{\ln S_t^{(i)} \ln S_t^{(j)}}(t + dt, W_t, \ln S_t, H_t) \left(\sum_{m=1}^n \sigma_{i,m}(H_t, \ln S_t) \sigma_{j,m}(H_t, \ln S_t) \right) dt \\
&\quad + \sum_{i=1}^n \sum_{j=1}^d V_{\ln S_t^{(i)} H_t^{(j)}}(t + dt, W_t, \ln S_t, H_t) \left(\sum_{m=1}^n \sigma_{i,m}(H_t, \ln S_t) b_j(H_t^{(j)}) \rho_{m,j} \right) dt.
\end{aligned} \tag{2.26}$$

We assume a sufficiently small dt so that $o(dt)$ terms are omitted when taking conditional expectations. The optimal allocation is given by the solution to the system of equations:

$$\sum_{j=1}^n 2f_{i,j}(t, W_t, \ln S_t, H_t) \pi_t^{(*,j)} = -f_i(t, W_t, \ln S_t, H_t), \quad i = 1, \dots, n. \tag{2.27}$$

With the representation of the value function in Equation (2.4) and assuming that $f(t, \ln S, H) = \exp(P_k(t, \ln S, H))$, the derivatives of value function with respect to each stock and state variable can be rewritten as,

$$\begin{aligned}
V_W(t+dt, W_t, \ln S_t, H_t) &= W_t^{-\gamma} \exp(P_k(t+dt, \ln S_t, H_t)) \\
V_{WW}(t+dt, W_t, \ln S_t, H_t) &= -\gamma W_t^{-\gamma-1} \exp(P_k(t+dt, \ln S_t, H_t)) \\
V_{W \ln S_t^{(i)}}(t+dt, W_t, \ln S_t, H_t) &= W_t^{-\gamma} \exp(P_k(t+dt, \ln S_t, H_t)) \frac{\partial P_k(t+dt, \ln S_t, H_t)}{\partial \ln S_t^{(i)}} \\
V_{WH_t^{(i)}}(t+dt, W_t, \ln S_t, H_t) &= W_t^{-\gamma} \exp(P_k(t+dt, \ln S_t, H_t)) \frac{\partial P_k(t+dt, \ln S_t, H_t)}{\partial H_t^{(i)}}.
\end{aligned} \tag{2.28}$$

Substituting (2.28) into (2.27), the optimal strategy can be approximated as follows:

$$\begin{aligned}
\sum_{j=1}^n g_{i,j}(t, W_t, \ln S_t, H_t) \pi_t^{(*,j)} &= g_i(t, W_t, \ln S_t, H_t), \quad i = 1, \dots, n \\
g_{i,j}(t, W_t, \ln S_t, H_t) &= \gamma \left(\sum_{m=1}^n \sigma_{i,m}(H_t, \ln S_t) \sigma_{j,m}(H_t, \ln S_t) \right) \\
g_i(t, W_t, \ln S_t, H_t) &= \left(\theta_i(H_t, \ln S_t) + \frac{1}{2} \sum_{j=1}^n \sigma_{i,j}^2(H_t, \ln S_t) - r(H_t) \right) \\
&\quad + \sum_{j=1}^n \frac{\partial P_k(t+dt, \ln S_t, H_t)}{\partial \ln S_t^{(j)}} \left(\sum_{m=1}^n \sigma_{i,m}(H_t, \ln S_t) \sigma_{j,m}(H_t, \ln S_t) \right) \\
&\quad + \sum_{j=1}^d \frac{\partial P_k(t+dt, \ln S_t, H_t)}{\partial H_t^{(j)}} \left(\sum_{m=1}^n \sigma_{i,m}(H_t, \ln S_t) b_j(H_t^{(j)}) \rho_{m,j} \right).
\end{aligned} \tag{2.29}$$

The existence and uniqueness of the approximation, $\pi_t^{(*,j)}$ is ensured by the invertibility of the matrix $\sigma(H_t, \ln S_t) \sigma(H_t, \ln S_t)^T$, together with the differentiability of the polynomial P_k . Note π^* does not depend on W_t , hence the drift and volatility of the wealth process are linear in W_t , and they both satisfy the conditions in Proposition 1.2 in [60], therefore the wealth process has a positive path-wise unique solution:

$$\begin{aligned}
dW_t &= \left(W_t r(H_t) + \sum_{i=1}^n \frac{1}{\gamma} W_t a(t, \ln S_t, H_t) \left(\theta_i(H_t, \ln S_t) + \sum_{j=1}^n \frac{1}{2} \sigma_{i,j}^2(H_t, \ln S_t) - r(H_t) \right) \right) dt \\
&\quad + \sum_{i=1}^n \frac{1}{\gamma} W_t a(t, \ln S_t, H_t) \left(\sum_{j=1}^n \sigma_{i,j}(H_t, \ln S_t) dB_t^{(j)} \right).
\end{aligned}$$

2.8 Relation to the BGSS

The main difference between the our method and BGSS centralize on the procedure to obtain the optimal allocation.

In our method, we expand the value function with respect to all state variables up to second order in Equation (2.25) and optimal allocation can be computed by Equation (2.6). At time t , we compute the optimal allocation with estimated value function at $t + \Delta t$ and use it to estimate value function at time t by a regression function. We move backward and obtain the value function and optimal allocation at each period. There are two ways to obtain the corresponding expected utility $V(t, W_0, \ln S_t^m, H_t^m)$ given state variable (W_0, S_t^m, H_t^m) . The first (VFI) approach is to make use of the estimation of function $V(t + \Delta t, W, \ln S, H)$ obtained from last step. After computing the optimal allocation π_t^m , we generate $\hat{W}_{t+\Delta t}^{m,n}(\pi_t^m), \hat{S}_{t+\Delta t}^{m,n}, \hat{H}_{t+\Delta t}^{m,n}$. $V(t, W_0, \ln S_t^m, H_t^m)$ can be estimated by

$$\hat{V}(t, W_0, S_t^m, X_t^m) \approx \frac{1}{N} \sum_{n=1}^N V(t + \Delta t, \hat{W}_{t+\Delta t}^{m,n}(\pi_t^m), \hat{S}_{t+\Delta t}^{m,n}, \hat{H}_{t+\Delta t}^{m,n}). \quad (2.30)$$

An alternative (PWI) way is to generate the optimal terminal wealth (at T). We set $\hat{W}_T^{m,n} = W_0, \hat{S}_T^{m,n} = S_T^m, \hat{H}_T^{m,n} = H_T^m$. For time $s \geq t$, optimal allocation $\pi_s^{m,n}$ can be obtained by $V(s + \Delta t, W, \ln S, H)$ which has been estimated in previous step. We simulate $\hat{S}_s^{m,n}, \hat{H}_s^{m,n}$ and compute the corresponding optimal wealth $\hat{W}_s^{m,n}$. The value $V(t, W_t^m, \ln S_t^m, H_t^m)$ can be estimated by

$$\hat{V}(t, W_0, S_t^m, H_t^m) \approx \frac{1}{N} \sum_{n=1}^N U(\hat{W}_T^{m,n}). \quad (2.31)$$

After computing the value of $V(t, W_0, \ln S_t^m, H_t^m)$, we regress it over (W_0, S_t^m, H_t^m) and obtain an approximation for $V(t, W, \ln S, H)$.

BGSS expands the value function solely with respect to the wealth level, and this is up to order four. For simplicity, we show the expansion of the value function to the second order in Equation (2.32). Instead of estimating the value function, the authors construct two regression functions, one over f_1 and the second over f_2 , while the optimal allocation is computed by their ratio. One possible flaw of such approach is that by estimating f_1 and f_2 separately, one may obtain incompatible results violating the intrinsic relation between these two functions, as they are both descendants (plain derivatives) of the value function. We avoid this by estimating directly the value function and then differentiating to produce f_1 and f_2 .

$$\begin{aligned} V(t, W_t, \pi, \ln S_t, H_t) &= f_1(t, W_t, \ln S_t, H_t)\pi^2 + f_2(t, W_t, \ln S_t, H_t)\pi + f_3(t, W_t, \ln S_t, H_t) \\ f_1(t, W_t, \ln S_t, H_t) &= \frac{1}{2} \mathbb{E}_t[V_{W_t W_t}(t + dt, (1 + r(H_t)dt)W_t, \ln S_{t+dt}, X_{t+dt})W_t^2 \sigma^2(H_t, \ln S_t)(dB_t)^2] \\ f_2(t, W_t, \ln S_t, H_t) &= \mathbb{E}_t[V_{W_t}(t + dt, (1 + r(H_t)dt)W_t, \ln S_{t+dt}, H_{t+dt})W_t(\theta(H_t, \ln S_t) \\ &\quad + \frac{1}{2} \sigma^2(H_t, \ln S_t) - r(H_t))dt] \\ f_3(t, W_t, \ln S_t, H_t) &= \mathbb{E}_t[V(t + dt, (1 + r(H_t)dt)W_t, \ln S_{t+dt}, H_{t+dt})] \\ \pi_t^* &= -\frac{f_2(t, W_t, \ln S_t, H_t)}{2f_1(t, W_t, \ln S_t, H_t)}. \end{aligned} \quad (2.32)$$

The second difference is that we assume a functional structure on the value function, i.e. exponential polynomial, followed by a log transformation. We use a polynomial of $(\ln S, H)$ to

estimate the transformed value function $\ln(-V(t, W, \ln S, H)) - (1 - \gamma) \ln W$. However, BGSS directly estimate the derivatives of the value function without any transformation.

2.9 Tables and Figures.

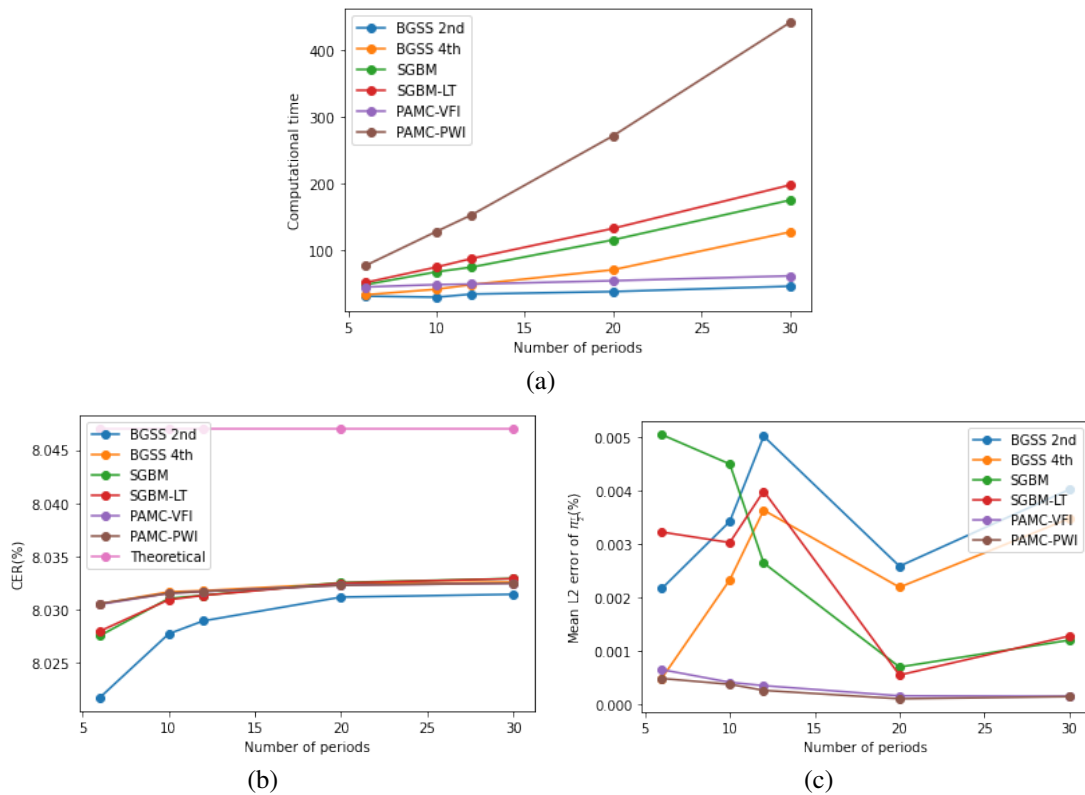


Figure 2.1: Different periods (Heston), (a) shows computational time versus number of period. (b) shows annualized certainty equivalent rate (CER) versus number of period. (c) shows mean L2 distance of optimal allocations at mid point versus number of period. We set $\gamma = 4$ and use other parameters in table 2.5 to produce above plots.

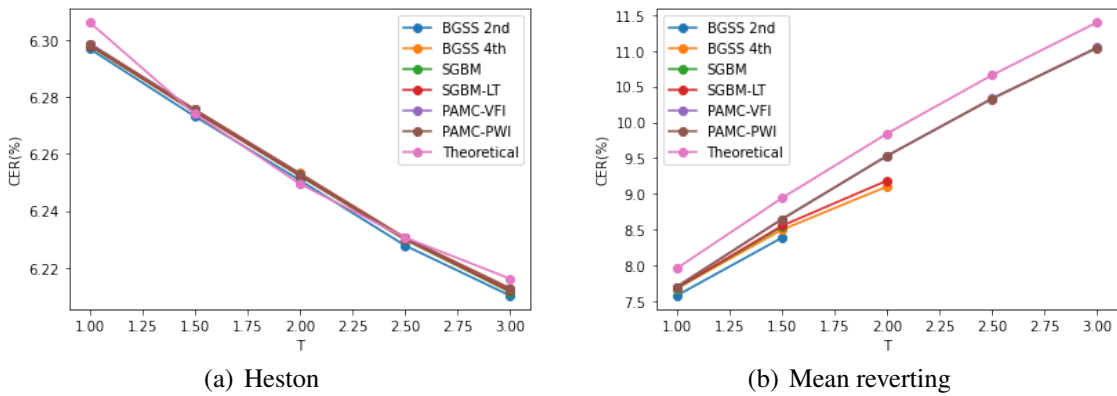


Figure 2.2: CER versus time to maturity T , $\gamma = 10$

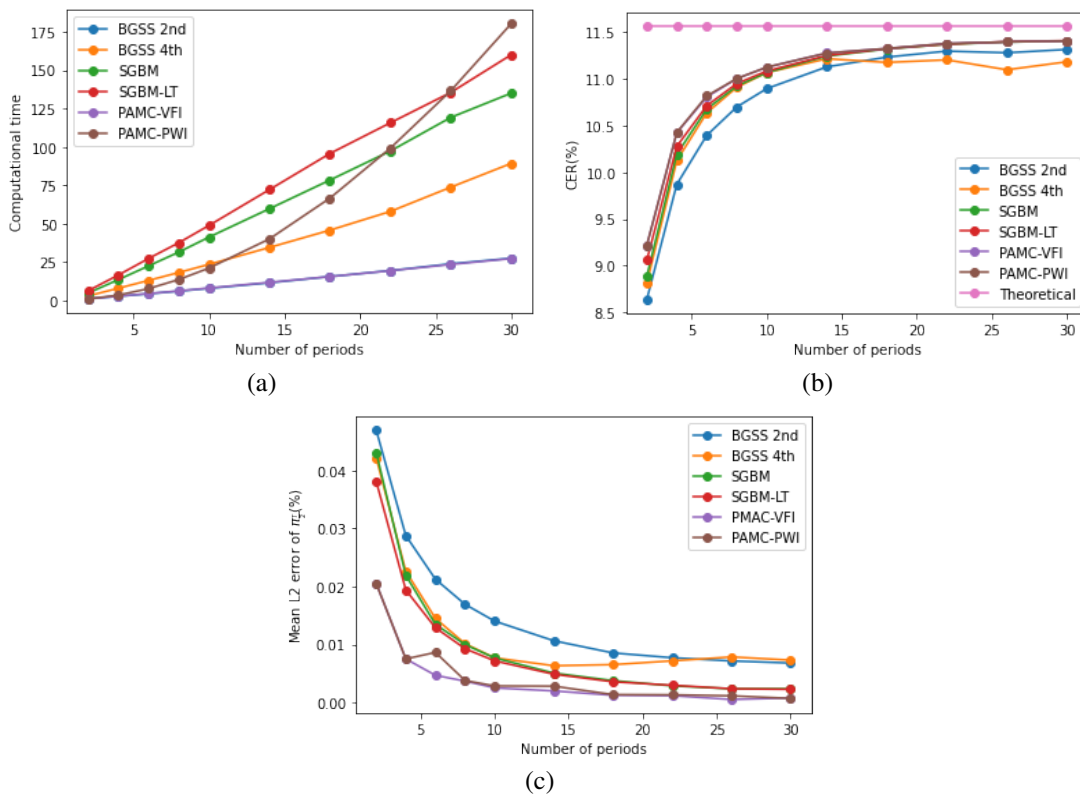


Figure 2.3: Different periods (Mean-reverting Model), (a) shows computational time versus number of period. (b) shows annualized certainty equivalent rate (CER) versus number of period. (c) shows mean L2 distance of optimal allocations at mid point versus number of period. We set $\gamma = 4$ and use other parameters in table 2.5 to produce above plots.

Algorithm 6: VFI

Input: S_0, W_0, H_0 , Initial value for all processes involved

Output: Optimal current trading strategy π_0^* and expected utility $\hat{V}(0, W_0, \ln S_0, H_0)$

- 1 initialization;
- 2 Generating n_r paths of $B_t^{(j,m)}, B_t^{(j,m)}, S_t^m, H_t^m, m = 1 \dots n_r$;
- 3 **if** $t = T - \Delta t$ **then**
- 4 **for** $m = 1 \dots n_r$ **do**
- 5 Directly compute optimal allocation $\pi_{T-\Delta t}^m$ with Equation (2.6) where the derivative of value function w.r.t state variable is 0 at time T ;
- 6 **for** $n = 1 \dots N$ **do**
- 7 Simulate wealth $\hat{W}_T^{m,n}(\pi_{T-\Delta t}^m)$ at the terminal time given that wealth, stock price allocation and other state variables at $T - \Delta t$ are $W_0, S_{T-\Delta t}^m, \pi_{T-\Delta t}^m$ and $H_{T-\Delta t}^m$;
- 8 Compute $\hat{v}^m = \ln(-\frac{1}{N} \sum_{n=1}^N U(\hat{W}_T^{m,n}(\pi_{T-\Delta t}^m))) - (1 - \gamma) \ln W_0$;
- 9 Regress \hat{v}^m over the polynomial of $(H_{T-\Delta t}^m, \ln S_{T-\Delta t}^m)$, and obtain the function $L_{T-\Delta t}(H, \ln S)$;
- 10 **for** $t = T - 2\Delta t$ **to** Δt **do**
- 11 **for** $m = 1 \dots n_r$ **do**
- 12 Using the estimation of transformed value function $L_{t+\Delta t}(H, \ln S)$ from last step, compute optimal allocation π_t^m with Equation (2.6) given S_t^m , and H_t^m ;
- 13 **for** $n = 1 \dots N$ **do**
- 14 Simulate wealth $\hat{W}_{t+\Delta t}^{m,n}(\pi_t^m)$, $\hat{S}_{t+\Delta t}^{m,n}$ and $\hat{H}_{t+\Delta t}^{m,n}$ given that wealth, stock price, allocation and other state variables at t are W_0, S_t^m, π_t^m and H_t^m ;
- 15 Compute $\hat{v}^m = \ln(\frac{1}{N} \sum_{n=1}^N (W_{t+\Delta t}^{m,n}(\pi_t^m))^{1-\gamma} \exp(L_{t+\Delta t}(\hat{H}_{t+\Delta t}^{m,n}, \ln \hat{S}_{t+\Delta t}^{m,n}))) - (1 - \gamma) \ln W_0$;
- 16 ; ;
- 16 Regress \hat{v}^m over the polynomial of $(H_t^m, \ln S_t^m)$, to produce the function $L_t(H, \ln S)$;
- 17 **if** $t = 0$ **then**
- 18 Compute π_0^* with $L_{\Delta t}(H, \ln S)$ and Equation (2.6) ;
- 19 Generate new paths of $S_t^z, H_t^z, z = 1 \dots N_0$, use the estimation of transformed value function $L_t(H, \ln S)$ to compute corresponding optimal allocation π_t^z and calculate the optimal terminal wealth W_T^z . The expected utility is ,
- 20
$$\hat{V}(0, W_0, \ln S_0, H_0) = \frac{1}{N_0} \sum_{n=1}^{N_0} U(W_T^z);$$
- 20 **return** $\pi_0^*, \hat{V}(0, W_0, \ln S_0, H_0)$;

Algorithm 7: PWI

Input: S_0, W_0, H_0 , initial values for all processes involved

Output: Optimal current trading strategy π_0^* and expected utility $\hat{V}(0, W_0, \ln S_0, H_0)$

1 initialization;

2 Generating n_r paths of $B_t^{(j,m)}, B_t^{(j,m)}, S_t^m, H_t^m, m = 1 \dots n_r$;

3 **if** $t = T - \Delta t$ **then**

4 **for** $m = 1 \dots n_r$ **do**

5 Directly compute optimal allocation $\pi_{T-\Delta t}^m$ with Equation (2.6) where the derivative of value function w.r.t state variable is 0 at time T ;

6 **for** $n = 1 \dots N$ **do**

7 Simulate wealth $\hat{W}_T^{m,n}(\pi_{T-\Delta t}^m)$ at the terminal given that wealth, stock price, allocation and other state variables at $T - \Delta t$ are $W_0, S_{T-\Delta t}^m, \pi_{T-\Delta t}^m$ and $H_{T-\Delta t}^m$;

8 Compute $\hat{v}^m = \ln(\frac{1}{N} \sum_{n=1}^N U(\hat{W}_T^{m,n}(\pi_{T-\Delta t}^m))) - (1 - \gamma) \ln(W_0)$;

9 Regress \hat{v}^m over the polynomial of $(H_{T-\Delta t}^m, \ln S_{T-\Delta t}^m)$, producing the function $L_{T-\Delta t}(H, \ln S)$

10 **for** $t = T - 2\Delta t$ **to** Δt **do**

11 **for** $m = 1 \dots n_r$ **do**

12 **for** $n = 1 \dots N$ **do**

13 Set $\hat{W}_t^{m,n} = W_0, \hat{S}_t^{m,n} = S_t^m$ and $\hat{H}_t^{m,n} = H_t^m$;

14 **for** $s = t$ **to** $T - \Delta t$ **do**

15 Using the estimation of transformed value function $L_{s+\Delta t}(H, \ln S)$ from previous step, compute optimal allocation $\pi_s^{m,n}$ with Equation(2.6), given $\hat{S}_s^{m,n}$ and $\hat{H}_s^{m,n}$;

16 Simulate wealth $\hat{W}_{s+\Delta t}^{m,n}, \hat{S}_{s+\Delta t}^{m,n}$ and $\hat{H}_{s+\Delta t}^{m,n}$ given the wealth, stock price allocation and other state variables at t are $\hat{W}_s^{m,n}, \hat{S}_s^{m,n}, \pi_s^{m,n}$ and $\hat{H}_s^{m,n}$;

17 Obtain terminal wealth $\hat{W}_T^{m,n}$. Compute

$\hat{v}^m = \ln(\frac{1}{N} \sum_{n=1}^N U(\hat{W}_T^{m,n})) - (1 - \gamma) \ln(W_0)$;

18 Regress \hat{v}^m over the polynomial of $(H_t^m, \ln S_t^m)$, and obtain the function $L_t(H, \ln S)$;

19 **if** $t = 0$ **then**

20 Compute π_0^* with $L_{\Delta t}(H, \ln S)$ and Equation (2.6) ;

21 Generate new paths of $S_t^z, H_t^z, z = 1 \dots N_0$, use the estimation of transformed value function $L_t(H, \ln S)$ to compute corresponding optimal allocation π_t^z and calculate the optimal terminal wealth W_T^z . The expected utility is ,

$$\hat{V}(0, W_0, \ln S_0, H_0) = \frac{1}{N_0} \sum_{n=1}^{N_0} U(W_T^z);$$

22 **return** $\pi_0^*, \hat{V}(0, W_0, \ln S_0, H_0)$;

Table 2.2: Parameter value for Merton's problem

Parameter	Value	Parameter	Value
T	1	σ	0.2
r	0.05	λ_S	0.22
Δ_t	0.1	<i>period</i>	10
S_0	1.0	W_0	1
N	2000	n_r	100
N_0	2000000		

Table 2.3: Parameter value for VAR model

Parameter	Value	Parameter	Value
T	10	Δ_t	0.25
R^f	$1.06^{0.25}$	<i>period</i>	40
a_r	0.277	b_r	0.060
a_d	-0.155	b_d	0.958
μ^r	0	μ^d	0
σ_r^2	0.0060	σ_d^2	0.0049
$\rho\sigma_r\sigma_d$	-0.0051	d_0	-3.6905
S_0	1.0	W_0	1
N	2000	n_r	100
N_0	2000000		

Table 2.4: Parameter value for the SV case, after [34]

Parameter	Value	Parameter	Value
T	1	ρ_{SV}	-0.54
θ_v	0.0257	σ_v	0.26
κ_v	1.33	λ_S	2.45
Δ_t	0.1	<i>period</i>	10
r	0.05	v_0	0.04
S_0	1.0	W_0	1
N	2000	n_r	100
N_0	2000000		

Table 2.5: Parameter value for mean-reverting model, after [19]

Parameter	Value	Parameter	Value
T	1	A	1
θ_t	0.1	σ	0.02
Δ_t	0.1	<i>period</i>	10
r_t	0.05	W_0	1
S_0	1.0	N	2000
n_r	100	N_0	2000000

Table 2.6: Parameter value for the Heston model with stochastic interest rate, after [35]

Parameter	Value	Parameter	Value
T	1	ρ_{SX}	-0.7
θ_X	0.0199	σ_X	0.2941
κ_X	2.8278	λ_S^{old}	2.2472
λ_X	-6.6932	λ_r	-0.1132
θ_r	0.0192	σ_r	0.0566
κ_r	0.1300	ν	-0.5973
Δ_t	0.1	<i>period</i>	10
r_0	θ_r	X_0	θ_X
S_0	1.0	W_0	1
N	2000	n_r	100
N_0	2000000		

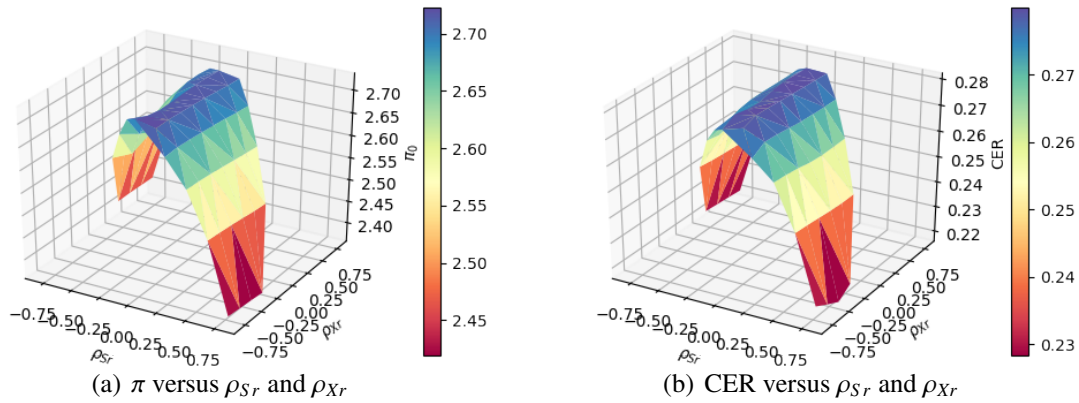


Figure 2.4: The optimal strategy and CER across different value of ρ_{Sr} and ρ_{Xr} (Heston model with stochastic interest rate), $\gamma = 4$. Results from PAMC-VFI and PAMC-PWI are visually overlapped.

Table 2.7: Results for GBM

	$\gamma = 2.0$	$\gamma = 4.0$	$\gamma = 6.0$	$\gamma = 8.0$	$\gamma = 10.0$
Theoretical					
Weights (π_0^*)	0.550	0.275	0.183	0.138	0.110
Expected utility ($V^*(0)$)	-0.940	-0.282	-0.153	-0.099	-0.070
CER (%)	6.41	5.77	5.56	5.45	5.38
BGSS 2nd					
Weights (π_0^{BGSS})	0.554	0.277	0.185	0.139	0.111
Relative error(%) in π	0.7	0.7	0.7	0.7	0.7
Expected utility ($V^{BGSS}(0)$)	-0.940	-0.282	-0.153	-0.099	-0.069
Relative error(%) in V	0.02	0.05	0.07	0.10	0.12
CER (%)	6.38	5.75	5.54	5.43	5.37
Computational time (seconds)	7.1	7.0	7.5	7.6	7.1
BGSS 4th					
Weights (π_0^{BGSS})	0.556	0.278	0.185	0.139	0.111
Relative error(%) in π	1.0	1.1	1.2	1.2	1.2
Expected utility ($V^{BGSS}(0)$)	-0.940	-0.282	-0.153	-0.099	-0.069
Relative error(%) in V	0.02	0.05	0.07	0.10	0.12
CER (%)	6.38	5.75	5.54	5.43	5.37
Computational time (seconds)	17.1	17.6	17.4	17.4	17.5
SGBM					
Weights (π_0^{BGSS})	0.554	0.277	0.185	0.139	0.111
Relative error(%) in π	0.8	0.8	0.8	0.8	0.8
Expected utility ($V^{BGSS}(0)$)	-0.940	-0.282	-0.153	-0.099	-0.069
Relative error(%) in V	0.009	0.03	0.05	0.08	0.10
CER (%)	6.39	5.75	5.54	5.43	5.37
Computational time (seconds)	16.0	16.7	16.1	16.6	16.6
SGBM-LT					
Weights (π_0^{SGBM})	0.554	0.277	0.185	0.139	0.111
Relative error(%) in π	0.7	0.9	0.9	0.9	0.9
Expected utility ($V^{SGBM}(0)$)	-0.940	-0.282	-0.153	-0.099	-0.069
Relative error(%) in V	0.02	0.05	0.07	0.10	0.12
CER (%)	6.39	5.75	5.54	5.43	5.37
Computational time (seconds)	20.0	21.7	20.1	21.6	21.6
PAMC (VFI)					
Weights (π_0^{SGBM})	0.550	0.275	0.183	0.138	0.110
Relative error (%) in π	0	0	0	0	0
Expected utility ($V^{SGBM}(0)$)	-0.940	-0.282	-0.153	-0.099	-0.069
Relative error (%) in V	0.01	0.07	0.07	0.11	0.10
CER (%)	6.38	5.75	5.54	5.43	5.37
Computational time (seconds)	6.4	7.8	7.9	8.1	8.1
PAMC(PWI)					
Weights (π_0^{SGBM})	0.550	0.275	0.183	0.138	0.110
Relative error (%) in π	0	0	0	0	0
Expected utility ($V^{SGBM}(0)$)	-0.940	-0.282	-0.153	-0.099	-0.069
Relative error (%) in V	0.01	0.04	0.06	0.11	0.17
CER (%)	6.39	5.75	5.54	5.43	5.36
Computational time (seconds)	21.4	21.8	21.9	21.1	21.8

Table 2.8: Results for VAR model

	$\gamma = 2.0$	$\gamma = 4.0$	$\gamma = 6.0$	$\gamma = 8.0$	$\gamma = 10.0$
COS					
Weights (π_0^{COS})	1.0	0.835	0.725	0.640	0.570
Expected utility ($V^{COS}(0)$)	-0.414	-0.0270	-0.00364	-0.000650	-0.000136
CER (%)	9.23	8.74	8.34	8.01	7.74
Computational time (seconds)	325.9	334.7	334.9	334.9	334.7
BGSS 2nd					
Weights (π_0^{BGSS})	1.0	0.763	0.608	0.486	0.401
Expected utility ($V^{BGSS}(0)$)	-0.414	-0.0272	-0.00388	-0.000762	-0.000172
CER (%)	9.23	8.71	8.20	7.76	7.45
Computational time (seconds)	55.3	56.7	56.5	53.6	53.2
BGSS 4th					
Weights (π_0^{BGSS})	1.0	0.831	0.693	0.577	0.484
Expected utility ($V^{BGSS}(0)$)	-0.414	-0.0270	-0.00372	-0.000690	-0.000151
CER (%)	9.23	8.74	8.30	7.92	7.61
Computational time (seconds)	109.1	273.4	320.1	325.8	346.9
SGBM					
Weights (π_0^{SGBM})	1.0	0.833	0.713	0.603	0.508
Expected utility ($V^{SGBM}(0)$)	-0.414	-0.0270	-0.00365	-0.000679	-0.000150
CER (%)	9.23	8.74	8.34	7.94	7.62
Computational time (seconds)	230.8	230.7	234.1	235.6	231.6
SGBM-LT					
Weights (π_0^{SGBM})	1.0	0.842	0.729	0.639	0.550
Expected utility ($V^{SGBM}(0)$)	-0.414	-0.0270	-0.00364	-0.000653	-0.000141
CER (%)	9.23	8.74	8.34	8.00	7.70
Computational time (seconds)	253.2	256.6	260.5	261.1	265.1
PAMC (VFI)					
Weights (π_0^{PAMC})	1.0	0.853	0.741	0.656	0.586
Expected utility ($V^{PAMC}(0)$)	-0.414	-0.0270	-0.00365	-0.000650	-0.000136
CER (%)	9.23	8.74	8.34	8.01	7.74
Computational time (seconds)	56.3	58.2	58.2	57.9	58.1
PAMC (PWI)					
Weights (π_0^{PAMC})	1.0	0.837	0.722	0.641	0.572
Expected utility ($V^{PAMC}(0)$)	-0.414	-0.0270	-0.00365	-0.000651	-0.000136
CER (%)	9.23	8.74	8.34	8.01	7.74
Computational time (seconds)	482.4	476.8	475.9	475.1	475.1

Table 2.9: Results for stochastic volatility

	$\gamma = 2.0$	$\gamma = 4.0$	$\gamma = 6.0$	$\gamma = 8.0$	$\gamma = 10.0$
Theoretical					
Weights (π_0^*)	1.287	0.660	0.442	0.335	0.268
Expected utility ($V^*(0)$)	-0.902	-0.264	-0.142	-0.091	-0.064
CER (%)	10.88	8.05	7.08	6.60	6.31
BGSS 2 nd					
Weights (π_0^{BGSS})	1.267	0.648	0.435	0.327	0.263
Relative error (%) in π	1.52	1.93	2.09	2.16	2.21
Expected utility ($V^{BGSS}(0)$)	-0.902	-0.264	-0.142	-0.091	-0.064
Relative error (%) in V	0.03	0.07	0.10	0.13	0.16
CER (%)	10.84	8.02	7.06	6.58	6.29
Computational time (seconds)	20.3	21.0	21.5	21.3	21.2
BGSS 4 th					
Weights (π_0^{BGSS})	1.275	0.657	0.442	0.333	0.267
Relative error (%) in π	0.92	0.56	0.51	0.50	0.50
Expected utility ($V^{BGSS}(0)$)	-0.902	-0.264	-0.142	-0.091	-0.064
Relative error (%) in V	0.02	0.06	0.08	0.12	0.15
CER (%)	10.85	8.03	7.06	6.58	6.29
Computational time (seconds)	37.8	39.7	38.1	38.9	38.0
SGBM					
Weights (π_0^{SGBM})	1.275	0.657	0.442	0.333	0.267
Relative error (%) in π	0.94	0.56	0.51	0.48	0.49
Expected utility ($V^{SGBM}(0)$)	-0.902	-0.264	-0.142	-0.091	-0.064
Relative error (%) in V	0.03	0.06	0.09	0.13	0.16
CER (%)	10.85	8.03	7.06	6.58	6.29
Computational time (seconds)	55.3	55.0	54.5	55.3	55.1
SGBM-LT					
Weights (π_0^{SGBM})	1.274	0.656	0.442	0.333	0.267
Relative error (%) in π	1.02	0.65	0.60	0.59	0.58
Expected utility ($V^{SGBM}(0)$)	-0.902	-0.264	-0.142	-0.091	-0.064
Relative error (%) in V	0.02	0.06	0.09	0.12	0.16
CER (%)	10.85	8.03	7.06	6.58	6.29
Computational time (seconds)	61.4	62.1	61.3	62.0	62.1
PAMC (VFI)					
Weights (π_0^{PAMC})	1.286	0.660	0.444	0.334	0.268
Relative error (%) in π	0.04	0.08	0.10	0.12	0.12
Expected utility ($V^{PAMC}(0)$)	-0.902	-0.264	-0.142	-0.091	-0.064
Relative error (%) in V	0.02	0.04	0.05	0.05	0.06
CER (%)	10.85	8.03	7.07	6.59	6.30
Computational time (seconds)	50.3	50.1	50.4	50.0	50.3
PAMC (PWI)					
Weights (π_0^{PAMC})	1.281	0.655	0.440	0.331	0.265
Relative error (%) in π	0.48	0.86	1.01	1.10	1.15
Expected utility ($V^{PAMC}(0)$)	-0.902	-0.264	-0.142	-0.091	-0.064
Relative error (%) in V	0.02	0.04	0.05	0.06	0.06
CER (%)	10.85	8.03	7.07	6.60	6.30
Computational time(seconds)	122.5	123.4	122.6	122.8	122.3

Table 2.10: Results for Heston model with different degree of polynomial

degree		Theoretical	1	2	3	1	2	3
			VFI			PWI		
$\gamma = 2$	Weight	1.287	1.286	1.287	1.280	1.281	1.281	1.286
	CER(%)	10.88	10.85	10.85	10.85	10.85	10.85	10.85
	Computational time		51.1	50.9	51.5	148.2	150.0	153.4
$\gamma = 10$	Weight	0.268	0.268	0.268	0.266	0.265	0.265	0.267
	CER(%)	6.31	6.30	6.30	6.30	6.30	6.30	6.30
	Computational time		53.8	54.3	55.0	154.8	158.6	161.9

Table 2.11: Error between numerical and theoretical allocation at mid point Heston Model

method	γ	
	2	10
	Mean of $L2$ distance	
BGSS 2 nd	6.8×10^{-5}	1.5×10^{-5}
BGSS 4 th	1.9×10^{-4}	1.2×10^{-5}
SGBM	9.0×10^{-5}	1.0×10^{-4}
SGBM -LT	8.7×10^{-5}	2.3×10^{-5}
(VFI) (degree=1)	5.1×10^{-6}	2.0×10^{-6}
(VFI) (degree=2)	5.1×10^{-6}	2.0×10^{-6}
(VFI) (degree=3)	6.2×10^{-6}	2.4×10^{-6}
(PWI) (degree=1)	4.8×10^{-6}	1.8×10^{-6}
(PWI) (degree=2)	4.4×10^{-6}	1.7×10^{-6}
(PWI) (degree=3)	4.3×10^{-6}	1.6×10^{-6}

Table 2.12: Results for mean-reverting case

	$\gamma = 2.0$	$\gamma = 4.0$	$\gamma = 6.0$	$\gamma = 8.0$	$\gamma = 10.0$
Theoretical					
Weights (π_0^*)	1.084	0.632	0.449	0.348	0.284
Expected utility ($V^*(0, x)$)	-0.859	-0.240	-0.126	-0.080	-0.056
CER (%)	16.38	11.56	9.64	8.60	7.95
BGSS 2nd					
Weights (π_0^{BGSS})	1.031	0.578	0.401	0.307	0.249
Relative error (%) in π	4.93	8.64	10.54	11.65	12.38
Expected utility ($V^{BGSS}(0)$)	-0.865	-0.244	-0.129	-0.083	-0.058
Relative error (%) in V	0.67	1.83	2.54	3.00	3.32
CER (%)	15.61	10.89	9.09	8.14	7.56
Computational time(seconds)	7.9	8.8	8.9	8.9	8.8
BGSS 4th					
Weights (π_0^{BGSS})	1.076	0.612	0.440	0.332	0.270
Relative error (%) in π	0.73	3.13	4.07	4.62	5.00
Expected utility ($V^{BGSS}(0)$)	-0.864	-0.243	-0.129	-0.082	-0.057
Relative error (%) in V	0.60	1.36	1.88	2.23	2.48
CER (%)	15.68	11.06	9.23	8.26	7.66
Computational time(seconds)	30.1	29.6	30.3	29.1	31.0
SGBM					
Weights (π_0^{SGBM})	1.070	0.612	0.429	0.330	0.269
Relative error (%) in π	1.26	3.23	4.36	5.06	5.54
Expected utility ($V^{SGBM}(0)$)	-0.864	-0.243	-0.129	-0.082	-0.057
Relative error (%) in V	0.55	1.36	1.88	2.21	2.46
CER (%)	15.75	11.06	9.23	8.26	7.66
Computational time(seconds)	39.8	39.9	40.7	39.9	39.4
SGBM-LT					
Weights (π_0^{SGBM})	1.072	0.613	0.430	0.331	0.269
Relative error (%) in π	1.12	3.00	4.16	4.89	5.39
Expected utility ($V^{SGBM}(0)$)	-0.864	-0.243	-0.129	-0.082	-0.057
Relative error (%) in V	0.52	1.32	1.82	2.16	2.40
CER (%)	15.78	11.07	9.24	8.27	7.67
Computational time(seconds)	47.3	47.9	47.0	47.3	47.6
PAMC (VFI)					
Weights (π_0^{PAMC})	1.092	0.635	0.448	0.346	0.282
Relative error (%) in π	0.70	0.44	0.16	0.62	0.95
Expected utility ($V^{PAMC}(0)$)	-0.863	-0.243	-0.128	-0.082	-0.057
Relative error (%) in V	0.41	1.18	1.64	1.95	2.16
CER (%)	15.90	11.12	9.28	8.30	7.70
Computational time (seconds)	7.6	7.8	7.8	7.8	7.9
PAMC (PWI)					
Weights (π_0^{PAMC})	1.093	0.640	0.452	0.349	0.285
Relative error (%) in π	0.78	1.16	0.79	0.46	0.21
Expected utility ($V^{PAMC}(0)$)	-0.858	-0.243	-0.128	-0.082	-0.057
Relative error (%) in V	0.33	1.18	1.64	1.95	2.17
CER (%)	16.00	11.12	9.28	8.30	7.70
Computational time (seconds)	20.4	20.5	20.6	20.6	20.6

Table 2.13: Results for mean-reverting case with different degree of polynomial

degree	Theoretical	1	2	3	1	2	3
		VFI			PWI		
$\gamma = 2$	Weight	1.084	1.001	1.092	1.092	1.016	1.093
	CER(%)	16.38	15.66	15.90	15.84	15.64	16.00
	Computational time		7.5	7.8	8.3	18.9	20.6
$\gamma = 10$	Weight	0.284	0.226	0.282	0.281	0.267	0.285
	CER(%)	7.95	7.53	7.70	7.70	7.52	7.70
	Computational time		7.3	7.9	8.5	19.0	20.6

Table 2.14: Error between numerical and theoretical allocation at mid point Mean-reverting Model

method \ γ	2	10
	Mean of $L2$ distance	
BGSS 2 nd	2.1×10^{-4}	6.7×10^{-5}
BGSS 4 th	1.5×10^{-4}	3.6×10^{-5}
SGBM	1.5×10^{-4}	3.3×10^{-5}
SGBM-LT	1.4×10^{-4}	3.1×10^{-5}
(VFI) (degree=1)	2.0×10^{-4}	8.8×10^{-5}
(VFI) (degree=2)	1.5×10^{-5}	1.5×10^{-5}
(VFI) (degree=3)	3.6×10^{-5}	1.5×10^{-5}
(PWI) (degree=1)	2.0×10^{-4}	8.9×10^{-5}
(PWI) (degree=2)	3.4×10^{-5}	1.7×10^{-5}
(PWI) (degree=3)	3.2×10^{-5}	1.6×10^{-5}

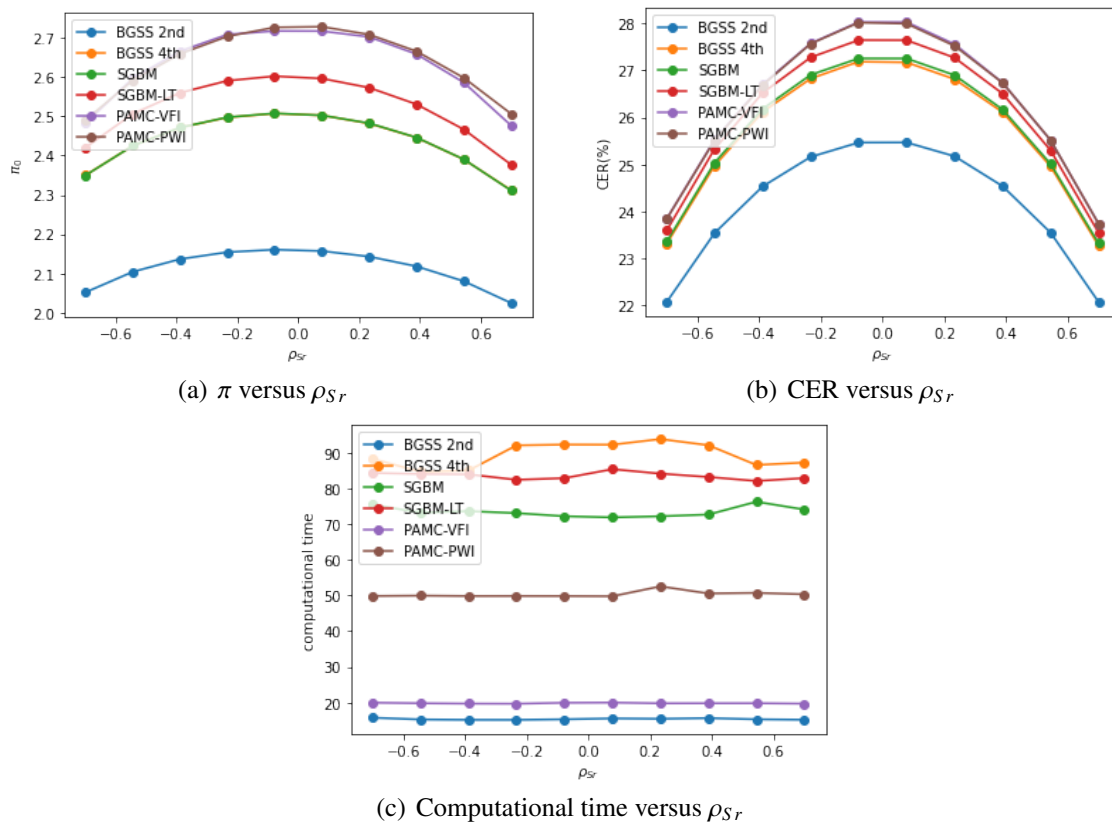


Figure 2.5: Comparison in Heston model with stochastic interest rate given $\rho_{Xr} = 0$: (a) optimal strategy, (b) CER and (c) computational time from PAMC, BGSS and SGBM across different value of ρ_{Sr} .

Chapter 3

Polynomial affine approach to the HARA utility with application to OU 4/2 model

Chapter summary:

This chapter designs a numerical methodology, named PAMH, to approximate an investor's optimal portfolio strategy in the contexts of expected utility theory (EUT) and mean-variance theory (MVT). Thanks to the use of hyperbolic absolute risk aversion utilities (HARA), the approach produces optimal solutions for decreasing relative risk aversion (DRRA) investors, as well as for increasing relative risk aversion (IRRA) agents. The accuracy and efficiency of the approximation is examined in a comparison to known closed-form solutions for a one dimensional ($n = 1$) geometric Brownian motion with a CIR stochastic volatility model (i.e. GBM 1/2 or Heston model), and a high dimensional (up to $n = 35$) stochastic covariance model. The former confirms the method works even when the theoretical candidate is not well-defined, while the latter illustrates low errors (up to 8% in certainty equivalent rate (CER)) and feasible computational time (less than one hour in a PC).

Given the potential of this method, we investigate a relevant practical setting with no closed-form solution, namely when assets follow an Ornstein–Uhlenbeck 4/2 stochastic volatility (SV, i.e. OU 4/2) model. We conduct sensitivity analyses of the optimal strategies for DRRA and IRRA investors with respect to key parameters; (e.g. risk aversion, minimum capital guarantee and 4/2's parameters). In particular, the efficient frontier for the IRRA case is presented. A comparison to important sub-optimal strategies in terms of CER is performed, indicating low CER performances due to ignorance of stochastic volatility for CRRA investors, i.e. a myopic strategy would be even better than ignoring SV. The analyses highlight the importance of efficient and precise numerical methods to obtain substantially higher CERs.

Status: Published in *Applied Mathematics and Computation*.

3.1 Introduction

Financial markets and the models that describe them are ceaselessly evolving. New stylized market phenomena emerge over time, and models to describe even the simplest equity markets are significantly refined each decade. For example, stochastic volatility (SV; see [32] for the ARCH model and [48] for the 1/2 continuous-time model, geometric Brownian motion

[GBM] 1/2) emerged in 1980s and 1990s; this is one of the most important stylized facts when describing market indexes, such as the S&P 500, or common stocks. This branch has led to many innovations, such as the trading of VIX since 2004, created by Chicago Board Options Exchange (CBOE) as an index tracking the instantaneous SV of the S&P 500, or the invention of VVIX in 2012, used for tracking the stochastic volatility of volatility (SVV). As recently as 2017 (see [45]), researchers are still crafting the right models for SV; there, the author introduced the GBM 4/2 model to better capture implied volatility surfaces and the patterns of historical volatilities. Many other stylized facts, such as stochastic market prices of risk, mean-reverting periods and Markov-switching market states (crisis, normal), also require constant attention to remain relevant in modern financial mathematics. All these facts highlight the need for numerical methods that can efficiently solve important financial challenges.

This chapter proposes a numerical method for portfolio optimization targeting investor with hyperbolic absolute risk aversion (HARA) risk preferences. We explore accuracy and time efficiency when working with advanced stochastic variance/covariance models. Given the importance and lack of solvability of the 4/2 family of models, we use the numerical approach to explore in detail the solutions for one member of the 4/2 family. Next we present an overview motivating our 4/2 application and the state of the art on numerical portfolio solutions.

Starting with the GBM in [8] seminal work, continuous-time stochastic differential equations (SDEs) are powerful tools to generate rich models capable of describing financial data. Unlike the GBM, the SV model of [48], named GBM 1/2, is able to produce volatility smiles and skews similar to those observed in equity option markets. However, because of the restrictions on the volatility of volatility, 1/2 volatility paths spend much more time close to 0 than is predicted by the empirical distribution of the volatility, among other drawbacks. The GBM 3/2 model of [49] was developed to overcome some of these limitations but it still admits extreme paths with spikes in instantaneous volatility. Twenty-five years later, a new influential model (see [45] for the GBM 4/2) unified the 1/2 and 3/2 models, better capturing the evolution of the implied volatility surface. The 4/2 model uniformly bounds the instantaneous variance away from zero when weights on 1/2 and 3/2 factors are positive. The GBM 4/2 was extended to capture mean-reverting of the underlying stock in [37], defining the Ornstein–Uhlenbeck 4/2 (OU 4/2) targeting commodities and currency markets.. However, the additional sources of randomness jeopardise the analytic solvability of important financial problems, including the target of this chapter: optimal investment allocation.

Portfolio optimization for continuous-time processes began in the late 60s with the seminal papers of [76] and [78]; this was in the setting of expected utility theory (EUT). The author used Hamilton-Jacobi-Bellman (HJB) to produce optimal trading strategies, value functions and the optimal wealth for stock prices modeled with a GBM. Moreover, [59] followed Merton's approach and obtained a closed-form solution of optimal strategies with the 1/2 model for a constant relative risk aversion (CRRA) utility, which is one of the most popular choices among investors. Then, [19] considered the same optimal portfolio problem and utility, when stock price follows exponential Ornstein–Uhlenbeck processes. They obtained analytic solutions up to a system of ordinary differential equations (ODEs). All the cases described above belong to quadratic-affine family defined in the celebrated paper of [70]. This latest family appears to be one of the broadest classes solvable in closed form with CRRA utilities. Nonetheless, many reasonable and interesting models do not match the definition of the quadratic-affine family,

and they are hence rarely solvable in the context of portfolio optimization. The examples considered in this chapter, namely, the OU 4/2 model and the embedded cases of OU 1/2 and OU 3/2, are not quadratic affine.

Moreover, CRRA is a somewhat narrow family of utilities; the larger class of HARA utilities is preferable due to the flexible capturing risk aversion preference. However, HARA is a challenging class with which to generate closed-form solutions; therefore, it has been studied to a lesser extent for advanced SDE models. Two notable exceptions are the works of [61], where the authors considered the stochastic market price of risk and SV, as well as non-mean reverting underlyings, solving the optimal allocation problem for incomplete markets. Optimal allocations for a bond-stock market incorporating regime switching, a stochastic short rate and further stochastic factors was presented in [33]. The target model in this chapter (i.e. the Ornstein–Uhlenbeck 4/2 model) has not yet been studied with CRRA or with HARA utilities due to the lack of closed-form solutions.

Another benefit of HARA utilities is their use as a bridge connecting EUT and another important branch of portfolio optimization, namely, mean-variance theory (MVT). [73] solved the optimal single-period investment allocation which laid the foundation for the later development of asset management. The existence of a variance term in the objective function does not allow for a direct application of the Bellman principle (i.e. time inconsistent problematic). [5] thus proposed a framework to derive a so-called time-consistent mean-variance (TCMV) strategy. An alternative solution is called a pre-commitment approach (see [89]), which is obtained by transforming the dynamic mean-variance portfolio problem into a stochastic linear quadratic (LQ) problem. In addition to the traditional HJB PDE, the LQ approach leads to a representation of the solution in terms of backward stochastic differential equations (BSDEs). The seminal papers, [66] and [65], found the associated stochastic Riccati equations (SREs) for the optimal mean-variance strategy in complete and incomplete market setting. These works are extended in [20], which obtained closed-form solution of mean-variance portfolio in the presence of correlation risk. TCMV solutions within the LQ approach were first presented in [50]. The recent work of [88] links TCMV portfolio to the solutions of BSDEs for generalized one-dimensional SV models.

The linear quadratic pre-commitment problem is a special case of a HARA utility; therefore, the MVT strategy can be studied as an EUT HARA portfolio choice problem. As mentioned before, closed-form solutions exist for GBM, OU and GBM 1/2 models, but more advanced models such as the OU 4/2 model must be studied with an efficient numerical method.

The lack of closed-form solutions promotes the emergence of many numerical approximation methods for optimal portfolio strategies, most of which focus on a CRRA-type investor. [11] analyzed dynamic portfolio selection by solving HJB partial differential equation (PDE) with a finite difference method. However, the numerical PDE method suffer from the curse of dimensionality, which limits its practical use (see [42] and [1]). In contrast, Monte Carlo based methods accommodate a variety of situations and are preferable in the case of a large amount of state variables and stochastic factors. Inspired by [72], [10] first applied the least-squares Monte Carlo method to the portfolio optimization problem with excellent results in terms of accuracy and time efficiency. Therefore, [40] expanded the value function based on a nonlinear decomposition and applied the inverse transformation on the value function, successfully improving the accuracy. [24] enhanced [10] by replacing the standard regression method by a techniques called the stochastic grid bundling method (SGBM) introduced in [53]. A Monte

Carlo based method was discussed in [9], which utilizes the martingale approach and is efficient for high dimensional portfolio selection. Recently, deep learning models have been successfully used in high-dimensional stochastic control problems. For example, [4] and [52] proposed deep learning-based algorithms, providing accurate estimates of optimal control and value function for discrete-time finite time horizon problems. An efficient deep reinforcement learning based algorithm, targeting non-linear PDEs and dynamic optimization problem in finance, was introduced in [42]. [84] considered the application of a deep-learning method to high-dimensional portfolio with serially-dependent models. [64] enhanced method introduced in [23] with the Lasso and shown good stability in both low and high dimensional portfolio choice problem.

The contributions of the chapter are summarized next:

1. A numerical method is presented to approximate optimal allocation and value function for a risk-averse investor in a general HARA setting, hence embedding both EUT (DRRA) and MVT (IRRA) cases. The method relies on the wealth and state variables separability of the value function to fit the value function via an exponential polynomial.¹ This work generalizes the family of exponential quadratic solutions (see [70]).
2. A high level of accuracy of the methodology and low computational time on a standard PC are demonstrated on two models, a one-dimensional stochastic volatility GBM 1/2 model (as per [61]), and, for CRRA utilities, a 35-dimensional multivariate stochastic covariance model (see [34]).
3. The optimal strategy, optimal wealth and value function are numerically studied for an OU 4/2 model (see [37]) in the context of EUT (decreasing RRA). Sensitivities to risk aversion level, minimum capital guarantee and 4/2 parameters are presented. The analysis confirms substantial changes in allocations due to relatively small changes in these parameters.
4. An efficient frontier of pre-commitment strategies for dynamic MVT (increasing RRA investor) is obtained. A sensitivity to 4/2 parameters and multipliers is presented, confirming the findings of the DRRA case.
5. The suboptimality of myopic strategies in terms of the certainty equivalent rate (CER), for OU 4/2 models, is corroborated. A similar analysis of CER performance in the popular OU 1/2 model confirms low CERs for investors ignoring SV, to the point that a myopic strategy may be preferable to a strategy that neglects SV.

The chapter is organized as follows: Section 3.2 introduces the investor's problem and methodology, and Section 3.3 examines the accuracy of the method by comparing it to the analytical solution of Heston's SV model and a multivariate stochastic covariance model. The optimal allocation, efficient frontier and sensitivity analysis with respect to the volatility group parameters are then studied in Section 3.4. Section 3.5 concludes with the detailed algorithm, and mathematical proof is provided in the Section 3.6 and 3.7.

¹See [90] for a CRRA application with neural networks.

3.2 Polynomial-affine method for HARA utilities

This section introduces a method to solve dynamic portfolio choice for a risk-averse investor with a HARA utility function. We assume that the stochastic processes describing the financial market are defined on a complete probability space $(\Omega, \mathcal{F}, \mathbb{P})$ with a right-continuous filtration $\{\mathcal{F}_t\}_{t \in [0, T]}$. We consider an economy with a money market account (M) and n stocks $S = (S^{(1)}, \dots, S^{(n)})$. We assume the log stock prices follow a general diffusion process with a n -dim state variable $X = (X^{(1)}, \dots, X^{(n)})$:

$$\begin{cases} \frac{dM_t}{M_t} = r dt \\ d \ln S_t^{(i)} = \theta_i(X_t, \ln S_t) dt + \sum_{j=1}^n \sigma_{i,j}(X_t, \ln S_t) dB_t^{(j)}, \quad i = 1, \dots, n \\ dX_t^{(j)} = a_j(X_t^{(j)}) dt + b_j(X_t^{(j)}) dB_t^{(X,j)} \\ \langle dB_t^{(j)}, dB_t^{(X,j)} \rangle = \rho_j dt, \quad j = 1, \dots, n \end{cases} \quad (3.1)$$

where $B_t^{(i)}, B_t^{(X,j)}$ for $i, j = 1, \dots, n$ are Brownian motions with correlation only when $i = j$, $|\rho_j| < 1$. r is the risk-free rate, $\theta(X_t, \ln S_t) = (\theta_1(X_t, \ln S_t), \dots, \theta_n(X_t, \ln S_t))$, $\sigma(X_t, \ln S_t) = (\sigma_{i,j}(X_t, \ln S_t))$ are the drift and volatility of the log price processes. We assume the matrix $\sigma(X_t, \ln S_t) \sigma(X_t, \ln S_t)^T$ is strictly definite positive, and the coefficients: $\theta_i, \sigma_{i,j}, a_j, b_j$ satisfy the non-Lipschitz conditions in Proposition 1.2 from [60] to ensure existence and uniqueness of a solution to the SDE.

There are many popular models embedded in this representation. For example, for one stock, Equation (3.1) is the Geometric Brownian Motion (GBM) when $\theta(X_t, \ln S_t)$ and $\sigma(X_t, \ln S_t)$ are constants. If we set $\theta(X_t, \ln S_t) = r + (\lambda_S - 0.5)X_t$, $\sigma(X_t, \ln S_t) = \sqrt{X_t}$, $a(X_t) = \kappa_X(\theta_X - X_t)$ and $b(X_t) = \sigma_X \sqrt{X_t}$, Equation (3.1) is exactly the Heston's 1/2 model. Furthermore, the exponential Ornstein–Uhlenbeck model can be obtained by setting $\theta(X_t, \ln S_t) = \kappa_S(\theta_S - \ln S_t) dt$, $\sigma(X_t, \ln S_t) = \sigma$.

For multiple stocks, (3.1) greatly overlaps with the largest family of solvable stochastic covariance models in the literature, this is the Quadratic-Affine defined in [70]. For simplicity of exposition, we choose the same number of state variables and stocks (n) and a convenient dependence structure among the Brownian vectors B and $B^{(X)}$, both assumptions can be relaxed for future analysis.

We consider an investor with risk preference as per a HARA utility, defined in [78], as follows:

$$U(W) = \frac{\gamma}{1-\gamma} \left(\frac{\omega}{\gamma} W - F \right)^{1-\gamma} \quad (3.2)$$

where $\omega > 0$, $\gamma \neq 1$ and $\frac{\omega}{\gamma} W - F > 0$. γ represents the investor's level of risk aversion. There is a lower bound on portfolio wealth W when $\gamma > 0$ and an upper bound on W when $\gamma < 0$. The relative risk aversion (RRA) of HARA utility is given by

$$RRA = -\frac{WU''(W)}{U'(W)} = \left(\frac{1}{\gamma} - \frac{F}{\omega W} \right)^{-1}, \quad (3.3)$$

which increases with wealth W when F is negative (IRRA) and decreases when F is positive (DRRA). A well-known example, of a positive F is the constant proportion portfolio insurance (CPPI) strategy obtained for a HARA investor when stock price follows a GBM; in this

case, F can be interpreted as a minimum capital guarantee. It is worth mentioning that the HARA utility in Equation (3.2) converges to other standard utilities with a specific choice of the parameters. Table 3.1 lists some special cases of HARA utility, which can consequently be adapted to our methodology.

Table 3.1: Special cases of the hyperbolic absolute risk aversion (HARA) utility

Parameter	Utility
$\gamma = -1$	Quadratic utility
$\gamma \rightarrow \infty, F = -1$	Exponential utility (CRAR)
$F = 0, \gamma > 0$	Power utility (CRRA)
$\omega = \gamma \rightarrow 1, F = 0$	Log utility

We assume that investors can freely trade at, highly frequent, discrete opportunities $t \in [0, \Delta t, 2\Delta t, \dots, T - \Delta t]$ up to a terminal time T . Let $\pi_t = (\pi_t^{(1)}, \dots, \pi_t^{(n)})$ denote the percentage of wealth allocated to the stocks at time t . The corresponding wealth process is,

$$\begin{aligned} \frac{dW_t}{W_t} &= \left(r + \sum_{i=1}^n \pi_t^{(i)} \left(\theta_i(X_t, \ln S_t) + \sum_{j=1}^n \frac{1}{2} \sigma_{i,j}^2(X_t, \ln S_t) - r \right) \right) dt \\ &+ \sum_{i=1}^n \pi_t^{(i)} \left(\sum_{j=1}^n \sigma_{i,j}(X_t, \ln S_t) dB_t^{(j)} \right). \end{aligned} \quad (3.4)$$

The investor wants to derive an investment strategy π_t that maximizes the expected utility from the terminal wealth W_T . The investor's problem at any time $t \in [0, T]$ can be written as

$$V(t, W, \ln S, X) = \max_{\pi_{s \geq t}} \mathbb{E}(U(W_T) | \mathcal{F}_t), \quad (3.5)$$

where $V(t, W, \ln S, X)$ is called the value function at time t .

The value function for a HARA utility and a large family of diffusion has been shown to have representation (see, for instance, [33]):

$$V(t, W, X, \ln S) = \frac{\gamma}{1 - \gamma} \left(\frac{\omega}{\gamma} W - Fd(t) \right)^{1-\gamma} f(t, X, \ln S) \quad (3.6)$$

where $d(t)$ is the price of a zero coupon bond. Moreover the structure of the value function within the quadratic-Affine model class of [70] is also of the form:

$$V(t, W, X, \ln S) = \frac{W^{1-\gamma}}{1 - \gamma} f(t, X, \ln S). \quad (3.7)$$

In both cases the function $f(t, X, \ln S)$ is exponential linear or quadratic. Inspired by these results we assume Equation (3.6) to be an approximation for the solution of problem (3.5), with the flexibility that $\ln f$ could be of any polynomial form.² In other words, we approximate the true $\ln f$ by a polynomial of order k , denoted P_k , via regression. It is not difficult to show

²If the model is solvable, $\ln f$ is often a linear or quadratic function. While, when the model is unsolvable, a polynomial function with higher degree provides flexibility in capturing the value function.

that the value function is indeed separable in W and X , e.g. in the form of (3.7), therefore the problem reduces to approximating f . It should be noted that, by the Stone-Weierstrass theorem, any continuous function on a compact support can be approximated arbitrarily well in the polynomial class. Although the support of f is not necessarily compact here, the PAMH method works with simulations on a finite horizon, hence an approximation of the space via a compact region. This can also be motivated with practical financial arguments, and it can be interpreted as an approximation of the value function on a compact support. With a good approximation of the value function, the estimation of the optimal strategy would also be accurate because it depends on the coefficient of the value function.³

Note that the coefficients in P_k are time-dependent and the order n is determined by the highest expected utility. With the representation of the value function in Equation (3.6), we obtain an approximation of the optimal allocation described in Theorem 3.2.1.

Theorem 3.2.1 *The optimal allocation $\pi_t^* = (\pi_t^{(*,1)}, \dots, \pi_t^{(*,n)})$ for investors with market dynamics shown in Equation (3.1) can be approximated by the unique solution to the system of equations:*

$$\sum_{j=1}^n g_{i,j}(t, W_t, \ln S_t, X_t) \pi_t^{(*,j)} = g_i(t, W_t, \ln S_t, X_t), \quad i = 1, \dots, n \quad (3.8)$$

where

$$\begin{aligned} g_{i,j}(t, W_t, \ln S_t, X_t) &= \omega W_t \left(\sum_{k=1}^n \sigma_{i,k}(X_t, \ln S_t) \sigma_{j,k}(X_t, \ln S_t) \right) \\ g_i(t, W_t, \ln S_t, X_t) &= \left(\frac{\omega}{\gamma} W_t - Fd(t+dt, X_t) \right) \left(\theta_i(X_t, \ln S_t) + \frac{1}{2} \sum_{j=1}^n \sigma_{i,j}^2(X_t, \ln S_t) - r \right) \\ &+ \sum_{j=1}^n \left(\frac{\omega}{\gamma} W_t - Fd(t+dt, X_t) \right) \frac{\partial P_k(t+dt, \ln S_t, X)}{\partial \ln S_t^{(j)}} \left(\sum_{k=1}^n \sigma_{i,k}(X_t, \ln S_t) \sigma_{j,k}(X_t, \ln S_t) \right) \\ &+ \sum_{j=1}^n \left(\frac{\omega}{\gamma} W_t - Fd(t+dt, X_t) \right) \frac{\partial P_k(t+dt, \ln S_t, X)}{\partial X_t^{(j)}} \sigma_{i,j}(X_t, \ln S_t) b_j(X_t^{(j)}) \rho_j. \end{aligned} \quad (3.9)$$

Under this strategy, the wealth process $W_t \geq Fd(t) \geq 0$ has a unique pathwise solution.

The Proof of Theorem 3.2.1 is given in Section 3.7. It should be noted that the previous result implicitly assumes existence and uniqueness of the solution to the optimal control problem. Given the generality of our model, this can not be ensured via explicit conditions, as it depends on the specific choice of models (see [59] and [18] for examples on one-dimensional models). Nonetheless, as explained in section 3, our numerical methodology delivers good results even when the solution can be not ensured.

The notation of the polynomial affine method for HARA utility (PAMH) and the step-by-step algorithm are presented in Section 3.6. To facilitate understanding and measure accuracy,

³The same principle can be applied to other basis functions or neural networks.

we apply the main result to the solvable cases of the 1/2 model (dimension $n = 1$), and to a popular stochastic covariance model (dimension up to $n = 35$). Then we focus on the application and financial implications for the OU 4/2 model. The methodology was run on a laptop with processor Intel(R) Xeon(R) CPU @ 2.30GHz and 25 GB RAM.

3.3 Accuracy of the approximation for GBM 1/2 model

In this section, the goodness of the methodology is examined by comparing it to the closed-form solution of the popular Heston's model (see [48]). We first provide a concise review of the GBM 1/2 model, its closed-form optimal strategy and value function. By implementing the Heston's 1/2 model, the accuracy and efficiency of our method is demonstrated. Moreover, we compare the optimal allocation and the expected utility at time 0 from our method with the theoretical results, and we report the annualized CER defined by,

$$U(W_0(1 + CER)^T) = V(0, W_0, \ln S_0, X_0). \quad (3.10)$$

3.3.1 Closed-form solution of GBM 1/2 model

The dynamics of Heston's model (see [48]) can be summarized as follows:

$$\begin{cases} \frac{dM_t}{M_t} = rdt \\ \frac{dS_t}{S_t} = (r + \lambda_S X_t)dt + \sqrt{X_t}dB_t^S \\ dX_t = \kappa_X(\theta_X - X_t)dt + \sigma_X \sqrt{X_t}dB_t^X. \end{cases} \quad \langle B^S, B^X \rangle_t = \rho_{SX} \quad (3.11)$$

[61] present the corresponding optimal trading strategy and value function for a HARA utility, which is given by

$$\begin{aligned} V(t, W, X) &= \frac{(\frac{\omega}{\gamma} W e^{r(T-t)} - F)^{1-\gamma}}{1-\gamma} e^{\gamma a(t) + \gamma b(t)X} \\ \pi^*(t, W, X) &= \frac{(\omega W - \gamma F e^{-r(T-t)})}{\omega \gamma W} (\lambda_S + \rho_{SX} \sigma_X b(t)). \end{aligned} \quad (3.12)$$

Here the functions $a(\tau)$ and $b(\tau)$ are

$$\begin{aligned} a(\tau) &= -\frac{\kappa_X \theta_X}{d_X} \left\{ \frac{d_X + b_X}{2} - \ln \frac{2d_X}{2d_X - (d_X + b_X)(1 - e^{-d_X(T-\tau)})} \right\} \\ b(\tau) &= \frac{2c_X(1 - e^{-d_X(T-\tau)})}{2d_X - (d_X + b_X)(1 - e^{-d_X(T-\tau)})} \end{aligned} \quad (3.13)$$

with auxiliary parameters $a_X = \frac{(1+\rho_{SX}^2(1-\gamma)/\gamma)\sigma_X^2}{2}$, $b_X = \sigma_X \rho_{SX} \lambda_S \frac{1-\gamma}{\gamma} - \kappa_X$, $c_X = \frac{1-\gamma}{2\gamma^2} \lambda_S^2$ and $d_X = \sqrt{b_X^2 - 4a_X c_X}$. [59] stated a sufficient condition for well-defined parametrization of the model, which is given by

$$\lambda_S < \frac{\kappa_X}{\sigma_X} \left(\sqrt{\rho_{SX}^2 + \frac{\gamma}{1-\gamma}} - \rho_{SX} \right). \quad (3.14)$$

Table 3.2: Parameter value for geometric Brownian motion (GBM) 1/2 model.

Parameter	Value	Parameter	Value
T	1	ρ_{SV}	-0.54
θ_v	0.0257	σ_v	0.26
κ_v	1.33	λ_S	2.45
Δt	0.1	<i>period</i>	10
r	0.05	X_0	0.04
S_0	1.0	M_0	1.0
W_0	1	n_r	100
N	2000	N_0	2000000
F	0.5	ω	γ

A violation of Equation (3.14) could render the closed-form solution invalid i.e. the HJB problem has no unique real solution; this could lead to an expected utility (3.12) of complex or infinitely large value. We consider such situation next to assess the performance of our numerical method.

3.3.2 Accuracy for DRRA investors

Next, we implement our method on the Heston 1/2 model. We start with the decreasing RRA case, where $F > 0$ and $\gamma > 0$. We use the parameter set given in [34] which can be found in Table 3.2.

A first order of the polynomial P_k is selected, which is identical the degree of the polynomial on the state variable in the exponential function of the closed form solution (see Equation (3.12)). To increase accuracy, we generate the paths of stock price and state variable with $dt = \frac{1}{60}$ which is finer than the re-balancing time interval $\Delta t = 0.1$. First, we consider an investor with DRRA (see Table 3.3), at time 0 with various investor's risk aversion levels γ . Both optimal allocation and expected utility from the PAMH are close to the theoretical values. The relative error of optimal allocation is less than 1% and the relative error of expected utility is less than 0.1%. The differences between CERs are also negligible—less than 0.02%. Furthermore, the PAMH is efficient, and all the results are obtained within a minute.

Figure 3.1 compares the expected utility and CER between the theoretical result and our method across different values of F . The results visually overlap, which demonstrates that the PAMH is able to obtain accurate results of optimal allocation and value function despite the choice of risk aversion level γ and minimum capital guarantee level F .

Table 3.3: Results for GBM 1/2 model with decreasing relative risk aversion (DRRA) investor.

	$\gamma = 2.0$	$\gamma = 4.0$	$\gamma = 6.0$	$\gamma = 8.0$	$\gamma = 10.0$
<i>Theoretical</i>					
<i>Weights</i> (π_0^*)	0.675	0.346	0.233	0.175	0.141
<i>Expected utility</i> ($V^*(0, x)$)	-3.440	-7.331	-21.494	-67.017	-213.738
<i>CER</i> (%)	8.14	6.66	6.15	5.90	5.75
<i>PAMH</i>					
<i>Weights</i> (π_0^{PAMH})	0.672	0.345	0.232	0.175	0.140
<i>Relative error</i> (%)	0.36	0.47	0.53	0.56	0.58
<i>Expected utility</i> ($V^{PAMH}(0, x)$)	-3.441	-7.334	-21.505	-67.057	-213.876
<i>Relative error</i> (%)	0.027	0.043	0.0054	0.060	0.065
<i>CER</i> (%)	8.13	6.65	6.15	5.89	5.74
<i>Computational time</i> (Seconds)	56.3	55.3	55.1	53.4	53.0

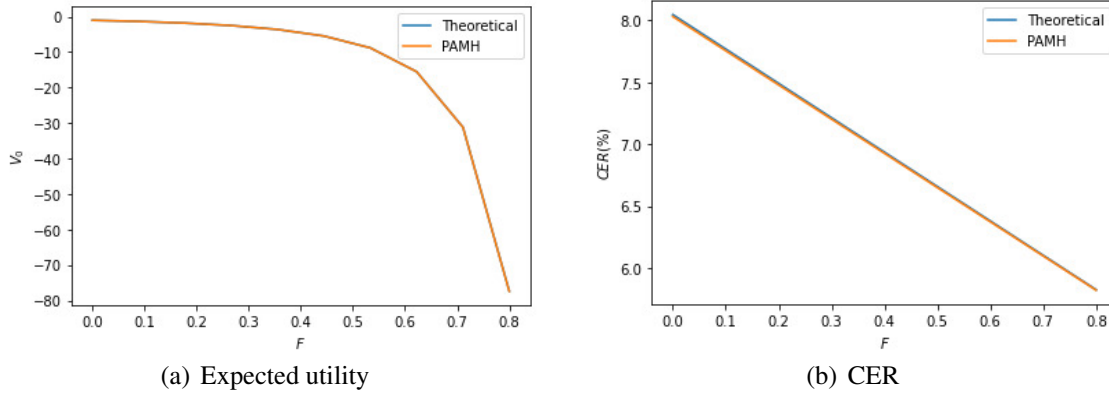


Figure 3.1: Expected utility and certainty equivalent rate (CER) versus F (geometric Brownian motion [GBM] 1/2 model).

Moreover, we investigate a parametrization where closed-form solutions are not well-defined (i.e., λ_S exceeds the upper bound given in Equation (3.14)). We let $F = 0$, so the investor's preference is modelled by a power utility function. Besides, we assume the positive correlation between volatility and stock price (i.e., $\rho_{SV} = 0.54$) and risk aversion level $\gamma = 0.3$. We consider a high frequency re-balancing strategy (i.e., $\Delta t = 0.001$) to ensure the stability of portfolio wealth, and set the number of simulations to compute expected utility at a fixed value $N_0 = 100000$.⁴ Figure 3.2 displays the expected utility and CER versus λ_S , well-defined closed-form solution holds when $\lambda_S < 1.579$ (blue vertical line). Before the condition is violated, the PAMH strategy achieves similar portfolio performance as the theoretical solution. Alternatively, when $\lambda_S > 1.579$, the theoretical approach can not ensure a viable solution. Nonetheless, as per Figure 3.2, our numerical methodology still provides a very good solution, with expected utility and CER increasing smoothly, even though the theoretical solution would actually deliver complex numbers. Note the expected utility shall explode in finite time

⁴This proves the stability of PAMH in case of violations of Equation (3.14), a larger N_0 would improve the precision of the approximated expected utility at the expense of computational time.

($\lambda_S = 5.5231$ in this setting), which can be detected with PAMH by increasing λ_S toward the divergent value. Hence PAMH solution would also produce divergent expected utility and CER.

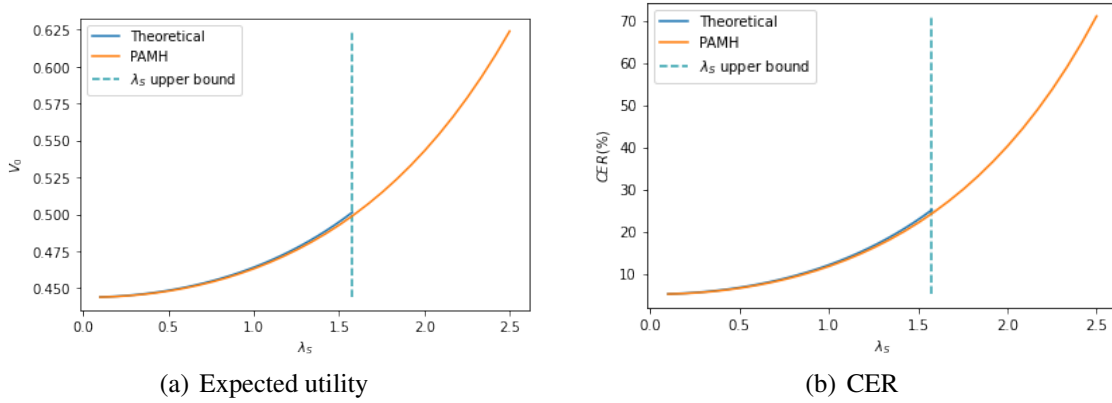


Figure 3.2: Expected utility and certainty equivalent rate (CER) versus λ_S with non-well-defined parametrization (geometric Brownian motion [GBM] 1/2 model).

3.3.3 Accuracy for IRRA investors

A HARA utility (3.2) coincides with the quadratic utility when $\gamma = -1$, $\omega = 1$ and F is negative, which correspond to the increasing RRA investor's preference. Table 3.4 compares the result from our PAMH methodology versus the known theoretical results ([61]). This is done in terms of optimal allocation and expected utility for a quadratic utility setting. Relative errors in optimal allocation and expected utility remain small for any value of F , while both the expectation and the standard deviation of terminal wealth increase with the absolute value of F .

Table 3.4: Results for GBM 1/2 model with increasing relative risk aversion (IRRA) investor.

	$F = -1.2$	$F = -1.4$	$F = -1.6$	$F = -1.8$	$F = -2.0$
<i>Theoretical</i>					
<i>Weights</i> (π_0^*)	0.433	1.015	1.597	2.179	2.761
<i>Expected utility</i> ($V^*(0, x)$)	-0.009	-0.047	-0.116	-0.217	-0.348
<i>CER</i> (%)	6.92	9.33	11.73	14.14	16.55
<i>PAMH</i>					
<i>Weights</i> (π_0^{PAMH})	0.423	0.989	1.555	2.121	2.688
<i>Relative error</i> (%)	2.29	2.54	2.61	2.64	2.66
<i>Expected utility</i> ($V^{PAMH}(0, x)$)	-0.009	-0.048	-0.118	-0.220	-0.353
<i>Relative error</i> (%)	1.51	1.45	1.44	1.43	1.43
<i>CER</i> (%)	6.82	9.10	11.39	13.67	15.96
$\mathbb{E}(W_T)$	1.086	1.130	1.175	1.220	1.264
<i>sd</i> (W_T)	0.065	0.151	0.236	0.321	0.407
<i>Computational time</i> (Seconds)	53.8	54.8	54.9	54.1	53.9

3.3.4 Application to a n-dim Heston model

To verify effectiveness and efficiency of the PAMH for a multi-dimensional portfolio choice problem, we applied the PAMH to a multi-factor stochastic volatility model, which is summarized by

$$\begin{cases} \frac{dM_t}{M_t} = r dt \\ d \ln S_t^{(i)} = \left(r + \sum_{j=1}^n (\lambda_s^{(j)} a_{i,j} - \frac{1}{2} a_{i,j}^2) X_t^{(j)} \right) dt + \sum_{j=1}^n a_{i,j} \sqrt{X_t^{(j)}} dB_t^{(j)}, \quad i = 1, \dots, n \\ dX_t^{(j)} = \kappa_{X,j} (\theta_{X,j} - X_t^{(j)}) dt + \sigma_{X,j} \sqrt{X_t^{(j)}} dB_t^{(X,j)} \\ \langle dB_t^{(j)}, dB_t^{(X,j)} \rangle = \rho_j dt, \quad j = 1, \dots, n. \end{cases} \quad (3.15)$$

$A = (a_{i,j})$ is a constant orthogonal matrix (i.e., AA^T is a identity matrix). Note that the multi-factor stochastic volatility model (3.15) is exactly the GBM 1/2 model (3.11) when the number of stocks is $n = 1$. The value function and optimal strategy for CRRA investors was solved in [34].

For simplicity, we let $\lambda_s^{(j)} = \lambda_s$, $\kappa_{X,j} = \kappa_X$, $\theta_{X,j} = \theta_X$, $\sigma_{X,j} = \sigma_X$, $S_0^{(i)} = S_0$, and $X_0^j = X_0$ (see Table 3.2). Hence, identical distributed stocks $S_t^{(i)}$ are included in investors' portfolio as n increases. The orthogonal matrix A is generated by the equation:

$$A = 2e^T e / (ee^T) - I, \quad (3.16)$$

where e is a $1 \times n$ all-ones vector, and I is a $n \times n$ identity matrix. In order to create a fair comparison across dimensions, and for the purpose of extend-ability of the setting to higher dimension, we increase the number of simulated paths linearly with dimension, i.e. $n_r = 100 * n$, and set the number of simulations to compute expected utility at a fixed value $N_0 = 100000$.⁵ Figure 3.3 (a) displays the expected utilities obtained with the PAMH and the theoretical solution versus number of stocks for a CRRA investor (i.e., $\gamma = 4$, $F = 0$ and $\omega = \gamma$). Expected utility increases with stocks because more assets allow investors to improve performance. The distance between expected utilities from our PAMH and theoretical solution stays small for any size of stocks involved. Figure 3.3 (b) plots the CER versus the number of stocks, we witness a similar result with (a) except that the theoretical solution slightly outperform PAMH when dimension is high, e.g. 8% relative difference at $n = 35$. In Figure 3.3 (c), we define the mean of relative strategy error (MRSE) as follows:

$$MRSE = \frac{1}{n} \sum_{i=1}^n \left| \frac{\pi_0^{i,PAMH} - \pi_0^{i,*}}{\pi_0^{i,*}} \right|,$$

which is the average of relative error of the difference in allocation compared to PAMH at time 0. The optimal strategy from the PAMH is very accurate, the mean relative strategy error is less than 1.4% when the number of stocks is as high as 35. We also consider the computational time in Figure 3.3 (d), which increases modestly with dimension n . It's concluded that PAMH exhibits excellent accuracy and efficiency on both low and high dimensional dynamic portfolio choice problem.

⁵This proves to be reasonable for $n = 35$, a larger N_0 would improve the precision of the approximated expected utility at the expense of computational time.

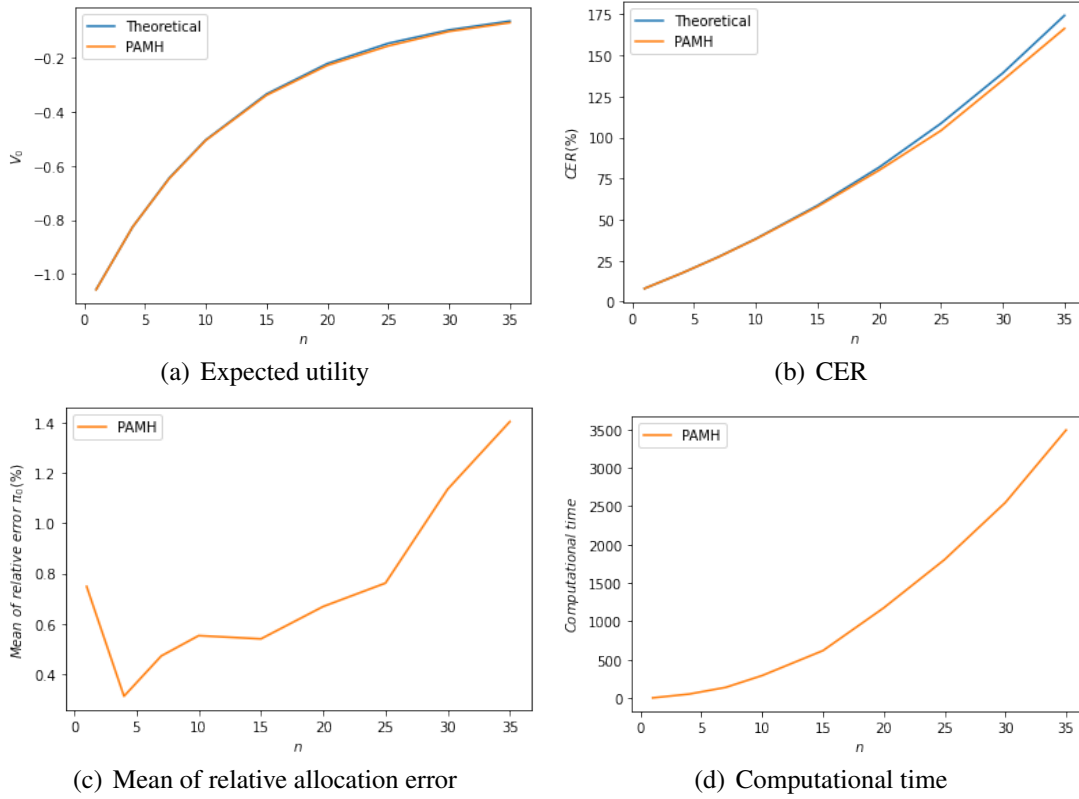


Figure 3.3: Expected utility, certainty equivalent rate (CER), mean of relative strategy error, and computational time versus dimension n (multi-factor stochastic volatility model).

3.4 Applications to the OU 4/2 family of models

Now that we have a reliable method to compute allocations and expected utilities, we turn our attention to an important practical model where the stock price follows the general OU 4/2 model: see Equation (3.17). Here, the state variable X_t is the variance driver which follows a CIR process with mean-reverting rate $\kappa_X > 0$, long run average $\theta_X > 0$ and volatility of volatility $\sigma_X > 0$. In the drift of the log stock price, the excess return is linear in the instantaneous variance $(a_S \sqrt{X_t} + \frac{b_S}{\sqrt{X_t}})^2$. This is the preferred setting in the finance/economics literature; see [78]. Moreover, the parameter ρ captures the leverage effect, while β_S controls the speed of reversion to the mean, where the latest is captured by L_S .

$$\begin{cases} \frac{dS_t^0}{S_t^0} = r dt \\ d \ln S_t = (L_S + (\lambda_S - \frac{1}{2})(a_S \sqrt{X_t} + \frac{b_S}{\sqrt{X_t}})^2 - \beta_S \ln S_t) dt + (a_S \sqrt{X_t} + \frac{b_S}{\sqrt{X_t}}) dB_t \\ dX_t = \kappa_X (\theta_X - X_t) dt + \sigma_X \sqrt{X_t} dB_t^X \\ \langle dB_t, dB_t^X \rangle = \rho dt \end{cases} \quad (3.17)$$

The nested case of a constant variance was solved in closed-form in [19] for a CRRA investor, no results are known in the presence of even simpler stochastic volatility like the 1/2 (Heston) model. Another nested case, the 4/2 model of [45] was solved recently in [18].

Similarly, the authors are not aware of solutions to even the constant variance case for the IRRA side of the problem.⁶

In Section 3.4.1, we consider a DRRA (i.e. $\gamma > 1$ & $F > 0$) HARA utility objective function. The optimal allocation, expected utility and CER are reported. In Section 3.4.2, we first demonstrate the connection between dynamic mean-variance portfolio and optimal portfolio with an IRRA preference. Then, we study the optimal allocation and the efficient frontier. In Section 3.4.3, we investigate the loss investor ignoring SV with a specific case of the OU 4/2 model (i.e. the OU 1/2 model). The sensitivity analysis and portfolio performance of the optimal strategy, myopic strategy and constant volatility strategy are reported for comparison purposes. Note that the myopic strategy is considered due to its simplicity and appeal in the industry. This is inspired by Merton's non-state variables solution, which fails to account for future movement of the state variable. The myopic strategy can be computed directly because it is obtained by assuming that the derivatives of the value function with respect to the state variables are 0 in the HJB equation. For the OU 4/2 model, the myopic strategy is given as follows:

$$\pi_t^{Myopic} = \frac{\omega W - \gamma F \exp(-r(T - t - \Delta t))}{\omega \gamma W (a_S \sqrt{X_t} + \frac{b_S}{\sqrt{X_t}})^2} (L_S - r + \lambda_S (a_S \sqrt{X_t} + \frac{b_S}{\sqrt{X_t}})^2 - \beta_S \ln S_t). \quad (3.18)$$

We compare the optimal portfolio versus myopic strategies in terms of allocation, expected utility, CER and efficient frontier. Furthermore, we analyze the sensitivity of optimal allocation to various parameters. The parameters used in the numerical example are listed in Table 3.5 and estimated from the data of the gold ETF and the volatility index of the gold ETF in [37].

Table 3.5: Parameter value for OU 4/2 model.

Parameter	Value	Parameter	Value
T	1	X_0	0.04
r	0.05	λ_S	0.572
Δt	$\frac{1}{60}$	<i>period</i>	60
S_0	120.0	M_0	1.0
W_0	1	n_r	100
κ_X	4.7937	θ_X	0.0395
σ_X	0.2873	a_S	1
b_S	0.002	ρ	-0.08
L	3.7672	β_S	0.78
N	2000	N_0	2000000
F	0.5	ω	γ

3.4.1 Analysis of a DRRA investor

We first consider the optimal portfolio for a DRRA investor. Here, a qualified polynomial P_k is selected. Note that there is no significant improvement by further increasing the order beyond

⁶[88] consider general SV models but closed-form solutions are not evident in the presence of mean-reverting assets.

2. Table 3.6 reports the optimal allocation, expected utility, CER and computational time. The myopic strategy can be directly computed from Equation (3.18), and the computational time for each strategy reflects the time required to compute the expected utility via simulation.

As expected, the optimal strategy from the PAMH always achieves a higher expected utility and CER than the myopic strategy, and there is no significant monotone relationship between the difference in CERs and the risk aversion level γ . Standard deviation of the estimates are given in Table 3.6, displayed in parentheses, by running the PAMH for 100 times. The myopic strategy is deterministic, so the standard deviation of expected utility and CER result solely from the simulation of stock price, while standard deviation for the PAMH results from both the simulation of stock price and the estimation of the strategy. Therefore, the PAMH is slightly more volatile than the myopic strategy. However, standard deviation for both, PAMH and myopic strategies, are small, which indicates the accuracy and stability of the reported results. Figure 3.4 illustrates the expected utility and CER from the PAMH versus the myopic strategy for different levels of the minimum capital guarantee level F , for $\gamma = 4$. The difference in expected utility is negligible, while the difference in CER grows as F decreases.⁷ Both optimal allocations from the PAMH and the myopic strategy place a large proportion of wealth on the risk-free asset when F increases which results in a diminishing difference in the CER.

Table 3.6: Results for OU 4/2 model with DRRA investor.

	$\gamma = 2.0$	$\gamma = 4.0$	$\gamma = 6.0$	$\gamma = 8.0$	$\gamma = 10.0$
<i>Myopic</i>					
<i>Weights</i> (π_0^{Myopic})	0.049 (0.00)	0.024 (0.00)	0.016 (0.00)	0.012 (0.00)	0.010 (0.00)
<i>Expected utility</i> ($V^{Myopic}(0, x)$)	-3.393 (0.001)	-7.132 (0.002)	-20.792 (0.006)	-64.629 (0.021)	-205.729 (0.072)
<i>CER</i> (%)	8.95 (0.009)	7.18 (0.006)	6.53 (0.003)	6.19 (0.003)	5.98 (0.002)
<i>Computational time</i> (seconds)	55.6 (2.5)	57.6 (1.6)	54.1 (1.4)	58.5 (1.3)	60.2 (1.6)
<i>PAMH</i>					
<i>Weights</i> (π_0^{PAMH})	0.036 (0.005)	0.013 (0.004)	0.008 (0.003)	0.005 (0.003)	0.004 (0.002)
<i>Expected utility</i> ($V^{PAMH}(0, x)$)	-3.389 (0.001)	-7.095 (0.003)	-20.630 (0.010)	-64.020 (0.036)	-203.565 (0.122)
<i>CER</i> (%)	9.02 (0.011)	7.28 (0.007)	6.62 (0.006)	6.27 (0.004)	6.05 (0.004)
<i>Computational time</i> (seconds)	166.5 (1.4)	165.5 (1.2)	161.5 (4.0)	164.5 (4.8)	161.4 (3.7)

⁷The differences between PAMH and Myopic strategy in terms of expected utility and CER gets significant as the time to maturity increases.

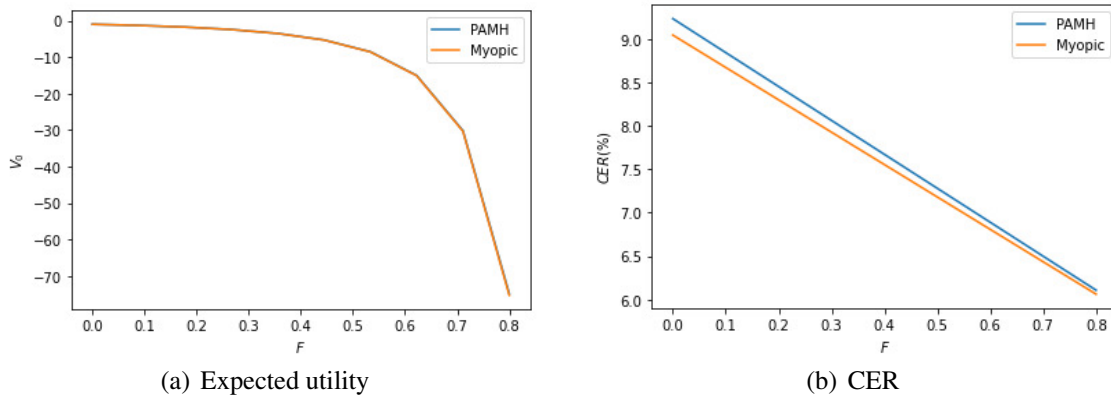


Figure 3.4: Expected utility and CER versus F (OU 4/2 model).

The relationship between optimal allocation and volatility group parameters a_S and b_S , is presented in Figure 3.5. Both the PAMH allocation and the myopic strategy change significantly with a_S and b_S ; the PAMH changes faster, which suggest that myopic approaches underestimate the importance of volatility. Furthermore, the figure also indicates that investors should put a larger proportion of their wealth on risky assets in more volatile periods.

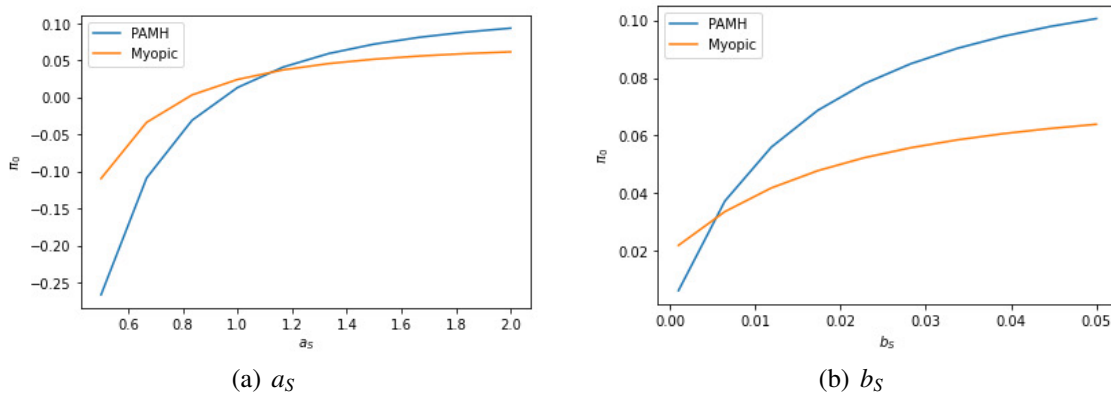


Figure 3.5: Optimal allocation for decreasing relative risk aversion (DRRA) investor versus a_S and b_S (OU 4/2 model).

3.4.2 Analysis of IRRA investors—the mean-variance case

In this section, we consider a dynamic mean-variance portfolio problem where investors maximize the expectation of the portfolio terminal wealth given a bound on the variance of terminal wealth. Formally, the investor problem is given by

$$V(t, W_t, X_t) = \max_{\pi_{\{s \geq t\}}} \mathbb{E}(W_T | \mathcal{F}_t) - \lambda \text{Var}(W_T | \mathcal{F}_t), \quad (3.19)$$

where λ denotes the Lagrange multiplier. Due to the variance term and the failure of iterated expectations, an application of dynamic programming does not lead to an optimal solution. [89] shows that the optimal strategy of Problem (3.19) can be found by solving a stochastic linear quadratic problem.

Theorem 3.4.1 *If $\pi_{s \geq t}^*$ is the optimal strategy for Problem (3.19), $\pi_{s \geq t}^*$ is the optimal strategy for*

$$\min_{\pi_{\{s \geq t\}}} \mathbb{E}((W_T - \mu)^2 | \mathcal{F}_t) \quad (3.20)$$

where $\mu = \frac{1}{2\lambda} + \mathbb{E}(W_T | \mathcal{F}_t)$.

Proof See [89], Theorem 3.1.

If two conditions are assumed—① the optimal strategy for Equation (3.19) exists, and ② the optimal strategy for (3.20) is unique—then the optimal strategy for (3.19) can be found by solving Equation (3.20). This is a special case of our investor's problem in Equation (3.2), when we set $\gamma = -1$, $F = -\mu$ and $\omega = 1$:

$$\max_{\pi_{\{s \geq t\}}} -\frac{1}{2} \mathbb{E}((-W_T - F)^2 | \mathcal{F}_t). \quad (3.21)$$

In this section, we obtain the optimal strategy of the dynamic mean-variance strategy by solving Auxiliary Problem (3.21). Note that, in this case, a negative F leads to IRRA investors, and its size determines the distribution of the optimal terminal wealth.

Table 3.7 compares the optimal strategy, expected utility and CER from the myopic strategy and the PAMH. The expected utility represented the value of (3.21) at time $t = 0$. The expectation and standard deviation of terminal wealth are also provided. The optimal strategy obtained from the PAMH is significantly different from the myopic strategy: PAMH always leads to a higher expectation and standard deviation of terminal wealth for the same fixed value of F . Standard deviation of estimates are reported in parentheses, obtained from 100 runs. All the results from PAMH are slightly more volatile because of the extra randomness from estimation of optimal strategy. The small standard deviation demonstrates the excellent accuracy and stability of the results from the PAMH. In addition, to illustrate the trade-off between expected return and volatility, we plot the efficient frontiers in Figure 3.6. The expectation of terminal wealth from both the PAMH and the myopic strategy is linear with the volatility. Not surprisingly, given a specific volatility level, the PAMH also always achieves a higher expected return than the myopic strategy. Furthermore, the difference increases as volatility increases.⁸

⁸Superiority of PAMH is more significant when the time to maturity get larger.

Table 3.7: Results for OU 4/2 model with IRRA investor.

	$F = -1.06$	$F = -1.1$	$F = -1.2$	$F = -1.3$	$F = -1.4$
<i>Myopic</i>					
$Weights(\pi_0^{Myopic})$	0.0017 (0.00)	0.0088 (0.00)	0.026 (0.00)	0.044 (0.00)	0.062 (0.00)
$Expected\ utility(V^{Myopic}(0, x))$	-0.00002 (0.0000001)	-0.00008 (0.000002)	-0.00072 (0.00002)	-0.0202 (0.00006)	-0.0397 (0.00012)
$CER(\%)$	5.30 (0.002)	6.07 (0.006)	7.99 (0.020)	9.90 (0.031)	11.82 (0.042)
$\mathbb{E}(W_T)$	1.054 (0.000002)	1.064 (0.00001)	1.089 (0.00003)	1.115 (0.00005)	1.141 (0.00007)
$sd(W_T)$	0.003 (0.00004)	0.016 (0.00014)	0.047 (0.00050)	0.078 (0.00075)	0.110 (0.00102)
$Computational\ time(Seconds)$	58.1 (7.2)	62.8 (5.9)	60.9 (4.9)	56.1 (4.7)	59.9 (4.5)
<i>PAMH</i>					
$Weights(\pi_0^{PAMH})$	0.0010 (0.0004)	0.0048 (0.0021)	0.0143 (0.0063)	0.0238 (0.0105)	0.0333 (0.0147)
$Expected\ utility(V^{PAMH}(0, x))$	-0.00002 (0.0000005)	-0.00007 (0.00002)	-0.00064 (0.00014)	-0.0180 (0.00039)	-0.0353 (0.00077)
$CER(\%)$	5.34 (0.008)	6.29 (0.041)	8.66 (0.124)	11.04 (0.208)	13.41 (0.291)
$\mathbb{E}(W_T)$	1.055 (0.00007)	1.069 (0.00039)	1.105 (0.00118)	1.141 (0.00197)	1.176 (0.00276)
$sd(W_T)$	0.004 (0.0002)	0.020 (0.0008)	0.061 (0.0025)	0.103 (0.0042)	0.144 (0.0058)
$Computational\ time(Seconds)$	229.6 (4.1)	232.7 (54.9)	255.4 (19.2)	249.7 (52.5)	242.0 (43.4)

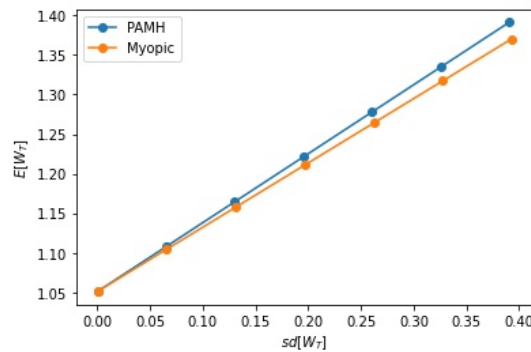


Figure 3.6: Efficient frontier (OU 4/2 model).

Next, we investigate the impact of volatility group parameters a_S and b_S on the optimal allocation, (see Figure 3.7) for a fixed $F = -1.2$. Both strategies increase with a_S and b_S , (i.e. they increase with the instantaneous volatility). However, the PAMH is much more sensitive

to volatility group parameters than the myopic strategy. It should be noted that a_S , which is the parameter controlling the GBM 1/2 part, could even change the sign of the allocation, leading to short positions on these mean reverting underlyings for investors.

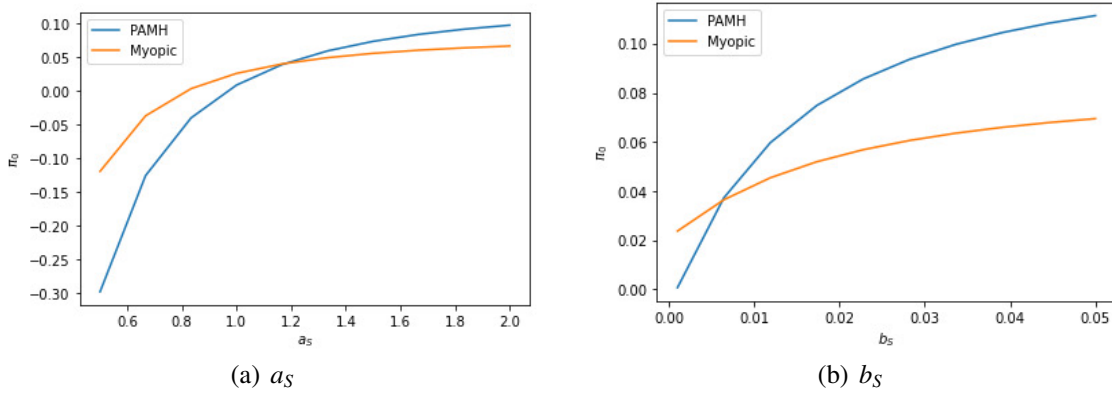


Figure 3.7: Optimal allocation for IRRA investor versus a_S and b_S (OU 4/2 model).

3.4.3 Suboptimality analysis for CRRA investors – the OU 1/2 model

We investigate the impact on performance when CRRA investors fail to account for SV. In particular, we focus on the OU 1/2 (Heston's) model, which is the most popular and important member of the OU 4/2 family (i.e. $b_S = 0$). The dynamics of the OU Heston are summarized as follows:

$$\begin{cases} \frac{dM_t}{M_t} = rdt \\ d \ln S_t = (L_S + (\lambda_S - \frac{1}{2})X_t - \beta_S \ln S_t)dt + \sqrt{X_t}dB_t \\ dX_t = \kappa_X(\theta_X - X_t)dt + \sigma_X \sqrt{X_t}dB_t^X \\ \langle dB_t, dB_t^X \rangle = \rho dt \end{cases} \quad (3.22)$$

The investor may neglect the SV feature of the financial time series and simply take the long run average of the variance as the instantaneous variance (i.e. $\sigma^2 = \mathbb{E}(X_t) = \theta_X$). This makes the OU 1/2 model degenerate into the exponential OU model

$$\begin{cases} \frac{dM_t}{M_t} = rdt \\ d \ln S_t = (L_S + (\lambda_S - \frac{1}{2})\sigma^2 - \beta_S \ln S_t)dt + \sigma dB_t \end{cases} \quad (3.23)$$

A CRRA-type investor would be able to use closed-form solutions for the exponential OU model as presented in [19]:

$$\pi_t^* = \frac{1}{\gamma} \left(\left(\frac{1}{\sigma^2} - \beta_S K(T-t) \right) (L_S + \lambda_S \sigma^2 - \beta_S \ln S_t - r) - \beta_S N(t, T) \right), \quad (3.24)$$

where $K(T-t)$, $N(t, T)$ can be obtained by solving ODEs, leading to $K(T-t) = R_2(T-t)$

$t)R_1^{-1}(T - t), R(t) = (R_1(t), R_2(t))$ and

$$\begin{aligned}
 R(T - t) &= \exp\left(\begin{pmatrix} \frac{1}{\gamma}\beta_S & -\frac{1}{\gamma}\beta_S^2\sigma^2 \\ \frac{1-\gamma}{\gamma\sigma^2} & -\frac{1}{\gamma}\beta_S \end{pmatrix} T - t\right) \begin{pmatrix} 1 \\ 0 \end{pmatrix} \\
 N(T - t) &= N(t, T) = \frac{\int_0^{T-t} \Theta K(T - s) \Phi_H(s, 0) ds}{\Phi_H(T - t, 0)} \\
 \Theta &= \frac{1}{2}\beta_S\sigma^2 - \beta_S r
 \end{aligned} \tag{3.25}$$

where

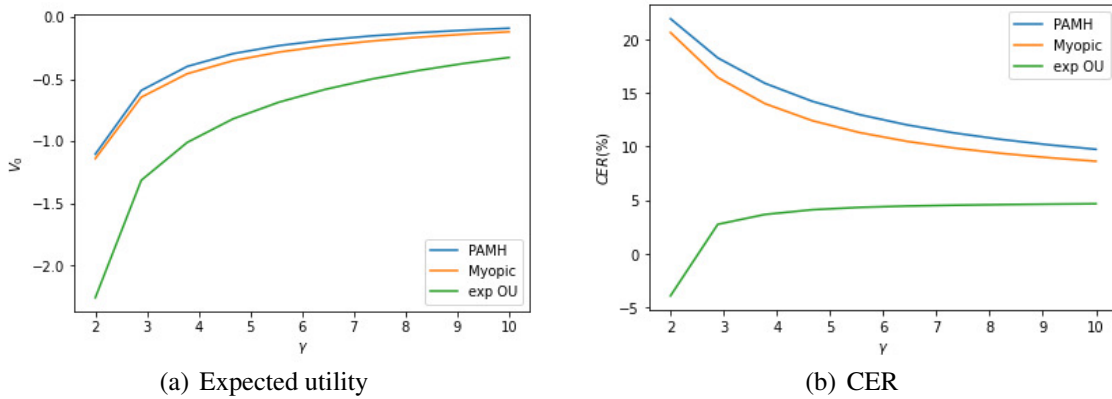
$$\frac{d\Phi_H(t, s)}{dt} = H(t)\Phi_H(t, s), H(t) = \frac{1}{\gamma}(\beta_S - \beta_S^2\sigma^2 K(T - t)) \quad \Phi_H(s, s) = 1. \tag{3.26}$$

The parameters for the OU 1/2 model from [37] are presented in Table 3.8,

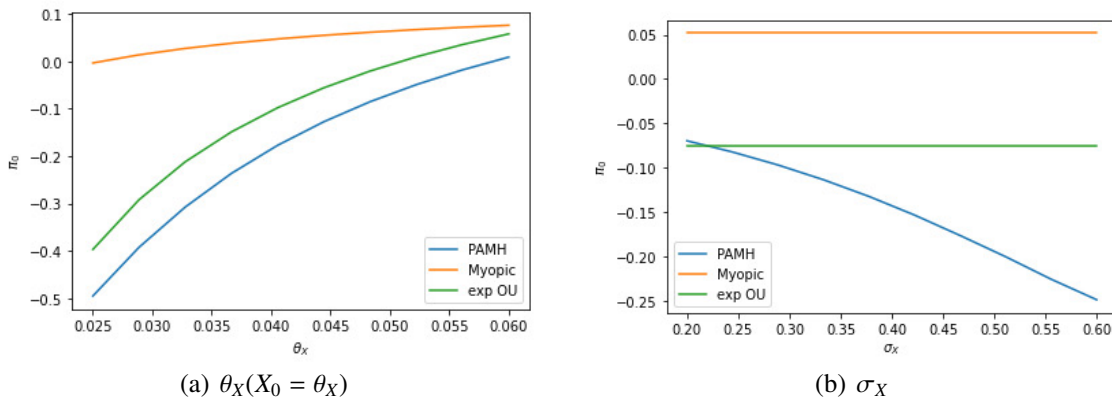
Table 3.8: Parameter values for OU 1/2 model.

Parameter	Value	Parameter	Value
T	3	X_0	0.04
r	0.05	λ_S	0.572
Δt	$\frac{1}{120}$	<i>period</i>	360
S_0	120.0	M_0	1.0
W_0	1	n_r	100
κ_X	5.028	θ_X	0.0426
σ_X	0.4149	ρ	-0.08
L	3.7672	β_S	0.78
N	2000	N_0	2000000
F	0	ω	γ

Figure 3.8 compares the portfolio performance of the myopic strategy, constant volatility strategy (exp OU) and PAMH optimal strategy for a CRRA-type investor in terms of expected value function and CER. The PAMH optimal strategy outperformed the other two sub-optimal strategies as expected. The myopic strategy achieves a higher expected value function and CER than the constant volatility strategy, which suggests that investors who fail to take the future movement of the volatility into consideration outperform those ignoring the SV.

Figure 3.8: Expected utility and CER versus γ (OU 1/2 model).

A sensitivity analysis of the three strategies at time $t = 0$ to the long run average θ_X and the volatility σ_X of instantaneous variance X_t are illustrated in Figure 3.9. With the fixed risk aversion level at $\gamma = 4$, all three strategies increase with θ_X , and both the PAMH and constant volatility strategy increase faster than the myopic strategy. Moreover, the PAMH strategy decreases with σ_X while the myopic strategy and constant volatility strategy remain constant.

Figure 3.9: Optimal allocation versus θ_X and σ_X (OU 1/2 model).

3.5 Conclusions

This chapter proposed a numerical scheme—the PAMH—for HARA utilities. The accuracy and time efficiency of PAMH are verified using closed-form solutions available for an one-dimensional problem, the GBM 1/2 (Heston’s) model, and for a multivariate stochastic covariance problem in dimension $n = 35$. The former was implemented on both, the case of DRRA, (i.e. EUT), and the case of IRRA, (i.e. MVT), while the latter was applied to the CRRA case only. In all cases the results are very close to the optimal levels in reasonable computational times. The method produces good solutions even in situations when verification theorems fail to deliver existence of a unique optimal.

The methodology was applied to the OU 4/2 model, which addresses two stylized facts of financial data: mean reversion and advanced SV. This is a powerful model for commodity

prices, volatility indexes, exchange rates and interest rates. We hence approximated the dynamic portfolio choice for the OU 4/2 model numerically and obtained optimal strategies for EUT and MVT.

For both, IRRA and DRRA, we witnessed large changes in optimal allocation due to variations in the volatility group parameters: a_S and b_S . For the DRRA case, the difference in CER between the PAMH strategy and the myopic strategy increased as the minimum capital guarantee level F decreased. As the optimal allocation for an IRRA investor coincides with the pre-commitment strategy in the context of a dynamic mean-variance portfolio, we displayed the corresponding efficient frontier. Here again, the myopic strategy performed quite poorly compared to the optimal. We also found low CER performances due to the ignorance of SV for CRRA investors. In this case, investors should prefer a myopic strategy to a strategy that neglects SV.

3.6 Notation and algorithm for our methodology

In this section we clarify the notation and present the algorithm step by step:

Notation	Meaning
$B_t^m, B_t^{m,X}$	Brownian motion at time t in m_{th} simulated path
S_t^m	Stock price at time t in m_{th} simulated path
X_t^m	Other state variables such as interest rate or volatility
n_r	Number of simulated paths
N	Number of simulations to compute expected utility for a given set (W_0, S_t^m, X_t^m)
$\hat{W}_{t+\Delta t}^{m,n}(\pi^m)$	The simulated wealth level at $t + \Delta t$ given the wealth, the allocation and other state variables at t are W_0, π^m, S_t^m , and X_t^m
$\hat{S}_{t+\Delta t}^{m,i}$	A simulated stock price at $t + \Delta t$ given S_t^m
$\hat{X}_{t+\Delta t}^{m,i}$	A simulated state variable at $t + \Delta t$ give X_t^m
$V(t, W, \ln S, X)$	Value function at time t given wealth W , stock price S and state variable X
\hat{v}^m	Estimation of $P_k(t, \ln S_t^m, X_t^m) = \log(f(t, \ln S_t^m, X_t^m))$ in Equation (3.6). Regressand in regression, superscript m indicates the corresponding regressor $(\ln S_t^m, X_t^m)$
$L_t(X, \ln S)$	The regression function to be used to approximate $P_k(t, \ln S, X)$
π_t^m	Optimal strategy at time t in m_{th} simulated path
$\hat{V}(0, W_0, \ln S_0, X_0)$	Estimation of expected utility at time 0.

Table 3.9: Notation and definitions

3.6.1 Algorithm

Next, we describe the algorithm step by step. We first generate the paths of stock prices S_t^m and state variables X_t^m according to their dynamics. Starting from $t = T - \Delta t$, which is the last period before the terminal, we compute the optimal strategy $\pi_{T-\Delta t}^m$ given $W_0, S_{T-\Delta t}^m, X_{T-\Delta t}^m$. Next, we obtain \hat{v}^m , which is the estimation of $P_k(T - \Delta t, \ln S_{T-\Delta t}^m, X_{T-\Delta t}^m)$, by taking the average of the simulated values. By regressing \hat{v}^m over the polynomial of $(X_{T-\Delta t}^m, \ln S_{T-\Delta t}^m)$, we obtain $L_{T-\Delta t}(X, \ln S)$ which is the approximation of the function $P_k(T - \Delta t, \ln S, X)$. The value

function at $t = T - \Delta t$ is then known immediately. We move backward and stop when the initial optimal strategy is obtained.

The state variable function f is separable with the wealth in Equation (3.6), so $P_k(t, \ln S_t^m, X_t^m)$ can be estimated assuming the wealth level starts at W_0 at each re-balancing time. To evaluate the expected utility, we regenerate the paths of stock price and state variables. The optimal strategy can be computed from $L_t(X, \ln S)$; hence, it is easy to obtain the optimal terminal wealth. The average of the utility of optimal terminal wealth denotes the expected utility.

Algorithm 8: PAMH

Input: S_0, W_0, X_0

Output: Optimal current trading strategy π_0^* and expected utility $\hat{V}(0, W_0, \ln S_0, X_0)$

- 1 Initialization;
 - 2 Generating n_r paths of $B_t^m, B_t^{m,X}, S_t^m, X_t^m$ for $m = 1 \dots n_r$;
 - 3 **while** $t = T - \Delta t$ **do**
 - 4 Directly compute optimal allocation $\pi_{T-\Delta t}^m$ with Equation (3.8) where the derivative of value function w.r.t state variable is 0 at time T ;
 - 5 Simulate wealth $\hat{W}_T^{m,i}(\pi_{T-\Delta t}^m)$ at the terminal given the wealth, stock price allocation and other state variables at $T - \Delta t$ are $W_0, S_{T-\Delta t}^m, \pi_{T-\Delta t}^m$ and $X_{T-\Delta t}^m$ for $i = 1 \dots N$;
 - 6 Compute $\hat{v}^m = \ln \left[\frac{1-\gamma}{\gamma} \frac{1}{N} \sum_{i=1}^N U(\hat{W}_T^{m,i}(\pi_{T-\Delta t}^m)) \right] - (1-\gamma) \ln \left[\frac{\omega}{\gamma} W_0 - Fd(T - \Delta t) \right]$ for $m = 1 \dots n_r$;
 - 7 Regress \hat{v}^m over the polynomial of $(X_{T-\Delta t}^m, \ln S_{T-\Delta t}^m)$, and obtain the function $L_{T-\Delta t}(X, \ln S)$
 - 8 **for** $t = T - 2\Delta t$ **to** Δt **do**
 - 9 Take the $L_{t+\Delta t}(X, \ln S)$ obtained from last step as $P_k(t + \Delta t, X, \ln S)$, we compute optimal allocation π_t^m with Equation (3.8) given W_0, S_t^m , and X_t^m ;
 - 10 Simulate wealth $\hat{W}_{t+\Delta t}^{m,i}(\pi_t^m)$, $\hat{S}_{t+\Delta t}^{m,i}$ and $\hat{X}_{t+\Delta t}^{m,i}$ given the wealth, stock price, allocation and other state variables at t are W_0, S_t^m, π_t^m and X_t^m for $i = 1 \dots N$;
 - 11 Compute
 - 12 $\hat{v}^m = \ln \left[\frac{1}{N} \sum_{i=1}^N \left(\frac{\omega}{\gamma} W_{t+\Delta t}^{m,i}(\pi_t^m) - Fd(t + \Delta t) \right)^{1-\gamma} \exp(L_{t+\Delta t}(\hat{X}_{t+\Delta t}^{m,i}, \ln \hat{S}_{t+\Delta t}^{m,i})) \right] - (1-\gamma) \ln \left[\frac{\omega}{\gamma} W_0 - Fd(t) \right]$ for $m = 1 \dots n_r$;
 - 13 Regress \hat{v}^m over the polynomial of $(X_t^m, \ln S_t^m)$, and obtain the function $L_t(X, \ln S)$;
 - 14 **while** $t = 0$ **do**
 - 15 Compute $g_{i,j}$ and g_j with $L_{\Delta t}(X, \ln S)$ obtained from the last step, so the optimal strategy is immediately known with Equation (3.8);
 - 16 Generate new paths of S_t^z, X_t^z for $z = 1 \dots N_0$, use the estimation of transformed value function $L_t(X, \ln S)$ to compute corresponding optimal allocation π_t^z and calculate the optimal terminal wealth W_T^z . The expected utility is ,

$$\hat{V}(0, W_0, \ln S_0, X_0) = \frac{1}{N_0} \sum_{n=1}^{N_0} U(W_T^z)$$
 - 17 **return** $\pi_0^*, \hat{V}(0, W_0, \ln S_0, X_0)$
-

3.7 Proof of Theorem 3.2.1

According to the Bellman equation, the value function can be rewritten as,

$$\begin{aligned} V(t, W, \ln S, X) &= \mathbb{E}_t(V(t + dt, W_{t+dt}, \ln S_{t+dt}, X_{t+dt}) \mid W, \ln S, X) \\ &= \max_{\pi_t} \mathbb{E}_t(V(t + dt, W_{t+dt}, \ln S_{t+dt}, X_{t+dt}) \mid W, \pi, \ln S, X). \end{aligned} \quad (3.27)$$

We expand $V(t + dt, W_{t+dt}, \ln S_{t+dt}, X_{t+dt})$ at $t + dt$ in terms of all the variables.

$$\begin{aligned} V(t + dt, W_{t+dt}, \ln S_{t+dt}, X_{t+dt}) &= V(t + dt, W_t, \ln S_t, X_t) + V_{W_t}(t + dt, W_t, \ln S_t, X_t)dW_t \\ &+ \frac{1}{2}V_{W_t W_t}(t + dt, W_t, \ln S_t, X_t)(dW_t)^2 \\ &+ \sum_{i=1}^n \left(V_{\ln S_t^{(i)}}(t + dt, W_t, \ln S_t, X_t)d \ln S_t^{(i)} + V_{X_t^{(i)}}(t + dt, W_t, \ln S_t, X_t)dX_t^{(i)} \right) \\ &+ \frac{1}{2} \sum_{i,j=1}^n \left(V_{\ln S_t^{(i)} \ln S_t^{(j)}}(t + dt, W_t, \ln S_t, X_t)(d \ln S_t^{(i)})(d \ln S_t^{(j)}) \right) \\ &+ \frac{1}{2} \sum_{i=1}^n \left(V_{X_t^{(i)} X_t^{(i)}}(t + dt, W_t, \ln S_t, X_t)(dX_t^{(i)})^2 \right) + \sum_{i=1}^n \left(V_{W_t \ln S_t^{(i)}}(t + dt, W_t, \ln S_t, X_t)dW_t d \ln S_t^{(i)} \right) \\ &+ \sum_{i=1}^n \left(V_{W_t X_t^{(i)}}(t + dt, W_t, \ln S_t, X_t)dW_t dX_t^{(i)} \right) + \sum_{i,j=1}^n \left(V_{\ln S_t^{(i)} X_t^{(j)}}(t + dt, W_t, \ln S_t, X_t)d \ln S_t^{(i)} dX_t^{(j)} \right) + o(dt). \end{aligned} \quad (3.28)$$

Substituting $dW_t, d \ln S_t, dX_t$ which can be found in Equation (3.1), taking conditional expectation on both sides, and rewriting $V(t, W_t, \ln S_t, X_t)$ in a quadratic form with respect to π leads to

$$\begin{aligned}
V(t, W_t, \ln S_t, X_t) &= \max_{\pi_t} \left(\sum_{i,j=1}^n f_{i,j}(t, W_t, \ln S_t, X_t) \pi_t^{(i)} \pi_t^{(j)} + \sum_{i=1}^n f_i(t, W_t, \ln S_t, X_t) \pi_t^{(i)} + f_0(t, W_t, \ln S_t, X_t) \right) \\
f_{i,j}(t, W_t, \ln S_t, X_t) &= \frac{1}{2} V_{W_t W_t}(t + dt, W_t, \ln S_t, X_t) W_t^2 \left(\sum_{k=1}^n \sigma_{i,k}(X_t, \ln S_t) \sigma_{j,k}(X_t, \ln S_t) \right) dt \\
f_i(t, W_t, \ln S_t, X_t) &= V_{W_t}(t + dt, W_t, \ln S_t, X_t) W_t \left(\theta_i(X_t, \ln S_t) + \frac{1}{2} \sum_{j=1}^n \sigma_{i,j}^2(X_t, \ln S_t) - r \right) dt \\
&\quad + \sum_{j=1}^n V_{W_t \ln S_t^{(j)}}(t + dt, W_t, \ln S_t, X_t) W_t \left(\sum_{k=1}^n \sigma_{i,k}(X_t, \ln S_t) \sigma_{j,k}(X_t, \ln S_t) \right) dt \\
&\quad + \sum_{j=1}^n V_{W_t X_t^{(j)}}(t + dt, W_t, \ln S_t, X_t) W_t \sigma_{i,j}(X_t, \ln S_t) b_j(X_t^{(j)}) \rho_j dt \\
f_0(t, W_t, \ln S_t, X_t) &= V(t + dt, W_t, \ln S_t, X_t) + V_{W_t}(t + dt, W_t, \ln S_t, X_t) W_t r dt \\
&\quad + \sum_{i=1}^n V_{\ln S_t^{(i)}}(t + dt, W_t, \ln S_t, X_t) \theta_i(X_t, \ln S_t) dt \\
&\quad + \sum_{i=1}^n \left(V_{X_t^{(i)}}(t + dt, W_t, \ln S_t, X_t) a_i(X_t^{(i)}) + \frac{1}{2} V_{X_t^{(i)} X_t^{(i)}}(t + dt, W_t, \ln S_t, X_t) b_i^2(X_t^{(i)}) \right) dt \\
&\quad + \frac{1}{2} \sum_{i,j=1}^n V_{\ln S_t^{(i)} \ln S_t^{(j)}}(t + dt, W_t, \ln S_t, X_t) \left(\sum_{k=1}^n \sigma_{i,k}(X_t, \ln S_t) \sigma_{j,k}(X_t, \ln S_t) \right) dt \\
&\quad + \sum_{i,j=1}^n V_{\ln S_t^{(i)} X_t^{(j)}}(t + dt, W_t, \ln S_t, X_t) \sigma_{i,j}(X_t, \ln S_t) b_j(X_t^{(j)}) \rho_j dt.
\end{aligned} \tag{3.29}$$

We assume a sufficiently small dt so that $o(dt)$ terms are omitted when taking conditional expectations. The optimal allocation is given by the solution to the system of equations:

$$\sum_{j=1}^n 2f_{i,j}(t, W_t, \ln S_t, X_t) \pi_t^{(*,j)} = -f_i(t, W_t, \ln S_t, X_t), \quad i = 1, \dots, n. \tag{3.30}$$

With the representation of the value function in Equation (3.6) and assuming that $f(t, \ln S, X) = \exp(P_k(t, \ln S, X))$, the derivatives of value function with respect to each stock and state variable can be rewritten as,

$$\begin{aligned}
V_W(t+dt, W_t, \ln S_t, X_t) &= \omega \left(\frac{\omega}{\gamma} W_t - Fd(t+dt) \right)^{-\gamma} \exp(P_k(t+dt, \ln S_t, X_t)) \\
V_{WW}(t+dt, W_t, \ln S_t, X_t) &= -\omega^2 \left(\frac{\omega}{\gamma} W_t - Fd(t+dt) \right)^{-\gamma-1} \exp(P_k(t+dt, \ln S_t, X_t)) \\
V_{W \ln S_t^{(i)}}(t+dt, W_t, \ln S_t, X_t) &= \omega \left(\frac{\omega}{\gamma} W_t - Fd(t+dt) \right)^{-\gamma} \exp(P_k(t+dt, \ln S_t, X_t)) \frac{\partial P_k(t+dt, \ln S_t, X_t)}{\partial \ln S_t^{(i)}} \\
V_{WX_t^{(i)}}(t+dt, W_t, \ln S_t, X_t) &= \omega \left(\frac{\omega}{\gamma} W_t - Fd(t+dt) \right)^{-\gamma} \exp(P_k(t+dt, \ln S_t, X_t)) \frac{\partial P_k(t+dt, \ln S_t, X_t)}{\partial X_t^{(i)}}
\end{aligned} \tag{3.31}$$

substituting Equation (3.31) into Equation (3.30), the optimal strategy can be approximated as follows:

$$\begin{aligned}
\sum_{j=1}^n g_{i,j}(t, W_t, \ln S_t, X_t) \pi_t^{(*,j)} &= g_i(t, W_t, \ln S_t, X_t), \quad i = 1, \dots, n \\
g_{i,j}(t, W_t, \ln S_t, X_t) &= \omega W_t \left(\sum_{k=1}^n \sigma_{i,k}(X_t, \ln S_t) \sigma_{j,k}(X_t, \ln S_t) \right) \\
g_i(t, W_t, \ln S_t, X_t) &= \left(\frac{\omega}{\gamma} W_t - Fd(t+dt) \right) \left(\theta_i(X_t, \ln S_t) + \frac{1}{2} \sum_{j=1}^n \sigma_{i,j}^2(X_t, \ln S_t) - r \right) \\
&\quad + \sum_{j=1}^n \left(\frac{\omega}{\gamma} W_t - Fd(t+dt) \right) \frac{\partial P_k(t+dt, \ln S_t, X_t)}{\partial \ln S_t^{(j)}} \left(\sum_{k=1}^n \sigma_{i,k}(X_t, \ln S_t) \sigma_{j,k}(X_t, \ln S_t) \right) \\
&\quad + \sum_{j=1}^n \left(\frac{\omega}{\gamma} W_t - Fd(t+dt) \right) \frac{\partial P_k(t+dt, \ln S_t, X_t)}{\partial X_t^{(j)}} \sigma_{i,j}(X_t, \ln S_t) b_j(X_t^{(j)}) \rho_j.
\end{aligned} \tag{3.32}$$

The existence and uniqueness of the approximation, $\pi_t^{(*,j)}$ is ensured by the invertibility of the matrix $\sigma(X_t, \ln S_t) \sigma(X_t, \ln S_t)^T$, together with the differentiability of the polynomial P_k . Note π^* depends on W_t in the form $\frac{(\frac{\omega}{\gamma} W_t - Fd(t+dt))}{W_t} a(t, \ln S_t, X_t)$, hence the drift and volatility of the wealth process are linear in W_t , and they both satisfy the conditions in Proposition 1.2 in [60], therefore the wealth process has a pathwise unique solution which always remains above the floor $Fd(t) \geq 0$:

$$\begin{aligned}
dW_t &= \left(W_t r + \sum_{i=1}^n \left(\frac{\omega}{\gamma} W_t - Fd(t+dt) \right) a(t, \ln S_t, X_t) \left(\theta_i(X_t, \ln S_t) + \sum_{j=1}^n \frac{1}{2} \sigma_{i,j}^2(X_t, \ln S_t) - r \right) \right) dt \\
&\quad + \sum_{i=1}^n \left(\frac{\omega}{\gamma} W_t - Fd(t+dt) \right) a(t, \ln S_t, X_t) \left(\sum_{j=1}^n \sigma_{i,j}(X_t, \ln S_t) dB_t^{(j)} \right).
\end{aligned}$$

Chapter 4

A neural network Monte Carlo approximation for expected utility theory

Chapter summary:

This chapter proposes an approximation method to create an optimal continuous-time portfolio strategy based on a combination of Neural Networks and Monte Carlo, named NNMC. This work is motivated by the increasing complexity of continuous-time models and stylized facts reported in the literature. We work within expected utility theory for portfolio selection with a Constant Relative Risk Aversion utility. The method extends a recursive polynomial exponential approximation framework, first documented in chapter 3, by adopting neural networks to fit the portfolio value function. We develop two architectures of network and explore several activation functions. The methodology is applied on four settings: a 4/2 stochastic volatility (SV) model with two types of market price of risk, a 4/2 model with jumps, and an Ornstein–Uhlenbeck 4/2 model. Closed-form solution in one case above is available, which helps in the comparison of accuracy. We report the accuracy of the various settings in terms of optimal strategy, portfolio performance and computational efficiency, highlighting the potential of NNMC to tackle complex dynamic models.

Status: Published in *Journal of Risk and Financial Management*.

4.1 Introduction

Optimally allocating to a collection of financial investments like stocks, bonds, commodities, has been a topic of concern to financial institutions and players since at least the pioneer work of Markowitz’s Mean-Variance portfolio theory in 1952. People then realized the importance of diversification and his work laid the foundations for the development of portfolio analysis in both academia and industry. These initial results were in discrete-time, but it was not long before continuous-time portfolio decisions were produced in the alternative paradigm of Expected Utility Theory, see [76]. The author assumed the investor is able to adjust their position continuously, and stock price process is modelled by a geometric Brownian motion (GBM). The optimal trading strategy and consumption policy that maximize the investor’s expected utility were obtained in closed-form by solving a Hamilton-Jacobi-Bellman equation.

The beauty and practicality of this continuous-time solution led many researchers on this

path, producing optimal closed-form strategies for a wide range of models. For example, [59] considered the stochastic volatility (SV) Heston model, [48]. [38] constructed a portfolio of stocks and fixed-income market products to hedge interest rate risk. Explicit solutions in the presence of regime switching, stochastic interest rate and stochastic volatility was presented in [33], the positive performance of their portfolio is confirmed by empirical study. For the commodities asset class, [19] modelled a mean-reverting risky asset by an exponential Ornstein–Uhlenbeck (OU) process and solved the investment problem for an insurer subject to random payment of insurance claim.

These models are particular cases of the quadratic-Affine family (see [70]), one of the broadest model solvable in closed-form. The value function for a model in this family is the product of a function of wealth and an exponential quadratic function. Nonetheless, the complexity of financial markets has continued increasing every decade, with researchers detecting new stylized facts and proposing new models outside the quadratic-Affine. Needless to say, investor must rely on these advanced models for better financial decision, however. Closed-form solutions are no longer guarantee. One example of these advanced models is the GBM 4/2 model, introduced in [45]. The model improves the Heston model in terms of better fitting of implied volatility surfaces and historical volatilities patterns. The optimal portfolio problem with the GBM 4/2 model is solvable for certain types of market price of risk (MPR, see [18]), while the optimal trading strategy has not been found yet with a MPR proportional to the instantaneous volatility. More recently, an OU 4/2 model, which unifies the mean-reverting drift and stochastic volatility in a single model, was presented in [37]. The model targets two asset classes: commodities and volatility indexes. The optimal portfolio with the OU 4/2 model is not closed-form. This motivates approximation methods for dynamic portfolio choice.

Most approximation methods follow the idea from martingale method (see [54]) or dynamic programming technique [10]. [26] proposed a simulation-based method seeking the financial replication of the optimal terminal wealth given in the martingale method. [30] developed a comprehensive approach for the same investment problems, and the application of Malliavin calculus enhances its accuracy. The work in [10] led to the BGSS method, which is inspired on the popular least-square Monte Carlo method of [72]. BGSS pioneered the recursive approximation method for dynamic portfolio choice. [24] enhanced BGSS with the Stochastic Grid Bundling Method (SGBM) for conditional expectation estimation introduced in [53]. More recently, a polynomial affine method for Constant Relative Risk Aversion utility (PAMC) was recently developed in [92]. The method takes advantage of the quadratic-Affine structure, leading to superior accuracy and efficiency in the approximation of the optimal strategy and value function. In this chapter, we extend the methodology in PAMC using neural networks.

The history of artificial neural networks goes back to [75], where the author created the so-called a “threshold logic” on the basis of the neural networks of the human brain in order to mimic human thoughts. Then deep learning has steadily evolved. Almost three decades later, back propagation, a widely used algorithm in neural network’s parameter fitting for supervised learning, was introduced, see [69]. The importance of back propagation was only fully recognized when [82] showed that it can provide interesting distribution representations. The universal approximation theorem (see [27]) illustrated that every bounded continuous function can be approximated by a network with an arbitrarily small error, which further verifies the effectiveness of the neural network. Neural networks recently attracted a lot of attention of applied scientists, which success in fields such as image recognition and natural language pro-

cessing because it is particular good at function approximation when the form of the target function is unknown. In the realm of dynamic portfolio analyses, [67] first predicted portfolio covariance matrix with the Elman network and achieved good estimation of the optimal mean-variance portfolio. More recently, [63] proposed a neural network, representing the portfolio strategy at each rebalancing time, for a constrained defined contribution (DC) allocation problem. [17] introduced a differential equation based method, where the value function with the Heston model is estimated by a deep neural network.

In this chapter, motivated by the lack of knowledge on the correct expression for the portfolio value function for unsolvable models, we approximate the optimal portfolio strategy for any given stochastic process model with a neural network fitting the value function. A successful fitting relies on a suitable network architecture that captures the connection between input and output variable, as well as reasonable activation functions. We design two architectures enriching an embedded quadratic-affine structure, and we consider three types of activation functions.

Given the lack of closed-form solutions for SV 4/2 models, we use them as our toy examples in the implementations. In particular, we first implement our methodology on the solvable case (i.e., GBM 4/2 with solvable MPR), so the accuracy and efficiency is demonstrated before it is applied to the unsolvable cases of: GBM 4/2 model with stochastic jumps, GBM 4/2 model with proportional instantaneous volatility MPR, and the OU 4/2 model. Furthermore, we show numerically which network architecture is preferable in each case.

The chapter is organized as follows, Section 4.2 introduces the dynamic portfolio choice problem, and presents the neural network architectures, activation functions and parameter training details. The step by step algorithm of our methodology is provided in Section 4.3. Sections 4.4 and 4.5 applies the methodology to the GBM 4/2 and the OU 4/2 models. Section 4.6 concludes.

4.2 Problem Setting and Architectures of the Deep Learning Model

We consider a frictionless market consisting of a money market account (cash, M) and one stock (S). We assume the stock price follows a generalized diffusion process incorporating a one-dimensional state variable X . All the processes are defined on a complete probability space $(\Omega, \mathcal{F}, \mathbb{P})$ with a right-continuous filtration $\{\mathcal{F}_t\}_{t \in [0, T]}$, summarized by the stochastic differential equations (SDE):

$$\begin{cases} \frac{dM_t}{M_t} = r(X_t)dt \\ dS_t = S_t \theta(X_t, S_t)dt + S_t \sigma(X_t, S_t)dB_t + S_t \mu_N dN_t \\ dX_t = a(X_t)dt + b(X_t)dB_t^X \\ \langle dB_t, dB_t^X \rangle = \rho dt. \end{cases} \quad (4.1)$$

B_t and B_t^X are Brownian motions with correlation ρ . $r(X_t)$ is the interest rate, $\theta(X_t, S_t)$ and $\sigma(X_t, S_t)$ are the drift and diffusion coefficients for the stock price. $a(X_t)$ and $b(X_t)$ are measurable functions of state variable X_t . N_t is a pure-jump process independent of B_t and B_t^X with stochastic intensity $\lambda_N X_t$ for constant $\lambda_N > 0$, and $\mu_N > -1$ denotes the jump size.

We consider an investor with risk preference represented by a constant relative risk aversion (CRRA) utility:

$$U(W) = \frac{W^{1-\gamma}}{1-\gamma}. \quad (4.2)$$

Investors can adjust their allocation at a predetermined set of rebalancing times $(0, \Delta t, 2\Delta t, \dots, T - \Delta t)$. The investors wish to derive a portfolio strategy π (percentage of wealth allocated to the stock) that maximizes their expected utility of terminal wealth, in other word, $\mathbb{E}(U(W_T))$. The value function, representing investor's conditional expected utility, has the following representation:

$$V(t, W, S, X) = \max_{\pi_{s \geq t}} \mathbb{E}(U(W_T) | t, W, S, X) = \frac{W^{1-\gamma}}{1-\gamma} f(t, S, X). \quad (4.3)$$

The value function is separated into a wealth factor $\frac{W^{1-\gamma}}{1-\gamma}$ and a state variable function f . The NNMC estimates the state variable function f with a neural network model NN and computes the optimal strategy π_t^* with the Bellman principle.

4.2.1 Architectures of the deep learning model

In this section, we present two neural network architectures to fit the value function. According to the separable property of the value function shown in Equation (4.3), the only unknown component is the state variable function f , which is therefore the target function for the neural network. The architectures of the networks are built around exponential polynomial functions, which are the most common form of solvable investor's value functions and used in the PAMC method (see [92]). This property of proposed networks ensures the new method generalizes PAMC.

The neural network is expected to achieve a better fit than a polynomial regression if the true state variable function is significantly different from the exponential polynomial function. Furthermore, we designed an initialization method for networks, which is better than a random initialization in terms of portfolio value function fitting.

4.2.1.1 Sum of exponential network

We first introduce the sum of exponential polynomial neural network (SEN), as illustrated in Figure 4.1. The amount of input depends on the number of state variables. For simplicity, we take two inputs as an example. The first hidden layer computes the monomial of inputs. The second hidden layer obtains the linear combinations of the neuron in the first layer, where the weights are fitted in NNMC. An exponential activation function is applied to the second layer. The final output calculates a linear combination of exponential polynomials, so the exponential polynomial is a specific case of this neural network.

We denote the sum of exponential network by NN^{SEN} ; the proposition next states the estimation of the corresponding optimal allocation.

Proposition 4.2.1 *Given the SEN approximation of the value function at the next rebalancing time $t + \Delta t$, (i.e. $NN^{SEN}[t + \Delta t, S_t, X_t]$), the optimal strategy at time t is given by*

$$\pi_t^{SEN} = \arg \max_{\pi} V(t, W_t, \pi_t, S_t, X_t), \quad (4.4)$$

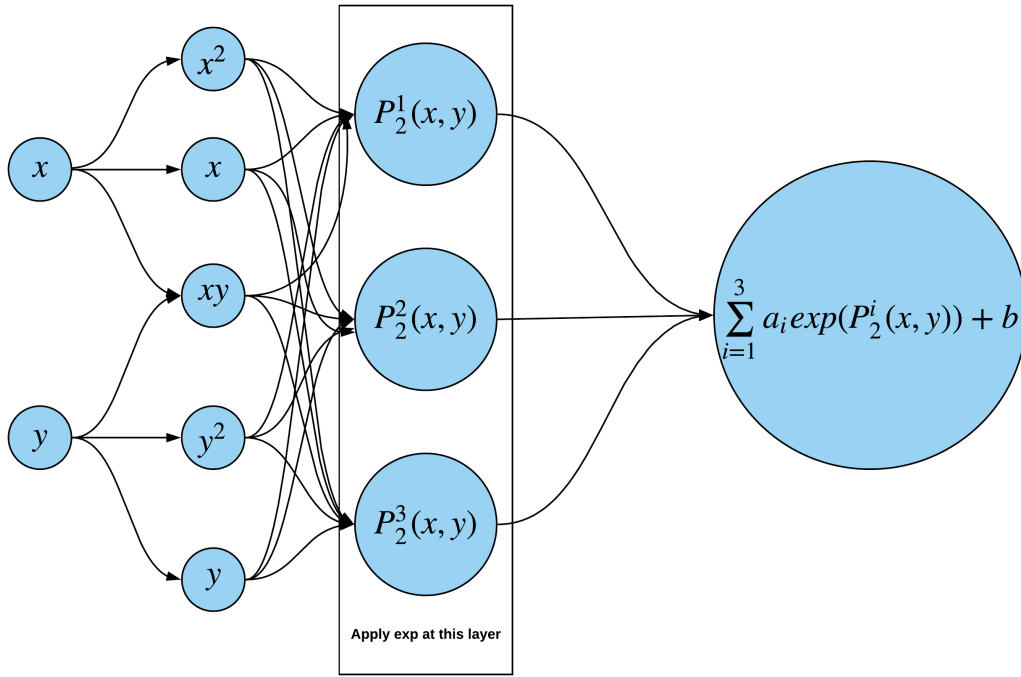


Figure 4.1: Sum of exponential network (SEN).

which is the solution of

$$f_2(t, W_t, S_t, X_t) + f_1(t, W_t, S_t, X_t)\pi_t + NN^{SEN}(t + \Delta t, S_t(1 + \mu_N), X_t)\lambda_N X_t \mu_N (1 + \pi_t \mu_N)^{-\gamma} = 0, \quad (4.5)$$

where

$$\begin{aligned} f_1(t, W_t, S_t, X_t) &= -\gamma NN^{SEN}(t + \Delta t, W_t, S_t, X_t)\sigma^2(X_t, S_t) \\ f_2(t, W_t, S_t, X_t) &= NN^{SEN}(t + \Delta t, W_t, S_t, X_t)(\theta(X_t, S_t) - r(X_t)) \\ &\quad + \frac{\partial NN^{SEN}(t + \Delta t, W_t, S_t, X_t)}{\partial S_t} S_t \sigma^2(X_t, S_t) \\ &\quad + \frac{\partial NN^{SEN}(t + \Delta t, W_t, S_t, X_t)}{\partial X_t} \sigma(X_t, S_t) b(X_t) \rho. \end{aligned} \quad (4.6)$$

Notably, $\pi_t^{SEN} = -\frac{f_2(t, W_t, S_t, X_t)}{f_1(t, W_t, S_t, X_t)}$ when S_t follows a diffusion process, i.e., $\lambda_N = 0$. $\pi_t^{SEN} = \frac{1}{\mu_N} \left(\left(-\frac{f_2(t, W_t, S_t, X_t)}{NN^{SEN}(t + \Delta t, S_t, X_t)\lambda_N X_t \mu_N} \right)^{-\frac{1}{\gamma}} - 1 \right)$ when S_t follows a jump process, i.e., $\sigma(X_t, S_t) = 0$.

Proof It follows similarly to Theorem 1 in [91]. According to the Bellman principle,

$$V(t, W_t, S_t, X_t) = \max_{\pi_t} \mathbb{E}_t(V(t + \Delta t, W_{t+\Delta t}, S_{t+\Delta t}, X_{t+\Delta t}) | W_t, S_t, X_t). \quad (4.7)$$

We substitute $V(t + \Delta t, W_{t+\Delta t}, S_{t+\Delta t}, X_{t+\Delta t})$ with $\frac{W^{1-\gamma}}{1-\gamma} NN^{SEN}(t + \Delta t, W_{t+\Delta t}, S_{t+\Delta t}, X_{t+\Delta t})$ and expand the right hand side of the equation with respect to W , S and X , then $V(t, W_t, S_t, X_t)$ is written as a function of strategy π_t . Equation (4.5) is obtained with the first order condition.

4.2.1.2 Improving Exponential Network

The architecture of an improving exponential network (IEN) is exhibited in Figure 4.2.

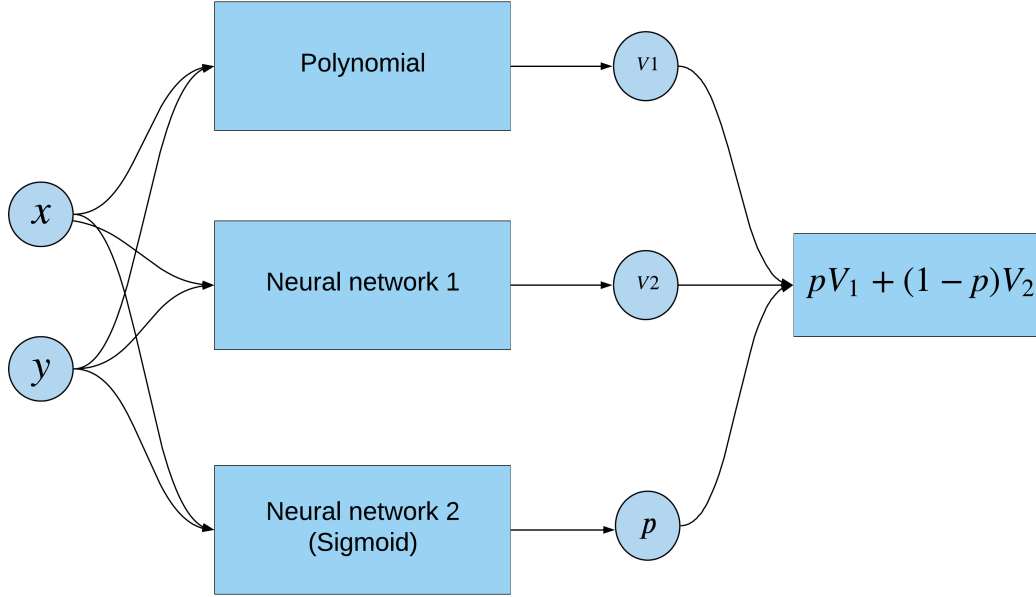


Figure 4.2: Improving exponential polynomial.

The target function of IEN is the log of the state variable function f (i.e. $\ln f$). The neural network consists of three parts. Node 1 is a polynomial with the output denoted by V_1 . Node 2 is an artificial neural network with an arbitrary number of hidden layers and neurons; we denote its output by V_2 . Node 3 is a single layer network with a Sigmoid function which computes a proportion $p \in [0, 1]$. The final output is the weighted average of the first two nodes $pV_1 + (1 - p)V_2$. The second node is the complement to the exponential polynomial function. Moreover, the similarity between the true value function and the exponential polynomial function is measured by p , which is fitted into the NNMC methodology. Therefore, the network automatically adjusts the weights on the exponential polynomial function and its supplement according to the generated data. Finally, the state variable function f is computed as

$$f = e^{pv_1 + (1-p)v_2} = (e^{v_1})^p \times (e^{v_2})^{1-p}, \quad (4.8)$$

which is the geometric weighted average of nodes 1 and 2. Letting NN^{IEN} denote the IEN, the estimation of optimal strategy is give in the next proposition.

Proposition 4.2.2 *Given the IEN approximation of the log value function at time $t + \Delta t$ (i.e., $NN^{IEN}[t + \Delta t, S_t, X_t]$), the optimal strategy at time t is given by*

$$\pi_t^{IEN} = \arg \max_{\pi} V(t, W_t, S_t, X_t), \quad (4.9)$$

which is the solution of

$$(f_2(t, W_t, S_t, X_t) + f_1(t, W_t, S_t, X_t)\pi_t) + \lambda_N X_t \exp\left(NN^{IEN}(t + \Delta t, S_t(1 + \mu_N), X_t)\right) \mu_N (1 + \pi_t \mu_N)^{-\gamma} = 0, \quad (4.10)$$

where

$$\begin{aligned}
f_1(t, W_t, S_t, X_t) &= -\gamma \exp\left(NN^{IEN}(t + \Delta t, S_t, X_t)\right) \sigma^2(X_t, S_t) \\
f_2(t, W_t, S_t, X_t) &= \exp\left(NN^{IEN}(t + \Delta t, S_t, X_t)\right) (\theta(X_t, S_t) - r(X_t)) \\
&\quad + \frac{\partial NN^{IEN}(t + \Delta t, W_t, S_t, X_t)}{\partial S_t} \exp\left(NN^{IEN}(t + \Delta t, S_t, X_t)\right) S_t \sigma^2(X_t, S_t) \\
&\quad + \frac{\partial NN^{IEN}(t + \Delta t, W_t, S_t, X_t)}{\partial X_t} \exp\left(NN^{IEN}(t + \Delta t, S_t, X_t)\right) \sigma(X_t, S_t) b(X_t) \rho.
\end{aligned} \tag{4.11}$$

Notably, $\pi_t^{IEN} = -\frac{f_2(t, W_t, S_t, X_t)}{f_1(t, W_t, S_t, X_t)}$ when S_t follows a diffusion process, in other word, $\lambda_N = 0$. $\pi_t^{IEN} = \frac{1}{\mu_N} \left(-\frac{f_2(t, W_t, S_t, X_t)}{\exp(NN^{IEN}(t + \Delta t, S_t, X_t)) \lambda_N X_t \mu_N} \right)^{-\frac{1}{\gamma}} - 1$ when S_t follows a jump process (i.e. $\sigma[X_t, S_t] = 0$).

Proof The proof follows similarly to Proposition 4.2.1.

4.2.2 Initialization, Stopping Criterion and Activation Function

In this section, we disclose more details on training the neural networks. The initialization of weights is the first step of network training, which may significantly impact the goodness of fit. A good initialization prevents the network's weights from converging to a local minimum and avoids slow convergence. Random initialization is most used when interpretability of network is usually weak. In contrast, both the SEN and the IEN are extensions of an exponential polynomial function; we suggest taking advantage of the results from the polynomial regression. Hence, the neural network searches the minimum near the exponential polynomial function used in the PAMC ensuring consistency. The polynomial regression initialization achieves superior results to the random initialization.

The coefficients of the exponential polynomial are first obtained with a regression model. The output of the SEN is a linear combination of exponential polynomial functions $\sum_{i=1}^N a_i \exp(P_n^i(x, y)) + b$, we substitute the coefficients from polynomial regression into $P_n^1(x, y)$ and set $a_1 = 1, a_2 = a_3 = \dots = a_n = b = 0$. For the initialization of the IEN, we substitute the coefficients into the first node and artificially make $p = 1$.

The training process minimizes the mean squared error (MSE) between network's the output and the simulated expected utility, and the sample data is split into a training set and a test set to reduce the overfitting problem. Adam is a back-propagation algorithm that combines the best properties of the AdaGrad and RMSProp algorithms to handle sparse gradients on noisy problems and provides excellent convergence speed. We applied the Adam on the training set for updating the network's weights, and the test set MSE was computed and recorded afterward. The test set MSE was expected to be convergent, so the training process was finished when the difference between the moving average of the recent 100 test set MSEs and the most recent test set MSE was less than a predetermined threshold, which was set at 0.00001 in the implementation.

The number of exponential polynomials is a hyperparameter in the SEN. We let the SEN be a sum of two exponential polynomial functions for simplicity. Node 2 in the IEN is an artificial neural network, which complements node 1 when the value function significantly deviates

from an exponential polynomial function. The number of hidden layers and neurons, as well as the activation function of node 2, are freely determined before fitting the value function. We assume node 2 is a single layer network with 10 neurons¹ and we implement several functions for comparison purposes, such as the logistic (sigmoid):

$$f(x) = \frac{1}{1 + e^{-x}}, \quad (4.12)$$

the Rectified linear unit (ReLU):

$$f(x) = \begin{cases} 0 & \text{if } x \leq 0 \\ x & \text{if } x > 0 \end{cases}, \quad (4.13)$$

and the Exponential linear unit (ELU):

$$f(x) = \begin{cases} 0 & \text{if } x \leq 0 \\ e^x - 1 & \text{if } x > 0 \end{cases}. \quad (4.14)$$

4.3 Notation and Algorithm of the Methodology

In this section, we clarify the notation and the step-by-step algorithm. The notation is displayed in Table 4.1.

Notation	Meaning
B_t^m	Brownian motion at time t in m_{th} simulated path
S_t^m	Stock price at time t in m_{th} simulated path
X_t^m	Other state variable such as interest rate or volatility
n_r	Number of simulated paths
N	Number of simulation to compute expected utility for a given set (W_0, S_t^m, X_t^m)
$\hat{W}_{t+\Delta t}^{m,n}(\pi^m)$	A simulated wealth level at $t + \Delta t$ given the wealth, allocation and other state variables at t are W_0, π^m and X_t^m
$\hat{S}_{t+\Delta t}^{m,n}$	A simulated stock price at $t + \Delta t$ given S_t^m
$\hat{X}_{t+\Delta t}^{m,n}$	A simulated state variable at $t + \Delta t$ give X_t^m
$V(t, W, S, X)$	Value function at time t given wealth W , stock price S and state variable X
$NN(t, X, S)$	The neural network used to fit $f(t, S_t, X_t)$ or $\ln [f(t, S_t, X_t)]$
\hat{v}^m	Estimation of $f(t, S_t^m, X_t^m)$ or $\ln [f(t, S_t^m, X_t^m)]$
$\pi_s^{m,n}$	Optimal strategy at time s given wealth, stock price and other state variables are $\hat{W}_s^{m,n}, \hat{S}_s^{m,n}$ and $\hat{X}_s^{m,n}$
$\hat{V}(0, W_0, S_0, X_0)$	Estimation of expected utility at time 0.

Table 4.1: Notations for NNMC for NNMC is listed here.

¹In our experiments, increasing the number of layers has little improvement in portfolio performance.

4.3.1 Algorithm

We first generate the paths of the stock price S_t^m and state variable X_t^m . The method starts from $t = T - \Delta t$ (i.e., the last rebalancing time before the terminal). We compute the optimal strategy $\pi_{T-\Delta t}^m$ given $W_0, S_{T-\Delta t}^m, X_{T-\Delta t}^m$ using the Equations (4.5) or (4.10). Next, \hat{v}^m is obtained through simulation, which estimates $f(T - \Delta t, S_{T-\Delta t}^m, X_{T-\Delta t}^m)$ when using SEN and $\ln[f(T - \Delta t, S_{T-\Delta t}^m, X_{T-\Delta t}^m)]$ when using IEN. The network $NN(T - \Delta t, X, S)$, approximating the state variable function, is trained with the input $(X_{T-\Delta t}^m, S_{T-\Delta t}^m)$ and output \hat{v}^m . We conduct a similar procedure at each rebalancing point and recursively approximate the value function and optimal strategy until the inception of the portfolio. To evaluate the expected utility, we regenerate the paths of stock price and state variables. The path-wise optimal strategy is computed from $NN(t, X, S)$, so the optimal terminal wealth is easy to obtain. The average of the utility of optimal terminal wealth approximates the expected utility. Algorithm 9 and 10 present the pseudo code for NNMC using SEN and IEN respectively. Simulation variance reduction methods, such as antithetic variates, could be incorporated into both algorithms to reduce the standard error of estimated expected utility.

4.4 Application to 4/2 model

[45] unified the 1/2 and 3/2 SV models and proposed the 4/2 SV model. The 4/2 model better captures the evolution of the implied volatility surface and uniformly bounds the instantaneous variance away from zero when weights on 1/2 and 3/2 factors are positive. We implement the NNMC on the 4/2 model and report the optimal allocation, expected utility, and the annualized CER defined by

$$U(W_0(1 + CER)^T) = V(0, W_0, S_0, X_0). \quad (4.15)$$

Three versions of the 4/2 model are considered; all are specific cases of the generalized model (4.1). The first assumes market price of risk proportional to the volatility driver. In other word, the value function and the optimal allocation are solvable in closed-form. The second incorporates stochastic jumps into the 4/2 model, while the last uses the preferred setting for the market price of risk in the economics/finance literature (i.e., proportional to the instantaneous volatility). The parameters used in this section are presented in Table 4.2² and are estimated from the S&P 500 and its volatility index (VIX) in [18].

4.4.1 A solvable case

[18] found the closed-form solution for an optimal dynamic portfolio when the stock price follows a 4/2 model with the market price of risk linear to the square root of the volatility driver $\sqrt{X_t}$. The dynamics of stock price S_t and volatility driver X_t are exhibited in Equation (4.16).

$$\begin{cases} \frac{dM_t}{M_t} = rdt \\ \frac{dS_t}{S_t} = (r + \lambda_S(a_S X_t + b_S))dt + (a_S \sqrt{X_t} + \frac{b_S}{\sqrt{X_t}})dB_t^S & \langle B_t^S, B_t^X \rangle = \rho t \\ dX_t = \kappa_X(\theta_X - X_t)dt + \sigma_X \sqrt{X_t}dB_t^X. \end{cases} \quad (4.16)$$

² Δ_t^{re} is the portfolio rebalancing interval, $\frac{1}{\Delta_t^{re}}$ indicates the rebalancing frequency. The Euler method with step size Δ_t^{si} is applied in generating the stock price and states variables.

Algorithm 9: NNMC-SEN

Input: S_0, W_0, X_0
Output: Optimal trading strategy π_0^* and expected utility $\hat{V}(0, W_0, S_0, X_0)$

- 1 initialization;
- 2 Generating n_r paths of B_t^m, S_t^m, X_t^m for $m = 1 \dots n_r$;
- 3 **while** $t = T - \Delta t$ **do**
- 4 Compute optimal allocation $\pi_{T-\Delta t}^m$ with Equation (4.5) ;
- 5 Simulate wealth $\hat{W}_T^{m,n}(\pi_{T-\Delta t}^m)$ given $W_0, S_{T-\Delta t}^m, \pi_{T-\Delta t}^m$ and $X_{T-\Delta t}^m$ at $T - \Delta t$ for $n = 1 \dots N$;
- 6 Compute $\hat{v}^m = \frac{1}{N} \sum_{n=1}^N U(\hat{W}_T^{m,n}(\pi_{T-\Delta t}^m)) \times \frac{1-\gamma}{W_0^{1-\gamma}}$ for $m = 1 \dots n_r$;
- 7 Train a network with input $(X_{T-\Delta t}^m, S_{T-\Delta t}^m)$ and output \hat{v}^m . Denote the network by $NN(T - \Delta t, X, S)$
- 8 **for** $t = T - 2\Delta t$ **to** Δt **do**
- 9 Compute optimal allocation π_t^m with $NN(t + \Delta t, X, S)$ and Equation (4.5) given W_0, S_t^m , and X_t^m ;
- 10 Simulate wealth $\hat{W}_{t+\Delta t}^{m,n}(\pi_t^m), \hat{S}_{t+\Delta t}^{m,n}$ and $\hat{X}_{t+\Delta t}^{m,n}$ given W_0, S_t^m, π_t^m and X_t^m at time t for $n = 1 \dots N$;
- 11 Compute $\hat{v}^m = [\frac{1}{N} \sum_{n=1}^N (W_{t+\Delta t}^{m,n}(\pi_t^m))^{1-\gamma} NN(t + \Delta t, \hat{X}_{t+\Delta t}^{m,n}, \hat{S}_{t+\Delta t}^{m,n})] \times \frac{1}{W_0^{1-\gamma}}$ for $m = 1 \dots n_r$;
- 12 Train a new network with input $(X_{T-\Delta t}^m, S_{T-\Delta t}^m)$ and output \hat{v}^m and denote it by $NN(t, X, S)$;
- 13 **while** $t = 0$ **do**
- 14 Compute π_0^* with $NN(\Delta t, X, S)$ and Equation (4.5);
- 15 Generate new paths of S_t^z, X_t^z for $z = 1 \dots N_0$, use the estimation of value function $NN(t, X, S)$ to compute π_t^z and W_T^z .
- 16 The expected utility is , $\hat{V}(0, W_0, S_0, X_0) = \frac{1}{N_0} \sum_{n=1}^{N_0} U(W_T^z)$
- 17 **return** $\pi_0^*, \hat{V}(0, W_0, S_0, X_0)$

Solving the associated Hamilton-Jacobi-Bellman (HJB) equation,

$$0 = \sup_{\pi} \left\{ V_t + W_t(r + \lambda_S(a_S X_t + b_S) + \kappa_X(\theta_X - X_t))V_X + \frac{1}{2} W_t^2 \pi^2 \left(a_S \sqrt{X_t} + \frac{b_S}{\sqrt{X_t}} \right)^2 V_{WW} + \frac{1}{2} \sigma_X^2 X_t V_{XX} + \pi W_t (a_S X_t + b_S) \sigma_X \rho V_{WX} \right\}, \quad (4.17)$$

the optimal trading strategy and value function are given by

$$V(t, W, X) = \frac{W^{1-\gamma}}{1-\gamma} e^{a(T-t)+b(T-t)X} \quad (4.18)$$

$$\pi_t^* = \frac{X}{aX + b} \left[\frac{\sigma_X \rho_S X b(T-t)}{\gamma} + \frac{\lambda_S}{\gamma} \right].$$

The functions $a(T - t)$ and $b(T - t)$ are

$$\begin{aligned} a(T - t) &= \gamma r(T - t) + \frac{2\kappa_X \theta_X}{k_2} \ln \frac{2k_3 e^{0.5(k_1+k_2)(T-t)}}{2k_3 + (k_1 + k_3)(e^{k_3(T-t)} - 1)} \\ b(T - t) &= \frac{k_0(e^{k_3(T-t)} - 1)}{2k_3 + (k_1 + k_3)(e^{k_3(T-t)} - 1)}, \end{aligned} \quad (4.19)$$

with auxiliary parameters $k_0 = \frac{1-\gamma}{\gamma} \lambda_S^2$, $k_1 = \kappa_X - \frac{1-\gamma}{\gamma} \rho_{SX} \sigma_X \lambda_S$, $k_2 = \sigma_X^2 + \frac{(1-\gamma)\sigma_X^2 \rho_{SX}^2}{\gamma}$ and $k_3 = \sqrt{k_1^2 - k_0 k_2}$.

The closed-form solution (see Equation (4.18)) reveals that the value function in this case is an exponential linear function. Hence we set the degree of polynomial to 1 when implementing NNMC with both the SEN and the IEN. Table 4.3 compares the optimal allocation, expected utility and CER from NNMC, the embedded PAMC and the theoretical solution. PAMC takes the least computational time. The optimal allocation obtained from PAMC is more accurate than results from NNMC, while the differences in expected utility and CER are not significant. Furthermore, SEN slightly outperforms IEN in terms of accuracy of optimal allocation and computation efficiency. Moreover, the ReLU activation function is superior to the sigmoid and ELU function when IEN is applied.

We repeat the estimation of expected utility (i.e., steps 14-16 in NNMC-SEN and steps 15-17 in NNMC-IEN) after the value function and optimal strategy are obtained. All approximation methods have similar standard deviations of the estimated expected utility and CERs. Moreover, standard deviation decreases with risk aversion level γ , which indicates that our approximation is more accurate for higher risk averse investors.

Figure 4.3 displays the expected utility and CER as a function of time to maturity T when $\gamma = 2$. The expected utility increases with maturity T as expected, while the CER decreases. Expected utility from PAMC, NNMC, and the theoretical solution are visually the same. The comparison in portfolio performance is clearer by showing the CER: PAMC and NNMC produce CERs that are slightly smaller than the theoretical result. Furthermore, ELU seems to be inferior to the ReLU and sigmoid function, and CER obtained from NNMC with the ELU activation function is slightly smaller than results from other methods when the investment horizon is small.

4.4.2 An unsolvable case, 4/2 Model with jumps

Next, we extend the 4/2 model to account for stochastic jumps. The dynamics of stock prices and volatility drivers are summarized by the SDE:

$$\begin{cases} \frac{dM_t}{M_t} = r dt \\ \frac{dS_t}{S_t} = (r + \lambda_S(a_S X_t + b_S) - \lambda_Q X_t \mu_N) dt + (a_S \sqrt{X_t} + \frac{b_S}{\sqrt{X_t}}) dB_t^S + \mu_N dN_t < B_t^S, B_t^X > = \rho t \\ dX_t = \kappa_X(\theta_X - X_t) dt + \sigma_X \sqrt{X_t} dB_t^X. \end{cases} \quad (4.20)$$

Volatility and market price of risk are the same with the 4/2 model given in Equation (4.16). N_t is an independent Poisson process with intensity $\lambda_N X_t$, μ_N is the jump size, and $\lambda_Q X_t$ captures the market price of jump risk.

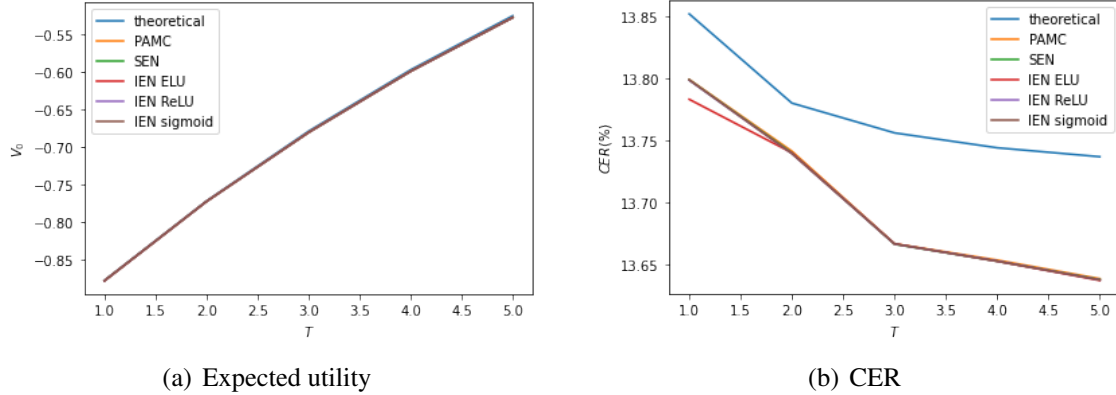


Figure 4.3: S_t follows the 4/2 model with market price of risk $\lambda_S \sqrt{X_t}$, (a) shows the Expected utilities obtained with theoretical results and approximation methods versus investment horizon T , (b) shows the CERs versus investment horizon T given $\gamma = 2$.

We use the set of jump risk parameters given in [71]: $\lambda_N = \lambda_Q = 0.1/\theta_X$ and $\mu_N = 0.1$. Notably, the stock is expected to jump once every 10 years if X_t stays at its mean level θ_X . The degree of polynomial in PAMC and NNMC was chosen to be 1. In this case, the optimal strategy cannot be solved explicitly given the approximation of the value function at the next rebalancing time (see Propositions 4.2.1 and 4.2.2), hence we solve Equation (4.5) and (4.10) with the Newton-Raphson method in NNMC. The optimal allocation, expected utility, CER obtained with NNMC and PAMC are reported in Table 4.4. When the stock follows the 4/2 model with jumps, PAMC is faster, followed by NNMC-SEN. Moreover, the accuracy of estimated expected utility and CER from PAMC and NNMC are similar, which suggests that neural networks fail to enhance the portfolio performance in this case. The standard deviations of these approximation methods have little difference.

Figure 4.4 exhibits the expected utility and CER as a function of investment horizon T . Portfolios with longer investment horizon are expected to achieve a better performance (i.e., higher expected utility) while CER decreases with T .

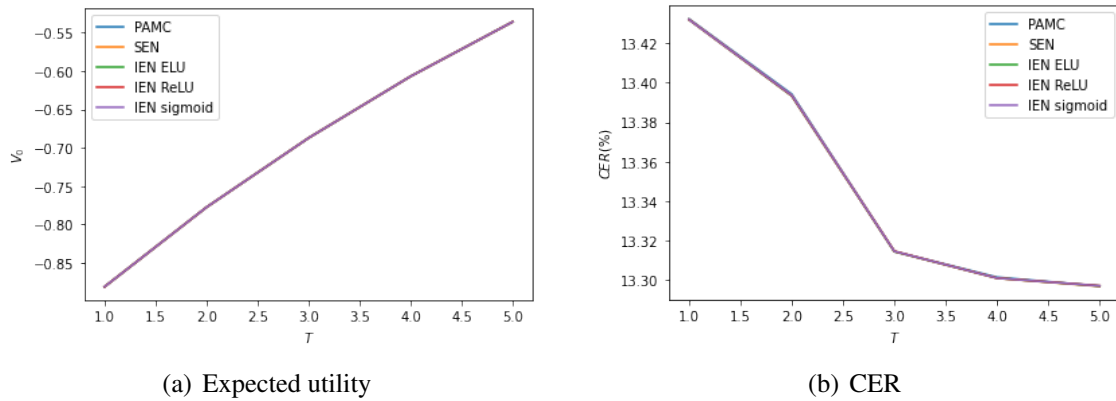


Figure 4.4: S_t follows a 4/2 model with stochastic jump, (a) shows the Expected utilities obtained with the approximation methods versus investment horizon T , (b) shows CERs versus investment horizon T given $\gamma = 2$.

4.4.3 An unsolvable case, market price of risk proportional to volatility

In this section, we consider an excess return, proportional to the instantaneous variance. The dynamics are given in Equation (4.21), and a closed-form solution has not been found yet. We report the optimal allocation and expected utility from PAMC and NNMC, as well as investigate the impact of maturity T . The degree of polynomial in PAMC and NNMC is still 1.

$$\begin{cases} \frac{dM_t}{M_t} = r dt \\ \frac{dS_t}{S_t} = (r + \lambda_S (a_S \sqrt{X_t} + \frac{b_S}{\sqrt{X_t}})^2) dt + (a_S \sqrt{X_t} + \frac{b_S}{\sqrt{X_t}}) dB_t^S & \langle B_t^S, B_t^X \rangle = \rho t \\ dX_t = \kappa_X (\theta_X - X_t) dt + \sigma_X \sqrt{X_t} dB_t^X. \end{cases} \quad (4.21)$$

Table 4.5 reports the optimal allocation, expected utility, and CER from PAMC and NNMC. PAMC is still the most efficient method, followed by the NNMC-SEN. All methods achieve similar portfolio performance in terms of the expected utility and CER as well as the corresponding standard deviation. Figure 4.5 plots the expected utility and CER versus maturity T when $\gamma = 2$, which further verifies the non-significant difference in expected utility and CER obtained from the methods.

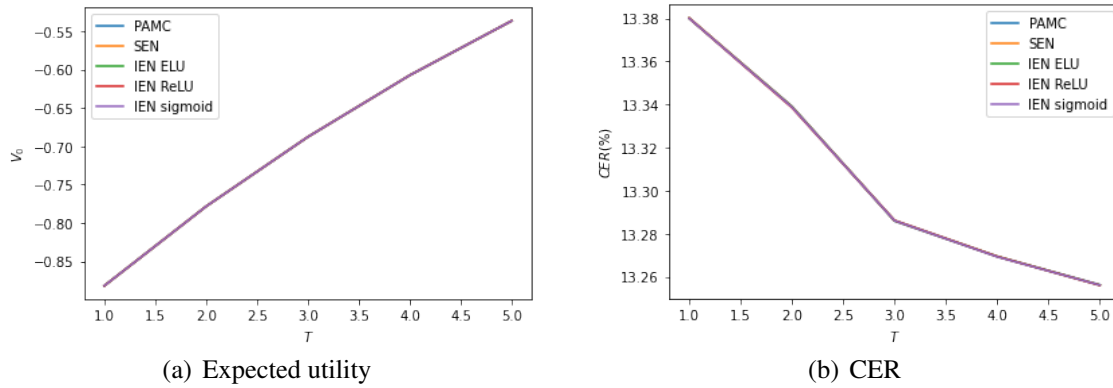


Figure 4.5: S_t follows the 4/2 model with market price of risk $\lambda_S (a_S \sqrt{X_t} + \frac{b_S}{\sqrt{X_t}})$, (a) shows the Expected utilities obtained with theoretical results and approximation methods versus investment horizon T , (b) shows the CERs versus investment horizon T given $\gamma = 2$.

4.5 Application to the OU 4/2 model

Motivated by the 4/2 stochastic volatility model and mean-reverting price pattern popular among various asset classes (e.g., commodities, exchange rates, volatility indexes), [37] define an Ornstein–Uhlenbeck 4/2 (OU 4/2) stochastic volatility model for volatility index option and commodity option valuation. Equation (4.22) presents the dynamics involved in the OU 4/2 model, which is a specific case of Equation (4.1) given $\theta(X_t, S_t) = (L_S + (\lambda_S - \frac{1}{2})(a_S \sqrt{X_t} + \frac{b_S}{\sqrt{X_t}})^2 - \beta_S \ln S_t)$, $\sigma(X_t, S_t) = (a_S \sqrt{X_t} + \frac{b_S}{\sqrt{X_t}})$, $a(X_t) = \kappa_X (\theta_X - X_t)$ and $b(X_t) = \sigma_X \sqrt{X_t}$. The parameters used in this section are reported in Table 4.6, which is estimated from the data of gold Exchange-traded fund (ETF) and the volatility index of gold ETF in [37]. There are

two state variables in the OU 4/2 model; hence, the input in both the SEN and the IEN are 2. Furthermore, the degree of polynomial in PAMC and NNMC is 2.

$$\begin{cases} \frac{dM_t}{M_t} = rdt \\ \frac{dS_t}{S_t} = (L_S + \lambda_S(a_S \sqrt{X_t} + \frac{b_S}{\sqrt{X_t}})^2 - \beta_S \ln S_t)dt + (a_S \sqrt{X_t} + \frac{b_S}{\sqrt{X_t}})dB_t \\ dX_t = \kappa_X(\theta_X - X_t)dt + \sigma_X \sqrt{X_t}dB_t^X \\ \langle dB_t, dB_t^X \rangle = \rho dt. \end{cases} \quad (4.22)$$

SEN performs worse than IEN when fitting the value function with the OU 4/2 model. Sometimes, SEN significantly deviates from the true value function, which results in poor portfolio performances and the occurrence of negative terminal wealth. Therefore, we exclude the results from NNMC-SEN in this section. Table 4.7 compares the optimal allocation, expected utility, and CER obtained for the OU 4/2 model. PAMC and NNMC-IEN produce similar optimal allocations, both outperforming NNMC-SEN. Furthermore, we also estimate the standard deviation of expected utility and CER, which demonstrates that NNMC leads to a less volatile estimation of expected utility and CER than PAMC in most cases. In contrast to the results for the 4/2 model, IEN is more efficient than SEN. We conclude that IEN is suitable for the model with complex structure and multiple state variables. The expected utility and CER as a function of the maturity T when $\gamma = 2$ is plotted in figure 4.6. Both the expected utility and CER increase with T . The expected utility and CER obtained from PAMC and NNMC-IEN visually overlap and are slightly higher than that of NNMC-SEN. Moreover, the selection of activation function in IEN makes little difference.

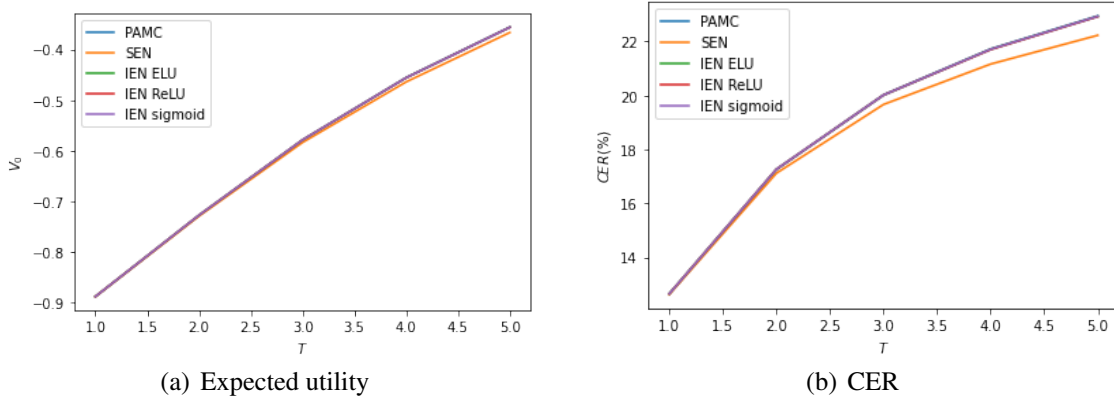


Figure 4.6: S_t follows the OU 4/2 model, (a) shows the Expected utilities obtained via approximation methods versus investment horizon T , (b) shows the CERs versus investment horizon T given $\gamma = 2$.

4.6 Conclusions

This chapter investigated fitting the value function in an expected utility, dynamic portfolio choice using a deep learning model. We proposed two architectures for the neural network, which extends the broadest solvable family of value function (i.e., the exponential polynomial function). We measured the accuracy and efficiency of various types of NNMC methods on

the 4/2 model and the OU 4/2 model. The difference in optimal allocation, expected utility and CER is insignificant when the stock price follows the 4/2 model. The embedded PAMC is superior to NNMC due to the lower parametric space, hence efficiency. Furthermore, when considering the OU 4/2 model, NNMC-SEN is inferior to a polynomial regression (PAMC) and to the NNMC-IEN in terms of expected utility and CER.

In summary, NNMC benefits from the popular exponential polynomial representation (embedded PAMC method) to propose network architecture flexible enough to reach beyond Affine models. Although the best setting, NNMC-IEN (ELU), is not as efficient as PAMC, neural networks demonstrate the way to tackle more advanced models along the lines of Markov switching, Lévy processes, and fractional Brownian processes.

Algorithm 10: NNMC-IEN

Input: S_0, W_0, X_0
Output: Optimal trading strategy π_0^* and expected utility $\hat{V}(0, W_0, S_0, X_0)$

- 1 initialization;
- 2 Generating n_r paths of B_t^m, S_t^m, X_t^m for $m = 1 \dots n_r$;
- 3 **while** $t = T - \Delta t$ **do**
- 4 Compute optimal allocation $\pi_{T-\Delta t}^m$ with Equation (4.10);
- 5 Simulate wealth $\hat{W}_T^{m,n}(\pi_{T-\Delta t}^m)$ given $W_0, S_{T-\Delta t}^m, \pi_{T-\Delta t}^m$ and $X_{T-\Delta t}^m$ at $T - \Delta t$
 for $n = 1 \dots N$;
- 6 Compute $\hat{v}^m = \ln [\text{sign}(1 - \gamma) \frac{1}{N} \sum_{n=1}^N U(\hat{W}_T^{m,n}(\pi_{T-\Delta t}^m))] - (1 - \gamma) \ln [W_0]$
 for $m = 1 \dots n_r$;
- 7 Train the network with input $(X_{T-\Delta t}^m, S_{T-\Delta t}^m)$ and output \hat{v}^m . Denote the network by
 $NN(T - \Delta t, X, S)$
- 8 **for** $t = T - 2\Delta t$ **to** Δt **do**
- 9 Compute optimal allocation π_t^m with $NN(t + \Delta t, X, S)$ and Equation (4.10) given
 W_0, S_t^m , and X_t^m ;
- 10 Simulate wealth $\hat{W}_{t+\Delta t}^{m,n}(\pi_t^m), \hat{S}_{t+\Delta t}^{m,n}$ and $\hat{X}_{t+\Delta t}^{m,n}$ given W_0, S_t^m, π_t^m and X_t^m at t
 for $n = 1 \dots N$;
- 11 Compute
- 12 $\hat{v}^m = \ln [\frac{1}{N} \sum_{n=1}^N (W_{t+\Delta t}^{m,n}(\pi_t^m))^{1-\gamma} \exp(NN(t + \Delta t, \hat{X}_{t+\Delta t}^{m,n}, \hat{S}_{t+\Delta t}^{m,n}))] - (1 - \gamma) \ln [W_0]$ for
 $m = 1 \dots n_r$;
- 13 Train a new network with input $(X_{T-\Delta t}^m, S_{T-\Delta t}^m)$ and output \hat{v}^m and denote it by
 $NN(t, X, S)$;
- 14 **while** $t = 0$ **do**
- 15 Compute π_0^* with $NN(\Delta t, X, S)$ and Equation (4.10);
- 16 Generate new paths of S_t^z, X_t^z for $z = 1 \dots N_0$, use the estimation of transformed
 value function $NN(t, X, S)$ to compute π_t^z and W_T^z .
- 17 The expected utility is , $\hat{V}(0, W_0, S_0, X_0) = \frac{1}{N_0} \sum_{n=1}^{N_0} U(W_T^z)$
- 18 **return** $\pi_0^*, \hat{V}(0, W_0, S_0, X_0)$

Table 4.2: Parameter values for 4/2 model.

Parameter	Value	Parameter	Value
T	1	X_0	0.04
r	0.05	λ_S	2.9428
Δ_t^{re}	$\frac{1}{10}$	Δ_t^{si}	$\frac{1}{60}$
S_0	1.0	M_0	1.0
W_0	1	n_r	100
N	2000	N_0	200000
κ_X	7.3479	θ_X	0.0328
σ_X	0.6612	a_s	0.9051
b_S	0.0023	ρ	-0.7689

Table 4.3: Results for the 4/2 model with market price of risk $\lambda_S \sqrt{X_t}$. We report the optimal weights, expected utility, and CER obtained with theoretical result and with the approximation method for different levels of risk aversion γ . The standard deviation of estimated expected utility and CER from 100 runs is displayed in parentheses.

	$\gamma = 2.0$	$\gamma = 4.0$	$\gamma = 6.0$	$\gamma = 8.0$	$\gamma = 10.0$
Theoretical					
Weights (π_0^*)	1.614	0.832	0.561	0.423	0.340
Expected utility (V_0^*)	-0.878	-0.253	-0.135	-0.087	-0.061
CER (%)	13.85	9.62	8.15	7.40	6.95
PAMC					
Weights (π_0^{PAMC})	1.615	0.833	0.561	0.423	0.340
Relative error(%)	0.001	0.05	0.05	0.04	0.04
Expected utility (V_0^{PAMC})	-0.879	-0.253	-0.135	-0.087	-0.061
	(0.0005)	(0.0002)	(0.0001)	(0.0001)	(0.0001)
Relative error (%)	0.04	0.04	0.05	0.06	0.08
CER (%)	13.80	9.60	8.14	7.40	6.95
	(0.065)	(0.033)	(0.023)	(0.017)	(0.014)
Computational time (seconds)	31.3	30.6	30.3	30.0	30.4
NNMC-SEN					
Weights (π_0^{SEN})	1.612	0.831	0.560	0.422	0.339
Relative error(%)	0.15	0.18	0.20	0.22	0.23
Expected utility (V_0^{SEN})	-0.879	-0.253	-0.135	-0.087	-0.061
	(0.0005)	(0.0002)	(0.0001)	(0.0001)	(0.0001)
Relative error(%)	0.05	0.04	0.05	0.06	0.06
CER (%)	13.80	9.60	8.14	7.40	6.95
	(0.065)	(0.033)	(0.026)	(0.017)	(0.014)
Computational time (seconds)	56.4	57.2	57.6	57.0	57.9
NNMC-IEN (ReLU)					
Weights ($\pi_0^{IEN ReLU}$)	1.612	0.831	0.560	0.422	0.339
Relative error(%)	0.14	0.19	0.22	0.25	0.27
Expected utility ($V_0^{IEN ReLU}$)	-0.879	-0.253	-0.135	-0.087	-0.061
	(0.0005)	(0.0002)	(0.0001)	(0.0001)	(0.0001)
Relative error(%)	0.05	0.04	0.05	0.06	0.06
CER (%)	13.80	9.60	8.14	7.40	6.95
	(0.065)	(0.033)	(0.023)	(0.017)	(0.014)
Computational time (seconds)	62.1	63.4	64.8	63.5	63.5
NNMC-IEN (sigmoid)					
Weights ($\pi_0^{IEN sigmoid}$)	1.612	0.831	0.560	0.422	0.339
Relative error(%)	0.15	0.20	0.23	0.27	0.27
Expected utility ($V_0^{IEN sigmoid}$)	-0.879	-0.253	-0.135	-0.087	-0.061
	(0.0005)	(0.0002)	(0.0001)	(0.0001)	(0.0001)
Relative error(%)	0.05	0.04	0.05	0.10	0.10
CER (%)	13.80	9.60	8.14	7.39	6.94
	(0.065)	(0.033)	(0.023)	(0.017)	(0.014)
Computational time (seconds)	63.6	62.2	63.1	79.2	75.1
NNMC-IEN (ELU)					
Weights ($\pi_0^{IEN ELU}$)	1.612	0.831	0.560	0.422	0.339
Relative error(%)	0.16	0.19	0.19	0.28	0.31
Expected utility ($V_0^{IEN ELU}$)	-0.879	-0.253	-0.135	-0.087	-0.061
	(0.0005)	(0.0002)	(0.0001)	(0.0001)	(0.0001)
Relative error(%)	0.06	0.10	0.05	0.18	0.20
CER (%)	13.78	9.58	8.14	7.38	6.93
	(0.065)	(0.034)	(0.023)	(0.017)	(0.014)
Computational time (seconds)	78.2	74.6	62.1	77.4	75.3

Table 4.4: Results for the 4/2 model with stochastic jumps. We report the optimal weights, expected utility and CER obtained via the approximation methods for different levels of risk aversion γ . The standard deviation of estimated expected utility and CER from 100 runs is displayed in parentheses.

	$\gamma = 2.0$	$\gamma = 4.0$	$\gamma = 6.0$	$\gamma = 8.0$	$\gamma = 10.0$
PAMC					
Weights (π_0^{PAMC})	1.545	0.797	0.537	0.405	0.325
Expected utility (V_0^{PAMC})	-0.882 (0.0006)	-0.255 (0.0003)	-0.136 (0.0002)	-0.087 (0.0001)	-0.061 (0.0001)
CER (%)	13.43 (0.075)	9.41 (0.039)	8.01 (0.027)	7.30 (0.020)	6.87 (0.016)
Computational time (seconds)	47.1	48.4	47.1	47.2	47.1
NNMC-SEN					
Weights (π_0^{SEN})	1.545	0.797	0.537	0.405	0.325
Expected utility (V_0^{SEN})	-0.882 (0.0006)	-0.255 (0.0003)	-0.136 (0.0002)	-0.087 (0.0001)	-0.061 (0.0001)
CER (%)	13.43 (0.075)	9.41 (0.040)	8.01 (0.027)	7.30 (0.020)	6.87 (0.016)
Computational time (seconds)	74.2	77.3	72.5	72.3	82.7
NNMC-IEN (ReLU)					
Weights ($\pi_0^{IEN ReLU}$)	1.544	0.796	0.536	0.405	0.325
Expected utility ($V_0^{IEN ReLU}$)	-0.882 (0.0006)	-0.255 (0.0003)	-0.136 (0.0002)	-0.087 (0.0001)	-0.061 (0.0001)
CER (%)	13.43 (0.075)	9.41 (0.040)	8.01 (0.027)	7.30 (0.020)	6.87 (0.016)
Computational time (seconds)	93.1	89.4	86.8	83.7	83.2
NNMC-IEN (sigmoid)					
Weights ($\pi_0^{IEN sigmoid}$)	1.544	0.796	0.537	0.404	0.324
Expected utility ($V_0^{IEN sigmoid}$)	-0.882 (0.0006)	-0.255 (0.0003)	-0.136 (0.0002)	-0.087 (0.0001)	-0.061 (0.0001)
CER (%)	13.43 (0.075)	9.41 (0.040)	8.01 (0.027)	7.30 (0.020)	6.87 (0.016)
Computational time (seconds)	93.1	92.7	90.3	83.5	82.1
NNMC-IEN (ELU)					
Weights ($\pi_0^{IEN ELU}$)	1.544	0.796	0.537	0.404	0.325
Expected utility ($V_0^{IEN ELU}$)	-0.882 (0.0006)	-0.255 (0.0003)	-0.136 (0.0002)	-0.087 (0.0001)	-0.061 (0.0001)
CER (%)	13.43 (0.075)	9.41 (0.040)	8.01 (0.027)	7.30 (0.020)	6.87 (0.016)
Computational time (seconds)	81.3	83.9	88.1	81.5	85.6

Table 4.5: Results for the 4/2 model with market price of risk $\lambda_S(a_S \sqrt{X_t} + \frac{b_S}{\sqrt{X_t}})$. We report the estimation of optimal weights, expected utility and CER obtained via approximations given different levels of risk aversion γ . The standard deviation of estimated expected utility and CER from 100 runs is displayed in parentheses.

	$\gamma = 2.0$	$\gamma = 4.0$	$\gamma = 6.0$	$\gamma = 8.0$	$\gamma = 10.0$
PAMC					
Weights (π_0^{PAMC})	1.539	0.789	0.531	0.400	0.321
Expected utility (V_0^{PAMC})	-0.882 (0.0005)	-0.255 (0.0002)	-0.136 (0.0001)	-0.087 (0.0001)	-0.061 (0.0001)
CER (%)	13.38 (0.065)	9.36 (0.033)	7.97 (0.022)	7.26 (0.017)	6.84 (0.013)
Computational time (seconds)	33.9	33.6	34.0	35.4	33.2
NNMC-SEN					
Weights (π_0^{SEN})	1.537	0.788	0.530	0.399	0.320
Expected utility (V_0^{SEN})	-0.882 (0.0005)	-0.255 (0.0002)	-0.136 (0.0001)	-0.087 (0.0001)	-0.061 (0.0001)
CER (%)	13.38 (0.065)	9.36 (0.033)	7.97 (0.022)	7.26 (0.017)	6.84 (0.013)
Computational time (seconds)	62.7	62.6	62.4	62.7	62.9
NNMC-IEN (ReLU)					
Weights ($\pi_0^{IEN ReLU}$)	1.537	0.788	0.530	0.399	0.320
Expected utility ($V_0^{IEN ReLU}$)	-0.882 (0.0005)	-0.255 (0.0002)	-0.136 (0.0001)	-0.087 (0.0001)	-0.061 (0.0001)
CER (%)	13.38 (0.065)	9.35 (0.033)	7.97 (0.022)	7.26 (0.017)	6.84 (0.013)
Computational time (seconds)	70.8	69.8	69.0	69.4	69.6
NNMC-IEN (sigmoid)					
Weights ($\pi_0^{IEN sigmoid}$)	1.537	0.788	0.530	0.399	0.320
Expected utility ($V_0^{IEN sigmoid}$)	-0.883 (0.0005)	-0.255 (0.0002)	-0.136 (0.0001)	-0.088 (0.0001)	-0.061 (0.0001)
CER (%)	13.38 (0.065)	9.35 (0.033)	7.97 (0.022)	7.26 (0.017)	6.84 (0.013)
Computational time (seconds)	69.0	68.0	68.9	68.4	68.7
NNMC-IEN (ELU)					
Weights ($\pi_0^{IEN ELU}$)	1.537	0.788	0.530	0.399	0.320
Expected utility ($V_0^{IEN ELU}$)	-0.882 (0.0005)	-0.255 (0.0002)	-0.136 (0.0001)	-0.087 (0.0001)	-0.061 (0.0001)
CER (%)	13.38 (0.065)	9.35 (0.033)	7.97 (0.022)	7.26 (0.017)	6.84 (0.013)
Computational time (seconds)	69.3	69.4	68.3	71.6	68.5

Table 4.6: Parameter value for the OU 4/2 model.

Parameter	Value	Parameter	Value
T	1	X_0	0.04
r	0.05	λ_S	0.572
Δ_t^{re}	$\frac{1}{60}$	Δ_t^{si}	$\frac{1}{60}$
S_0	120.0	M_0	1.0
W_0	1	n_r	100
κ_X	4.7937	θ_X	0.0395
σ_X	0.2873	a_S	1
b_S	0.002	ρ	-0.08
L	3.7672	β_S	0.78
N	2000	N_0	200,000

Table 4.7: Results for the OU 4/2 model. We report the estimation of optimal weights, expected utility and CER obtained via approximations for different levels of risk aversion γ . The standard deviation of estimated expected utility and CER from 100 runs is provided in parentheses.

	$\gamma = 2.0$	$\gamma = 4.0$	$\gamma = 6.0$	$\gamma = 8.0$	$\gamma = 10.0$
PAMC					
Weights (π_0^{PAMC})	0.068	0.026	0.015	0.010	0.008
Expected utility (V_0^{PAMC})	-0.888 (0.0006)	-0.255 (0.0003)	-0.136 (0.0002)	-0.087 (0.0002)	-0.061 (0.0001)
CER (%)	12.65 (0.073)	9.28 (0.047)	8.00 (0.035)	7.32 (0.028)	6.90 (0.024)
Computational time (seconds)	103.9	104.6	104.4	104.5	104.3
NNMC-SEN					
Weights (π_0^{SEN})	0.134	0.056	0.042	0.040	0.029
Expected utility (V_0^{SEN})	-0.888 (0.0006)	-0.256 (0.0003)	-0.136 (0.0002)	-0.087 (0.0001)	-0.061 (0.0001)
CER (%)	12.62 (0.076)	9.26 (0.045)	7.97 (0.032)	7.29 (0.025)	6.87 (0.020)
Computational time (seconds)	439.5	477.5	434.3	446.9	449.7
NNMC-IEN (ReLU)					
Weights ($\pi_0^{IEN ReLU}$)	0.070	0.028	0.016	0.011	0.007
Expected utility ($V_0^{IEN ReLU}$)	-0.888 (0.0006)	-0.255 (0.0003)	-0.136 (0.0002)	-0.087 (0.0002)	-0.061 (0.0001)
CER (%)	12.65 (0.072)	9.29 (0.045)	8.00 (0.033)	7.32 (0.026)	6.90 (0.022)
Computational time (seconds)	190.3	190.6	190.4	187.8	185.1
NNMC-IEN (sigmoid)					
Weights ($\pi_0^{IEN sigmoid}$)	0.067	0.026	0.015	0.010	0.007
Expected utility ($V_0^{IEN sigmoid}$)	-0.888 (0.0006)	-0.255 (0.0003)	-0.136 (0.0002)	-0.087 (0.0001)	-0.061 (0.0001)
CER (%)	12.65 (0.072)	9.28 (0.044)	8.00 (0.033)	7.32 (0.026)	6.90 (0.022)
Computational time (seconds)	185.7	186.0	185.2	181.4	181.9
NNMC-IEN (ELU)					
Weights ($\pi_0^{IEN ELU}$)	0.072	0.031	0.015	0.010	0.008
Expected utility ($V_0^{IEN ELU}$)	-0.888 (0.0006)	-0.255 (0.0003)	-0.136 (0.0002)	-0.087 (0.0001)	-0.061 (0.0001)
CER (%)	12.65 (0.072)	9.28 (0.044)	8.00 (0.033)	7.32 (0.026)	6.90 (0.022)
Computational time (seconds)	185.6	184.1	188.1	195.1	193.7

Chapter 5

Derivatives-based portfolio decisions. An expected utility insight

Chapter summary:

This chapter challenges the use of stocks in portfolio construction, demonstrating that deep out-of-the-money Asian products, conveniently designed straddles and basket options could be better choices. Our results are obtained under the assumptions of the Black–Scholes–Merton setting, uncovering a hidden benefit of derivatives that complements their well-known gains for hedging, in market incompleteness, while also transferable to more advanced settings.

The analysis relies on the infinite number of optimal choices of derivatives for a maximized expected utility (EUT) agent, proposing risk exposure minimization as an additional optimization criterion inspired by regulations.

Status: Accepted by *Annals of Finance*.

5.1 Introduction

Financial derivatives such as futures, options and swaps play essential roles in current financial markets. They are used for hedging and speculation as well as for arbitrage opportunities. The history of derivatives is as old as the history of commerce. Derivatives have grown into an indispensable asset class since the 1970s, in part due to the increase in volatility and complexity of global financial markets. The popularity of derivatives is such that some market analysts, such as [74], place the size of derivatives at more than 10 times the total world gross domestic product (GDP). Vanilla European and American options usually come to mind first when discussing options. Beyond that, a wide variety of options are traded in centralized exchanges or over-the-counter (OTC) markets, and some investors are even able to define their own products and terms. The enduring appeal of derivatives lies in their diversity and hence the capacity to fulfill their needs of financial players.

This chapter uncovers an additional benefit of derivatives. It addresses a basic, yet poorly understood question for investors: what is the best financial derivative to include in a portfolio? We challenge the common practice of using the underlying stock; instead, we demonstrate that Asian derivatives, straddles or baskets could be more convenient choices. Our analysis and results are obtained under the safe assumptions of a Black–Scholes–Merton model, which not

only uncovers the hidden “in plain sight” benefits of derivatives, but also highlights their potential for applications in more advanced settings incorporating market incompleteness, jumps and transaction costs, among others.

Derivative valuation in the context of continuously trading markets was initiated by the seminal papers of [8] and [77]. The authors solved associated partial differential equations (PDEs) and obtained the price function of a European option in closed form, when the underlying asset follows a geometric Brownian motion (GBM). Their work (i.e. Black–Scholes–Merton formula) laid the foundation for the development of derivative pricing. Their results have been extended in many directions; most relevant to this study are extensions to the pricing of many other types of options, such as American options (see [7]) lookback options (see [44]) and geometric average Asian options (see [56]), to mention a few. The distinctive exercise rights and structure of payoff reflect the complexity of financial derivatives.

This chapter focuses on the benefits of derivatives from the portfolio investment perspective for a maximized expected utility (EUT) agent. Investment incorporating derivatives have been studied from multiple perspectives. [47] found a buy-and-hold strategy that minimizes the mean-squared distance to the terminal wealth of [76] continuously rebalancing portfolio. Moreover, an elasticity approach was introduced in [58], by which the author obtained the optimal strategy of a portfolio with path-dependent options. [79] studied a portfolio of volatility derivatives (options or swaps) for a constant absolute risk aversion (CARA) investor. In additions, [71] investigated the optimal portfolio in a stock-derivatives market with Heston’s SV model and jumps. Their results demonstrated the improvement in performance when using derivatives to complete the market, while showing that an infinite number of derivatives can be used with the same optimal performance for the portfolio. In contrast to the existing literature, this chapter investigates how to best select derivatives.

For this purpose, in addition to a maximized EUT, we develop a second optimization criterion for the portfolio manager as a way of selecting the best derivative. We choose risky asset exposure minimization motivated by two facts. First, the maximization of the utility can be achieved by an infinitely number of equally optimal derivatives (as per [71]). Second, minimizing risk exposure, as a second optimization criterion, aligns with practical needs in the industry. In general, investment companies face many constraints in the construction of their portfolios, many of which are imposed by regulatory agencies. The key factor behind regulatory constraints is the intention to control the exposure of a portfolio to risky assets, protecting an investor’s capital in the case of a market crash. Some of these risks are difficult to accurately model, which highlights the importance of minimizing exposure.

Our findings demonstrate that derivatives can be used to reduce risk exposure with no impact on the level of satisfaction of the investor (e.g. maximum utility). We investigate the selection of derivatives in three specific option classes: (i) American, European and Asian calls and puts; (ii) American, European and Asian synthetic straddles; and (iii) basket options. We further compare one-asset and multi-asset options in various realistic situations, and we consider the relationship between risky asset exposure and portfolio rebalancing frequency.

The contributions of the chapter are summarized as follows:

1. Given the infinite number of choices of equally optimal financial derivatives for an EUT investor, we explore an additional optimization criterion, namely, risk exposure minimization, to help investors make a practical derivative selection.

2. We demonstrate, in the context of two one-factor (e.g. GBM) assets, that the minimum number of derivatives needed not only to maximize EUT performance, but also to minimize risk exposure is exactly two.
3. In a comparison of the most popular types of simple one-asset options (e.g. American, European and Asian calls and puts), we illustrate that the deepest out-of-the-money Asian products are the best choices for minimizing risk exposure.
4. To avoid illiquid out-of-the-money options, which also require plenty of rebalancing, we explore optimal selections among straddles. We demonstrate the existence of an optimal strike price for risk exposure minimization, which is likely a better practical choice than out-of-the-money calls and puts.
5. Given the setting of two assets in the portfolio, we study the optimality of multi-asset derivatives. We determine that a basket option could be a better selection than one-asset Asian calls and puts in many realistic situations.
6. Several analyses are performed to solidify our findings; in particular, the relationship between risky asset exposure and portfolio rebalancing frequency is investigated, and the results are put to the test for a variety of parametric choices.

The chapter is organized as follows. Section 5.2 describes the EUT problem for an investor allocating directly among financial derivatives. Given the vast number of optimal derivatives available for this problem, Section 5.2 defines a criterion based on an additional optimization problem that aids in selecting a single optimal solution. Section 5.3 then explores two cases of one-asset options available to a portfolio investor: (1) calls and puts and (2) straddles. Thereafter, Section 5.4 focuses on the benefit of multi-asset derivatives such as basket options, and Section 5.5 concludes this study. Section 5.6 presents all the proofs and complementary analyses in support of our findings.

5.2 Mathematical setting and results

Let $(\Omega, \mathcal{F}, \mathbb{P})$ be a complete probability space with a right-continuous filtration $\{\mathcal{F}_t\}_{t \in [0, T]}$. We consider a frictionless market, in which trading occurs without transaction costs or market impact, comprising a money market account M_t and two risky assets $S_t = [S_t^{(1)}, S_t^{(2)}]^T$, with the following dynamics:

$$\begin{cases} \frac{dM_t}{M_t} = rdt \\ dS_t = \text{diag}(S_t) [(r \cdot \mathbb{1} + \text{diag}(\sigma)\Lambda)dt + \text{diag}(\sigma)dB_t], \end{cases} \quad (5.1)$$

where $B_t = [B_t^{(1)}, B_t^{(2)}]^T$ are Brownian motions modelling the risk of two underlying assets, whose correlation is denoted by $\rho \in (-1, 1)$. Here, r is the risk-free rate and $\mathbb{1}$ denote the vector of ones, $\Lambda = [\lambda^{(1)}, \lambda^{(2)}]^T$ are constants capturing the market price of risk of B_t , and $\sigma = [\sigma^{(1)}, \sigma^{(2)}]^T$ captures the volatility of the two underlying assets.

We now introduce a set of admissible financial derivatives on the assets S_t , for a fixed $n \geq 1$:

$$\Omega_0^{(n)} = \left\{ O_t = [O_t^{(1)}, O_t^{(2)}, \dots, O_t^{(n)}]^T \mid O_t^{(i)} \neq 0, i = 1, \dots, n \text{ and } \text{rank}(\Sigma_t) = 2, t \in [0, T] \right\},$$

where Σ_t represents the variance matrix of O_t . The element (i, j) , $i = 1, \dots, n$, $j = 1, 2$, of Σ_t , denoted by f_t^{ij} , represents the sensitivity of $O_t^{(i)}$ to the underlying asset $S_t^{(j)}$, i.e. $f_t^{ij} = \frac{dO_t^{(i)}}{dS_t^{(j)}} S_t^{(j)} \sigma^{(j)}$. Note that Ω_O is an infinite set, which could contain standardized exchange-traded options and non-standardized OTC options available to a generic investor. The reader should observe that f_t^{ij} depends on derivative type, style, underlying price, strike price, time to maturity and other factors, and Σ_t is a full-rank matrix, which allows us to continue working in a complete market if $n \geq 2$. For simplicity, we also assume that the derivatives in $\Omega_O^{(n)}$ will be rolled over, always keeping the same time to maturity and a non-zero value.

We are now ready to create a derivatives-based dynamic portfolio choice problem for a risk-averse investor. The investor preference is measured by the widely used and algebraically simple CRRA utility.¹ We assume that an investor allocates in an element of Ω_O ; that is, a specific $O_t = [O_t^{(1)}, O_t^{(2)}, \dots, O_t^{(n)}]^T$ ($n \geq 2$). Note that by arbitrage arguments, the dynamics of the derivatives-based assets and the market account are as follows:

$$\begin{cases} \frac{dM_t}{M_t} = rdt \\ dO_t = \text{diag}(O_t) [(r \cdot \mathbb{1} + \Sigma_t \Lambda)dt + \Sigma_t dB_t]. \end{cases} \quad (5.2)$$

The investor is not prohibited from trading on the underlying assets. This would be equivalent to setting $n = 2$ and taking $O_t = S_t$.

Let $\Omega_\pi^{(O)}$ denote the space of admissible strategies satisfying the standard conditions, where the element $\pi_t = [\pi_t^{(1)}, \pi_t^{(2)}, \dots, \pi_t^{(n)}]^T$ represents the proportions of the investor's wealth in the options $O_t = [O_t^{(1)}, O_t^{(2)}, \dots, O_t^{(n)}]^T$ with the remaining $1 - \mathbb{1}^T \pi_t$ invested in the cash account M_t . The wealth process W_t satisfies

$$\frac{dW_t}{W_t} = (r + \pi_t^T \Sigma_t \Lambda)dt + \pi_t \Sigma_t dB_t. \quad (5.3)$$

A CRRA utility function represents the investor's preference on the terminal wealth W_T , which is given by

$$U(W_T) = \frac{W_T^{1-\gamma}}{1-\gamma}, \quad (5.4)$$

Moreover, $\gamma > 0$, $\gamma \neq 1$ measures the investor's level of risk aversion. The investor's objective is to derive an investment strategy π_t^* that maximizes the EUT of the terminal wealth W_T . Then, the investor's problem can be written as follows:

$$V(t, W) = \max_{\pi_{s \geq t} \in \Omega_\pi^{(O)}} \mathbb{E}(U(W_T) | \mathcal{F}_t), \quad (5.5)$$

and $V(t, W)$ denotes the value function at time t . According to the principles of stochastic control, we state the Hamilton-Jacobi-Bellman (HJB) equation for the value function V :

$$\sup_{\pi_t} \left\{ V_t + W_t V_W (r + \pi_t^T \Sigma_t \Lambda) + \frac{1}{2} W_t^2 V_{WW} (\pi_t^T \Sigma_t \Phi \Phi^T \Sigma_t^T \pi_t) \right\} = 0, \quad (5.6)$$

where $\Phi = \begin{bmatrix} 1 & 0 \\ \rho & \sqrt{1-\rho^2} \end{bmatrix}$.

¹The can easily be extended to other utility functions.

Proposition 5.2.1 (Solution for V and π_t^*) *The value function has the representation:*

$$V(t, W) = \frac{W^{1-\gamma}}{1-\gamma} \exp\left((1-\gamma)\left(r + \frac{1}{2} \frac{\Lambda^T (\Phi\Phi^T)^{-1} \Lambda}{\gamma}\right)(T-t)\right). \quad (5.7)$$

Moreover, π_t^* is an optimal strategy if it satisfies $\Sigma_t^T \pi_t^* = \eta_t^*$, where η_t^* is given by

$$\eta_t^* = \begin{bmatrix} \eta_t^{(1)} \\ \eta_t^{(2)} \end{bmatrix} = \frac{(\Phi\Phi^T)^{-1} \Lambda}{\gamma}. \quad (5.8)$$

Proof See Section 5.6.1.

Proposition 5.2.1 highlights three important implications. First, for any given element in $\Omega_O^{(n)}$, if $n > 2$ numerous, indeed infinitely many, strategies, all produce the same maximum value function. This can be interpreted as a redundant market case. Second, if $n = 2$, then a unique optimal strategy exists for the problem. Finally, if $n = 1$, there is no optimal solution: the value function cannot reach the global maximum; this is actually an incomplete market situation.

In summary, as there are a host of tradeable derivatives in the financial market, hence a myriad of elements exist in $\Omega_O^{(n)}$. This means there are an infinite number of choices of the portfolio composition O_t that can deliver the same optimal solution to the EUT problem. The next section takes advantage of this pool of optimal solutions to design a criterion that allows investors to select the best portfolio composition, with the corresponding strategy. This extra criterion is motivated by investor needs. Adding such a criterion will lead to an additional optimization problem, the solution of which is explored below.

5.2.1 Derivative selection criterion: minimizing ℓ_1 risk exposure

In this section, we propose a derivative selection criterion. Proposition 5.2.1 illustrates that, given $O_t \in \Omega_O^{(n)}$, with $n \geq 2$, an optimal strategy $\pi_t^* \in \Omega_\pi^{(O)}$ exists that maximizes the EUT of terminal wealth. From the traditional dynamic portfolio choice perspective, derivative selection does not benefit the investor, because regardless of the derivative chosen, the optimal strategy always achieves the same EUT.

In reality, investors are always concerned with the size of their risky allocations. For example, market conditions may change over time, and a risky investor could suffer large, unexpected losses especially during crisis periods. Regulatory constraints also force the investor to keep increasingly large percentages of wealth in cash. This means that strategies with smaller exposure on the risky products are naturally preferable to the investor. In this regard, we design a simple derivative selection criterion aimed at capturing this practical dilemma:

$$\min_{O_t \in \Omega_O^{(n)}} \left\| \arg \max_{\pi_{s \geq t} \in \Omega_\pi^{(O)}} \mathbb{E}(U(W_T) \mid \mathcal{F}_t) \right\|_1, \quad (5.9)$$

where $\|\pi_{s \geq t}\|_1 = \sum_{i=1}^n |\pi_t^{(i)}|$ represents the ℓ_1 norm of allocations at time t . Note that this objective is equivalent to maximizing the cash position while shorting less.

As we mentioned before, it is suboptimal for the investor to choose a portfolio composition size $n < 2$ based on the unhedgeable risk resources and incompleteness of the market. However, the investor might be interested in a redundant ($n > 2$) market situation, hoping to reduce their risky asset exposure. In the next proposition, we demonstrate that the best choice of n , for problem (5.9), is actually $n = 2$.

Proposition 5.2.2 *Assume that an optimal solution for problem (5.9) exists for $n \geq 2$, then, (5.9) leads to the same minimal ℓ_1 norm for any $n \geq 2$. In addition, an optimal strategy exists for problem (5.9) such that the number of non-zero allocations is less than or equal to 2.*

Proof See Section 5.6.2.

Proposition 5.2.2 demonstrates that redundancy will not offer any additional help with the investor's risky asset exposure. In other words, working with $n = 2$ is sufficient for problem (5.9). This allows us to work with the simplest case given a complete market setting (i.e. $n = 2$).

5.3 Applications to one-asset derivatives

In this section, we solve the derivative selection problem—that is, (5.9)—for $n = 2$, within subsets of the derivative set $\Omega_O^{(2)}$. The derivative selection problem is rewritten as

$$\min_{O_t \in \Omega_O^{(2,1)}} \left\| \arg \max_{\pi_{s \geq t} \in \Omega_\pi^{(O)}} \mathbb{E}(U(W_T) \mid \mathcal{F}_t) \right\|_1, \quad (5.10)$$

where $\Omega_O^{(2,1)}$ captures one-asset (single-stock) derivatives, which can be represented as follows:

$$\Omega_O^{(2,1)} = \left\{ O_t = [O_t^{(1)}, O_t^{(2)}]^T \mid O_t \in \Omega_O^{(2)}, O_t^{(i)} = g(S^{(i)}), i = 1, 2, t \in [0, T] \right\}.$$

In this situation, the option's variance matrix for a portfolio composition $O_t = [O_t^{(1)}, O_t^{(2)}]^T \in \Omega_O^{(2,1)}$ is defined by

$$\Sigma_t = \begin{bmatrix} f_t^{(1)} & 0 \\ 0 & f_t^{(2)} \end{bmatrix}, \quad (5.11)$$

which, provided $f_t^{(1)}$ and $f_t^{(2)}$ are nonzero, is a rank 2 (non-singular) diagonal matrix. By Itô's lemma, the sensitivity of $O_t^{(i)}$ is a function of the option Delta, spot price $S_t^{(i)}$, stock volatility $\sigma^{(i)}$ and the option price $O_t^{(i)}$:

$$f^{(i)} = \frac{\partial O_t^{(i)}}{\partial S_t^{(i)}} \frac{S_t^{(i)} \sigma^{(i)}}{O_t^{(i)}}. \quad (5.12)$$

The next proposition states the fundamental principle of one-asset option selection.

Proposition 5.3.1 (Fundamental principle of one-asset option selection) *A portfolio composition:*

$O_t^* = [O_t^{(1)*}, O_t^{(2)*}]^T \in \Omega_O^{(2,1)}$ is optimal for problem (5.10) if and only if

$$O_t^{(i)*} = \arg \max_{O_t^{(i)}} \left| \frac{dO_t^{(i)}}{dS_t^{(i)}} \frac{1}{O_t^{(i)}} \right|. \quad (5.13)$$

Proof See Section 5.6.3.

Note that both option Delta and price must be bounded away from 0 and ∞ to avoid the sub-optimal incomplete market case, such that the option sensitivity $f^{(i)} \in (0, \infty)$ and variance matrix Σ_t is non-singular. In other words, we could witness an infinitely large allocation as $f^{(i)} \rightarrow 0$ (to be explained in Section 5.3.1), which would also lead to a suboptimal solution (incomplete market) and hence a departure from the investor's target (i.e. maximizing utility and minimizing risk exposure).

The fundamental principle of one-asset option selection illustrates that the selection of one-asset options is separable. Investors can first pick the option with the largest relative sensitivity to $S_t^{(1)}$ among all one-asset options on $S_t^{(1)}$ as $O_t^{(1)*}$, and they can then select $O_t^{(2)*}$ in a similar way. Based on this principle, we consider the case where $\Omega_O^{(2,1)}$ is a subset of put and call options in Section 5.3.1. Then, the best option style and strike price for minimizing $\|\pi_t\|_1$ is quantified.

Selection of put and call options is studied first due to their popularity. Nonetheless, calls and puts have a problem: their optimal is on the boundary of the strike price range. This could lead to illiquid choices (high out-of-the-money options) or, even worse, incomplete market suboptimality on the limit as the strike price goes to zero (puts) or infinity (calls). In Section 5.3.2, we investigate derivative selection in a subset of straddles. Straddles are also popular products, which avoid the boundary optimality of calls and puts. Note that the selection of $O_t^{(1)*}$ and $O_t^{(2)*}$ is independent, and the procedures are similar; hence, for simplicity, we only present the result for $O_t^{(2)*}$.

The chosen parameters are presented in Table 5.1.² These parameters are considered to be plausible.

Table 5.1: Parameter Value

Parameter	Value	Parameter	Value
$\sigma^{(1)}$	0.13	$\sigma^{(2)}$	0.2
r	0.05	ρ	0.4
$\lambda^{(1)}$	0.52	$\lambda^{(2)}$	0.6
Investment horizon T	1	Time to maturity of options \hat{T}	2
$S_0^{(1)}$	40	$S_0^{(2)}$	30
$\eta_t^{(1)}$	0.083	$\eta_t^{(2)}$	0.117
γ	4.0		

²See Section 5.6.9 for analysis of other parameter choices.

The option variance matrix may not be solvable in closed form. Therefore, we approximate the sensitivity of European, American and arithmetic average Asian options via the finite difference method: the Delta of option O_t is given by

$$\text{Delta} = \frac{O_t(S + \Delta S) - O_t(S - \Delta S)}{2\Delta S}. \quad (5.14)$$

Here, $O_t(S)$ is the simulated option price given spot price S . In addition, we estimate the sensitivity of American options with the generalized infinitesimal perturbation analysis approach introduced by [16].

5.3.1 Put and call options

We first consider the derivative selection problem (5.10) on the subset denoted by $\Omega_O^{(2, \text{put call})}$ that contains only European-, American- and Asian-style put and call options:

$$\Omega_O^{(2, \text{put call})} = \left\{ O_t = [O_t^{(1,j)}, O_t^{(2,j)}]^T \mid O_t^{(i,j)} = g^{(j)}(S^{(i)}), i = 1, 2, t \in [0, T] \right\}.$$

For both practical and theoretical reasons, the strike price $K^{(i,j)}$ of a given option $O_t^{(i,j)}$ is bounded within $[A^{(i,j)}, B^{(i,j)}]$, where $j \in \{\text{Euro Call}, \text{Asian Call}, \text{Amer Call}, \text{Euro Put}, \text{Asian Put}, \text{Amer Put}\}$. The put option strike price is bounded away from 0; that is, $A^{(i,j)} > 0$, where $j \in \{\text{Euro Put}, \text{Asian Put}, \text{Amer Put}\}$. Similarly, the call option strike excludes ∞ . Both conditions ensure the non-zero option price assumption. For simplicity, we also assume that all the options have the same time to maturity $\hat{T} = 2$, and we search the optimal portfolio composition in terms of option type, style and strike price.

European put and call prices and their sensitivities are solved by the well-known Black–Scholes–Merton model (see [8]). Let $O_t^{(i, \text{Euro Call})}$ and $O_t^{(i, \text{Euro Put})}$ be a call and put option on $S_t^{(i)}$ given in Equation (5.1). The Black–Scholes–Merton model indicates that

$$\begin{aligned} O_t^{(i, \text{Euro Call})} &= S_t^{(i)} N(d_1) - K^{(i, \text{Euro Call})} e^{-r(\hat{T}-t)} N(d_2) \\ O_t^{(i, \text{Euro Put})} &= K^{(i, \text{Euro Put})} e^{-r(\hat{T}-t)} N(-d_2) - S_t^{(i)} N(-d_1) \\ \frac{\partial O_t^{(i, \text{Euro Call})}}{\partial S_t^{(i)}} &= N(d_1) \qquad \frac{\partial O_t^{(i, \text{Euro Put})}}{\partial S_t^{(i)}} = -N(-d_1), \end{aligned} \quad (5.15)$$

where N is the cumulative distribution function of a standard normal random variable and

$$d_1 = \frac{\ln(S_t^{(i)} / K^{(i, \text{Euro Call/Put})}) + (r + \frac{1}{2}(\sigma^{(i)})^2)(\hat{T} - t)}{\sigma^{(i)} \sqrt{\hat{T} - t}}, \quad d_2 = d_1 - \sigma^{(i)} \sqrt{\hat{T} - t}. \quad (5.16)$$

The proposition next demonstrates the existence of an optimal portfolio composition $O_t^* \in \Omega_O^{(2, \text{put call})}$, given the assumption that $O_t^{(i,j)} \in \mathbb{C}^1$ and the Delta is non-zero.

Proposition 5.3.2 (Existence of optimal portfolio composition in put and call subset) *Assume $O_t^{(i,j)}(S^{(i)}, K^{(i,j)}) \in \mathbb{C}^1$ on $(0, \infty) \times [A^{(i,j)}, B^{(i,j)}]$,³ the optimal portfolio composition for problem (5.10) within the subset $\Omega_O^{(2, \text{put call})}$ exists.*

³ $\frac{\partial O_t^{(i,j)}}{\partial K^{(i,j)}}$ on boundary is defined as the one-sided derivative.

Proof See Section 5.6.4.

It is easy to show the expression for this optimal composition, in the case of the European options, as clarified in the following corollary.

Corollary 5.3.3 *The risk exposure to an European call option decreases with $K^{(i,Euro\ Call)}$ and converges to 0 as $K^{(i,Euro\ Call)} \rightarrow \infty$. Similarly, the risk exposure to an European put option increases with $K^{(i,Euro\ Put)}$ and converges to 0 as $K^{(i,Euro\ Put)} \rightarrow 0$. Therefore, the optimal European call is achieved when $K^{(i,Euro\ Call)} = B^{(i,Euro\ Call)}$ and the optimal European put is achieved when $K^{(i,Euro\ Put)} = A^{(i,Euro\ Put)}$.*

Proof See Section 5.6.5.

Corollary 5.3.3 demonstrates that $\|\pi_t\|_1$ can vanish if the European call option's strike price approaches infinity. These extreme options cannot be found in the market, but more importantly, they would also lead to a violation of the non-singular matrix Σ_t condition, creating an incomplete market situation. This is known as the problem of “boundary optimality.” The corollary thus illustrates the importance of our derivative selection.

Figure 5.1 (a) exhibits $\pi_0^{(2,j)}$ —that is, the allocation on call options $O_t^{(2,j)}$ at $t = 0$ —as a function of strike price and spot price ratio $K^{(2,j)}/S_t^{(2)}$; for example, $K^{(2,j)}/S_t^{(2)} = 1$ indicates at-the-money options. The analytical sensitivity of European calls is obtained with Equation (5.12) and (5.15), with which the optimal strategy is known immediately. Note that the European call option reduces to $S_t^{(2)}$ when $K^{(2,Euro\ Call)} = 0$, and the allocation hence converges to the optimal strategy on $S_t^{(2)}$. The allocation on the European call obtained by the finite difference method is also plotted to verify the accuracy of numerical approximation. Allocations obtained via analytical and numerical approaches visually overlap except when $K^{(2,Euro\ Call)}$ is extremely large. The allocation to Asian calls is similar to that of European calls when the strike prices are small, but it decreases faster. Asian calls are consequently preferable to European calls given the same upper bound on strike price; that is, $B^{(2,Euro\ call)} = B^{(2,Asian\ call)}$.

The allocation on put options is illustrated in Figure 5.1 (b). The absolute allocations for European, American⁴ and Asian puts increase with strike price because of the decreasing instantaneous sensitivity. The absolute allocation on Asian puts is the smallest when $K^{(2,Asian\ Put)}$ is small, but the opposite occurs as the strike price rises. Figure 5.1 not only confirms Corollary 5.3.3—that is $\pi_t^{(2,Euro\ Call)} \rightarrow 0$ as $K^{(2,Euro\ Call)} \rightarrow \infty$ and $\pi_t^{(2,Euro\ Put)} \rightarrow 0$ as $K^{(2,Euro\ Put)} \rightarrow 0$ —but also demonstrates a similar conclusion for Asian and American options.

In summary, the absolute allocation on a put or call option is monotone with strike price; hence, the optimal choice of $O_t^{(2,j)}$ is on the boundary. This means we only need to compare the allocation $\pi_t^{(2,j)}$ on the deepest out-of-the-money option to obtain the option with the smallest absolute allocation.

⁴We assume stocks which pay no dividends, so American call is identical to the European call in (a). In addition, the allocation on American put is shown in (b) when $K^{(2,Amer\ Put)} < 37.7$, i.e. the region, in which the American put should be held and not yet exercised.

Next, we consider the case where options of different style⁵ share an identical boundary:

$$\begin{aligned} [S_t^{(2)}, R^B S_t^{(2)}] &= [A^{(2,j)}, B^{(2,j)}], \quad j \in \{\text{Euro Call}, \text{Asian Call}\} \\ [R^A S_t^{(2)}, S_t^{(2)}] &= [A^{(2,j)}, B^{(2,j)}], \quad j \in \{\text{Euro Put}, \text{Asian Put}, \text{Amer Put}\}. \end{aligned}$$

Here, $R^A \leq 1$, and $R^B \geq 1$. As we move the lower bound of put option strike price $R^A S_t^{(2)}$ and the upper bound of call option strike price $R^B S_t^{(2)}$, the optimal choice of $O_t^{(2,j)}$ is shown in Figure 5.1 (c). The Asian option is preferable compared to American and European options. Asian calls dominate when both R^A and R^B are large, whereas Asian puts dominate when both R^A and R^B are small.

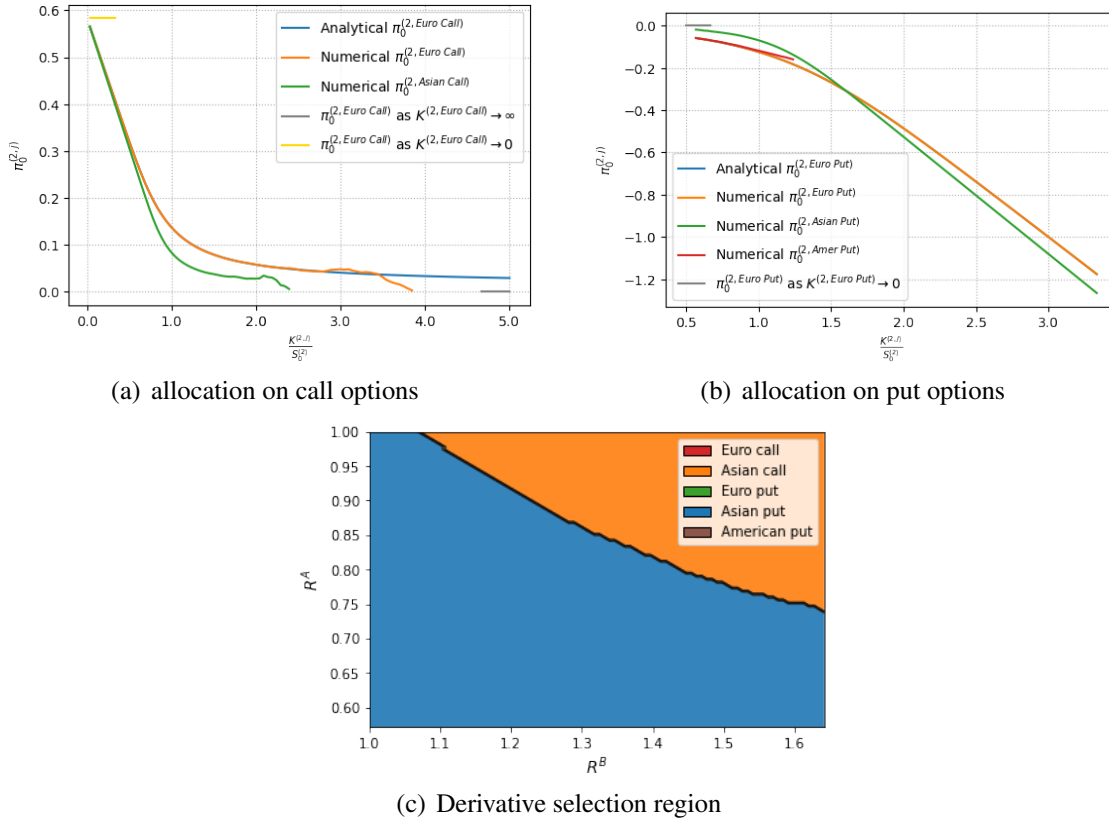


Figure 5.1: Allocation on options versus strike price

Figure 5.2 displays the performance of the portfolio $O_t = [O_t^{(1, \text{Euro Call})}, O_t^{(2, \text{Euro Call})}]^T$ versus strike prices for different rebalancing frequencies. The portfolio performance is measured by annualized certainty equivalent (CER), defined as

$$U(W_0 \exp(\text{CER} * T)) = V(0, W_0). \quad (5.17)$$

The theoretical optimal CER (orange wireframe) is plotted as the benchmark, which can only be achieved by continuously rebalancing. We also present the incomplete market CER (i.e.

⁵The actual range of American put strike price is the intersection of $[A^{(i, \text{Amer Put})}, B^{(i, \text{Amer Put})}]$ and the region of $K^{(i, \text{Amer Put})}$ such that the option is not exercised immediately, hence American option is not considered when $[A^{(i, \text{Amer Put})}, B^{(i, \text{Amer Put})}]$ is mutually exclusive with that region.

the green wireframe) for comparison purposes, for example obtained through the lack of an asset to hedge the risk in $B_t^{(2)}$. A portfolio with in-the-money call options is insensitive to the rebalancing frequency, and the loss from occasional rebalancing is not significant. On the other hand, the CER of a portfolio with two deep out-of-the-money calls could be even smaller than that of an incomplete market CER when the portfolio is only rebalanced 10 times per year, whereas it approaches complete market CER as the rebalancing frequency increases.

This is important for investors reducing their risk exposure with deep out-of-the-money options. These products lack liquidity; hence, the trading strategy might fail because investors cannot adjust their position quickly enough. In summary, the best (out-of-the-money) options are those requiring more frequent rebalancing, as Figure 5.2 demonstrates. This points at future research addressing the trade-off between exposure and rebalancing.

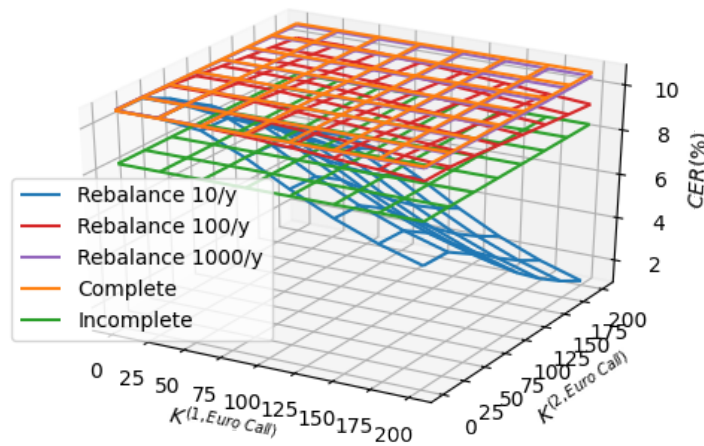


Figure 5.2: Certainty equivalent rate (CER) versus strike price with different rebalancing frequencies

5.3.2 Straddles

Next, we consider the derivative selection in a subset of options called straddles:

$$\Omega_O^{(2, \text{straddle})} = \left\{ O_t = [O_t^{(1,j)}, O_t^{(2,j)}]^T \mid O_t^{(i,j)} = g^{(j)}(S^{(i)}), i = 1, 2, t \in [0, T] \right\}.$$

where $j \in \{\text{Euro Strad}, \text{Asian Strad}, \text{Amer Strad}\}$. A straddle is an option synthesized by simultaneously taking a long position in a call and a put option; hence, the terminal payoff of a European straddle is $|S_T^{(i)} - K^{(i, \text{Euro Strad})}|$, where $K^{(i, \text{Euro Strad})}$ denotes the strike price. The European straddle price and Delta are obtained with the Black–Scholes–Merton model:

$$\begin{aligned} O_t^{(i, \text{Euro Strad})} &= S_t^{(i)}(2N(d_1) - 1) - K^{(i, \text{Euro Strad})} e^{-r(\hat{T}-t)}(2N(d_2) - 1) \\ \frac{\partial O_t^{(i, \text{Euro Strad})}}{\partial S_t^{(i)}} &= 2N(d_1) - 1. \end{aligned} \tag{5.18}$$

d_1 and d_2 are defined in Equation (5.16). We substitute the straddle's Delta into Equation (5.12), and the sensitivity of straddle $O_t^{(i, Euro Strad)}$ is given by

$$f^{(i, Euro Strad)} = \frac{(2N(d_1) - 1)S_t^{(i)}\sigma^{(i)}}{O_t^{(i, Euro Strad)}}. \quad (5.19)$$

The non-singular variance matrix condition requires non-zero sensitivity $f^{(i, Euro Strad)}$, such that $2N(d_1) - 1 \neq 0$ and the feasible region for the strike price is as follows:

$$K^{(i, Euro Strad)} \in \left[0, S_t^{(i)} \exp\left(r + \frac{1}{2}(\sigma^{(i)})^2(\hat{T} - t)\right) \cup \left(S_t^{(i)} \exp\left(r + \frac{1}{2}(\sigma^{(i)})^2(\hat{T} - t)\right), \infty\right). \quad (5.20)$$

It is easy to verify that $O_t^{(i, Euro Strad)} \in (0, \infty)$ and $O_t^{(i, j)}(S_t^{(i)}, K^{(i, j)}) \in \mathbb{C}^1$. We define the feasible region for the straddle $O_t^{(i, j)}$ by analogy: $K^{(i, j)} \in [0, A^{(i, j)}] \cup (A^{(i, j)}, \infty)$, where $j \in \{Euro Strad, Asian Strad\}$, and $K^{(i, j)} \in [0, A^{(i, j)}] \cup (A^{(i, j)}, B^{(i, j)}]$, where $j \in \{Amer Strad\}$. Here, $A^{(i, Amer Strad)}$ is the point Delta of $O_t^{(i, Amer Strad)}$ equal to 0, and $B^{(i, Amer Strad)}$ is the maximum strike price such that the American put is not immediately exercised. The next theorem shows the existence of an optimal straddle (i.e. an optimal strike price).

Proposition 5.3.4 (Existence of optimal portfolio composition in the straddle subset) *There exists a portfolio composition $O_t^* = [O_t^{(1, *)}, O_t^{(2, *)}]^T$ with finite strike prices $K^{(i, j, *)}$, such that O_t^* is optimal for problem (5.10) within $\Omega_O^{(2, straddle)}$. Here the optimal strike price, $K^{(i, j, *)}$ is the solution of the equation:*

$$\frac{\partial^2 O_t^{(i, j)}}{\partial S_t^{(i)} \partial K^{(i, j)}} O_t^{(i, j)} - \frac{\partial O_t^{(i, j)}}{\partial S_t^{(i)}} \frac{\partial O_t^{(i, j)}}{\partial K^{(i, j)}} = 0. \quad (5.21)$$

Proof See Section 5.6.6.

Next, we quantify the derivative selection within the subset of straddles. Here, we only illustrate the optimal choice of $O_t^{(2, j)}$ because of the separable selection within a one-asset option subset (see Proposition 5.3.1). We first compute the optimal strike price of American straddle $B^{(i, Amer Strad)} = 37.7$ and the unfeasible point $A^{(2, j)}$ for European, Asian and American straddles; this is where the Delta of $O_t^{(2, j)}$ is equal to 0. From the formulas above, we have $A^{(2, Euro Strad)} = S_t^{(2)} \exp\left(r + \frac{1}{2}(\sigma^{(2)})^2(\hat{T} - t)\right) = 34.5$, $A^{(2, Asian Strad)} = 31.9$ and $A^{(2, Amer Strad)} = 32.9$, which are all obtained with Brent's algorithm.

Figure 5.3 depicts the allocation $\pi_0^{(2, j)}$, where $j \in \{Euro Strad, Asian Strad, Amer Strad\}$ versus the ratio of spot price to strike price. The allocation $\pi_0^{(2, j)}$ has the shape of a hyperbola, and it approaches $\pm\infty$ as $K^{(2, j)} \uparrow\downarrow A^{(2, j)}$, which forms a ‘‘cliff.’’ In contrast to the put and call option, the optimal straddle is found in the interior regardless of the option style. The boundary optimality issue is thus avoided, and it's plausible that the straddle minimum risk exposure will have acceptable liquidity. Moreover, the optimal straddle minimizing the risk exposure lies on the left branch; that is, $K^{(2, j)} \in [0, A^{(2, j)})$. The Asian straddle is superior to European and American straddles because of its smaller absolute allocation.

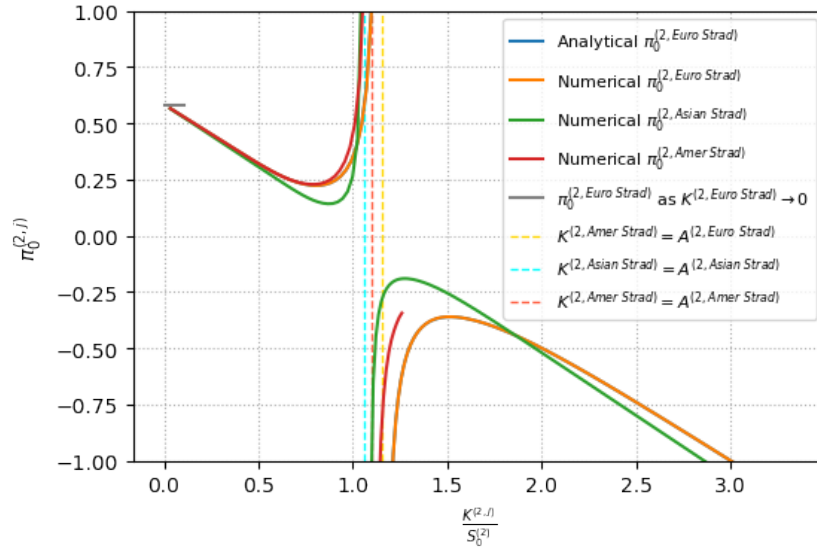


Figure 5.3: Allocation on straddle versus $\frac{K^{(i,j)}}{S_0^{(i,j)}}$

The allocation on the European straddle $\pi_t^{(i,Euro Strad)}$ is solved in closed form with Equation (5.19):

$$\pi_t^{(i,Euro Strad)} = \frac{\eta_t^{(i)}}{f^{(i,Euro Strad)}} = \frac{\eta_t^{(i)}(2S_t^{(i)}(2N(d_1) - 1) - K^{(i,Euro Strad)}e^{-r(\hat{T}-t)}(2N(d_2) - 1))}{(2N(d_1) - 1)S_t^{(i)}\sigma^{(i)}}, \quad (5.22)$$

which is a function of the ratio of strike price to spot price $K^{(i,Euro Strad)}/S_t^{(i)}$.

In the subset of put and call $\Omega_O^{(2,put call)}$ (previous section), the optimal option is always found at the boundary. Therefore, investors stick to the option by rolling over with the same strike price. The optimal option in $\Omega_O^{(2,straddle)}$ depends on the spot price and time-dependent optimal ratio $K^{(i,Euro Strad)}/S_t^{(i)}$, and the investor should roll from the current holding to new straddles at each rebalancing time to minimize risk exposure. In this regard, Figure 5.4 (a) plots the optimal strike and spot price ratio of European straddle $K^{(i,Euro Strad)}/S_t^{(i)}$ versus time t . Both $K^{(1,Euro Strad)}/S_t^{(1)}$ and $K^{(2,Euro Strad)}/S_t^{(2)}$ increase with time t , while $K^{(2,Euro Strad)}/S_t^{(2)}$ grows faster.

The connection between portfolio CER and rebalancing frequency is demonstrated in Figure 5.4 (b). As expected, the portfolio CER approaches the theoretical result as rebalancing frequency rises. Note that the CER of the rolling straddle portfolio is close to the theoretical CER even when the rebalancing frequency is less than 10 times per year, suggesting that rebalancing even relatively infrequently causes only a small loss. This is another benefit of choosing straddles over out-of-the-money calls or puts.

In conclusion, straddles are an ideal option class for two reasons. First, the optimal straddle for minimizing risk exposure happens to be an active and liquid option. In addition, a rolling straddle portfolio is insensitive to the rebalancing frequency, thus reducing an investor's additional costs, such as transaction costs (although transaction cost is not exactly modelled yet).

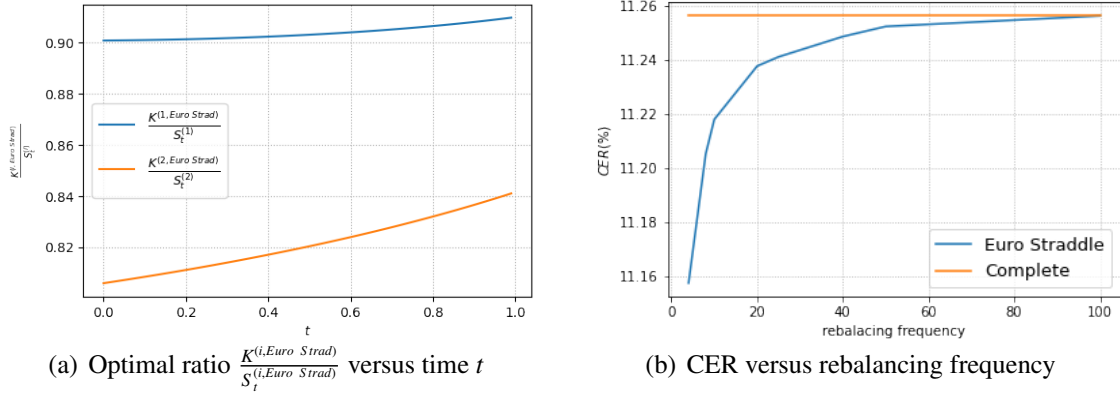


Figure 5.4: Straddle analysis

5.4 Multi-asset option selection

Multi-asset options are commonly traded in the OTC market. In this section, we explore the benefits of including such options in an investor's portfolio. A subset of multi-asset options is defined as follows:

$$\Omega_O^{(2,multi\ asset)} = \left\{ O_t = [O_t^{(1,j_1)}, O_t^{(2,j_2)}]^T \mid O_t^{(1,j_1)} = g^{(j_1)}(S^{(1)}), j_1 = \text{one-asset option}; \right. \\ \left. O_t^{(2,j_2)} = g^{(j_2)}(S^{(1)}, S^{(2)}), j_2 = \text{multi-asset option}, t \in [0, T] \right\}.$$

Assume the portfolio composition $O_t \in \Omega_O^{(2,multi\ asset)}$ consists of a one-asset option and a multi-asset option. The variance matrix then has the representation

$$\Sigma_t = \begin{bmatrix} f_t^{(11)} & 0 \\ f_t^{(21)} & f_t^{(22)} \end{bmatrix}. \quad (5.23)$$

The next proposition states the fundamental principle of derivative selection in the subset of multi-asset options.

Proposition 5.4.1 (Fundamental principle of multi-asset option selection) *If a portfolio composition $O_t^* = [O_t^{(1),*}, O_t^{(2),*}]^T$ is optimal for problem (5.10) within $\Omega_O^{(2,multi\ asset)}$, then*

$$O_t^{(1),*} = \arg \max_{O_t^{(1,j_1)}} \left| \frac{dO_t^{(1,j_1)}}{dS_t^{(1)}} \frac{1}{O_t^{(1,j_1)}} \right|. \quad (5.24)$$

Proof See Section 5.6.7.

Proposition 5.4.1 demonstrates a necessary condition for multi-asset option selection and reveals the sequential selection property for problem (5.10) within $\Omega_O^{(2,multi\ asset)}$. Investors should pick the one-asset option with the largest relative sensitivity to $S_t^{(1)}$ first, and they should then search for the optimal multi-asset option (see Equation (5.45)) given a fixed $f_t^{(11)}$.

Now, we illustrate the multi-asset portfolio selection with an example of basket options. The subset of basket option is given by

$$\Omega_O^{(2, \text{call basket})} = \left\{ O_t = [O_t^{(1, j_1)}, O_t^{(2, j_2)}]^T \mid O_t^{(1, j)} = g^{(j_1)}(S^{(1)}), j_1 = \text{European call}; \right. \\ \left. O_t^{(2, j_2)} = g^{(j_2)}(S^{(1)}, S^{(2)}), j_2 = \text{Basket Call or Basket Put}, t \in [0, T] \right\}.$$

Notably, $\Omega_O^{(2, \text{call basket})} \subset \Omega_O^{(2, \text{multi asset})}$. The basket option, simultaneously hedging the risk on a combination of two assets, has the following payoff:⁶

$$\begin{cases} O_T^{(2, j_2)} = (S_T^{(1)} + S_T^{(2)} - K^{(2, j_2)})^+ & j_2 = \text{Basket Call} \\ O_T^{(2, j_2)} = (K^{(2, j_2)} - S_T^{(1)} - S_T^{(2)})^+ & j_2 = \text{Basket Put.} \end{cases} \quad (5.25)$$

Furthermore, $K^{(i, j_i)} \in [A^{(i, j_i)}, B^{(i, j_i)}]$, where $j_1 = \text{Euro Call}$ and $j_2 \in \{\text{Basket Call}, \text{Basket Put}\}$, denotes the strike price of call and basket options. The existence of optimal portfolio composition within the subset of basket option is demonstrated in the next proposition.

Proposition 5.4.2 (Existence of optimal portfolio composition in the subset of basket option)

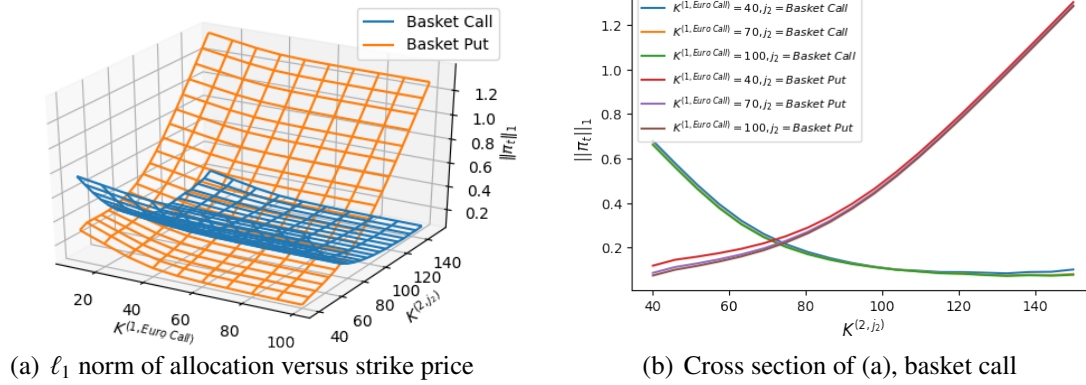
Let the basket option price $O_t^{(2, j_2)}$ be a function of $(S_t^{(1)}, S_t^{(2)}, K^{(2, j_2)})$ and $O_t^{(2, j_2)} \in \mathbb{C}^1$ on $(0, \infty) \times (0, \infty) \times [A^{(2, j_2)}, B^{(2, j_2)}]$, then the optimal portfolio composition for problem (5.10) within the subset $\Omega_O^{(2, \text{call basket})}$ exists.

Proof See Section 5.6.8.

The risky asset exposure (see Equation (5.45)) is broken down into the allocation on $O_t^{(1, j_1)}$ and $O_t^{(2, j_2)}$. Note that allocation on $O_t^{(2, j_2)}$ depends only on $f_t^{(22)}$ because $B_t^{(2)}$ is solely hedged by the basket option $O_t^{(2, j_2)}$. Figure 5.5 (a) illustrates how risky asset exposure varies with $K^{(1, j_1)}$ and $K^{(2, j_2)}$. Allocation on $O_t^{(1, j_1)}$ is scaled by the relative sensitivity $f_t^{(11)}$ (see Equation (5.45)); hence, risky asset exposure decreases with $K^{(1, j_1)}$, and out-of-the-money $O_t^{(1, j_1)}$ is preferable regardless of the choice of $O_t^{(2, j_2)}$, for example one-asset or multi-asset options. In addition, risky asset exposure is monotonic with $K^{(2, j_2)}$ except when $K^{(1, j_1)}$ is extremely small. We plot the cross section of (a) in Figure 5.5 (b) for illustration purposes. Given an at-the-money or out-of-the-money $O_t^{(1, j_1)}$, $\|\pi_t\|_1$ decreases when $j_2 = \text{Basket Call}$ and increases when $j_2 = \text{Basket Put}$. Therefore, out-of-the-money basket options minimize risky asset exposure. Moreover, $\|\pi_t\|_1$ is insensitive to $K^{(1, j_1)}$ because investing in basket options generally leads to a smaller allocation on $O_t^{(1, j_1)}$.

Similarly to put and call options, with the parameters listed in Table 5.1, the optimal basket call is achieved when the strike price $K^{(2, j_2)}$ is at the upper bound, while the optimal basket put is achieved when strike price $K^{(2, j_2)}$ is at the lower bound.

⁶Investor can choose the weight on each asset of basket option in OTC market, we only consider equal weighted case in this chapter .

Figure 5.5: $\|\pi_t\|_1$ versus strike price (Basket option)

Given the similarities between one-asset calls/puts and basket calls/puts, investors could be interested in the best among those choices. To answer this question, we fix the strike price of a European call $O_t^{(1, j_1)}$, letting the lower bound of a put option strike price and the upper bound of a call option strike price be proportional to the spot price:

$$\begin{aligned} [S_t^{(2)}, R^B S_t^{(2)}] &= [A^{(2, j_2)}, B^{(2, j_2)}], & j_2 \in \{\text{Euro Call}, \text{Asian Call}\}; \\ [S_t^{(1)} + S_t^{(2)}, R^B (S_t^{(1)} + S_t^{(2)})] &= [A^{(2, j_2)}, B^{(2, j_2)}], & j_2 \in \{\text{Basket Call}\}; \\ [R^A S_t^{(2)}, S_t^{(2)}] &= [A^{(2, j_2)}, B^{(2, j_2)}], & j_2 \in \{\text{Euro Put}, \text{Asian Put}, \text{Amer Put}\}; \\ [R^A (S_t^{(1)} + S_t^{(2)}), S_t^{(1)} + S_t^{(2)}] &= [A^{(2, j_2)}, B^{(2, j_2)}], & j_2 \in \{\text{Basket Put}\}, \end{aligned}$$

where $R^A \leq 1$ and $R^B \geq 1$.

By letting the ratio R^A and R^B vary, the optimal choice of $O_t^{(2, j_2)}$ is studied in Figure 5.6. One can observe that when $O_t^{(1, j_1)}$ is an at-the-money-option—that is, $K^{(1, j_1)} = 40$ —a one-asset Asian option dominates for a small R^B , while a basket call is superior to other options when R^B is large. However, basket calls become less preferable as $K^{(1, j_1)}$ increases. As mentioned above, compared with one-asset options, investors have a smaller absolute allocation on $O_t^{(1, j_1)}$ and a larger absolute allocation on $O_t^{(2, j_2)}$ with a basket option. Furthermore, the allocation on $O_t^{(1, j_1)}$ is scaled by the relative sensitivity $f_t^{(11)}$ (see Equation (5.35) and (5.45)), which explains why a basket call has an advantage over one-asset options when $K^{(1, j_1)}$ is small but loses its dominant position as $K^{(1, j_1)}$ rises. The optimal choice of $O_t^{(2, j_2)}$ with other sets of parameters is demonstrated in Section 5.6.9.

5.5 Conclusions

This chapter reveals the benefit of using options to minimize the total risk exposure of a portfolio, while maintaining an optimal level of utility. We demonstrate that the farther out-of-the-money calls or puts are, the better choices they are, particularly the Asian type. Given the lack of liquidity on those type of options, we explored straddle options and found that optimal choices are close to at-the-money options, which are hence likely liquid products. We also

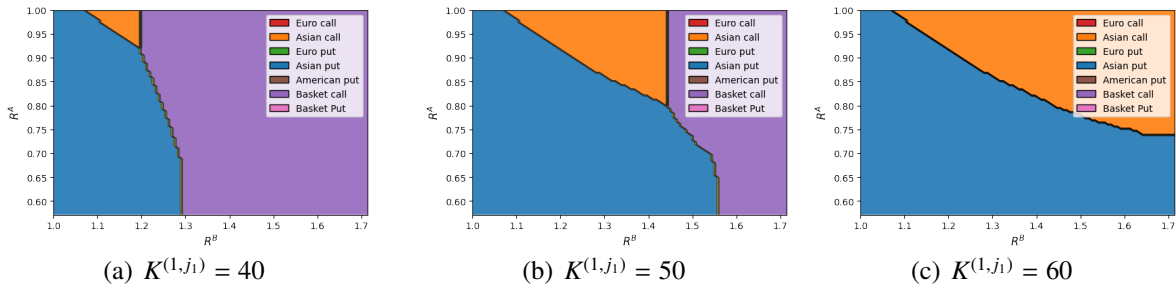


Figure 5.6: Derivatives selection $O_t^{(2,j_2)}$

explored multi-asset derivatives and can confirm that basket options are preferable to one-asset options in terms of minimizing risk exposure.

5.6 Proofs

5.6.1 Proof of Proposition 5.2.1

We assume $V(t, W) = \frac{W^{1-\gamma}}{1-\gamma} \exp(h(T-t))$, which is substituted into Equation (5.6). Then, $h(T-t)$ satisfies:

$$\sup_{\pi_t} \left\{ \frac{h'(T-t)}{1-\gamma} + r + \pi_t^T \Sigma_t \Lambda - \frac{\gamma}{2} (\pi_t^T \Sigma_t \Phi \Phi^T \Sigma_t \pi_t) \right\} = 0, \quad (5.26)$$

Denote $\eta_t = \Sigma_t^T \pi_t$, then problem (5.26) can be rewritten as,

$$\sup_{\eta_t} \left\{ \frac{h'(T-t)}{1-\gamma} + r + \eta_t^T \Lambda - \frac{\gamma}{2} (\eta_t^T \Phi \Phi^T \eta_t) \right\} = 0. \quad (5.27)$$

which implies the optimal strategy

$$\eta_t^* = \frac{(\Phi \Phi^T)^{-1} \Lambda}{\gamma}. \quad (5.28)$$

With $\eta_t^* = \Sigma_t^T \pi_t^*$, there are infinitely many choice of π_t^* if $n > 2$. Next, we substitute η_t^* into Equation (5.27) and derive the ordinary differential equation (ODE) for $h(T-t)$:

$$\begin{cases} \frac{h'(T-t)}{1-\gamma} + r + \frac{\Lambda^T (\Phi \Phi^T)^{-1} \Lambda}{2\gamma} = 0 \\ h(T) = 0. \end{cases} \quad (5.29)$$

where the terminal condition results from $V(t, W) = U(W)$. The solution to Equation (5.29) is

$$h(T-t) = (1-\gamma) \left(r + \frac{\Lambda^T (\Phi \Phi^T)^{-1} \Lambda}{2\gamma} \right) (T-t), \quad (5.30)$$

5.6.2 Proof of Proposition 5.2.2

Let $O_{t,n} = [O_t^{(1)}, O_t^{(2)}, \dots, O_t^{(n)}]^T$ with variance matrix Σ_t of rank 2 be an optimal subset of options for problem (5.9). $\pi_{t,n}^*$ is a strategy maximizing the expected utility if and only if $\Sigma_t^T \pi_{t,n}^* = \eta_t^*$. Therefore, $O_{t,n}$ and $\pi_{t,n}^*$ is an optimal pair for (5.9) when $\pi_{t,n}^*$ is an optimal solution for

$$\begin{aligned} & \underset{\pi_t}{\text{minimize}} && \|\pi_t\|_1 \\ & \text{subject to} && \Sigma_t^T \pi_t = \eta_t^*. \end{aligned} \quad (5.31)$$

According to the principle 4.5 in [80], problem (5.31) is equivalent to

$$\begin{aligned} & \underset{\delta_t}{\text{minimize}} && \mathbb{1}^T \delta_t \\ & \text{subject to} && \hat{\Sigma}_t^T \delta_t = \eta_t^*, \\ & && \delta_t \geq 0 \end{aligned} \quad (5.32)$$

where $\delta_t = [\alpha_t^{(1)}, \alpha_t^{(2)}, \dots, \alpha_t^{(n)}, \beta_t^{(1)}, \beta_t^{(2)}, \dots, \beta_t^{(n)}]^T$ satisfies $\alpha_t^{(i)} = \frac{|\pi_t^{(i)}| + \pi_t^{(i)}}{2}$, and $\beta_t^{(i)} = \frac{|\pi_t^{(i)}| - \pi_t^{(i)}}{2}$, with

$$\hat{\Sigma}_t = \begin{bmatrix} \Sigma_t \\ -\Sigma_t \end{bmatrix} = \begin{bmatrix} f_t^{11} & f_t^{12} \\ \dots & \dots \\ f_t^{n1} & f_t^{n2} \\ -f_t^{11} & -f_t^{12} \\ \dots & \dots \\ -f_t^{n1} & -f_t^{n2} \end{bmatrix}. \quad (5.33)$$

Theorems 2.3 and 2.4 in [6] lists the necessary and sufficient conditions for the extreme point δ_t , i.e.

1. $\delta_t = [\delta_t^{(1)}, \delta_t^{(2)}, \dots, \delta_t^{(n)}, \delta_t^{(n+1)}, \delta_t^{(n+2)}, \dots, \delta_t^{(2n)}]^T$.
2. the \hat{q}_{th} and \hat{p}_{th} rows in $\hat{\Sigma}_t$ are linear independent, $\delta_t^{(i)} = 0$ if $i \neq \hat{q}$ or \hat{p} .
3. δ_t is feasible solution.

Without loss of generality, we assume the p_{th} and q_{th} rows in Σ are linear independent, and we consider 4 cases:

$$\begin{aligned} \delta_t^{[1]} &= \begin{cases} [\delta_t^{[1,(1)}, \delta_t^{[1,(2)}, \dots, \delta_t^{[1,(n)}, \delta_t^{[1,(n+1)}, \delta_t^{[1,(n+2)}, \dots, \delta_t^{[1,(2n)}]^T \\ \delta_t^{[1,(i)} = 0 & \text{if } i \neq q \text{ or } p \end{cases} \\ \delta_t^{[2]} &= \begin{cases} [\delta_t^{[2,(1)}, \delta_t^{[2,(2)}, \dots, \delta_t^{[2,(n)}, \delta_t^{[2,(n+1)}, \delta_t^{[2,(n+2)}, \dots, \delta_t^{[2,(2n)}]^T \\ \delta_t^{[2,(i)} = 0 & \text{if } i \neq q + n \text{ or } p \end{cases} \\ \delta_t^{[3]} &= \begin{cases} [\delta_t^{[3,(1)}, \delta_t^{[3,(2)}, \dots, \delta_t^{[3,(n)}, \delta_t^{[3,(n+1)}, \delta_t^{[3,(n+2)}, \dots, \delta_t^{[3,(2n)}]^T \\ \delta_t^{[3,(i)} = 0 & \text{if } i \neq q \text{ or } p + n \end{cases} \\ \delta_t^{[4]} &= \begin{cases} [\delta_t^{[4,(1)}, \delta_t^{[4,(2)}, \dots, \delta_t^{[4,(n)}, \delta_t^{[4,(n+1)}, \delta_t^{[4,(n+2)}, \dots, \delta_t^{[4,(2n)}]^T \\ \delta_t^{[4,(i)} = 0 & \text{if } i \neq q + n \text{ or } p + n \end{cases} \end{aligned} \quad (5.34)$$

It is clear that there is a non-negative strategy in $\delta_t^{[1]}$, $\delta_t^{[2]}$, $\delta_t^{[3]}$ and $\delta_t^{[4]}$ because the i_{th} row in $\hat{\Sigma}$ is the opposite of the $(i+n)_{th}$ row, and the non-negative strategy is feasible and an extreme point. This proves the existence of an extreme point for problem (5.32). Now, theorem 2.7 in [6] guarantees that there is an optimal solution which is an extreme point for problem (5.32).

With the second necessary and sufficient conditions of the extreme point, we know that an optimal solution δ_t^* for problem (5.32) has at most two non-zero elements. This would imply an optimal solution, denoted by $\pi_{t,n}^* = [\pi_{t,n}^{(1)}, \pi_{t,n}^{(2)}, \dots, \pi_{t,n}^{(n)}]^T$, for problem (5.31) with at most two non-zero elements, which would also be the optimal strategy for (5.9).

Without loss of generality, we assume $\pi_{t,n}^{(i)} = 0$, $i \neq x, y$. $O_{t,2} = [O_t^{(x)}, O_t^{(y)}]$ and $\pi_{t,2}^* = [\pi_{t,n}^{(x)}, \pi_{t,n}^{(y)}]^T$ is a feasible strategy for problem (5.9) with $n = 2$. We show that it is an optimal pair by contradiction.

If there is a feasible solution $\hat{O}_{t,n} = [\hat{O}_t^{(1)}, \hat{O}_t^{(2)}]$ and $\hat{\pi}_{t,2}^* = [\hat{\pi}_{t,2}^{(1)}, \hat{\pi}_{t,2}^{(2)}]^T$ such that $\|\hat{\pi}_{t,2}^*\|_1 < \|\pi_{t,2}^*\|_1$, then $\hat{\pi}_{t,n}^* = [\hat{\pi}_{t,2}^{(1)}, \hat{\pi}_{t,2}^{(2)}, 0, \dots, 0]^T$ is a feasible strategy for (5.9) such that $\|\hat{\pi}_{t,n}^*\|_1 < \|\pi_{t,n}^*\|_1$, which is contradiction to our previous conclusion. Note that $\|\pi_{t,2}^*\|_1 = \|\pi_{t,n}^*\|_1$, so problem (5.9) with $n = 2$ and with $n \geq 2$ have the same minimum ℓ_1 norm of allocation.

5.6.3 Proof of Proposition 5.3.1

Let $O_t \in \Omega_O^{(2,1)}$ with non-singular variance matrix Σ_t (see Equation (5.11)), the optimal strategy space Ω_{π}^O contains a unique strategy, i.e. $\pi_t = (\Sigma_t^T)^{-1} \eta_t^*$, and ℓ_1 norm of π_t is given by

$$\|\pi_t\|_1 = \left| \frac{\eta_t^{(1)}}{f_t^{(1)}} \right| + \left| \frac{\eta_t^{(2)}}{f_t^{(2)}} \right|. \quad (5.35)$$

A non-zero denominator is guaranteed by the non-singular variance matrix assumption. $O_t^* = [O_t^{(1)*}, O_t^{(2)*}]^T \in \Omega_O^{(2,1)}$ with variance matrix

$$\Sigma_t^* = \begin{bmatrix} f_t^{(1)*} & 0 \\ 0 & f_t^{(2)*} \end{bmatrix}. \quad (5.36)$$

For $O_t \in \Omega_O^{(2,1)}$, if $|f_t^{(1)}| \leq |f_t^{(1)*}|$ and $|f_t^{(2)}| \leq |f_t^{(2)*}|$ hold, then it is easy to see $\|\pi_t\|_1 \geq \|\pi_t^*\|_1$, so O_t^* is a optimal portfolio composition.

If $|f_t^{(1)}| \leq |f_t^{(1)*}|$ or $|f_t^{(2)}| \leq |f_t^{(2)*}|$ does not hold, then there is a $O_t^{**} \in \Omega_O^{(2,1)}$, such that the corresponding strategy $\|\pi_t^{**}\|_1 < \|\pi_t^*\|_1$, hence O_t^* is not the optimal.

We have shown that, for any $O_t \in \Omega_O^{(2,1)}$, $|f_t^{(1)}| \leq |f_t^{(1)*}|$ and $|f_t^{(2)}| \leq |f_t^{(2)*}|$ is a sufficient and necessary condition for O_t^* to be an optimal portfolio composition for problem (5.10). Therefore,

$$O_t^{(i)*} = \arg \max_{O_t^{(i)}} \left| \frac{dO_t^{(i)}}{dS_t^{(i)}} \frac{1}{O_t^{(i)}} \right|. \quad (5.37)$$

5.6.4 Proof of Proposition 5.3.2

$O_t^* = [O_t^{(1)*}, O_t^{(2)*}]^T$ is the optimal portfolio composition for problem (5.10) if and only if it has the largest absolute sensitivity (see Proposition 5.3.1), i.e.

$$O_t^{(i)*} = \arg \max_{O_t^{(i)}} \left| \frac{dO_t^{(i,j)}}{dS_t^{(i)}} \frac{1}{O_t^{(i,j)}} \right|. \quad (5.38)$$

For convenience, we write the absolute sensitivity as a function of strike price $KK^{(i,j)}$.

$$h(K^{(i,j)}, j) = \left| \frac{dO_t^{(i,j)}}{dS_t^{(i)}} \frac{1}{O_t^{(i,j)}} \right|$$

$h(K^{(i,j)}, j)$ is continuous because $O_t^{(i,j)} \in \mathbb{C}^1$ and $O_t^{(i,j)} \neq 0$. According to the extreme value theorem, there is a $\hat{K}^{(i,j)} \in [A^{(i,j)}, B^{(i,j)}]$ that achieves the largest $h(K^{(i,j)}, j)$, hence minimizes ℓ_1 norm of allocation $\|\pi_t^*\|_1$. $O_t^{(i)*}$ is the optimal for problem (5.10) when the strike price $K^{(i,j)}$ is one of the $\hat{K}^{(i,j)}$ where:

$j \in \{\text{Euro Call, Asian Call, Amer Call, Euro Put, Asian Put, Amer Put}\}$

This guarantees the existence of optimal composition in $\Omega_O^{(2, \text{put call})}$.

5.6.5 Proof of Corollary 5.3.3

We first prove the following lemma,

Lemma 5.6.1 *The inequality*

$$\frac{\phi(x-c)}{N(x-c)} - c \leq \frac{\phi(x)}{N(x)} \quad (5.39)$$

holds for $\forall x \in (-\infty, \infty), c \in (0, \infty)$, where ϕ and N are respectively the density function and distribution function of a standard normal random variable.

Proof Let us define the "reversed hazard rate" function:

$$Y(x) = \frac{\phi(x)}{N(x)}.$$

We want to show

$$Y(x-c) - c \leq Y(x).$$

We first demonstrate $Y'(x) \geq -1$ for all x . To see this, note:

$$Y' + 1 = \frac{\phi}{N^2} \left(\frac{\phi'}{\phi} N - \phi + \frac{N^2}{\phi} \right) = \frac{\phi}{N^2} f.$$

Using $\phi' = -x\phi$, we have $f' = \left(1 + \frac{xN}{\phi}\right)N$. It is not difficult to see that $x + Y \geq 0$ (use the fact that $g = (x+Y)N \rightarrow 0$ as $x \rightarrow -\infty$ and $g' = N \geq 0$). Hence we know $\left(1 + \frac{xN}{\phi}\right) \geq 0$, which implies $f' \geq 0$. Moreover $f(x) \geq \lim_{x \rightarrow -\infty} f(x) = 0$, therefore $Y' + 1 \geq 0$.

Now we complete the proof, using $Y' \geq -1$ for all x , and the mean value theorem, we conclude "by contradiction" that

$$\frac{Y(x) - Y(x-c)}{c} \geq -1$$

for all x and c , which implies

$$Y(x) \geq Y(x-c) - c.$$

Next, we show that absolute value of optimal allocation on an European call decreases to 0 as $K^{(i, \text{Euro Call})} \rightarrow \infty$ and absolute value of allocation on an European put increases with $K^{(i, \text{Euro Put})}$ and converges to 0 as $K^{(i, \text{Euro Put})} \rightarrow 0$. We first abbreviate $K^{(i, \text{Euro Call})}$ to K . Equation (5.12) and (5.15) shows the sensitivity of an European call,

$$\frac{\partial O_t^{(i, \text{Euro Call})}}{\partial S_t^{(i)}} \frac{1}{O_t^{(i, \text{Euro Call})}} \sigma^{(i)} S_t^{(i)} = \frac{N(d_1) \sigma^{(i)} S_t^{(i)}}{S_t^{(i)} N(d_1) - K e^{-r(\hat{T}-t)} N(d_2)} = \frac{\sigma^{(i)}}{1 - e^{-r(\hat{T}-t)} \frac{K}{S_t^{(i)}} \frac{N(d_2)}{N(d_1)}},$$

where

$$d_1 = \frac{\ln(S_t^{(i)}/K) + (r + \frac{1}{2}(\sigma^{(i)})^2)(\hat{T} - t)}{\sigma^{(i)} \sqrt{\hat{T} - t}} = a \left(\ln(S_t^{(i)}/K) + r(\hat{T} - t) \right) + b \quad (5.40)$$

$$d_2 = d_1 - \sigma^{(i)} \sqrt{\hat{T} - t} = a \left(\ln(S_t^{(i)}/K) + r(\hat{T} - t) \right) + b - c \quad (5.41)$$

with $c = \sigma^{(i)} \sqrt{\hat{T} - t} > 0$, $b = \frac{1}{2}c$ and $a = \frac{1}{c}$. Let us rewrite the sensitivity as follows:

$$\frac{\partial O_t^{(i, Euro Call)}}{\partial S_t^{(i)}} \frac{1}{O_t^{(i, Euro Call)}} \sigma^{(i)} S_t^{(i)} = \frac{\sigma^{(i)}}{1 - e^{\frac{b-x}{a}} G(x)}$$

where $x = a(\ln(S_t/K) + r(\hat{T} - t)) + b$ and $G(x) = \frac{N(d_2)}{N(d_1)} = \frac{N(x-c)}{N(x)}$.

We would like to show $H(x) = e^{\frac{b-x}{a}} G(x)$ is increasing in K , hence decreasing in x . Its first derivative leads to:

$$\begin{aligned} H'(x) &= -\frac{e^{\frac{b-x}{a}}}{a} G(x) + e^{\frac{b-x}{a}} G'(x) = -\frac{e^{\frac{b-x}{a}}}{a} \frac{N(x-c)}{N(x)} + e^{\frac{b-x}{a}} \frac{n(x-c)N(x) - N(x-c)n(x)}{N^2(x)} \\ &= -\frac{e^{\frac{b-x}{a}}}{a} \frac{N(x-c)}{N(x)} + e^{\frac{b-x}{a}} \left(\frac{n(x-c)}{N(x-c)} - \frac{n(x)}{N(x)} \right) \frac{N(x-c)}{N(x)} \\ &= e^{\frac{b-x}{a}} \left[-\frac{1}{a} + \left(\frac{n(x-c)}{N(x-c)} - \frac{n(x)}{N(x)} \right) \right] \frac{N(x-c)}{N(x)} \\ &= e^{\frac{b-x}{a}} \left[-c + \left(\frac{n(x-c)}{N(x-c)} - \frac{n(x)}{N(x)} \right) \right] \frac{N(x-c)}{N(x)} \end{aligned}$$

It's easy to see $H'(x) < 0$ with Lemma 5.6.1. The sensitivity of an European call is positive and increases with K .

As $K \rightarrow \infty$, $O_t^{(i, Euro call)} \rightarrow 0$, so $Ke^{-r(\hat{T}-t)}N(d_2) \rightarrow 0$. Furthermore,

$$\begin{aligned} H(x) &= \frac{Ke^{-r(\hat{T}-t)}N(d_2)}{S_t^{(i)}N(d_1)} \xrightarrow{\text{L'Hôpital's rule}} \frac{e^{-r(\hat{T}-t)}N(d_2) - \phi(d_1) \frac{S_t^{(i)}}{K\sigma^{(i)}\sqrt{\hat{T}-t}}}{-\frac{S_t^{(i)}\phi(d_1)}{K\sigma^{(i)}\sqrt{\hat{T}-t}}} \\ &\xrightarrow{\text{L'Hôpital's rule}} \frac{-\phi(d_1) \frac{S_t^{(i)}}{(K)^2\sigma^{(i)}\sqrt{\hat{T}-t}} - \phi(d_1) \frac{d_1 S_t^{(i)}}{(K\sigma^{(i)}\sqrt{\hat{T}-t})^2} + \frac{\phi(d_1)S_t^{(i)}}{(K)^2\sigma^{(i)}\sqrt{\hat{T}-t}}}{-\phi(d_1) \frac{S_t^{(i)}d_1}{(K\sigma^{(i)}\sqrt{\hat{T}-t})^2} + \frac{S_t^{(i)}\phi(d_1)}{(K)^2\sigma^{(i)}\sqrt{\hat{T}-t}}} \\ &= \frac{-S_t^{(i)}\sigma^{(i)}\sqrt{\hat{T}-t} - S_t^{(i)}d_1 + S_t^{(i)}\sigma^{(i)}\sqrt{\hat{T}-t}}{-S_t^{(i)}d_1 + S_t^{(i)}\sigma^{(i)}\sqrt{\hat{T}-t}} \rightarrow 1. \end{aligned}$$

Hence,

$$\frac{\partial O_t^{(i, Euro Call)}}{\partial S_t^{(i)}} \frac{1}{O_t^{(i, Euro Call)}} \sigma^{(i)} S_t^{(i)} = \frac{\sigma^{(i)}}{1 - H(x)} \rightarrow \infty.$$

Moreover, the absolute value of allocation on $O_t^{(i, Euro Call)}$ is decreasing with K and

$$\left| \pi_t^{(i, Euro Call)} \right| = \frac{\left| \eta_t^{(i)} \right|}{\left| \frac{\partial O_t^{(i, Euro Call)}}{\partial S_t^{(i)}} \frac{1}{O_t^{(i, Euro Call)}} \sigma^{(i)} S_t^{(i)} \right|} \rightarrow 0 \quad \text{as } K \rightarrow \infty. \quad (5.42)$$

The proof for European put follows similarly.

5.6.6 Proof of Proposition 5.3.4

Suppose for any $O_t \in \Omega_O^{(2, \text{straddle})}$, $O_t^{(i,j)}$ satisfies these four conditions:

1. $\frac{\partial O_t^{(i,j)}}{\partial S_t^{(i)}} = 0 \iff K^{(i,j)} = A^{(i,j)}$.
2. $\left| \frac{\partial O_t^{(i,j)}}{\partial S_t^{(i)}} \right|$ has an upper bound.
3. $O_t^{(i,j)} \in (0, \infty)$ and $O_t^{(i,j)} \rightarrow \infty$ as $K^{(i,j)} \rightarrow \infty$, where $j \in \{\text{Euro Strad}, \text{Asian Strad}\}$.
4. $O_t^{(i,j)}(S^{(i)}, K^{(i,j)}) \in \mathbb{C}^1$.

All four assumptions are not restrictive in a Black-Scholes setting. Proposition 5.3.1 illustrates that $O_t^* = [O_t^{(1),*}, O_t^{(2),*}]^T$ is the optimal portfolio composition for problem (5.10) if it has the largest absolute sensitivity, i.e.

$$O_t^{(i),*} = \arg \max_{O_t^{(i,j)}} \left| \frac{dO_t^{(i,j)}}{dS_t^{(i)}} \frac{1}{O_t^{(i,j)}} \right|. \quad (5.43)$$

For convenience, we write the absolute sensitivity as a function of strike price $K^{(i,j)}$:

$$h(K^{(i,j)}, j) = \left| \frac{dO_t^{(i,j)}}{dS_t^{(i)}} \frac{1}{O_t^{(i,j)}} \right|.$$

With the four assumptions above, it's easy to see,

$$\begin{cases} h(0, j) \in (0, \infty) & j \in \{\text{Euro Strad}, \text{Asian Strad}, \text{Amer Strad}\} \\ h(B^{(i, \text{Amer Strad})}, \text{Amer Strad}) \in (0, \infty) \\ h(K^{(i,j)}, j) \rightarrow 0 & \text{as } K^{(i,j)} \uparrow \downarrow A^{(i,j)}, j \in \{\text{Euro Strad}, \text{Asian Strad}, \text{Amer Strad}\} \\ h(K^{(i,j)}, j) \rightarrow 0 & \text{as } K^{(i,j)} \rightarrow \infty, j \in \{\text{Euro}, \text{Asian}\}. \end{cases} \quad (5.44)$$

When $K^{(i,j)} \in [0, A^{(i,j)})$ and $j \in \{\text{Euro Strad}, \text{Asian Strad}, \text{Amer Strad}\}$, $h(K^{(i,j)}, j)$ is continuous because

$O_t^{(i,j)}(S^{(i)}, K^{(i,j)}) \in \mathbb{C}^1$. Besides, there is a Z such that $h(K^{(i,j)}, j) < h(0, j)$ when $K^{(i,j)} \in (Z, A^{(i,j)})$.

According to the extreme value theorem, there is a $K^{(l,i,j)}$ such that h attains the maximum in $[0, Z]$, hence $h(K^{(l,i,j)}, j) \geq h(0, j)$. $K^{(l,i,j)}$ is proven to be the maximum point for $h(K^{(i,j)}, j)$ in $[0, A^{(i,j)})$.

Let M be a real number in $(A^{(i,j)}, \infty)$ where $j \in \{\text{Euro Strad}, \text{Asian Strad}\}$, it's obvious that $h(M, j) > 0$. There is a $Z > 0$ such that $h(K^{(i,j)}, j) < h(M, j)$ when $K^{(i,j)} \in (A^{(i,j)}, A^{(i,j)} + \frac{1}{Z}) \cup (Z, \infty)$. According to the extreme value theorem, there is a $K^{(r,i,j)}$ such that h attains the maximum in $[A^{(i,j)} + \frac{1}{Z}, Z]$, i.e. $h(K^{(r,i,j)}, j) > h(M, j)$. Then, $K^{(r,i,j)}$ is the maximum point for $h(K^{(i,j)}, j)$ in $(A^{(i,j)}, \infty)$.

As for American straddle ($j = \text{Amer Strad}$), $h(B^{(i,j)}, j) > 0$. There is a $Z > 0$ such that $h(K^{(i,j)}, j) < h(B^{(i,j)}, j)$ when $K^{(i,j)} \in (A^{(i,j)}, A^{(i,j)} + \frac{1}{Z})$. And there is a $K^{(r,i,j)}$ such that h attains the maximum in $[A^{(i,j)} + \frac{1}{Z}, B^{(i,j)}]$, hence $h(K^{(r,i,j)}, j) \geq h(B^{(i,j)}, j)$. $h(K^{(r,i,j)}, j)$ is the maximum point on the right branch $[A^{(i,j)}, B^{(i,j)}]$. $O_t^{(i),*}$ is the optimal for the problem (5.10) when the strike price K is either $K^{(l,i,j)}$ or $K^{(r,i,j)}$ where $j \in \{\text{Euro Strad}, \text{Asian Strad}, \text{Amer Strad}\}$. The existence of the optimal composition in a straddle subset is proven.

5.6.7 Proof of Proposition 5.4.1

Let $O_t \in \Omega_O^{(2, multi\ asset)}$ with non-singular variance matrix Σ_t (see Equation (5.23)), the optimal strategy space Ω_π^O contains a unique strategy, i.e. $\pi_t = (\Sigma_t^T)^{-1} \eta_t^*$. The allocation and its ℓ_1 norm can be written as

$$\begin{aligned} \pi^{(1,j)} &= \frac{1}{f_t^{(11)}} (\eta_t^{(1)} - \frac{f_t^{(21)}}{f_t^{(22)}} \eta_t^{(2)}) & \pi^{(2,j)} &= \frac{\eta_t^{(2)}}{f_t^{(22)}} \\ \|\pi_t\|_1 &= \frac{1}{|f_t^{(11)}|} \left| \eta_t^{(1)} - \frac{f_t^{(21)}}{f_t^{(22)}} \eta_t^{(2)} \right| + \frac{|\eta_t^{(2)}|}{|f_t^{(22)}|}. \end{aligned} \quad (5.45)$$

If $O_t^* = [O_t^{(1),*}, O_t^{(2),*}]^T \in \Omega_O^{(2, multi\ asset)}$ achieves minimum ℓ_1 norm of allocation and

$$O_t^{(1),*} \neq \arg \max_{O_t^{(1,j_1)}} \left| \frac{dO_t^{(1,j_1)}}{dS_t^{(1)}} \frac{1}{O_t^{(1,j_1)}} \right|. \quad (5.46)$$

Then there is a $O_t^{**} = [O_t^{(1),**}, O_t^{(2),**}]^T$, such that

$$\left| \frac{dO_t^{(1),*}}{dS_t^{(1)}} \frac{1}{O_t^{(1),*}} \right| < \left| \frac{dO_t^{(1),**}}{dS_t^{(1)}} \frac{1}{O_t^{(1),**}} \right|. \quad (5.47)$$

Therefore, let $O_t^{(2),**} = O_t^{(2),*}$, this implies $|f_t^{(11),*}| < |f_t^{(11),**}|$, $f_t^{(21),*} = f_t^{(21),**}$ and $f_t^{(22),*} = f_t^{(22),**}$. Equation (5.45) indicates $\|\pi_t^*\|_1 > \|\pi_t^{**}\|_1$, which proves by contradiction that

$$O_t^{(1),*} = \arg \max_{O_t^{(1,j_1)}} \left| \frac{dO_t^{(1,j_1)}}{dS_t^{(1)}} \frac{1}{O_t^{(1,j_1)}} \right|. \quad (5.48)$$

is a necessary condition for O_t^* to be the optimal portfolio composition for problem (5.10) within $\Omega_O^{(2, multi\ asset)}$.

5.6.8 Proof of Proposition 5.4.2

Recall $f_t^{(ik)}$ in the variance matrix Σ_t can be written as

$$f_t^{(ik)} = \frac{\partial O_t^{(i,j_i)}}{\partial S_t^{(k)}} S_t^{(k)} \sigma^{(k)}. \quad (5.49)$$

According to the non-singular variance matrix assumption, $f_t^{(11)}, f_t^{(22)} \neq 0$. In addition, $O_t^{(1,j_1)}$ is an European call option, hence $f_t^{(11)}$ is continuous with respect to $K^{(1, Euro\ Call)}$ on $[A^{(1, Euro\ Call)}, B^{(1, Euro\ Call)}]$, $f_t^{(21)}$ and $f_t^{(22)}$ are continuous with respect to $K^{(2,j_2)}$ on $[A^{(2,j_2)}, B^{(2,j_2)}]$ because $O_t^{(2,j_2)} \in \mathbb{C}^1$. $\|\pi_t\|_1$ (see Equation (5.45)) is continuous on the closed set $[A^{(1, Euro\ Call)}, B^{(1, Euro\ Call)}] \times [A^{(2,j_2)}, B^{(2,j_2)}]$, so there is a portfolio with strike price $[\hat{K}^{(1, Euro\ Call)}, \hat{K}^{(2,j_2)}]^T$ that achieves minimum risky asset exposure with any j_2 . O_t^* is the optimal for problem (5.10) within $\Omega_O^{(2, call\ basket)}$ when the strike price is in $[\hat{K}^{(1, Euro\ Call)}, \hat{K}^{(2,j_2)}]^T$, where $j_2 \in \{Basket\ Call, Basket\ Put\}$.

5.6.9 Comparison between the one-asset option and multi-asset option subsets

In this section, we exhibit the optimal choice of $O_t^{(2,j_2)}$ given different set of parameters. In contrast to the two positive correlated underlying assets considered in Section 5.4, i.e. $\rho = 0.4$ (see Table 5.1), we let correlation $\rho = -0.4$ while all other parameters remain unchanged, here a similar derivatives selection is conducted.

Results are presented in Figure 5.7. Unlike the case of two positive correlated underlying assets (see Figure 5.6), one-asset option is no longer preferable in minimizing risky asset exposure while basket put becomes competitive. Especially when $O_t^{(1,j_1)}$ is an at-the-money European call, i.e. $K^{(1,j_1)} = 40$, a basket put is superior to other options, i.e. larger area.

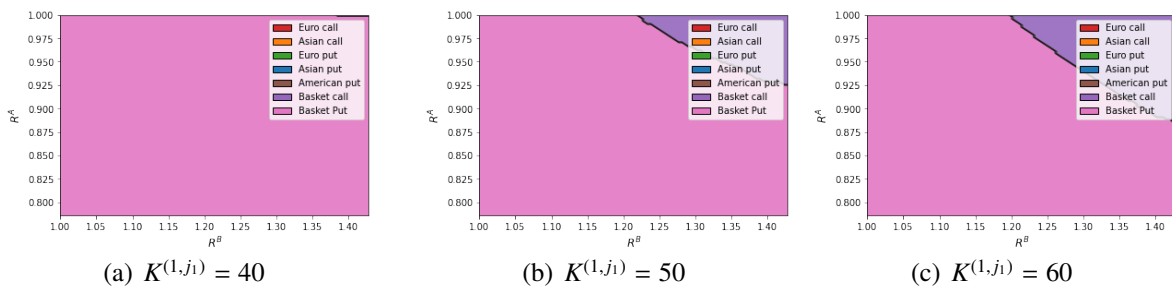


Figure 5.7: Derivatives selection $O_t^{(2,j_2)}$ ($\rho = -0.4$)

Next, we consider the case when the parameters of the two underlying assets are exchanged, i.e. $\lambda^{(1)} = 0.6$, $\lambda^{(2)} = 0.52$, $\sigma^{(1)} = 0.2$, $\sigma^{(2)} = 0.13$ while all other parameters are given in Table 5.1, the optimal choice of $O_t^{(2,j_2)}$ is shown in Figure 5.8. Compared with Figure 5.6, basket put instead of basket call is selected in the largest region. Furthermore, the one-asset Asian option is preferable when $K^{(1,j_1)}$ is regardless of the underlying assets' parameters.

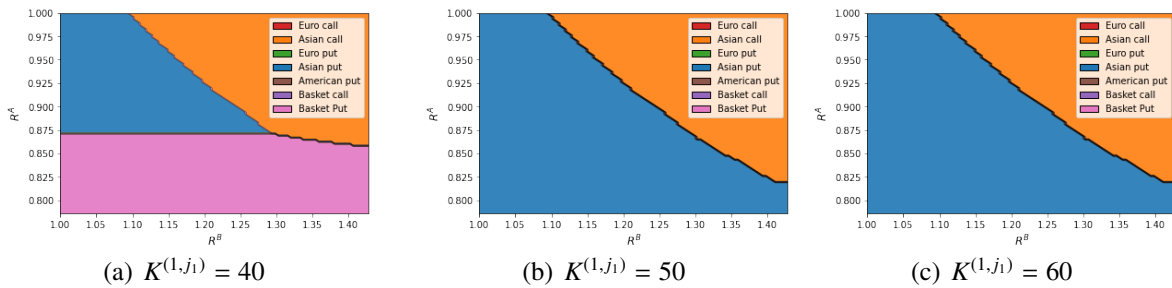


Figure 5.8: Derivatives selection $O_t^{(2,j_2)}$ (exchange assets' parameter)

Chapter 6

Optimal market completion through financial derivatives with applications to volatility risk

Chapter summary:

This chapter investigates the optimal choices of financial derivatives to complete a financial market in the framework of stochastic volatility (SV) models. We introduce an efficient and accurate simulation-based method, applicable to generalized diffusion models, to approximate the optimal derivatives-based portfolio strategy. We build upon the double optimization approach (i.e. expected utility maximization and risk exposure minimization) proposed in the chapter 5; demonstrating that strangle options are the best choices for market completion within equity options. Furthermore, we explore the benefit of using volatility index derivatives and conclude that they could be more convenient substitutes when only long-term maturity equity options are available.

Status: Submitted to *Quantitative Finance*.

6.1 Introduction

Financial markets are often modelled as a system of contingents on states mirroring the real-world economy. This generates a concept widely used in economic and finance literature, namely the complete market, which is simply described as ‘a market for every good’. Earlier studies assumed that the number of securities equals the number of states of nature and investigated the optimal allocation, placing all of the capital at once (see [2], [3]). Recognizing that investors benefit from adjusting allocation with a change of market status, more recent researchers have focused on the idea of a dynamically complete market, which is defined as a market wherein any contingent claim can be replicated by a self-financing strategy.

The study of portfolio choice in a dynamically complete market under a continuous-time framework can be traced back to the seminal work of [76], who computed the optimal allocation and consumption policy with a dynamic programming technique, assuming that the stock price follows a geometric Brownian motion (GBM). In this framework, the uncertainty is reflected in the Brownian motion, which captures the randomness of a stock’s return; hence,

investors can achieve the best portfolio performance with investments only on the stock and a cash account.

However, the financial market is ever evolving, and becoming increasingly complex; for instance, substantial evidence suggests that a single Brownian motion or source of randomness is insufficient to explain the movements of a single stock or index. Researchers have had to incorporate so-called stylized facts such as stochastic volatility (SV) or stochastic interest rates in their modelling to mimic this new reality. These stylized facts are captured via adding new ‘state variables’ (e.g. a new random processes for SV). These state variables have been recognized as important factors in the portfolio allocation process.

The importance of adding financial derivatives into a portfolio for market completion was demonstrated in [71], confirming that investors can improve portfolio performance when adding as many linearly independent equity options as new state variables in the portfolio composition. They do this to hedge the risk of the new state variables, thereby achieving significant improvement in portfolio performance compared to incomplete market investment (e.g. investing solely on stock and cash account). This work was extended in many directions. For example, [34] constructed an optimal portfolios with the addition of options to hedge new state variables accounting for stochastic correlation. Moreover, [62] solved derivative-based strategies under an asset–liability management (ALM) framework with the mean–variance criterion. In a similar setting, the optimal complete and incomplete strategies for the 4/2 SV model were derived in [18], which demonstrated the superiority of the complete market portfolio.

Although the literature cited above strongly supports the addition of derivatives to complete the market, investors may complete market in many ways due to the variety of derivatives in the market. Therefore, investors effectively have a non-unique solution to the problem (i.e. an infinite number of strategies, each linked to a choice of derivative, producing the same maximum expected utility). The problem of infinitely many solutions and the optimal choice of derivatives was studied in the recent paper [36] in the context of the Black—Scholes—Merton model. The paper proposed an optimization criterion (i.e. additional to the maximization of the utility, namely risk exposure minimization) to produce a unique, meaningful solution, thus deriving a practical derivative selection methodology for investors. The risk exposure minimization criterion can be motivated from many angles, especially in terms of regulatory constraints intended to control investors’ exposure to risky assets and hence to protect investors’ capital in the event of a market crash. In this chapter, we follow the same derivatives selection framework and explore the optimal product for market completion in the popular setting of SV models, with emphasis on the celebrated Heston model (see [48]).

There are two major hurdles for our derivatives-based portfolio allocation problem. First, given the complexity of advanced models with many state variables jeopardizes the solvability of the utility maximization allocation problem, closed-form solutions are often unavailable. This hurdle can be overcome using approximation methods for dynamic portfolio choice problems. [10], inspired by the least-squares Monte Carlo method (see [72]), recursively estimated the value function and optimal allocation following a dynamic programming principle. This method was later named the BGSS and [24] utilized the stochastic grid bundling method for conditional expectation estimation, introduced in [53], further enhancing the accuracy of BGSS. Additionally, [91] targeted unsolvable continuous-time models, proposing an efficient and accurate simulation-based method, namely the polynomial affine method for constant relative risk aversion utility (PAMC). The second hurdle appears in the complexity of derivatives’

price dynamics which, in contrast to traditional asset classes, could lead to highly non-linear stochastic differential equations. In this chapter, we overcome the two hurdles simultaneously by unifying the PAMC and an options' Greek approximation technique. Notably, the broad applicability of this methodology laid the foundation for the derivatives selection study within a generalized model family.

As mentioned above, our focus is on investors who are particularly concerned about volatility risk and seek the best derivatives to attain market completion. The seminal paper by [48] recognized the mean-reverting pattern of volatilities and introduced the well-known Heston (GBM 1/2) model. Later, extensions, such as the GBM 3/2 (see [49]) and GBM 4/2 (see [45]), were developed to better capture the volatility surface. These lead to notable successes in the valuation of European equity options, and semi-closed-form solutions for the option price and Greeks are generally accessible using Fourier transformation. Popular equity options, such as call, put, straddle and strangle options, are ideal products for investors to manage the volatility risk. Furthermore, the volatility index (VIX), a measure of the stock market's volatility based on S&P 500 index options provided by the Chicago Board Options Exchange (CBOE), affords investors an alternative way to assess the volatility risk. The effectiveness of VIX products in the portfolio performance enhancement has been confirmed in the literature: see [31], [15] and [87]. Hence, in this chapter we compare two categories of derivatives, namely equity options and VIX options in terms of optimal dynamic completion.

The contributions of the chapter are as follows:

1. The multitude of financial derivatives available in the market offers investors non-unique optimal choice in terms of expected utility theory (EUT) maximization. Hence we extend the additional optimization criterion proposed in [36], namely risk exposure minimization, from the family of GBM to SV models. This aids investors with practical derivative selection in a popular stock markets modeling setting.
2. The PAMC-indirect numerical method is proposed to approximate the optimal allocation for a constant relative risk aversion (CRRA) investor investing in the derivatives market. The superior accuracy and efficiency of the methodology are verified on the Heston model.
3. Targeting equity and volatility risk, we first consider the optimal choice among equity options (e.g. calls, puts, straddles and strangles). We demonstrate that strangles are the best options for minimizing risk exposure.
4. We also investigate the usage of financial derivatives on the VIX as a means of completing the market, and we conclude that investors would prefer VIX options to equity strangles when only long-term maturity options are available.

The remainder of this chapter is organized as follows: Section 6.2 presents the investor's problem (i.e. the two criteria for optimal allocation [utility maximization] and optimal market completion [risk exposure minimization]). Section 6.3 details an efficient approximation method for derivatives-based portfolio allocation. The optimal market completion targeting volatility risk within an equity option and a VIX option is studied in Section 6.4, followed by the conclusion in Section 6.5. Section 6.6 presents the mathematical proofs, while Section 6.7 provides

an alternative approximation method and a numerical examination of accuracy and efficiency for the two methods.

6.2 Investor's problem

In this section, we introduce a market completion framework using financial derivatives. We define a complete probability space $(\Omega, \mathcal{F}, \mathbb{P})$ with a right-continuous filtration $\{\mathcal{F}_t\}_{t \in [0, T]}$. The market is frictionless (i.e. no transaction cost and market impact), and a risk-free cash account M_t , a stock S_t and an investor with constant relative risk aversion (CRRA) utility, $U(W) = \frac{W^{1-\gamma}}{1-\gamma}$ exist. The market dynamics are summarized as follows:

$$\begin{cases} \frac{dM_t}{M_t} = r dt \\ \frac{dS_t}{S_t} = (r + \lambda^S \sigma^S) dt + \sigma^S dB_t^S \\ dH_t = \mu^H dt + \sigma^H dB_t^H \\ \langle dB_t^S, dB_t^H \rangle = \rho_{SH} dt. \end{cases} \quad (6.1)$$

where B_t^H and B_t^S are Brownian motions with correlation $\rho_{SH} \in (-1, 1)$, and the interest rate r is constant. State variable H_t follows a generalized diffusion process, where $\mu^H = \mu^H(t, H_t)$ denotes the drift and $\sigma^H = \sigma^H(t, H_t)$ denotes volatility. The market price of risk and the volatility of stock could be functions of both the stock price and the state variable, respectively; that is $\lambda^S = \lambda^S(t, H_t, \ln S_t)$ and $\sigma^S = \sigma^S(t, H_t, \ln S_t)$.

In this market, the number of investable risky assets is less than the number of risk drivers, hence market incompleteness. To eliminate the welfare loss resulting from the unhedgeable risk drivers, we introduce a set of financial derivatives:

$$\Omega_O^{(n)} = \left\{ \bar{O}_t = [O_t^{(1)}, O_t^{(2)}, \dots, O_t^{(n)}]^T \mid O_t^{(i)} \neq 0, i = 1, \dots, n \text{ and } \text{rank}(\Sigma_t) = 2, t \in [0, T] \right\}.$$

We assume that an investor allocates in an element of Ω_O ; that is, a specific $\bar{O}_t = [O_t^{(1)}, O_t^{(2)}, \dots, O_t^{(n)}]^T$ ($n \geq 2$). Note that by arbitrage arguments, the dynamics of the extended market are as follows:

$$\begin{cases} \frac{dM_t}{M_t} = r dt \\ d\bar{O}_t = \text{diag}(\bar{O}_t) [(r \cdot \mathbb{1} + \Sigma_t \Lambda) dt + \Sigma_t dB_t] \\ dH_t = \mu^H dt + \sigma^H dB_t^H \\ \langle dB_t^S, dB_t^H \rangle = \rho_{SH} dt, \end{cases} \quad (6.2)$$

where $B_t = [B_t^S, B_t^H]^T$ and Σ_t represents the $n \times 2$ variance matrix of \bar{O}_t ; the first column ($i, 1$) represents the sensitivity of $O_t^{(i)}$ to the underlying asset S_t (i.e. $\frac{\partial O_t^{(i)}}{\partial S_t} S_t \frac{1}{O_t^{(i)}} \sigma^S$); and the second column ($i, 2$) represents the sensitivity of $O_t^{(i)}$ to the state variable H_t (i.e. $\frac{\partial O_t^{(i)}}{\partial H_t} \frac{1}{O_t^{(i)}} \sigma^H$). $\Lambda = [\lambda^S, \lambda^H]^T$, where $\lambda^H = \lambda^H(t, H_t, \ln S_t)$ denotes the market price of volatility risk. Rank 2 variance matrix Σ_t guarantees the completeness of the market. For simplicity, we also assume that the derivatives in $\Omega_O^{(n)}$ will be rolled over, always maintaining the same time to maturity and a non-zero value. Note that the investor is not prohibited from trading on the stock, which is included in $\Omega_O^{(n)}$ as a special derivative.

Let $\Omega_\pi^{(O)}$ denote the space of admissible strategies satisfying the standard conditions, where the element $\pi_t = [\pi_t^{(1)}, \pi_t^{(2)}, \dots, \pi_t^{(n)}]^T$ represents the proportions of the investor's wealth in the derivatives $\bar{O}_t = [O_t^{(1)}, O_t^{(2)}, \dots, O_t^{(n)}]^T$, with the remaining $1 - \mathbb{1}^T \pi_t$ invested in the cash account M_t . The investor's wealth process W_t satisfies

$$\frac{dW_t}{W_t} = (r + \pi_t^T \Sigma_t \Lambda) dt + \pi_t^T \Sigma_t dB_t. \quad (6.3)$$

The investor's objective is to maximize the expected utility of their wealth at terminal T ; hence, their problem at time $t \in [0, T]$ can be written as

$$V(t, W, H, \ln S) = \max_{\pi_{s \geq t} \in \Omega_\pi^{(O)}} \mathbb{E}(U(W_T) | \mathcal{F}_t). \quad (6.4)$$

The associated Hamilton-Jacobi-Bellman (HJB) equation for the value function V follows the principles of stochastic control and is given by

$$\begin{aligned} \sup_{\pi_t} \left\{ V_t + W_t V_W (r + \pi_t^T \Sigma_t \Lambda) + \frac{1}{2} W_t^2 V_{WW} (\pi_t^T \Sigma_t \Phi \Phi^T \Sigma_t^T \pi_t) + W_t V_{WH} \sigma^H (\pi_t^T \Sigma_t A) + W_t V_{W \ln S} \sigma^S (\pi_t^T \Sigma_t B) \right\} \\ + V_H \mu^H + \frac{1}{2} V_{HH} (\sigma^H)^2 + V_{\ln S} (r + \lambda^S \sigma^S) + \frac{1}{2} V_{\ln S \ln S} (\sigma^S)^2 + V_{H \ln S} \sigma^H \sigma^S \rho_{SH} = 0, \end{aligned} \quad (6.5)$$

where $\Phi = \begin{bmatrix} 1 & 0 \\ \rho_{SH} & \sqrt{1 - \rho_{SH}^2} \end{bmatrix}$, $A = [\rho_{SH}, 1]^T$ and $B = [1, \rho_{SH}]^T$.

Next, we define a new artificial market, which consists of three assets: a risk-free money account M_t and two pure factor assets $S_t^{(S)}$ and $S_t^{(H)}$:

$$\begin{cases} \frac{dM_t}{M_t} = r dt \\ \frac{dS_t^{(S)}}{S_t^{(S)}} = (r + \lambda^S) dt + dB_t^S \\ \frac{dS_t^{(H)}}{S_t^{(H)}} = (r + \lambda^H) dt + dB_t^H \\ dH_t = \mu^H dt + \sigma^H dB_t^H \\ \langle dB_t^S, dB_t^H \rangle = \rho_{SH} dt \end{cases} \quad (6.6)$$

Compared to the original market, the market state variable is still H_t ; nonetheless, here the investor can put their money in the hypothetical pure factor assets $S_t^{(S)}$ and $S_t^{(H)}$, which have a unit exposure on B_t^S and B_t^H , respectively. Let $\eta_t = [\eta_t^{(1)}, \eta_t^{(2)}]^T$ be the allocation on the pure factors (also known as exposures in the literature: see [71]); \hat{W}_t denotes the investor's wealth process, and $\hat{V}(t, \hat{W}, H, \ln S)$ represents the value function in the artificial market. Similarly, the associated HJB equation is given by

$$\begin{aligned} \sup_{\eta_t} \left\{ \hat{V}_t + \hat{W}_t \hat{V}_{\hat{W}} (r + \eta_t^T \Lambda) + \frac{1}{2} \hat{W}_t^2 \hat{V}_{\hat{W}\hat{W}} (\eta_t^T \Phi \Phi^T \eta_t) + \hat{W}_t \hat{V}_{\hat{W}H} \sigma^H (\eta_t^T A) + \hat{W}_t \hat{V}_{\hat{W} \ln S} \sigma^S (\eta_t^T B) \right\} \\ + \hat{V}_H \mu^H + \frac{1}{2} \hat{V}_{HH} (\sigma^H)^2 + V_{\ln S} (r + \lambda^S \sigma^S) + \frac{1}{2} \hat{V}_{\ln S \ln S} (\sigma^S)^2 + \hat{V}_{H \ln S} \sigma^H \sigma^S \rho_{SH} = 0. \end{aligned} \quad (6.7)$$

If the solution of the associated HJB PDEs exists, then it is easy to verify that,

$$\hat{V}(t, \hat{W}, H, \ln S) = V(t, W, H, \ln S) \quad (6.8)$$

$$\hat{W}_t = W_t \quad (6.9)$$

$$\Sigma_t^T \pi_t^* = \eta_t^*. \quad (6.10)$$

Furthermore, if the number of derivatives in O_t is greater than 2 (i.e. $n \geq 2$), there are infinitely many optimal strategies, all producing the same maximum value function.

Aside from the expected utility maximization, the investor is also concerned with the size of their risky allocations. For instance, on the other hand, an institutional investor may have to keep their gross allocation exposure under a certain level due to regulatory constraints. On the other hand, a small exposure is important for capital safety regarding unmodellable risk, such as financial crisis. Hence, we consider an additional derivative selection criterion, namely risk exposure minimization, introduced in [36]:

$$\min_{\bar{O}_t \in \Omega_O^{(n)}} \left\| \arg \max_{\pi_{s \geq t} \in \Omega_\pi^{(O)}} \mathbb{E}(U(W_T) \mid \mathcal{F}_t) \right\|_1, \quad (6.11)$$

where $\|\pi_{s \geq t}\|_1 = \sum_{i=1}^n |\pi_t^{(i)}|$ represents the ℓ_1 norm of allocations at time t . Note that this objective is equivalent to maximizing the cash position while shorting less. [36] demonstrated that the redundancy offers no additional help with either the investor's expected utility or their risky asset exposure in the case of two one-factor assets. In the next proposition, we demonstrate a generalized conclusion, which applies to any diffusion model.

Proposition 6.2.1 *Assume that an optimal solution for Problem (6.11) exists for $n \geq 2$; then, (6.11) leads to the same minimal ℓ_1 norm for any $n \geq 2$. In addition, an optimal strategy exists for Problem (6.11) such that the number of non-zero allocations is less than or equal to 2.¹*

Proof See Section 6.6.1.

Proposition 6.2.1 demonstrates that investors do not need to consider the portfolio composition O_t with size $n > 2$. Working with $n = 2$ is sufficient for both Problems (6.4) and (6.11). We hence only study the simplest case given a complete market setting (i.e. $n = 2$).

6.3 Polynomial affine method for CRRA utilities in financial derivatives market

In this section, we introduce a methodology to compute derivatives-based portfolio strategies. This method is required to find the optimal candidate composition $\bar{O}_t \in \Omega_O^{(2)}$ for risk exposure minimization.

¹The result can be easily extended to higher dimension. When model contains $m \geq 2$ independent risk factors (Brownian motions), an optimal strategy exists for Problem (6.11) such that the number of non-zero allocations is less than or equal to m .

Complexity in assets' dynamic models often jeopardizes the analytic solvability of HJB PDE; this means that closed-form solutions are not always available. Motivated by this fact, [91] proposed a simulation-based method to approximate the optimal strategy for continuous-time portfolios within EUT (i.e. the PAMC). The original PAMC method is only applicable to asset classes, such as equity, fixed income and currency, where assets' dynamics are known explicitly. However, with proper modifications, the PAMC is easily extended to financial derivatives markets. The new method, namely the PAMC-indirect, is introduced in Section 6.3.1. Furthermore, an alternative method is described in Section 6.7. The performances of both methodologies are demonstrated in the case of the Heston model, and the comparison to the theoretical solution confirms the excellent accuracy and efficiency of the PAMC-indirect method.

6.3.1 The PAMC-indirect

Inspired by the quadratic affine model family (see [70]), the PAMC approach assumes that the value function has the following representation:

$$V(t, W, H, \ln S) = \frac{W^{1-\gamma}}{1-\gamma} f(t, H, \ln S), \quad (6.12)$$

where $f(t, H, \ln S)$ is approximated by an exponential polynomial function of order k ; that is, $\exp\{P_k\}$. The PAMC method utilizes the Bellman equation and the fact that the value function at re-balancing time is the conditional expectation of the value function at $t + \Delta t$; that is,

$$V(t, W_t, H_t, \ln S_t) = \max_{\pi_t} \mathbb{E}(V(t + \Delta t, W_{t+\Delta t}, H_{t+\Delta t}, \ln S_{t+\Delta t}) \mid \mathcal{F}_t).$$

The PAMC expands the value function at $t + \Delta t$ with respect to wealth W , state variable H and log stock price $\ln S$, and it considers a sufficiently small re-balancing interval Δt such that the infinitesimal $o(\Delta t)$ terms are omitted. Then, the value function $V(t, W_t, H_t, \ln S_t)$ is rewritten as a quadratic function of the portfolio strategy, and the optimal strategy is immediately solved with the first order condition given the information at $t + \Delta t$. Proposition 6.3.1 displays the estimation of optimal strategy η_t^* in the artificial pure factor market (6.6).

Proposition 6.3.1 *Given the approximation of the value function at the next re-balancing time $t + \Delta t$ (i.e. $\frac{W^{1-\gamma}}{1-\gamma} \exp\{P_k\}(t + \Delta t, H, \ln S)$), the optimal strategy at time t is given by*

$$\eta_t^* = \frac{1}{\gamma} (\Phi \Phi^T)^{-1} (\Lambda + \frac{\partial P_k}{\partial H} \sigma^H A + \frac{\partial P_k}{\partial \ln S} \sigma^S B). \quad (6.13)$$

Proof See Section 6.6.2.

The PAMC-indirect inherits the recursive approximation structure of the PAMC. After the generation of paths of asset price and state variables, the optimal pure factor strategies at last re-balancing time $T - \Delta t$ can be directly computed with Equation (6.13) because $P_k(T, H, \ln S) = 0$; the path-wise expected utilities are obtained through simulation. Furthermore, the expected

utilities are regressed over stock price $S_{T-\Delta t}$ and state variable $H_{T-\Delta t}$, and the regression function approximates the $V(T - \Delta t, W, H, \ln S)$. Then, the method moves backward, and similar procedures are conducted at each re-balancing time until the optimal initial strategy of the pure factor portfolio (i.e. η_0^*) is obtained.

Finally, the PAMC-indirect calculates the portfolio variance matrix Σ_t , which depends on the option price O_t , Delta $\frac{\partial O_t}{\partial S_t}$ and the sensitivity to the state variable $\frac{\partial O_t}{\partial H_t}$. The optimal derivatives strategy π_0^* is solved with Equation (6.10). Only in some special cases (e.g. the Black-Scholes model) are option prices solved analytically. A variety of approximation methods for option price and Greeks are available in the existing literature. The choice of such methods should be determined by the option style and underlying assets model. For example, an accurate Fourier transform (FT) approximation is an ideal choice when the semi-closed-form solution of an option is available (e.g. the Heston model, the Ornstein–Uhlenbeck 4/2 model), while a simple Monte Carlo simulation is universal for options with a deterministic exercise date; and a least-squares Monte Carlo method is applicable when considering American style options.

We clarify the notation in Table 6.1 and detail the PAMC-indirect in Algorithm 11.

Notation	Meaning
$B_t^{m,S}, B_t^{m,H}$	Brownian motion at time t in m^{th} simulated path
S_t^m	Stock price at time t in m^{th} simulated path
$S_t^{m,S}$	Pure factor asset S_t^S at time t in m^{th} simulated path
$S_t^{m,H}$	Pure factor asset S_t^H at time t in m^{th} simulated path
H_t^m	State variable Stock price at time t in m^{th} simulated path
O_t^m	Derivatives price at time t in m^{th} simulated path
n_r	Number of simulated paths
Σ_t^m	Variance matrix of portfolio composition at time t in m^{th} simulated path
N	Number of simulations to compute expected utility for a given set (W_0, S_t^m, H_t^m)
$\hat{W}_{t+\Delta t}^{m,n}(\pi^m)$	The simulated wealth level at $t + \Delta t$ given the wealth, the allocation and other state variables at t are W_0, π^m, S_t^m , and H_t^m
$\hat{S}_{t+\Delta t}^{m,n}$	A simulated stock price at $t + \Delta t$ given S_t^m
$\hat{H}_{t+\Delta t}^{m,n}$	A simulated state variable at $t + \Delta t$ given H_t^m
$\hat{O}_{t+\Delta t}^{m,n}$	A simulated option price at $t + \Delta t$
$V(t, W, \ln S, H)$	Value function at time t given wealth W , stock price S and state variable H
\hat{v}^m	Estimation of $P_k(t, \ln S_t^m, H_t^m) = \log(f(t, \ln S_t^m, H_t^m))$ in Equation (6.12). Regressand in regression; superscript m indicates the corresponding regressor $(\ln S_t^m, H_t^m)$
$L_t(H, \ln S)$	The regression function to be used to approximate $P_k(t, \ln S, H)$
η_t^m	Optimal strategy at time t in m^{th} simulated path

Table 6.1: Notation and definitions

6.4 Derivatives selection

In this section, we study derivative selection for market completion—that is, (6.11)—for $n = 2$ within subsets of the derivative set $\Omega_O^{(2)}$. The derivative selection problem is rewritten as

$$\min_{\bar{O}_t \in \Omega_O^{(2,C)}} \left\| \arg \max_{\pi_{s \geq t} \in \Omega_\pi^{(O)}} \mathbb{E}(U(W_T) \mid \mathcal{F}_t) \right\|_1, \quad (6.14)$$

where $\Omega_O^{(2,C)}$ is a derivative set defined by

$$\Omega_O^{(2,C)} = \left\{ \bar{O}_t = [S_t, O_t^{(C)}]^T \mid O_t^{(C)} \in C, t \in [0, T] \right\}.$$

The portfolio composition $\bar{O}_t \in \Omega_O^{(2,C)}$ consists of a stock S_t and a derivative security $O_t^{(C)}$; superscript C represents the candidate set of derivative type; and T_{op} denotes the time to maturity of $O_t^{(C)}$. This setting coincides with a popular practical strategic investment implementation (i.e. the elimination unhedgeable risk factors of a pure-stock portfolio with financial derivatives). We use the Heston SV model given in Equation (6.15) as the proxy of the market dynamics.

$$\begin{cases} \frac{dM_t}{M_t} = r dt \\ \frac{dS_t}{S_t} = (r + \lambda X_t) dt + \sqrt{X_t} dB_t^S \\ dX_t = \kappa^X (\theta^X - X_t) dt + \sigma^X \sqrt{X_t} dB_t^X \\ dO_t^{(C)} = (r + \lambda \frac{\partial O_t^{(C)}}{\partial S_t} S_t X_t + \lambda^X \frac{\partial O_t^{(C)}}{\partial X_t} \sigma^X X_t) dt + \frac{\partial O_t^{(C)}}{\partial S_t} S_t \sqrt{X_t} dB_t^S + \frac{\partial O_t^{(C)}}{\partial X_t} \sigma^X \sqrt{X_t} dB_t^X \\ \langle B^S, B^X \rangle_t = \rho_{SX} \end{cases}. \quad (6.15)$$

The Heston model is a specific case of the generalized diffusion model (6.1) with $\lambda^S = \lambda \sqrt{X_t}$, $\lambda^H = \lambda^X \sqrt{X_t}$, $\sigma^S = \sqrt{X_t}$, $\mu^X = \kappa^X (\theta^X - X_t)$ and $\sigma^H = \sigma^X \sqrt{X_t}$. We employed a representative market-calibrated set of parameters (see Table 6.2), given in [71], to investigate the best product to account for volatility risk. The optimal allocation for the model (6.15) can be written explicitly with Equations (6.13) and (6.10) as follows

$$\begin{aligned} \pi_t^S &= \frac{1}{\gamma(1 - \rho_{SX}^2)} (\lambda - \rho_{SX} \lambda^X) - \pi_t^O \frac{S_t}{O_t^{(C)}} \frac{\partial O_t^{(C)}}{\partial S_t} \\ \pi_t^O &= \left(\frac{O_t^{(C)}}{\gamma \sigma^X (1 - \rho_{SX}^2)} (\lambda^X - \rho_{SX} \lambda) + \frac{O_t^{(C)}}{\gamma} \frac{\partial P_k}{\partial X_t} \right) \frac{1}{\frac{\partial O_t^{(C)}}{\partial X_t}}. \end{aligned} \quad (6.16)$$

The representation indicates that the optimal allocation on option π_t^O solely depends on the choice of option $O_t^{(C)}$ (i.e. π_t^O is a function of the option's sensitivity to the instantaneous variance and option price), while the optimal allocation on the stock π_t^S is determined by the ratio of the option's sensitivity to the instantaneous variance and the sensitivity to the stock.

Table 6.2: Parameter value for the Heston model.

Parameter	Value	Parameter	Value
T	1 year	ρ_{SX}	-0.4
θ^X	0.0169	σ^X	0.25
κ^X	5.0	λ	4.0
λ^X	-7.1	T_{op}	0.1 year
Δt	$\frac{1}{60}$	$period$	60
r	0.05	X_0	θ^X
S_0	1.0	M_0	1.0
W_0	1	γ	4
N	2000	n_r	100

6.4.1 Derivatives selection within options on stock

We start the selection among four popular equity options. Specifically, the candidate set is given by

$$C = \{Call\ option, Put\ option, Straddle, Strangle\}.$$

For simplicity, we only consider European-style derivatives. Call (i.e. payoff $(S - K)^+$) and put (i.e. payoff $(K - S)^+$) options are the most common products traded in the market. Additionally, a straddle (i.e. payoff $(S - K)^+ + (K - S)^+$) is a commonly used product when investors expect the underlying asset to deviate from the spot price; hence, the long position of a straddle is approximately a long position on volatility. Compared with a straddle synthesized by purchasing a call and a put with the same strike price and maturity, a strangle (i.e. payoff $(S - K_1)^+ + (K_2 - S)^+$) has a more flexible structure, as it takes long positions on out-of-the-money (OTM) put and call, which is a cheaper way to acquire exposure to volatility.²

Figure 6.1 displays the risk exposure $\|\pi_t\|_1$ of portfolios as a function of derivative moneyness K/S_0 , where K is the strike price of the options. Figure 6.1 (a) exhibits risk exposure given options with maturity $T_{op} = 0.1$, and Figure 6.1 (b) displays results when the option maturity is $T_{op} = 0.5$. In both cases, investors reduce their risk exposure with OTM put and call options. Puts and calls could lead to illiquid choices, whereas a straddle achieves minimum $\|\pi_t\|_1$ when it is near at-the-money (ATM). The optimal moneyness of a straddle option shifts to the right as maturity T_{op} increases. The risk exposure with a strangle decreases as its component put option moves deeper OTM. Furthermore, even the strangle consisting of a near-ATM put and call outperforms other options. We consequently conclude that the strangle minimizes the risk exposure.

The turning point on the left tail of the strangle's risk exposure in Figure 6.1 is further studied in Figure 6.2, where we illustrate how the optimal moneyness of an OTM call, an allocation on stock π_t^S and an allocation on strangle π_t^O vary with the moneyness of an OTM put. Note the practical range selected for the moneyness of an OTM call; that is, $K^{Call}/S_0 \in [S_0, 110\%S_0]$. It is shown that, if the strike price of the put option starting at the spot price moves in the direction of OTM, the corresponding optimal moneyness of the call option also becomes deeply OTM.

²Elements in variance matrix Σ_t , which are functions of option prices and Greeks, can be obtained with numerical integration method (see [81] chapter 11). Specifically, we utilized the formula given in [48] and compute numerical integration with the Newton-Cotes formulas.

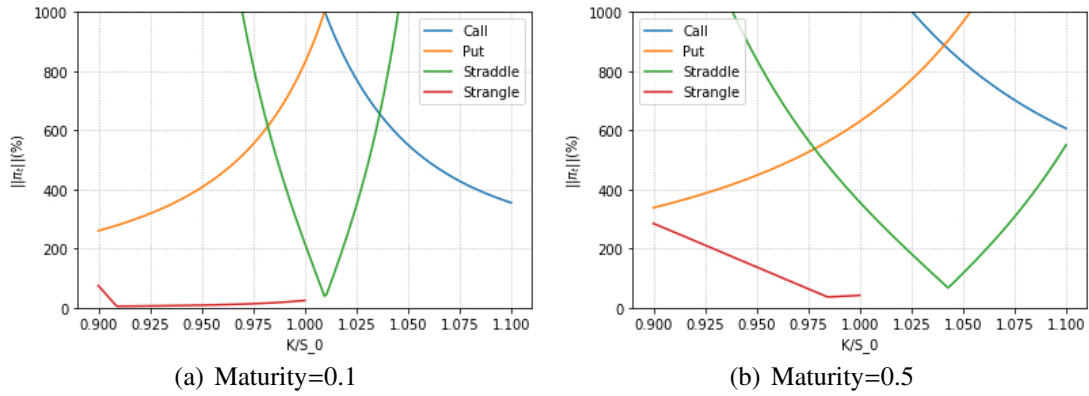


Figure 6.1: The $\|\pi_t\|_1$ versus moneyness: The Y-axis is the risk exposure of a portfolio containing different derivatives. The X-axis indicates the moneyness K/S_0 of calls, puts and straddles. The strangle is synthesized with an OTM put and an OTM call. Given moneyness of the OTM put indicated by the X-axis, the strike price of the OTM call is the one achieving minimum $\|\pi_t\|_1$ within the range $[S_0, 110\%S_0]$.

The OTM call reaches the boundary earlier than the put, which leads to the turning point. Before the turning point, allocation on the stock π_t^S continues to be small, and π_t^O gradually approaches 0; hence, the total risk exposure $\|\pi_t\|_1$ assumes a decreasing trend. However, π_t^S increases rapidly after the turning point, and $\|\pi_t\|_1$ consequently rises as π_t^O continues to drop. Moreover, Figures 6.2 (a) and (b) compare strangles with maturity $T_{op} = 0.1$ and $T_{op} = 0.5$, respectively. The turning point for a longer maturity strangle is more easily reached, which makes it less preferable.

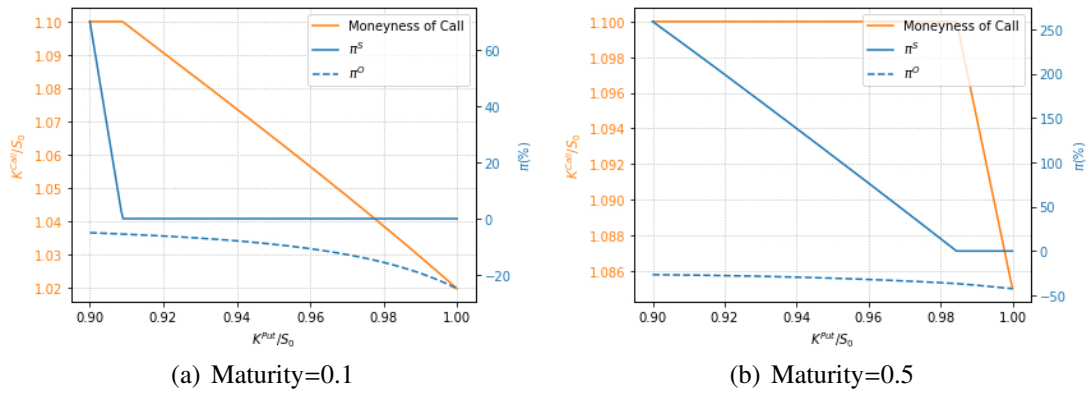


Figure 6.2: Impact of the OTM put’s moneyness on the strangle. Left vertical axis indicates the optimal moneyness of the OTM call within $[100\%S_0, 110\%S_0]$. Right vertical axis indicates the allocation on the stock and the strangle.

Equation (6.16) demonstrates that the allocation on the option is determined by the ratio of the Vega to the option price. Therefore, in Figure 6.3, we investigate the relationship between the Vega of the strangle and the time to maturity to provide further insight for the comparison of maturity in Figures 6.1 and 6.2. Figure 6.3 (a) illustrates the Vega versus the maturity of an

ATM strangle (the moneyness of component put option $K/S_0 = 100\%$) and an OTM strangle (the moneyness of component put option $K/S_0 = 95\%$). For an especially short-term maturity strangle, the terminal payoff do not have sufficient time to react to the change in volatility state, therefore, the Vega is small. For the long-term maturity strangle, a change in the instantaneous variance also has a small impact on the option price because of its mean-reverting nature. Hence, the Vegas of both strangles are concave in time to maturity, which peaks at around 0.3 years. The impact from time to maturity on the ratio of Vega to price is illustrated in Figure 6.3 (b), where $\frac{\partial O_t^{(C)}}{\partial X_t} / O_t^{(C)}$ is always positive and monotonically decreases with maturity, which leads to an increasing $|\pi_t^O|$. In Figure 6.2, π_t^S is close to 0 before the boundary, and $|\pi_t^O|$ increases with maturity; hence, we conclude that a short-term maturity strangle is preferable.

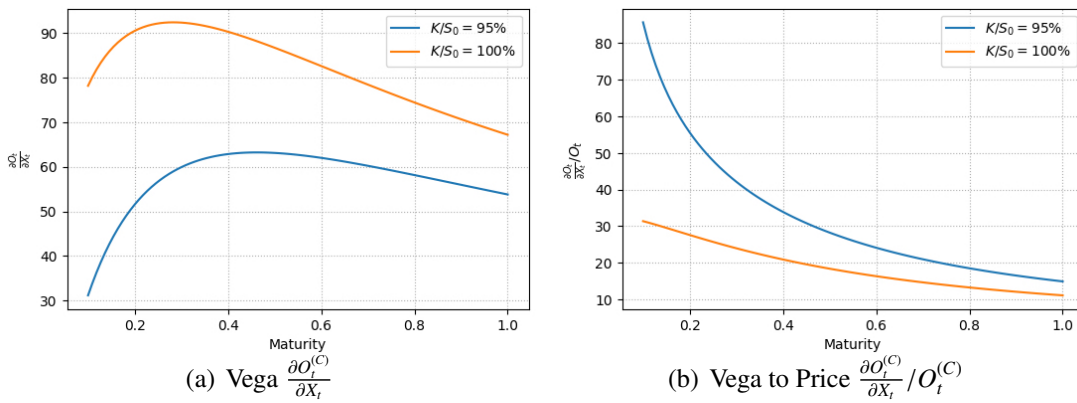


Figure 6.3: Sensitivity of strangle option price $O_t^{(C)}$ to instantaneous variance X_t versus time to maturity T_{op} . The legend indicates the moneyness of component put, and the call option is the one achieving minimum risk exposure. Note that there is no boundary for the strike price of the component call.

6.4.2 Derivatives selection within VIX products

Next, we study an investor who has access to the VIX of the stock at hand, such as the VIX for the S&P 500. In this case, the investor has direct access to the volatility risk by investing in products based on the VIX. The VIX has drawn investors' attention since its origin in 1993; not only is it a real-time indicator of the market sentiment, but also products such as VIX futures and VIX options are popular for hedging volatility risk. In this section, we explore products on the VIX. We consider a candidate set

$$C = \{VIX \text{ call}, VIX \text{ put}, VIX \text{ straddle}, \text{Strangle}\}.$$

Note that a strangle is the best option for minimizing risk exposure considered in Section 6.4.1. VIX calls and VIX puts are call and put options, respectively, based on the value of the VIX. A VIX straddle is an instrument synthesized by the long position of a VIX call and a VIX put with the same strike price.

Given the definition of VIX as specified in the CBOE white paper [14], [68] solved the VIX^2 in closed-form as a function of instantaneous variance X_t . Under the Heston model, we have

$$VIX_t^2 = \frac{1}{\tau} (a_\tau X_t + b_\tau) \quad (6.17)$$

$$a_\tau = \frac{1 - \exp -\kappa_v^* \tau}{\kappa_v^*}, \quad b_\tau = \theta_v^* (\tau - a_\tau) \quad \kappa_v^* = \kappa_v + \lambda^X \sigma_v, \quad \theta_v^* = \frac{\kappa_v \theta_v}{\kappa_v^*}, \quad \tau = \frac{30}{365},$$

where VIX_t^2 is linear with the instantaneous variance X_t . Computing a VIX option's price and Greeks is easy via Monte Carlo simulation; this method enable us to find elements in the variance matrix Σ_t .

Unlike options on the stock, by investing in VIX products, the investor acquires exposure only on the volatility risk; hence, the variance matrix Σ_t is diagonal. Moreover, the equity-neutral position of VIX products leads to a specific case of Equation (6.16):

$$\pi_t^S = \frac{1}{\gamma(1 - \rho_{SX}^2)} (\lambda - \rho_{SX} \lambda^X)$$

$$\pi_t^O = \left(\frac{O_t^{(C)}}{\gamma \sigma^X (1 - \rho_{SX}^2)} (\lambda^X - \rho_{SX} \lambda) + \frac{O_t^{(C)}}{\gamma} \frac{\partial P_k}{\partial X_t} \right) \frac{1}{\frac{\partial O_t^{(C)}}{\partial X_t}}. \quad (6.18)$$

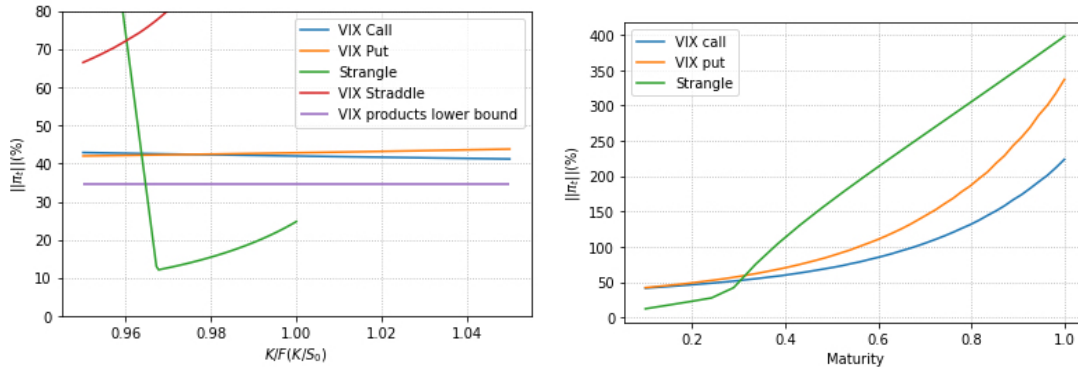
In this case, the allocation on the stock is invariant to the choice of VIX products, which thus becomes a natural lower bound for risk exposure (i.e. $\|\pi_t\|_1 \geq |\pi_t^S|$).

The risk exposure when investors hedge the volatility risk with VIX calls and puts is displayed in Figure 6.4 (a). On the one hand, calls and puts on the VIX have similar properties as those on the stock: OTM options tend to achieve smaller risk exposure. On the other hand, a VIX straddle is less ineffective in hedging the volatility risk because it is relatively insensitive to the volatility, and a larger risk exposure $\|\pi_t\|_1$ is needed for investors compared to the cases of VIX calls and puts. The risk exposure with the equity strangle is displayed for comparison purpose; here, the turning point resulting from the boundary of moneyness on the OTM call is still evident. Moreover, the strangle achieves a much smaller risk exposure than the VIX products. We therefore conclude that equity strangle is superior when the time to maturity T_{op} for candidate products is small ($T_{op} = 0.1$).

Figure 6.4 (b) illustrates how the option maturity T_{op} affects the risk exposure $\|\pi_t\|_1$. It indicates that an OTM VIX call and an OTM VIX put are preferable in (a), and a similar conclusion is verified numerically for any $T_{op} \in (0, 1]$. Therefore, risk exposure for the best VIX call ($K = 105\%S_0$) and VIX put ($K = 95\%S_0$) are plotted in Figure 6.4 (b). In addition, the minimum risk exposure within a pre-specified region of moneyness is also displayed. As the volatility time series exhibits a mean-reverting property, the VIX options with long-term maturity are insensitive to the instantaneous variance; hence, it has little effect in hedging the volatility risk. The figure also suggests that a large allocation on the long-term maturity VIX option is needed, such that the risk exposure increases rapidly with maturity. A strangle achieves smaller risk exposure when short-term maturity products are available in the market, aligning with the result in Figure 6.4 (a).

According to Figures 6.1 and 6.2, the boundary of the OTM call is reached faster as T_{op} increases, and the boundary significantly restricts risk exposure, thus reducing the effect of the

strangle. This leads to a steep slope of risk exposure for the strangle in Figure 6.4 (b). In summary, the investor should make a choice between VIX products and an equity strangle, depending on the situation. If the investor has access to short-term maturity options, then the strangle is preferable. However, when only long-term maturity products are available, the investor should choose call options on the VIX for market completion.



(a) The $\|\pi_t\|_1$ versus moneyness: the time to maturity of both VIX options and the strangle is 0.1 year. The X-axis indicates moneyness of VIX options and the OTM put in the strangle; the strike price of the OTM call is the one achieving minimum price $K^{Put} \in [95\%S_0, 100\%S_0]$ and the OTM call strike price $K^{Call} \in [100\%S_0, 105\%S_0]$.

(b) The $\|\pi_t\|_1$ versus maturity: the strike price of VIX calls is $105\%S_0$. The strike price of VIX puts is $95\%S_0$. The green line shows the smallest $\|\pi_t\|_1$ is achieved by the strangle given the OTM put strike price $K^{Put} \in [95\%S_0, 100\%S_0]$ and the OTM call strike price $K^{Call} \in [100\%S_0, 105\%S_0]$.

Figure 6.4: The $\|\pi_t\|_1$ for VIX products

6.5 Conclusion

This chapter explored optimal derivatives-based portfolios to complete a market characterized by volatility risk as a state variable. An accurate and high-speed approximation for optimal allocations is proposed, for the unsolvable problem of optimal derivative exposure. In addition to the traditional portfolio decision objective (i.e. EUT maximization), we work with an additional criterion, namely risk exposure minimization, for derivative selection. This aids in the selection of a meaningful product out of many that maximize the utility. We found that strangle options are the best equity option product for managing volatility risk. Moreover, we demonstrated that options based on the VIX are superior to equity strangles in some realistic situations.

There are many interesting potential extensions to this line of research. For instance, we could incorporate multi-factor models considering the stochastic interest rates, stochastic correlations, jumps and stochastic market prices of risk, to mention a few. These are more realistic settings, solvable within our numerical method, hence providing investors with valuable insight into optimal high-dimensional portfolios and multi-asset derivatives for sensible practical investment.

6.6 Proofs

6.6.1 Proof of Proposition 6.2.1

Let $O_{t,n} = [O_t^{(1)}, O_t^{(2)}, \dots, O_t^{(n)}]^T$ with variance matrix Σ_t of rank 2 be an optimal subset of options for problem (6.11). $\pi_{t,n}^*$ is a strategy maximizing the expected utility if and only if $\Sigma_t^T \pi_{t,n}^* = \eta_t^*$. Therefore, $O_{t,n}$ and $\pi_{t,n}^*$ is an optimal pair for (6.11) when $\pi_{t,n}^*$ is an optimal solution for

$$\begin{aligned} & \underset{\pi_t}{\text{minimize}} && \|\pi_t\|_1 \\ & \text{subject to} && \Sigma_t^T \pi_t = \eta_t^*. \end{aligned} \quad (6.19)$$

According to principle 4.5 in [80], problem (6.19) is equivalent to

$$\begin{aligned} & \underset{\delta_t}{\text{minimize}} && \mathbb{1}^T \delta_t \\ & \text{subject to} && \hat{\Sigma}_t^T \delta_t = \eta_t^*, \\ & && \delta_t \geq 0 \end{aligned} \quad (6.20)$$

where $\delta_t = [\alpha_t^{(1)}, \alpha_t^{(2)}, \dots, \alpha_t^{(n)}, \beta_t^{(1)}, \beta_t^{(2)}, \dots, \beta_t^{(n)}]^T$ satisfies $\alpha_t^{(i)} = \frac{|\pi_t^{(i)}| + \pi_t^{(i)}}{2}$, and $\beta_t^{(i)} = \frac{|\pi_t^{(i)}| - \pi_t^{(i)}}{2}$, with

$$\hat{\Sigma}_t = \begin{bmatrix} \Sigma_t \\ -\Sigma_t \end{bmatrix} = \begin{bmatrix} f_t^{11} & f_t^{12} \\ \dots & \dots \\ f_t^{n1} & f_t^{n2} \\ -f_t^{11} & -f_t^{12} \\ \dots & \dots \\ -f_t^{n1} & -f_t^{n2} \end{bmatrix}. \quad (6.21)$$

Theorems 2.3 and 2.4 in [6] lists the necessary and sufficient conditions for the extreme point δ_t , i.e.

1. $\delta_t = [\delta_t^{(1)}, \delta_t^{(2)}, \dots, \delta_t^{(n)}, \delta_t^{(n+1)}, \delta_t^{(n+2)}, \dots, \delta_t^{(2n)}]^T$.
2. the \hat{q}^{th} and \hat{p}^{th} rows in $\hat{\Sigma}_t$ are linear independent, $\delta_t^{(i)} = 0$ if $i \neq \hat{q}$ or \hat{p} .
3. δ_t is feasible solution.

Without loss of generality, we assume the p^{th} and q^{th} rows in Σ are linear independent, and we consider 4 cases:

$$\begin{aligned} \delta_t^{[1]} &= \begin{cases} [\delta_t^{[1,(1)}, \delta_t^{[1,(2)}, \dots, \delta_t^{[1,(n)}, \delta_t^{[1,(n+1)}, \delta_t^{[1,(n+2)}, \dots, \delta_t^{[1,(2n)}]^T \\ \delta_t^{[1,(i)} = 0 & \text{if } i \neq q \text{ or } p \end{cases} \\ \delta_t^{[2]} &= \begin{cases} [\delta_t^{[2,(1)}, \delta_t^{[2,(2)}, \dots, \delta_t^{[2,(n)}, \delta_t^{[2,(n+1)}, \delta_t^{[2,(n+2)}, \dots, \delta_t^{[2,(2n)}]^T \\ \delta_t^{[2,(i)} = 0 & \text{if } i \neq q + n \text{ or } p \end{cases} \\ \delta_t^{[3]} &= \begin{cases} [\delta_t^{[3,(1)}, \delta_t^{[3,(2)}, \dots, \delta_t^{[3,(n)}, \delta_t^{[3,(n+1)}, \delta_t^{[3,(n+2)}, \dots, \delta_t^{[3,(2n)}]^T \\ \delta_t^{[3,(i)} = 0 & \text{if } i \neq q \text{ or } p + n \end{cases} \\ \delta_t^{[4]} &= \begin{cases} [\delta_t^{[4,(1)}, \delta_t^{[4,(2)}, \dots, \delta_t^{[4,(n)}, \delta_t^{[4,(n+1)}, \delta_t^{[4,(n+2)}, \dots, \delta_t^{[4,(2n)}]^T \\ \delta_t^{[4,(i)} = 0 & \text{if } i \neq q + n \text{ or } p + n \end{cases} \end{aligned} \quad (6.22)$$

It is clear that there is a non-negative strategy in $\delta_i^{[1]}$, $\delta_i^{[2]}$, $\delta_i^{[3]}$ and $\delta_i^{[4]}$ because the i^{th} row in $\hat{\Sigma}$ is the opposite of the $(i+n)^{\text{th}}$ row, and the non-negative strategy is feasible and an extreme point. This proves the existence of an extreme point for problem (6.20). Now, theorem 2.7 in [6] guarantees that there is an optimal solution which is an extreme point for problem (6.20).

With the second necessary and sufficient conditions of the extreme point, we know that an optimal solution δ_i^* for problem (6.20) has at most two non-zero elements. This would imply an optimal solution, denoted by $\pi_{t,n}^* = [\pi_{t,n}^{(1)}, \pi_{t,n}^{(2)}, \dots, \pi_{t,n}^{(n)}]^T$, for problem (6.19) with at most two non-zero elements, which would also be the optimal strategy for (6.11).

Without loss of generality, we assume $\pi_{t,n}^{(i)} = 0$, $i \neq x, y$. $O_{t,2} = [O_t^{(x)}, O_t^{(y)}]$ and $\pi_{t,2}^* = [\pi_{t,n}^{(x)}, \pi_{t,n}^{(y)}]^T$ is a feasible strategy for problem (6.11) with $n = 2$. We show that it is an optimal pair by contradiction.

If there is a feasible solution $\hat{O}_{t,n} = [\hat{O}_t^{(1)}, \hat{O}_t^{(2)}]$ and $\hat{\pi}_{t,2}^* = [\hat{\pi}_{t,2}^{(1)}, \hat{\pi}_{t,2}^{(2)}]^T$ such that $\|\hat{\pi}_{t,2}^*\|_1 < \|\pi_{t,2}^*\|_1$, then $\hat{\pi}_{t,n}^* = [\hat{\pi}_{t,2}^{(1)}, \hat{\pi}_{t,2}^{(2)}, 0, \dots, 0]^T$ is a feasible strategy for (6.11) such that $\|\hat{\pi}_{t,n}^*\|_1 < \|\pi_{t,n}^*\|_1$, which is contradiction to our previous conclusion. Note that $\|\pi_{t,2}^*\|_1 = \|\pi_{t,n}^*\|_1$, so problem (6.11) with $n = 2$ and with $n \geq 2$ have the same minimum ℓ_1 norm of allocation.

6.6.2 Proof of Proposition 6.3.1

According to the Bellman equation, the value function can be rewritten as,

$$\begin{aligned} V(t, W, \ln S, H) &= \mathbb{E}_t(V(t+dt, W_{t+dt}, H_{t+dt}, \ln S_{t+dt}) \mid W, H, \ln S) \\ &= \max_{\eta} \mathbb{E}_t(V(t+dt, W_{t+dt}, H_{t+dt}, \ln S_{t+dt}) \mid W, \eta, H, \ln S). \end{aligned} \quad (6.23)$$

We expand $V(t+dt, W_{t+dt}, H_{t+dt}, \ln S_{t+dt})$ at $t+dt$ in terms of all the variables.

$$\begin{aligned} V(t+dt, W_{t+dt}, H_{t+dt}, \ln S_{t+dt}) &= V(t+dt, W_t, \ln S_t, H_t) + V_{W_t}(t+dt, W_t, H_t, \ln S_t) d\hat{W}_t \\ &+ \frac{1}{2} V_{W_t W_t}(t+dt, W_t, H_t, \ln S_t) (d\hat{W}_t)^2 + V_{\ln S_t}(t+dt, W_t, H_t, \ln S_t) d \ln S_t + V_{H_t}(t+dt, W_t, H_t, \ln S_t) dH_t \\ &+ \frac{1}{2} V_{\ln S_t \ln S_t}(t+dt, W_t, H_t, \ln S_t) d \ln S_t d \ln S_t + \frac{1}{2} V_{H_t H_t}(t+dt, W_t, \ln S_t, H_t) dH_t dH_t \\ &+ V_{W_t \ln S_t}(t+dt, W_t, H_t, \ln S_t) d\hat{W}_t d \ln S_t + V_{W_t H_t}(t+dt, W_t, H_t, \ln S_t) d\hat{W}_t dH_t \\ &+ V_{\ln S_t H_t}(t+dt, W_t, \ln S_t, H_t) d \ln S_t dH_t + o(dt). \end{aligned} \quad (6.24)$$

Substituting $d\hat{W}_t$, $d \ln S_t$, dH_t which can be found in Equation (6.1), taking conditional expectation on both sides, and rewriting $V(t, W_t, H_t, \ln S_t)$ in a quadratic form with respect to η leads to

$$\begin{aligned}
V(t, W_t, H_t, \ln S_t) &= \max_{\eta_t} \left(\sum_{i,j=1}^2 f_{i,j}(t, W_t, H_t, \ln S_t) \eta_t^{(i)} \eta_t^{(j)} + \sum_{i=1}^2 f_i(t, W_t, H_t, \ln S_t) \eta_t^{(i)} + f_0(t, W_t, H_t, \ln S_t) \right) \\
f_{i,j}(t, W_t, H_t, \ln S_t) &= \frac{1}{2} V_{W_t W_t}(t+dt, W_t, H_t, \ln S_t) \hat{W}_t^2 (\Phi \Phi^T)_{i,j} dt \\
f_i(t, W_t, H_t, \ln S_t) &= V_{W_t}(t+dt, W_t, H_t, \ln S_t) \hat{W}_t \Lambda_i dt + V_{W_t \ln S_t}(t+dt, W_t, H_t, \ln S_t) \hat{W}_t \sigma_S B_i dt \\
&\quad + V_{W_t H_t}(t+dt, W_t, H_t, \ln S_t) \hat{W}_t \sigma_H A_i dt \\
f_0(t, W_t, H_t, \ln S_t) &= V(t+dt, W_t, H_t, \ln S_t) + V_{W_t}(t+dt, W_t, H_t, \ln S_t) \hat{W}_t r dt \\
&\quad + V_{\ln S_t}(t+dt, W_t, H_t, \ln S_t) (\lambda^S \sigma^S - \frac{1}{2} (\sigma^S)^2) dt + V_{H_t}(t+dt, W_t, H_t, \ln S_t) \mu^H dt \\
&\quad + \frac{1}{2} V_{H_t H_t}(t+dt, W_t, H_t, \ln S_t) (\sigma^H)^2 dt + \frac{1}{2} V_{\ln S_t \ln S_t}(t+dt, W_t, H_t, \ln S_t) (\sigma^S)^2 dt \\
&\quad + V_{\ln S_t H_t}(t+dt, W_t, H_t, \ln S_t) \sigma^S \sigma^H dt.
\end{aligned} \tag{6.25}$$

We assume a sufficiently small dt so that $o(dt)$ terms are omitted when taking conditional expectations. The optimal allocation is given by the solution to the system of equations:

$$\sum_{j=1}^2 2f_{i,j}(t, W_t, H_t, \ln S_t) \eta_t^{(*,j)} = -f_i(t, W_t, H_t, \ln S_t), \quad i = 1, 2. \tag{6.26}$$

With the representation of the value function in Equation (6.12) and assuming that $f(t, H, \ln S) = \exp(P_k(t, H, \ln S))$, the derivatives of value function with respect to each stock and state variable can be rewritten as,

$$\begin{aligned}
V_W(t+dt, W_t, H_t, \ln S_t) &= \hat{W}_t^{-\gamma} \exp(P_k(t+dt, H_t, \ln S_t)) \\
V_{WW}(t+dt, W_t, H_t, \ln S_t) &= -\gamma \hat{W}_t^{-\gamma-1} \exp(P_k(t+dt, H_t, \ln S_t)) \\
V_{W \ln S_t}(t+dt, W_t, H_t, \ln S_t) &= \hat{W}_t^{-\gamma} \exp(P_k(t+dt, H_t, \ln S_t)) \frac{\partial P_k(t+dt, H_t, \ln S_t)}{\partial \ln S_t} \\
V_{WH_t}(t+dt, W_t, H_t, \ln S_t) &= \hat{W}_t^{-\gamma} \exp(P_k(t+dt, H_t, \ln S_t)) \frac{\partial P_k(t+dt, H_t, \ln S_t)}{\partial H_t}.
\end{aligned} \tag{6.27}$$

Substituting Equation (6.27) into Equation (6.26), the optimal strategy can be approximated as follows:

$$\begin{aligned}
\sum_{j=1}^2 g_{i,j}(t, W_t, H_t, \ln S_t) \eta_t^{(*,j)} &= g_i(t, W_t, H_t, \ln S_t), \quad i = 1, 2 \\
g_{i,j}(t, W_t, H_t, \ln S_t) &= \gamma (\Phi \Phi^T)_{i,j} \\
g_i(t, W_t, H_t, \ln S_t) &= \Lambda_i + \frac{\partial P_k(t+dt, H_t, \ln S_t)}{\partial \ln S_t} \sigma^S B_i + \frac{\partial P_k(t+dt, H_t, \ln S_t)}{\partial H_t} \sigma^S A_i,
\end{aligned} \tag{6.28}$$

Then, the optimal strategy can be rewritten in matrix form:

$$\eta_t^* = \frac{1}{\gamma} (\Phi \Phi^T)^{-1} \left(\Lambda + \frac{\partial P_k}{\partial H} \sigma^H A + \frac{\partial P_k}{\partial \ln S} \sigma^S B \right). \quad (6.29)$$

6.7 Alternative approximation method and comparison

6.7.1 Direct method

We introduced an alternative method for derivatives-based portfolio strategy, namely PAMC-direct method, which is straightforward application of the PAMC. At each re-balancing time, the path-wise option price O_t , Delta $\frac{\partial O_t}{\partial S_t}$ and the sensitivity to the state variable $\frac{\partial O_t}{\partial H_t}$ are approximated, so the instantaneous dynamics of derivatives are obtained. In this way, derivatives can be taken as an asset with dynamics known explicitly, the PAMC method is directly applied. Next proposition shows the estimation of optimal strategy π_t^* in PAMC-direct.

Proposition 6.7.1 *Given the approximation of the value function at the next re-balancing time $t + \Delta t$ (i.e. $\frac{W^{1-\gamma}}{1-\gamma} \exp\{P_k\}(t + \Delta t, H, \ln S)$), the optimal strategy at time t is given by*

$$\pi_t^* = \frac{1}{\gamma} (\Sigma_t \Phi \Phi^T \Sigma_t^T)^{-1} (\Sigma_t \Lambda + \frac{\partial P_k}{\partial H} \sigma^H \Sigma_t A + \frac{\partial P_k}{\partial \ln S} \sigma^S \Sigma_t B). \quad (6.30)$$

Proof Similar to Section 6.6.2.

We continue to use the notation in Table 6.1 and describe the step by step algorithm of the

PAMC-direct in Algorithm 12.

Algorithm 12: PAMC-direct method

Input: S_0, W_0, H_0
Output: Optimal trading strategy π_0^*

- 1 initialization;
- 2 Generating n_r paths of $B_t^m, B_t^{m,H}, S_t^m, H_t^m$ for $m = 1 \dots n_r$;
- 3 Apply approximation methods and obtain the price of $O_t(H_t^m, \ln S_t^m)$ as well as its sensitivity $\frac{\partial O_t}{\partial S_t}(H_t^m, \ln S_t^m)$ and $\frac{\partial O_t}{\partial H_t}(H_t^m, \ln S_t^m)$ for $t = 0, \Delta t, \dots, T$;
- 4 **while** $t = T - \Delta t$ **do**
- 5 **for** $m = 1 \dots n_r$ **do**
- 6 Compute the variance matrix $\Sigma_{T-\Delta t}^m$ with derivatives price and sensitivity obtained in step 3;
- 7 Directly compute optimal allocation $\pi_{T-\Delta t}^m$ with Equation (6.30) where the $P_k = 1$ at time T ;
- 8 **for** $n = 1 \dots N$ **do**
- 9 Generate $\hat{S}_T^{m,n}$ and $\hat{H}_T^{m,n}$ given $S_{T-\Delta t}^m$ and $H_{T-\Delta t}^m$ and obtain $\hat{O}_T^{m,n}$;
- 10 Compute wealth $\hat{W}_T^{m,n}(\pi_{T-\Delta t}^m)$ at the terminal given the wealth at $W_{T-\Delta t} = W_0$, the transformed value function is estimated by

$$\hat{v}^m = \ln \left[(1 - \gamma) \frac{1}{N} \sum_{n=1}^N U(\hat{W}_T^{m,n}(\pi_{T-\Delta t}^m)) \right] - (1 - \gamma) \ln W_0;$$
- 11 Regress \hat{v}^m over the polynomial of $H_{T-\Delta t}^m$ and $\ln S_{T-\Delta t}^m$, and obtain the function $L_{T-\Delta t}(H, \ln S)$;
- 12 **for** $t = T - 2\Delta t$ to Δt **do**
- 13 **for** $m = 1 \dots n_r$ **do**
- 14 Compute the variance matrix Σ_t^m with derivatives price and sensitivity obtained in step 3;
- 15 Directly compute optimal allocation π_t^m with Equation (6.30) where the $P_k = L_{t+\Delta t}(H, \ln S)$;
- 16 **for** $n = 1 \dots N$ **do**
- 17 Generate $\hat{S}_{t+\Delta t}^{m,n}$ and $\hat{H}_{t+\Delta t}^{m,n}$ given S_t^m and H_t^m and obtain $\hat{O}_{t+\Delta t}^{m,n}$;
- 18 Compute wealth $\hat{W}_{t+\Delta t}^{m,n}(\pi_t^m)$ at the terminal given the wealth at $W_t = W_0$, the transformed value function is estimated by

$$\hat{v}^m = \ln \left[\frac{1}{N} \sum_{n=1}^N (W_{t+\Delta t}^{m,n}(\pi_t^m))^{1-\gamma} \exp(L_{t+\Delta t}(\hat{H}_{t+\Delta t}^{m,n}, \ln \hat{S}_{t+\Delta t}^{m,n})) \right] - (1 - \gamma) \ln W_0;$$
- 19 Regress \hat{v}^m over the polynomial of H_t^m and $\ln S_t^m$, and obtain the function $L_t(H, \ln S)$;
- 20 **while** $t = 0$ **do**
- 21 Compute the variance matrix Σ_0 with derivatives price and sensitivity obtained in step 3, and the optimal allocation π_0^* is obtained with Equation (6.30) and where the $P_k = L_{\Delta t}(H, \ln S)$;
- 22 **return** π_0^*

6.7.2 Comparison between the PAMC-direct method and the PAMC-indirect method

In this section, we implement the PAMC-direct method and the PAMC-indirect method on the Heston SV model given in Equation (6.15) for comparison purpose. The derivatives-based portfolio given the Heston model was first studied in [71], where the author constructed a portfolio with derivative securities and a stock so that volatility risk is able to be managed. The optimal strategy stock-derivatives portfolio is solved in closed-form. The accuracy and efficiency of the PAMC-direct and the PAMC-indirect are examined in comparison with the analytical solution.

We continue to use the market-calibrated set of parameters in Table 6.2. For simplicity, we let O_t be a delta-neutral straddle because the delta-neutral position keeps the straddle near-the-money, and the liquidity should not be a concern.

Figure 6.5 (a) and (b) compares the optimal allocation on the stock and straddle across different values of risk aversion level γ . We let the re-balancing frequency of the PAMC-indirect method be 60 times per year, i.e. investors roughly adjust their positions weekly. Optimal allocation from the PAMC-indirect method and theoretical solution (re-balancing continuously) are visually overlapped, the PAMC-indirect method exhibits very excellent accuracy in this case. The allocation from the PAMC-direct method with 60 re-balances per year is subject to a substantial error, on the other hand, the gap to the theoretical solution shrinks if we let the re-balancing frequency be 300 times per year (roughly daily re-balance). We expect the gap will vanish as re-balancing frequency continues to increase. The computational times of the PAMC-direct and PAMC-indirect methods are compared in figure 6.5 (c), the time required for the PAMC-indirect method is significantly smaller than the time for the PAMC-direct method. The PAMC-indirect is superior to the PAMC-direct with regard to both accuracy and computational efficiency, we hence use only the PAMC-indirect in section 6.4.

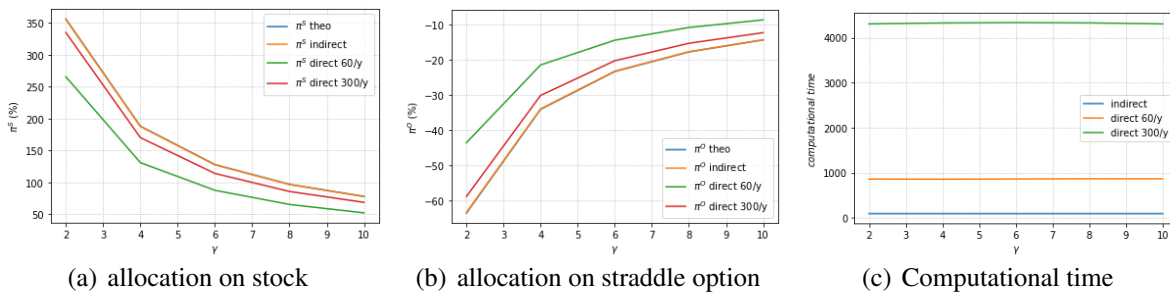


Figure 6.5: Allocation on straddle versus γ

Algorithm 11: PAMC-indirect

Input: S_0, W_0, H_0
Output: Optimal trading strategy π_0^*

- 1 Initialization;
- 2 Generating n_r paths of $B_t^{m,S}, B_t^{m,H}, S_t^m, H_t^m, S_t^{m,S}, S_t^{m,H}$ for $m = 1 \dots n_r$;
- 3 **while** $t = T - \Delta t$ **do**
- 4 **for** $m = 1 \dots n_r$ **do**
- 5 Directly compute optimal allocation $\eta_{T-\Delta t}^m$ with Equation (6.13) where $P_k = 1$ at time T ;
- 6 **for** $n = 1 \dots N$ **do**
- 7 Generate $\hat{S}_T^{m,n,S}$ and $\hat{S}_T^{m,n,H}$ given $S_{T-\Delta}^{m,S}$ and $S_{T-\Delta}^{m,H}$;
- 8 Compute wealth $\hat{W}_T^{m,n}(\eta_{T-\Delta t}^m)$ at the terminal time given the wealth at $W_{T-\Delta t} = W_0$, the transformed value function is estimated by

$$\hat{v}^m = \ln \left[(1 - \gamma) \frac{1}{N} \sum_{n=1}^N U(\hat{W}_T^{m,n}(\pi_{T-\Delta t}^m)) \right] - (1 - \gamma) \ln W_0;$$
- 9 Regress \hat{v}^m over the polynomial of $H_{T-\Delta t}^m$ and $\ln S_{T-\Delta t}^m$, and obtain the function $L_{T-\Delta t}(H, \ln S)$;
- 10 **for** $t = T - 2\Delta t$ to Δt **do**
- 11 **for** $m = 1 \dots n_r$ **do**
- 12 Directly compute optimal allocation η_t^m with Equation (6.13) where $P_k = L_{t+\Delta t}(H, \ln S)$;
- 13 **for** $n = 1 \dots N$ **do**
- 14 Generate $\hat{S}_{t+\Delta t}^{m,n}, \hat{H}_{t+\Delta t}^{m,n}, \hat{S}_{t+\Delta t}^{m,n,S}$ and $\hat{S}_{t+\Delta t}^{m,n,H}$ given $S_t^m, H_t^m, S_t^{m,S}$ and $S_t^{m,H}$;
- 15 Compute wealth $\hat{W}_{t+\Delta t}^{m,n}(\eta_t^m)$ at the terminal given the wealth at $W_t = W_0$, the transformed value function is estimated by

$$\hat{v}^m = \ln \left[\frac{1}{N} \sum_{n=1}^N (W_{t+\Delta t}^{m,n}(\pi_t^m))^{1-\gamma} \exp(L_{t+\Delta t}(\hat{H}_{t+\Delta t}^{m,n}, \ln \hat{S}_{t+\Delta t}^{m,n})) \right] - (1 - \gamma) \ln W_0;$$
- 16 Regress \hat{v}^m over the polynomial of H_t^m and $\ln S_t^m$, and obtain the function $L_t(H, \ln S)$;
- 17 **while** $t = 0$ **do**
- 18 η_0^* is obtained with Equation (6.13) and where the $P_k = L_{\Delta t}(H, \ln S)$;
- 19 Apply approximation methods and obtain the price of $O_0(H_0, \ln S_0)$ as well as its sensitivity $\frac{\partial O_0}{\partial S_0}(H_0, \ln S_0)$ and $\frac{\partial O_0}{\partial H_0}(H_0, \ln S_0)$;
- 20 Compute the variance matrix Σ_0 , and the optimal allocation $\pi_0^* = (\Sigma_0^T)^{-1} \eta_0^*$;
- 21 **return** π_0^*

Chapter 7

Summary and Future Research

The thesis studies numerical methods for dynamic portfolio choice problems as well as their applications. We first introduced a competitive numerical method (i.e. PAMC) to approximate the optimal strategy and value function for a CRRA-type investor in Chapter 2. The outstanding accuracy and efficiency of the PAMC were verified on a variety of continuous- and discrete-time models. Chapter 3 extended PAMC to the wider HARA utility family and proposed the PAMH. An important application of the PAMH was illustrated, where the optimal strategy and value function for the OU 4/2 model within both EUT and MVT were obtained. Furthermore, we demonstrated an innovation of fitting the portfolio value function with neural networks in Chapter 4, two architectures as extensions of exponential polynomial functions were proposed. The last two chapters investigated the portfolio decision in derivatives markets. Chapter 5 constructed a derivatives selection framework and explored an additional optimization criterion, namely, risk exposure minimization, to help investors make a practical derivatives selection. This framework was applied to volatility risk in Chapter 6. The optimal choices among equity options and VIX options to complete a financial market were studied relying on an extension method of the PAMC.

Our approximation methodologies in Chapters 2, 3, and 4 can be extended on several fronts. First, our methods are applicable to continuous-time (differentiable) models and specific discrete-time models (e.g. the VAR model); the application to other discrete-time models would be an interesting research topic. Currently, our methodologies are developed within a hypothetical trading environment where all costs and constraints associated with transactions are non-existent. These realistic considerations could be incorporated into the asset allocation process. Furthermore, a variety of variance reduction techniques might be applied to enhance the quality of the simulation in our methodologies. Many institutional investors in the capital market have distinct peculiarities in managing portfolios. For example, pension funds undertake legal obligations of future payments, while in an asset-liability management framework balancing portfolio return and surplus risk is suitable. Banks and property and casualty (P&C) insurers face significant cash flow uncertainty due to the nature of their liabilities, hence assets' liquidity and redemption period should be accounted in their portfolios. We suggest for future research variants of our methods, targeting specific investors, that could be more robust to instruct the investment decision.

Chapters 5 and 6 investigated the derivatives selection in a low-dimensional setting, i.e. portfolios consisting of two derivatives. One could incorporate multi-factor models taking into

account: stochastic interest rates, currency risk, stochastic correlations, jumps, and stochastic market prices of risk. In these cases, besides the equity and VIX derivatives, other products such as fixed-income and foreign exchange derivatives should be involved in the portfolio. These realistic settings will provide investors with a more comprehensive insight into optimal high-dimensional portfolios and multi-asset derivatives for sensible practical investment. Moreover, in Chapter 5, we witness that sensitivity to rebalancing frequency is a potential concern for derivatives-based portfolios. Another possible improvement to the derivatives selection criterion would consider the trade-off between risk exposure reduction and trading cost. Finally, we propose the additional portfolio criterion of risk exposure minimization for a derivatives-based portfolio. However, the choice of the objective function is subjective. People can consider other risk metrics (e.g. L_2 norm of the investment size), which will likely lead to different derivatives choices. Investigating the relation between metrics and derivative choices would also be an interesting extension of this work.

Bibliography

- [1] Johan Andreasson and Pavel V Shevchenko. Bias-corrected least-squares monte carlo for utility based optimal stochastic control problems. *Available at SSRN 2985828*, 2019.
- [2] Kenneth J Arrow. The role of securities in the optimal allocation of risk-bearing. *The review of economic studies*, 31(2):91–96, 1964.
- [3] Kenneth J Arrow and Gerard Debreu. Existence of an equilibrium for a competitive economy. *Econometrica: Journal of the Econometric Society*, pages 265–290, 1954.
- [4] Achref Bachouch, Côme Huré, Nicolas Langrené, and Huyen Pham. Deep neural networks algorithms for stochastic control problems on finite horizon: numerical applications. *Methodology and Computing in Applied Probability*, pages 1–36, 2021.
- [5] Suleyman Basak and Georgy Chabakauri. Dynamic mean-variance asset allocation. *The Review of Financial Studies*, 23(8):2970–3016, 2010.
- [6] Dimitris Bertsimas and John N Tsitsiklis. *Introduction to linear optimization*, volume 6. Athena Scientific Belmont, MA, 1997.
- [7] Petter Bjerksund and Gunnar Stensland. Closed-form approximation of american options. *Scandinavian Journal of Management*, 9:S87–S99, 1993.
- [8] Fischer Black and Myron Scholes. The pricing of options and corporate liabilities. *Journal of political economy*, 81(3):637–654, 1973.
- [9] Phelim Boyle, Junichi Imai, and Ken Seng Tan. Computation of optimal portfolios using simulation-based dimension reduction. *Insurance: Mathematics and Economics*, 43(3):327–338, 2008.
- [10] Michael W Brandt, Amit Goyal, Pedro Santa-Clara, and Jonathan R Stroud. A simulation approach to dynamic portfolio choice with an application to learning about return predictability. *The Review of Financial Studies*, 18(3):831–873, 2005.
- [11] Michael J Brennan, Eduardo S Schwartz, and Ronald Lagnado. Strategic asset allocation. *Journal of Economic dynamics and Control*, 21(8-9):1377–1403, 1997.
- [12] Mark Broadie and Weiwei Shen. Numerical solutions to dynamic portfolio problems with upper bounds. *Computational Management Science*, 14(2):215–227, 2017.

- [13] Andrea Buraschi, Paolo Porchia, and Fabio Trojani. Correlation risk and optimal portfolio choice. *The Journal of Finance*, 65(1):393–420, 2010.
- [14] CGM CBOE. Cboe vix white paper. <https://cdn.cboe.com/resources/vix/vixwhite.pdf>, 2003.
- [15] Hsuan-Chi Chen, San-Lin Chung, and Keng-Yu Ho. The diversification effects of volatility-related assets. *Journal of Banking & Finance*, 35(5):1179–1189, 2011.
- [16] Nan Chen and Yanchu Liu. American option sensitivities estimation via a generalized infinitesimal perturbation analysis approach. *Operations Research*, 62(3):616–632, 2014.
- [17] Shun Chen and Lei Ge. A learning-based strategy for portfolio selection. *International Review of Economics & Finance*, 71:936–942, 2021.
- [18] Yuyang Cheng and Marcos Escobar-Anel. Optimal investment strategy in the family of $4/2$ stochastic volatility models. *Quantitative Finance*, pages 1–29, 2021.
- [19] Mei Choi Chiu and Hoi Ying Wong. Optimal investment for an insurer with cointegrated assets: Crra utility. *Insurance: Mathematics and Economics*, 52(1):52–64, 2013.
- [20] Mei Choi Chiu and Hoi Ying Wong. Mean–variance portfolio selection with correlation risk. *Journal of Computational and Applied Mathematics*, 263:432–444, 2014.
- [21] Mei Choi Chiu and Hoi Ying Wong. Dynamic cointegrated pairs trading: mean–variance time-consistent strategies. *Journal of Computational and Applied Mathematics*, 290:516–534, 2015.
- [22] Peter Christoffersen, Steven Heston, and Kris Jacobs. The shape and term structure of the index option smirk: Why multifactor stochastic volatility models work so well. *Management Science*, 55(12):1914–1932, 2009.
- [23] Fei Cong and Cornelis W Oosterlee. Multi-period mean–variance portfolio optimization based on monte-carlo simulation. *Journal of Economic Dynamics and Control*, 64:23–38, 2016.
- [24] Fei Cong and Cornelis W Oosterlee. Accurate and robust numerical methods for the dynamic portfolio management problem. *Computational Economics*, 49(3):433–458, 2017.
- [25] John C Cox and Chi-fu Huang. Optimal consumption and portfolio policies when asset prices follow a diffusion process. *Journal of economic theory*, 49(1):33–83, 1989.
- [26] Jaksa Cvitanic, Levon Goukasian, Fernando Zapatero, et al. Monte carlo computation of optimal portfolios in complete markets. *Journal of Economic Dynamics and Control*, 27(6):971–986, 2003.
- [27] George Cybenko. Approximation by superpositions of a sigmoidal function. *Mathematics of control, signals and systems*, 2(4):303–314, 1989.

- [28] Matt Davison, Marcos Escobar-Anel, and Yichen Zhu. Optimal market completion through financial derivatives with applications to volatility risk. *arXiv preprint arXiv:2202.08148*, 2022.
- [29] Michel Denault, Erick Delage, and Jean-Guy Simonato. Dynamic portfolio choice: a simulation-and-regression approach. *Optimization and Engineering*, 18(2):369–406, 2017.
- [30] Jerome B Detemple, Ren Garcia, and Marcel Rindisbacher. A monte carlo method for optimal portfolios. *The journal of Finance*, 58(1):401–446, 2003.
- [31] James S Doran. Volatility as an asset class: Holding vix in a portfolio. *Journal of Futures Markets*, 40(6):841–859, 2020.
- [32] Robert F Engle. Autoregressive conditional heteroscedasticity with estimates of the variance of united kingdom inflation. *Econometrica: Journal of the Econometric Society*, pages 987–1007, 1982.
- [33] M Escobar, D Neykova, and R Zagst. Hara utility maximization in a markov-switching bond–stock market. *Quantitative Finance*, 17(11):1715–1733, 2017.
- [34] Marcos Escobar, Sebastian Ferrando, and Alexey Rubtsov. Optimal investment under multi-factor stochastic volatility. *Quantitative Finance*, 17(2):241–260, 2017.
- [35] Marcos Escobar, Sebastian Ferrando, and Alexey Rubtsov. Dynamic derivative strategies with stochastic interest rates and model uncertainty. *Journal of Economic Dynamics and Control*, 86:49–71, 2018.
- [36] Marcos Escobar-Anel, Matt Davison, and Yichen Zhu. Derivatives-based portfolio decisions. an expected utility insight. *arXiv preprint arXiv:2201.03717*, 2022.
- [37] Marcos Escobar-Anel and Zhenxian Gong. The mean-reverting 4/2 stochastic volatility model: Properties and financial applications. *Applied Stochastic Models in Business and Industry*, 2020.
- [38] Christian Riis Flor and Linda Sandris Larsen. Robust portfolio choice with stochastic interest rates. *Annals of Finance*, 10(2):243–265, 2014.
- [39] Lorenzo Garlappi and Georgios Skoulakis. Numerical solutions to dynamic portfolio problems: The case for value function iteration using taylor approximation. *Computational Economics*, 33(2):193–207, 2009.
- [40] Lorenzo Garlappi and Georgios Skoulakis. Solving consumption and portfolio choice problems: The state variable decomposition method. *The Review of Financial Studies*, 23(9):3346–3400, 2010.
- [41] Lorenzo Garlappi and Georgios Skoulakis. Taylor series approximations to expected utility and optimal portfolio choice. *Mathematics and Financial Economics*, 5(2):121, 2011.

- [42] Maximilien Germain, Huyên Pham, and Xavier Warin. Neural networks-based algorithms for stochastic control and pdes in finance. *arXiv preprint arXiv:2101.08068*, 2021.
- [43] William N Goetzmann, Stephen J Brown, Martin J Gruber, and Edwin J Elton. Modern portfolio theory and investment analysis. *John Wiley & Sons*, 237, 2014.
- [44] M Barry Goldman, Howard B Sosin, and Mary Ann Gatto. Path dependent options:” buy at the low, sell at the high”. *The Journal of Finance*, 34(5):1111–1127, 1979.
- [45] Martino Grasselli. The 4/2 stochastic volatility model: a unified approach for the heston and the 3/2 model. *Mathematical Finance*, 27(4):1013–1034, 2017.
- [46] Nils H Hakansson. Optimal investment and consumption strategies under risk for a class of utility functions. In *Stochastic Optimization Models in Finance*, pages 525–545. Elsevier, 1975.
- [47] Martin B Haugh and Andrew W Lo. Asset allocation and derivatives. *Quantitative Finance*, 1:45–72, 2001.
- [48] Steven L Heston. A closed-form solution for options with stochastic volatility with applications to bond and currency options. *The review of financial studies*, 6(2):327–343, 1993.
- [49] Steven L Heston. A simple new formula for options with stochastic volatility. 1997.
- [50] Ying Hu, Hanqing Jin, and Xun Yu Zhou. Time-inconsistent stochastic linear–quadratic control. *SIAM journal on Control and Optimization*, 50(3):1548–1572, 2012.
- [51] John Hull. Using hull-white interest rate trees. *Journal of Derivatives*, 3(3):26–36, 1996.
- [52] Côme Huré, Huyên Pham, Achref Bachouch, and Nicolas Langrené. Deep neural networks algorithms for stochastic control problems on finite horizon: convergence analysis. *SIAM Journal on Numerical Analysis*, 59(1):525–557, 2021.
- [53] Shashi Jain and Cornelis W Oosterlee. The stochastic grid bundling method: Efficient pricing of bermudan options and their greeks. *Applied Mathematics and Computation*, 269:412–431, 2015.
- [54] Ioannis Karatzas, John P Lehoczky, and Steven E Shreve. Optimal portfolio and consumption decisions for a “small investor” on a finite horizon. *SIAM journal on control and optimization*, 25(6):1557–1586, 1987.
- [55] Ioannis Karatzas, Steven E Shreve, I Karatzas, and Steven E Shreve. *Methods of mathematical finance*, volume 39. Springer, 1998.
- [56] Angelien GZ Kemna and Antonius CF Vorst. A pricing method for options based on average asset values. *Journal of Banking & Finance*, 14(1):113–129, 1990.

- [57] Ralph SJ Koijen, Theo E Nijman, and Bas JM Werker. When can life cycle investors benefit from time-varying bond risk premia? *The review of financial studies*, 23(2):741–780, 2009.
- [58] Holger Kraft. Elasticity approach to portfolio optimization. *Mathematical Methods of Operations Research*, 58(1):159–182, 2003.
- [59] Holger Kraft*. Optimal portfolios and heston’s stochastic volatility model: an explicit solution for power utility. *Quantitative Finance*, 5(3):303–313, 2005.
- [60] Holger Kraft. *Optimal portfolios with stochastic interest rates and defaultable assets*, volume 540. Springer Science & Business Media, 2012.
- [61] François Legendre and Djibril Togola. Explicit solutions to dynamic portfolio choice problems: A continuous-time detour. *Economic Modelling*, 58:627–641, 2016.
- [62] Danping Li, Yang Shen, and Yan Zeng. Dynamic derivative-based investment strategy for mean–variance asset–liability management with stochastic volatility. *Insurance: Mathematics and Economics*, 78:72–86, 2018.
- [63] Yuying Li and Peter A Forsyth. A data-driven neural network approach to optimal asset allocation for target based defined contribution pension plans. *Insurance: Mathematics and Economics*, 86:189–204, 2019.
- [64] Zhongyu Li, Ka Ho Tsang, and Hoi Ying Wong. Lasso-based simulation for high-dimensional multi-period portfolio optimization. *IMA Journal of Management Mathematics*, 31(3):257–280, 2020.
- [65] Andrew EB Lim. Quadratic hedging and mean-variance portfolio selection with random parameters in an incomplete market. *Mathematics of Operations Research*, 29(1):132–161, 2004.
- [66] Andrew EB Lim and Xun Yu Zhou. Mean-variance portfolio selection with random parameters in a complete market. *Mathematics of Operations Research*, 27(1):101–120, 2002.
- [67] Chi-Ming Lin, Jih-Jeng Huang, Mitsuo Gen, and Gwo-Hshiung Tzeng. Recurrent neural network for dynamic portfolio selection. *Applied Mathematics and Computation*, 175(2):1139–1146, 2006.
- [68] Yueh-Neng Lin. Pricing vix futures: Evidence from integrated physical and risk-neutral probability measures. *Journal of Futures Markets: Futures, Options, and Other Derivative Products*, 27(12):1175–1217, 2007.
- [69] Seppo Linnainmaa. The representation of the cumulative rounding error of an algorithm as a taylor expansion of the local rounding errors. *Master’s Thesis (in Finnish)*, Univ. Helsinki, pages 6–7, 1970.

- [70] Jun Liu. Portfolio selection in stochastic environments. *The Review of Financial Studies*, 20(1):1–39, 2006.
- [71] Jun Liu and Jun Pan. Dynamic derivative strategies. *Journal of Financial Economics*, 69(3):401–430, 2003.
- [72] Francis A Longstaff and Eduardo S Schwartz. Valuing american options by simulation: a simple least-squares approach. *The review of financial studies*, 14(1):113–147, 2001.
- [73] Harry Markowitz. Portfolio selection. *The journal of finance*, 7(1):77–91, 1952.
- [74] J.B. Maverick. How big is the derivatives market?, Aug 2020.
- [75] Warren S McCulloch and Walter Pitts. A logical calculus of the ideas immanent in nervous activity. *The bulletin of mathematical biophysics*, 5(4):115–133, 1943.
- [76] Robert C Merton. Lifetime portfolio selection under uncertainty: The continuous-time case. *The review of Economics and Statistics*, pages 247–257, 1969.
- [77] Robert C Merton. Theory of rational option pricing. *The Bell Journal of economics and management science*, pages 141–183, 1973.
- [78] Robert C Merton. Optimum consumption and portfolio rules in a continuous-time model. In *Stochastic Optimization Models in Finance*, pages 621–661. Elsevier, 1975.
- [79] Hui Mi and Lixia Xu. Optimal investment with derivatives and pricing in an incomplete market. *Journal of Computational and Applied Mathematics*, 368:112522, 2020.
- [80] Ronald L Rardin and Ronald L Rardin. *Optimization in operations research*, volume 166. Prentice Hall Upper Saddle River, NJ, 1998.
- [81] Fabrice D Rouah. *The Heston model and its extensions in Matlab and C*. John Wiley & Sons, 2013.
- [82] David E Rumelhart, Geoffrey E Hinton, and Ronald J Williams. Learning representations by back-propagating errors. *nature*, 323(6088):533–536, 1986.
- [83] Paul A Samuelson. Lifetime portfolio selection by dynamic stochastic programming. *The review of economics and statistics*, pages 239–246, 1969.
- [84] Ka Ho Tsang and Hoi Ying Wong. Deep-learning solution to portfolio selection with serially dependent returns. *SIAM Journal on Financial Mathematics*, 11(2):593–619, 2020.
- [85] Jules H van Binsbergen and Michael W Brandt. Solving dynamic portfolio choice problems by recursing on optimized portfolio weights or on the value function? *Computational Economics*, 29(3-4):355–367, 2007.
- [86] Oldrich Vasicek. An equilibrium characterization of the term structure. *Journal of financial economics*, 5(2):177–188, 1977.

- [87] Geoffrey J Warren. Can investing in volatility help meet your portfolio objectives? *The Journal of Portfolio Management*, 38(2):82–98, 2012.
- [88] Tingjin Yan and Hoi Ying Wong. Open-loop equilibrium strategy for mean–variance portfolio problem under stochastic volatility. *Automatica*, 107:211–223, 2019.
- [89] Xun Yu Zhou and Duan Li. Continuous-time mean-variance portfolio selection: A stochastic lq framework. *Applied Mathematics and Optimization*, 42(1):19–33, 2000.
- [90] Yichen Zhu and Marcos Escobar-Anel. A neural network monte carlo approximation for expected utility theory. *Journal of Risk and Financial Management*, 14(7):322, 2021.
- [91] Yichen Zhu and Marcos Escobar-Anel. Polynomial affine approach to hara utility maximization with applications to ornsteinuhlenbeck 4/2 models. *Applied Mathematics and Computation*, 418:126836, 2022.
- [92] Yichen Zhu, Marcos Escobar-Anel, and Matt Davison. A polynomial-affine approximation for dynamic portfolio choice. *Submitted to Computational economics*, 2020.

Curriculum Vitae

Name: Yichen Zhu

Post-Secondary Education and Degrees: South China University of Technology
Guangzhou, Guangdong
2013 - 2017 B.Sc.

University of Western Ontario
London, ON
2017 - 2018 M.Sc.

University of Western Ontario
London, ON
2018 - 2022 Ph.D.

Related Work Experience: Teaching Assistant
The University of Western Ontario
2017 - 2022

Publications:

Yichen Zhu, Marcos Escobar-Anel and Matt Davison. “A polynomial-affine approximation for dynamic portfolio choice.” Second round of revision to *Computational Economics*.

Yichen Zhu, Marcos Escobar-Anel. “Polyomial affine approach to the HARA utility with application to OU 4/2 model.” Published in *Applied Mathematics and Computation*.

Yichen Zhu, Marcos Escobar-Anel. “A neural network Monte Carlo approximation for expected utility theory.” Published in *Journal of Risk and Financial Management*.

Marcos Escobar-Anel, Matt Davison and Yichen Zhu. “Derivatives-based portfolio decisions. An expected utility insight.” Accepted by *Annals of Finance*.

Matt Davison, Marcos Escobar-Anel and Yichen Zhu. “Optimal market completion through financial derivatives with applications to volatility risk.” Submitted to *Quantitative Finance*.